



---

**Universidad de Valladolid**

PROGRAMA DE DOCTORADO  
EN INVESTIGACIÓN BIOMÉDICA

TESIS DOCTORAL:

**"Calcium signaling modulators: a novel  
pharmacological intervention to delay aging  
in *Caenorhabditis elegans*"**

Presentada por **PALOMA GARCÍA CASAS** para optar  
al grado de  
Doctora por la Universidad de Valladolid

Dirigida por:  
**Dr. Javier Álvarez Martín**  
**Dra. Mayte Montero Zoccola**  
**Dra. Rosalba Inés Fonteriz García**



## FUNDING

This research work has been possible thanks to the following funding:

Ayudas para contratos predoctorales para la formación de doctores 2015 contemplada en el Subprograma Estatal de Formación, del Programa Estatal de Promoción del Talento y su Empleabilidad, en el marco del Plan Estatal de Investigación Científica y Técnica e Innovación 2013-2016. Cofinanciadas por el Fondo Social Europeo (Orden ECC/1402/2013, de 22 de julio).





## PUBLICATIONS AND COMMUNICATIONS

Part of the results shown in this thesis are published in the following publications:

- **García-Casas P**, Arias-Del-Val J, Alvarez-Illera P, Fonteriz RI, Montero M, Alvarez J. Inhibition of Sarco-Endoplasmic Reticulum Ca<sup>2+</sup> ATPase Extends the Lifespan in *C. elegans* Worms. *Front Pharmacol*. 2018 Jun 25;9:669.
- **García-Casas P**, Arias-Del-Val J, Alvarez-Illera P, Wojnicz A, de Los Ríos C, Fonteriz RI, Montero M, Alvarez J. The Neuroprotector Benzothiazepine CGP37157 Extends Lifespan in *C. elegans* Worms. *Front Aging Neurosci*. 2019 Jan 17;10:440.

In addition some works related to this research have been presented in the following meetings:

- **XIV International Meeting of the Calcium European Society (2016)**. Pilar Álvarez-Illera, Adolfo Sánchez-Blanco, Paloma García-Casas, Silvia López-Burillo, Rosalba I Fonteriz, Javier Álvarez and Mayte Montero. “*Long term monitoring of Ca<sup>2+</sup> dynamics in C. elegans pharynx: an in vivo energy balance sensor*”. Valladolid, Spain, 2016. **Poster**
- **VI Spanish Worm Meeting (2017)**. García-Casas P, Arias-del-Val J, Alvarez-Illera P, Fonteriz RI, Montero M, Alvarez J. “*Effect of Sarco-Endoplasmic Reticulum Ca<sup>2+</sup>-ATPase (SERCA) inhibition on C. elegans life span and pharynx Ca<sup>2+</sup> signaling*” Valencia, Spain. **Oral communication**.
- **VI Spanish Worm Meeting (2017)**., Alvarez-Illera P, García-Casas P, Arias-del-Val J, Fonteriz RI, Montero M, Alvarez J. “*From young to adult: in vivo monitoring of Ca<sup>2+</sup> dynamics in C. elegans pharynx*” Valencia, Spain. **Oral communication**.
- **EMBO Workshop: C. elegans development, cell biology and gene expression (2018)**. Garcia-Casas P, Arias-del-Val J, Alvarez-Illera P, Wojnicz A, de los Ríos C, Fonteriz RI, Montero M, Alvarez J. “*Benzothiazepine CGP37157 extends lifespan in C. elegans worms*”. Barcelona, Spain. **Poster**.
- **EMBO Workshop: C. elegans development, cell biology and gene expression (2018)**. García-Casas P, Arias-del-Val J, Alvarez-Illera P, Fonteriz RI, Montero

M, Alvarez J. *"Inhibition of Sarco-Endoplasmic Reticulum Ca<sup>2+</sup> ATPase extends the lifespan in C. elegans worms"*. Barcelona, Spain. **Poster.**

- **EMBO Workshop: C. elegans development, cell biology and gene expression (2018).** Alvarez-Illera P, García-Casas P, Arias-del-Val J, Sanxhez-Blanco A, Fonteriz RI, Montero M, Alvarez J. *"Long-term monitoring of cytosolic and mitochondrial Ca<sup>2+</sup> dynamics in C. elegans pharynx"*. Barcelona, Spain. **Poster.**
- **VII Spanish Worm Meeting (2019)** Garcia-Casas P, Arias-del-Val J, Alvarez-Illera P, Fonteriz RI, Montero M, Alvarez J. *"Inhibition of Sarco-Endoplasmic Reticulum Ca<sup>2+</sup> ATPase extends the lifespan in C. elegans worms"*. Barcelona Spain. **Poster.**
- **VII Spanish Worm Meeting (2019)** Garcia-Casas P, Arias-del-Val J, Alvarez-Illera P, Wojnicz A, de los Ríos C, Fonteriz RI, Montero M, Alvarez J *"The neuroprotector benzothiazepine CGP37157 extends the lifespan in C. elegans worms"*. Barcelona, Spain. **Poster**
- **8th ECS Workshop. Calcium Signaling in Aging and Neurodegenerative Diseases (2019).** Garcia-Casas P, Arias-del-Val J, Alvarez-Illera P, Fonteriz RI, Montero M, Alvarez J. *"Inhibition of Sarco-Endoplasmic Reticulum Ca<sup>2+</sup> ATPase extends the lifespan in c. elegans worms"*. Coimbra, Portugal. **Oral communication.**
- **8th ECS Workshop. Calcium Signaling in Aging and Neurodegenerative Diseases (2019).** Alvarez-Illera P, Garcia-Casas P, Fonteriz RI, Montero M, Alvarez J. *"Mitochondrial Ca<sup>2+</sup> dynamics in MCU knockout C. elegans worms"* Coimbra, Portugal. **Poster.**
- **8th ECS Workshop. Calcium Signaling in Aging and Neurodegenerative Diseases (2019).** Garcia-Casas P, Arias-del-Val J, Alvarez-Illera P, Wojnicz A, de los Ríos C, Fonteriz RI, Montero M, Alvarez J. *"The Neuroprotector CGP37157 extends lifespan in C. elegans worms"*. Coimbra, Portugal. **Poster**

# INDEX

<b>ABBREVIATIONS</b>	<b>9</b>
<b>C.ELEGANS STRAINS</b>	<b>13</b>
<b>ABSTRACT</b>	<b>17</b>
<b>INTRODUCTION</b>	<b>21</b>
<b>I.CAENORHABDITIS ELEGANS BIOLOGY</b>	<b>23</b>
I.1 C. elegans as a model organism	23
I.2 C. elegans life cycle	26
I.3 C. elegans adult hermaphrodite anatomy	27
I.3.1 Cuticle	28
I.3.2 Epithelial system	29
I.3.3 Nervous system	29
I.3.4 Muscular system	30
I.3.5 Excretory system	31
I.3.6 Reproductive system	32
I.3.7 Digestive system	33
I.4 C. elegans pharynx	34
I.4.1 Pharynx anatomy	34
I.4.2 Pharyngeal nervous system	35
I.4.3 Pharyngeal action potentials	37
I.4.3.1 Nicotinic acetylcholine receptor: EAT-2 and EAT-18	38
I.4.3.2 T-type calcium channel: CCA-1	38
I.4.3.3 L-Type calcium channel: EGL-19	38
I.4.3.4 Glutamate gated chloride channel: AVR-15	39
I.4.3.5 Potassium channel: EXP-2	39
I.4.4 Pharyngeal motility	39
<b>II. AGING</b>	<b>40</b>
II.1 Theories of aging	40
II.2 Cellular and molecular hallmarks of aging	41
II.3 Loss of proteostasis as an aging promoter	43
II.3.1 The stress response	44
II.3.2 The degradation system: Ubiquitin/Proteasome (UPS)	45
II.3.3 The disposal system: Autophagy	45
II.4 Nutrient sensing pathways and aging regulation	48
II.4.1 IIS: Insulin/insulin-like growth factor (IGF-1) signaling pathway	48
II.4.2 Mechanistic target of rapamycin (mTOR) signaling pathway	51
II.4.3 Adenosine monophosphate-activated protein kinase (AMPK) pathway	54
II.4.4 Sirtuins pathway	56
II.5 Mitochondrial dysfunction	57
II.6 Delaying aging: the intricate network machinery of Caloric Restriction	59

<b>III. CALCIUM SIGNALING PATHWAY</b>	<b>63</b>
III.1 Calcium signaling dynamics	63
III.1.1 Cytosolic Ca <sup>2+</sup> concentration increase (ON reactions)	64
III.1.2 Restoration of cytosolic Ca <sup>2+</sup> concentration (OFF reactions)	65
III.2 Mitochondrial Ca <sup>2+</sup> dynamics	66
III.3 <i>C. elegans</i> Ca <sup>2+</sup> signaling toolkit	67
III.4 Mitochondria-ER Associated Membranes (MAMs)	69
III.5 Ca <sup>2+</sup> signaling and nutrient signaling pathways	70
<b>IV. AGING AND CALCIUM SIGNALING</b>	<b>72</b>
IV.1 Dysregulation of Ca <sup>2+</sup> signaling in aging and neurodegeneration	72
IV.2 <i>C. elegans</i> : insights in Ca <sup>2+</sup> signaling, aging, and neurodegeneration	73
<b>MOTIVATION AND AIMS</b>	<b>75</b>
<b>METHODS AND MATERIALS</b>	<b>79</b>
<b>I. C. ELEGANS STRAINS</b>	<b>81</b>
I.1 <i>C. elegans</i> control strains	81
I.1.1 Wildtype strain (N2)	81
I.1.2 Control strains with fluorescent indicators	81
I.1.2.1 Strains with cytosolic calcium probes	81
I.1.2.2 Strains with mitochondrial calcium probes	81
I.1.2.3 Strains with stress reporters	82
I.2 <i>C. elegans</i> mutant strains	83
I.2.1 Nutrient sensitive pathways mutants	83
I.2.1.1 IGF-1 signaling pathway mutants	83
I.2.1.2 mTOR signaling pathway mutants	83
I.2.1.3 AMPK signaling pathway mutants	84
I.2.1.4 Sirtuins signaling pathway mutants	84
I.2.2 Mitochondrial mutants	84
I.2.3 Caloric restriction mutants	84
<b>II. C. ELEGANS LABORATORY MAINTENANCE</b>	<b>86</b>
II.1 Nematode Growth Medium (NGM)	86
II.1.1 NGM FuDR agar plates	87
II.1.2 NGM agar plates for pharmacological treatments	87
II.2 <i>E. coli</i> OP50: worm's bacterial food source	87
II.2.1 Active OP50 culture	87
II.2.2 Heat-inactivated OP50 culture	88
II.3 Seeded NGM plates	88
<b>III. PHARMACOLOGICAL TREATMENTS</b>	<b>89</b>
III.1 Intracellular Ca <sup>2+</sup> modulators	89
III.1.1 Sarco-Endoplasmic Reticulum Ca <sup>2+</sup> ATPase inhibitors	89
III.1.1.1 Thapsigargin	89
III.1.1.2 2,5-di-tert-butylhydroquinone (2,5-BHQ)	90
III.1.2 Mitochondrial Na <sup>+</sup> /Ca <sup>2+</sup> exchanger (mNCX) inhibitor	90
III.1.2.1 CGP37157	90
III.2 $\gamma$ -cyclodextrin inclusion compounds	91

<b>IV. WORM'S POPULATION SYNCHRONIZATION</b>	<b>93</b>
<b>V. IN VIVO C. ELEGANS ASSAYS</b>	<b>95</b>
V.1 C. elegans lifespan assay	95
V.2 C. elegans Ca <sup>2+</sup> dynamics assay	96
V.2.1 Cameleons	96
V.2.2 Sample preparation and equipment	97
V.2.3 Recording settings	98
V.2.4 Statistical analysis	99
V.3 Electropharyngeogram (EPG)	100
V.3.1 Sample preparation and equipment	101
V.4 Confocal imaging	103
V.5 Evaluation of drug induced stress assay	103
V.6 C. elegans tracking assay	104
V.7 Fertility assay	104
<b>VI. BIOCHEMICAL ASSAYS</b>	<b>105</b>
VI.1 Measurement of CGP37157 in C. elegans worms	105
VI.1.1 Sample preparation	105
VI.1.2 HPLC-MS/MS	105
VI.2 ATP assessment in C. elegans worms	106
<b>VII. SOLUTIONS AND REAGENTS</b>	<b>107</b>
VII.1 Solutions	107
VII.1.1 M9 Buffer	107
VII.1.2 Bleaching solution	107
VII.1.3 KPO <sub>4</sub> Buffer 1M	107
VII.2 Materials	108
<b>RESULTS</b>	<b>109</b>
<b>I. SERCA INHIBITION AND AGING IN C. ELEGANS</b>	<b>111</b>
I.1 2,6-BHQ: inactive isomer of 2,5-BHQ	111
I.2 Effects of SERCA inhibitors in C. elegans lifespan	112
I.2.1 2,5-BHQ extends C. elegans lifespan	112
I.2.1.1 Oral administration of 2,5-BHQ extends <i>C. elegans</i> lifespan	112
I.2.1.2 C. elegans lifespan extension of 2,5-BHQ is not dependent on its method of administration or the presence of active OP50.	115
I.2.2 Thapsigargin (Tg) extends C. elegans lifespan	116
I.3 SERCA inhibitors do not extend lifespan inducing caloric restriction	119
I.4 SERCA inhibitors require functional mitochondria to extend C. elegans lifespan	121
I.5 Effect of SERCA inhibitors in nutrient sensing pathways C. elegans mutants	122
I.5.1 DAF-2 is not required for SERCA inhibitors lifespan extension	123
I.5.2 AMPK is required for SERCA inhibitors lifespan extension	124
I.5.3 mTOR is required for SERCA inhibitors lifespan extension	126
I.5.4 Sirtuins pathway is not required for SERCA inhibitors lifespan extension	128
I.5.5 DAF-16 is required for SERCA inhibitors lifespan extension	129
I.6 Effects of SERCA inhibitors in the ER stress response	131
I.6.1 SERCA inhibitors do not trigger ER stress response	131

<b>II. Na<sup>+</sup>/Ca<sup>2+</sup> ENCHANGER INHIBITION AND AGING IN C. ELEGANS</b>	<b>133</b>
II.1 Effects of CGP37157 in <i>C. elegans</i> lifespan	133
II.1.1 CGP37157 extends <i>C. elegans</i> lifespan	133
II.1.2 CGP37157 does not extend <i>C. elegans</i> lifespan inducing caloric restriction	136
II.1.3 CGP37157 requires functional mitochondria to increase <i>C. elegans</i> lifespan	137
II.1.4 Effects of CGP37157 in nutrient sensing pathways <i>C. elegans</i> mutants lifespan	138
II.1.4.1 Effects of CGP37157 in IIS, AMPK, and Sirtuins pathways mutants longevity.	138
II.1.4.2 mTOR pathway is required for CGP37157 <i>C. elegans</i> lifespan extension	140
II.2 Effective concentration of CGP37157 per worm	142
II.3 Effects of CGP37157 treatment on in vivo <i>C. elegans</i> Ca <sup>2+</sup> dynamics	143
II.3.1 Effects of CGP37157 in pharyngeal Ca <sup>2+</sup> dynamics	144
II.3.1.1 CGP37157 induces changes in the pharyngeal cytosolic Ca <sup>2+</sup> oscillations	144
II.3.1.2 CGP37157 induces changes in the pharyngeal mitochondrial Ca <sup>2+</sup> oscillations	146
II.3.2 Effects of CGP37157 in vulva Ca <sup>2+</sup> dynamics	148
II.4 Effects of CGP37157 in the electrophysiological properties of pharyngeal muscle	152
II.5 Effects of CGP37157 in several biomarkers of <i>C. elegans</i> aging	154
II.5.1 Effects of CGP37157 in <i>C. elegans</i> fertility	154
II.5.2 Effects of CGP37157 in <i>C. elegans</i> locomotion	155
II.5.3 Effects of CGP37157 in <i>C. elegans</i> hsp-12.6 expression	156
II.5.4 Effects of CGP37157 in <i>C. elegans</i> mitochondrial function	157
II.6 Effects of CGP37157 in <i>C. elegans</i> sarcopenia during aging	158
II.7 Effects of CGP37157 in <i>C. elegans</i> body wall muscle cells mitochondrial distribution and morphology.	159
<b>DISCUSSION</b>	<b>161</b>
<b>CONCLUSIONS</b>	<b>177</b>
<b>FUTURE PERSPECTIVES</b>	<b>183</b>
<b>BIBLIOGRAPHY</b>	<b>187</b>

## FIGURE AND TABLE INDEX

### FIGURES

#### INTRODUCTION

Figure 1: Anatomical differences between <i>C. elegans</i> hermaphrodite and male	23
Figure 2: <i>C. elegans</i> life cycle	26
Figure 3: <i>C. elegans</i> anatomical structure	27
Figure 4: <i>C. elegans</i> structure and composition of the adult cuticle	28
Figure 5: <i>C. elegans</i> adult nervous system structure	29
Figure 6: <i>C. elegans</i> body wall muscle structure	31
Figure 7: <i>C. elegans</i> excretory system structure	32
Figure 8: <i>C. elegans</i> reproductive system structure	33
Figure 9: <i>C. elegans</i> digestive system	33
Figure 10: <i>C. elegans</i> pharynx anatomy	34
Figure 11: <i>C. elegans</i> pharynx muscular anatomy	35
Figure 12: Organization of pharyngeal nervous system	36
Figure 13: Pharyngeal muscle action potential	38
Figure 14: Hallmarks of aging	42
Figure 15: Protein homeostasis maintenance	43
Figure 16: Molecular pathways that regulate autophagosome formation in <i>C. elegans</i>	47
Figure 17: Insulin/IGF-1 signaling in <i>C. elegans</i> regulation of aging	49
Figure 18: Upstream and downstream regulation of TORC1/2 complexes in <i>C. elegans</i>	52
Figure 19: Effects of TORC1 and TORC2 in <i>C. elegans</i> aging	54
Figure 20: AMPK upstream regulators and downstream effects	56
Figure 21: Mitochondrial dysfunction with age	58
Figure 22: Different regimes of dietary restriction activate different signaling pathways	59
Figure 23: Interaction between nutrient signaling pathways	60
Figure 24: Caloric restriction signaling pathways	61
Figure 25: Metabolic regulation of aging in <i>C. elegans</i>	62
Figure 26: Calcium transient	64
Figure 27: Neuronal calcium signaling toolkit in <i>C. elegans</i>	67
Figure 28: MAM-resident proteins	69
Figure 29: Regulation of AMPK and mTOR signaling pathways by calcium signaling	71

#### METHODS AND MATERIALS

Figure 30: Thapsigargin molecule structure	89
Figure 31: 2,5-BHQ and 2,6-BHQ molecule structures	90
Figure 32: molecular structure of CGP37157	91
Figure 33: $\gamma$ -CD inclusion compounds	91
Figure 34: worms population synchronization	93
Figure 35: ratiometric imaging of cameleon YC3.6	96
Figure 36: $\text{Ca}^{2+}$ imaging sample preparation	97
Figure 37: Zeiss Axiovert configuration for $\text{Ca}^{2+}$ measurements	98
Figure 38: representative traces of a $\text{Ca}^{2+}$ recording with a cameleon probe	99
Figure 39: EPG recording stereotypical wave	101
Figure 40: Schematic representation of an EPG assay	102

## RESULTS

<b>Figure 41:</b> Effects of 2,5-BHQ and 2,6-BHQ in ER [Ca <sup>2+</sup> ] of HeLa cells	112
<b>Figure 42:</b> Effects of 2,5-BHQ and 2,6-BHQ inclusion compounds in AQ2038 <i>C. elegans</i> lifespan	113
<b>Figure 43:</b> Effects of 2,5-BHQ and 2,6-BHQ incorporated in the NGM media in AQ2038 <i>C. elegans</i> lifespan	115
<b>Figure 44:</b> Effects of thapsigargin in AQ2038 <i>C. elegans</i> lifespan	117
<b>Figure 45:</b> Effects of SERCA inhibitors in DA1113 ( <i>eat-2</i> ) mutants lifespan	120
<b>Figure 46:</b> Effects of SERCA inhibitors in MQ1333 ( <i>nuo-6</i> ) mutants lifespan	121
<b>Figure 47:</b> Effects of SERCA inhibitors in CB1370 ( <i>daf-2</i> ) mutants lifespan	123
<b>Figure 48:</b> Effects of SERCA inhibitors in RB157 ( <i>aak-2</i> ) and AGD397 ( <i>aak-1;aak-2</i> ) mutants lifespan	125
<b>Figure 49:</b> Effects of SERCA inhibitors in DR142 ( <i>daf-15</i> ) and RB1206 ( <i>rsks-1</i> ) mutants lifespan	127
<b>Figure 50:</b> Effects of SERCA inhibitors in VC199 ( <i>sir-2.1</i> ) mutants lifespan	129
<b>Figure 51:</b> Effects of SERCA inhibitors in CF1038 ( <i>daf-16</i> ) mutants lifespan	130
<b>Figure 52:</b> Effects of 2,5-BHQ and 2,6-BHQ 250 μM in SJ4005 GFP expression	131
<b>Figure 53:</b> Effects of thapsigargin 10 nM in SJ4005 GFP expression	132
<b>Figure 54:</b> ER stress response is not induced by SERCA inhibition	132
<b>Figure 55:</b> Effects of CGP37157 in AQ2038 <i>C. elegans</i> lifespan	134
<b>Figure 56:</b> Effects of CGP37157 in DA1113 ( <i>eat-2</i> ) <i>C. elegans</i> lifespan	136
<b>Figure 57:</b> Effects of CGP37157 in MQ1333 ( <i>nuo-6</i> ) <i>C. elegans</i> lifespan	137
<b>Figure 58:</b> Effects of CGP37157 in CB1370 ( <i>daf-2</i> ), CF1038 ( <i>daf-16</i> ), RB754 ( <i>aak-2</i> ), AGD397 ( <i>akk-1;aak-2</i> ), VC199 ( <i>sir-2.1</i> ), and CF1038 ( <i>daf-16</i> ) <i>C. elegans</i> mutants lifespan	139
<b>Figure 59:</b> Effects of CGP37157 in DR142 ( <i>daf-15</i> ) and RB1206 ( <i>rsks-1</i> ) <i>C. elegans</i> mutants lifespan	141
<b>Figure 60:</b> Representative pharyngeal cytosolic Ca <sup>2+</sup> traces of untreated, and treated with CGP37157, AQ2038 worms	144
<b>Figure 61:</b> Changes in height, width and frequency of pharyngeal cytosolic Ca <sup>2+</sup> peaks at day 5 of treatment with CGP37157	145
<b>Figure 62:</b> Representative mitochondrial Ca <sup>2+</sup> traces of untreated and treated with CGP37157 AQ3055 worms in pharyngeal muscle cells	146
<b>Figure 63:</b> Changes in height, width and frequency of pharyngeal mitochondrial Ca <sup>2+</sup> peaks at day 5 of treatment with CGP37157	147
<b>Figure 64:</b> Representative cytosolic vulva Ca <sup>2+</sup> transients traces of untreated, and treated with CGP37157, AQ2121 worms	149
<b>Figure 65:</b> Changes in height, width and frequency of cytosolic vulva Ca <sup>2+</sup> transients at day 2 of treatment with CGP37157	149
<b>Figure 66:</b> Changes in height, width and frequency of cytosolic vulva Ca <sup>2+</sup> transients at day 12 of treatment with CGP37157	150
<b>Figure 67:</b> Comparison of the changes observed in height, width and frequency of cytosolic vulva Ca <sup>2+</sup> transients between day 2 and day 12 of treatment with CGP37157	151
<b>Figure 68:</b> Representative traces of EPGs from control and treated worms	152
<b>Figure 69:</b> Effects of CGP37157 in the electrophysiological properties of pharyngeal muscle cells	153
<b>Figure 70:</b> Effects of CGP37157 in <i>C. elegans</i> fertility	154
<b>Figure 71:</b> Effects of CGP37157 in <i>C. elegans</i> locomotion	155
<b>Figure 72:</b> Effects of CGP37157 in <i>C. elegans hsp16.2</i> expression in day 3 TJ375 worms	156
<b>Figure 73:</b> Effects of CGP37157 in <i>C. elegans</i> ATP levels	157
<b>Figure 74:</b> Effects of CGP37157 in <i>C. elegans</i> sarcopenia development in body wall muscle cells	158
<b>Figure 75:</b> Effects of CGP37157 in <i>C. elegans</i> body wall muscle cells mitochondrial distribution and morphology	159



## DISCUSSION

Figure 76: Proposed mechanism for the effect of SERCA inhibitors \_\_\_\_\_ 167

## TABLES

### INTRODUCTION

Table 1: <i>C. elegans</i> nomenclature _____	25
Table 2: <i>C. elegans</i> <i>ncx</i> genes and their expression pattern _____	68

### METHODS AND MATERIALS

Table 3: <i>C. elegans</i> control strains _____	82
Table 4: <i>C. elegans</i> mutant strains _____	85
Table 5: Nematode Growth Medium (NGM) composition _____	86
Table 6: M9 buffer composition _____	107
Table 7: Bleaching solution composition _____	107
Table 8: KPO <sub>4</sub> Buffer composition _____	107

### RESULTS

Table 9: Lifespan assays performed with 2,5-BHQ and 2,6-BHQ inclusion compounds in AQ2038 worms _____	114
Table 10: Lifespan assays performed with 2,5-BHQ and 2,6-BHQ incorporated in the NGM media in AQ2038 worms _____	116
Table 11: Lifespan assays performed with thapsigargin in AQ2038 worms _____	118
Table 12: Lifespan assays performed with SERCA inhibitors in DA113 ( <i>eat-2</i> ) worms _____	119
Table 13: Lifespan assays performed with SERCA inhibitors in MQ1333 ( <i>nuo-6</i> ) worms _____	122
Table 14: Lifespan assays performed with SERCA inhibitors in CB1370 ( <i>daf-2</i> ) worms _____	123
Table 15: Lifespan assays performed with SERCA inhibitors in RB157 ( <i>aak-2</i> ) and AGD397 ( <i>aak-1;aak-2</i> ) worms _____	124
Table 16: Lifespan assays performed with SERCA inhibitors in DR412 ( <i>daf-15</i> ) and RB1206 ( <i>rsk-1</i> ) worms _____	126
Table 17: Lifespan assays performed with SERCA inhibitors in VC199 ( <i>sir-2.1</i> ) worms _____	128
Table 18: Lifespan assays performed with SERCA inhibitors in CF1038 ( <i>daf-16</i> ) worms _____	130
Table 19: Lifespan assays performed with CGP37157 in AQ2038 wild type worms _____	135
Table 20: Lifespan assays performed with CGP37157 in DA1113 ( <i>eat-2</i> ) worms _____	137
Table 21: Lifespan assays performed with CGP37157 in MQ1333 ( <i>nuo-6</i> ) worms _____	138
Table 22: Lifespan assays performed with CGP37157 in CB1370 ( <i>daf-2</i> ), CF1038 ( <i>daf-16</i> ), RB754 ( <i>aak-2</i> ), AGD397 ( <i>akk-1;aak-2</i> ), VC199 ( <i>sir-2.1</i> ), and CF1038 ( <i>daf-16</i> ) mutant worms _____	140
Table 23: Lifespan assays performed with CGP37157 in DR142 ( <i>daf-15</i> ) and RB1206 ( <i>rsk-1</i> ) mutant worms _____	142
Table 24: HPLC-MS determination of CGP37157 in a known size sample of worms _____	143





**ABBREVIATIONS**



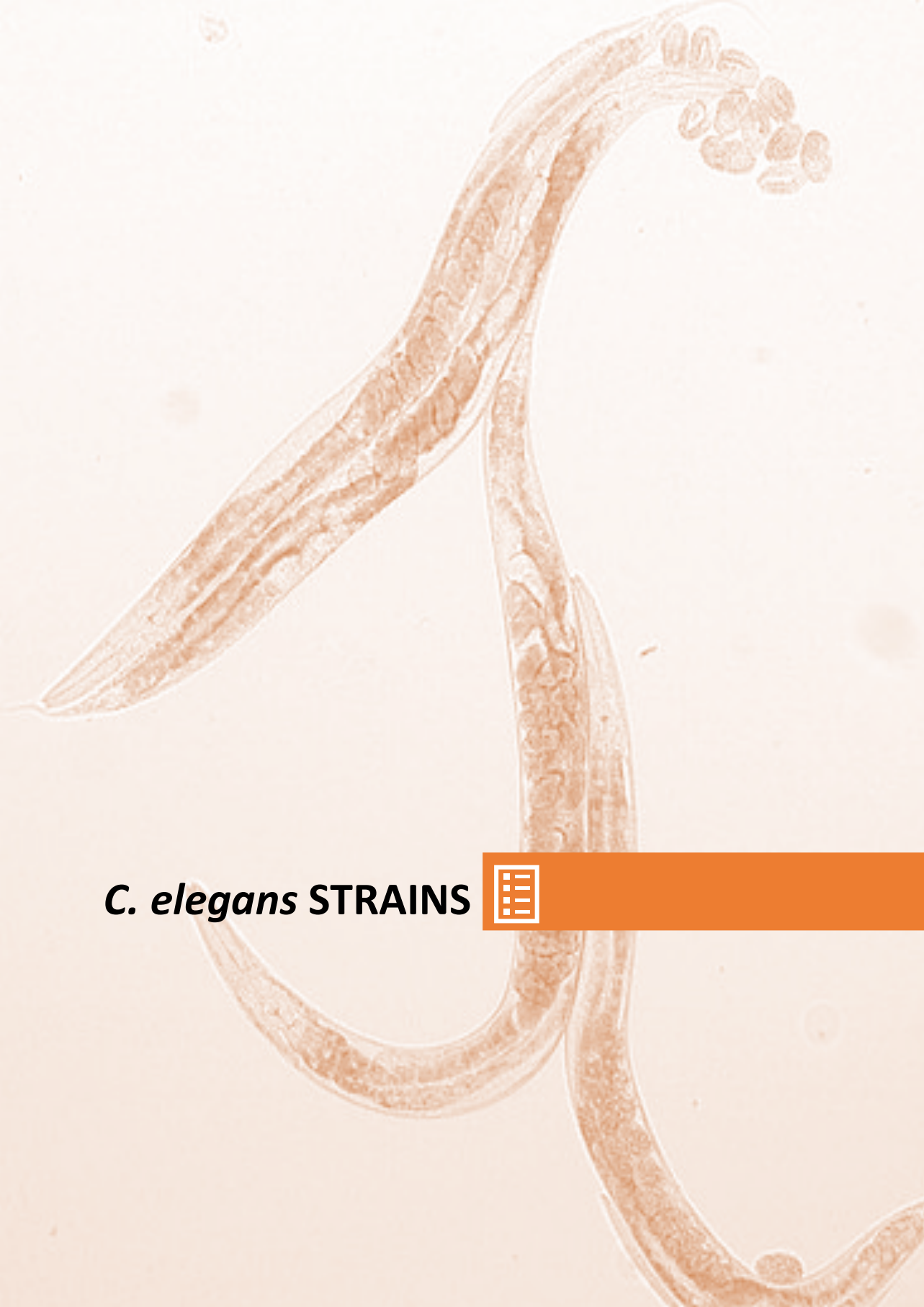




- **γ-CD:** gamma-cyclodextrin
- **[Ca<sup>2+</sup>]<sub>cyt</sub>:** cytosolic Ca<sup>2+</sup> concentration
- **[Ca<sup>2+</sup>]<sub>ER</sub>:** endoplasmic reticulum Ca<sup>2+</sup> concentration
- **2,5-BHQ:** 2,5-di-tert-butylhydroquinone
- **2,6-BHQ:** 2,6-di-tert-butylhydroquinone
- **ACh:** acetylcholine
- **AMPK:** adenosine monophosphate-activated protein kinase
- **ATF-4:** activating transcription factor-4
- **ATF-6:** activating transcription factor-6
- **ATG:** autophagy related proteins
- **BLPS:** body lengths per second
- **CaMKKβ:** Ca<sup>2+</sup>/calmodulin-dependent protein kinase kinase β
- **CGP37157:** 7-chloro-5-(2-chlorophenyl)-1,5-dihydro-4,1-benzothiazepin-2(3H)-one
- **CR:** caloric restriction
- **DIC:** differential interference contrast optics
- **DR:** dietary restriction
- **EAT-2:** *C. elegans* nicotinic acetylcholine receptor
- **EPG:** electropharyngeogram
- **EPSP:** excitatory post-synaptic potential
- **ER:** endoplasmic reticulum
- **ETC:** electron transport chain
- **FRET:** fluorescence resonance-energy transfer
- **FuDR:** 5-fluoro-2'-deoxyuridine
- **GFP:** green fluorescent protein
- **HS:** heat Shock
- **HSF:** heat shock transcriptional factors
- **HSPs:** heat shock proteins
- **HVA:** high voltage activated current
- **I1-I5:** pharyngeal interneurons
- **IGF-1:** insulin-like growth factor 1
- **IIS:** insulin/Insulin-like growth factor signaling pathway
- **ILPs:** insulin-like peptide ligands
- **IPSPs:** small notch hyperpolarizations
- **IRE-1:** inositol-requiring-kinase-1



- **LKB1**: serine/threonine kinase 11
- **M1-M5**: pharyngeal motoneurons
- **MAMs**: Mitochondria-ER Associated Membranes
- **mc**: pharyngeal marginal cells
- **MCs**: pharyngeal MC neurons
- **mTOR**: mechanistic target of rapamycin
- **NMJ**: neuromuscular junction
- **NSMs**: neurosecretory-motor neurons
- **O/N**: overnight
- **OP50**: *E. coli* bacterial strain
- **PAS**: Phagophore assembly site
- **PERK**: protein kinase RNA-like endoplasmic reticulum kinase
- **pm1-pm8**: pharyngeal muscular segments
- **RNAi**: RNA of interference
- **ROS**: Radical oxygen species
- **SIRT**s: sirtuins: silent information regulator proteins.
- **TAK1**: transforming growth factor- $\beta$ -activated kinase 1
- **Tg**: thapsigargin
- **UPS**: Ubiquitin/Proteasome system
- **VDCC**: voltage dependent  $\text{Ca}^{2+}$  channels
- **WHO**: World Health Organization
- **XBP-1**: X-box binding protein 1



***C. elegans* STRAINS**



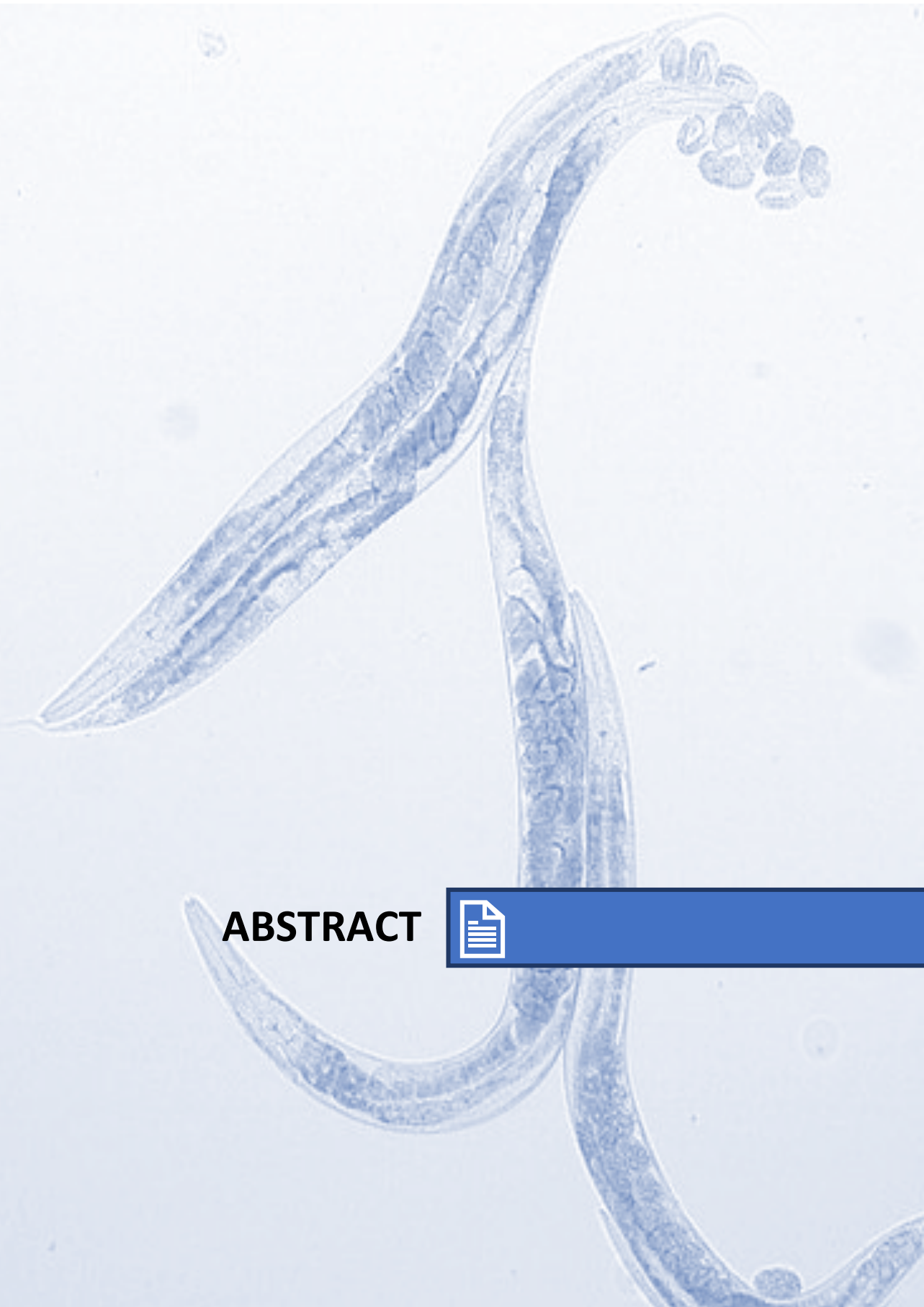




<i>C. elegans</i> control strains					
STRAIN	GENOTYPE	PROBE	GROUP	METHOD	ORTHOLOG
N2	Wild type	-	-	Transcriptomics RT-PCR	-
AQ2038	<i>pmyo2::YC2.1</i>	Cameleon YC2.1	Cytosolic Ca <sup>2+</sup> probe	Lifespan Ca <sup>2+</sup> dynamics	-
AQ2121	<i>pmyo3::YC2.1</i>	Cameleon YC2.1	Cytosolic Ca <sup>2+</sup> probe	Ca <sup>2+</sup> dynamics Motility assay	-
AQ3055	<i>pmyo-2::2mt8::YC3.60</i>	Cameleon YC3.6	Mitochondrial Ca <sup>2+</sup> probe	Ca <sup>2+</sup> dynamics	-
SJ4103	<i>zcls14[myo3::GFP(mit)]</i>	GFP	Mitochondrial GFP	Confocal imaging	-
SJ4005	<i>zcls4[hsp-4::GFP]</i>	GFP	ER stress	Stress induction	BiP
TJ375	<i>gpls1hsp-16.2p::GFP]</i>	GFP	Cytosolic stress	Stress induction	CRYAA CRYAB HSPB1

<i>C. elegans</i> mutant strains						
STRAIN	GENOTYPE	MUTATED GENE	ORTHOLOG	GROUP	PATHWAY	PHENOTYPE
CB1370	<i>daf-2 (e1370) III</i>	<i>daf-2</i>	IGF1R INSR	NSP	IGF-1	- Temperature sensitive - Long-lived
CF1038	<i>daf-16 (mu86) I</i>	<i>daf-16</i>	FoXO1,3,4	NSP	IGF-1	- Dauer defective - Short-lived
DR412	<i>daf-15(m81)/unc-24(e138) IV</i>	<i>daf-15</i>	RAPTOR	NSP	mTOR	- Long-lived
RB1206	<i>rsks-1(ok125)</i>	<i>rsks-1</i>	S6K	NSP	mTOR	- Long-lived
RB754	<i>aak-2(ok524) X</i>	<i>aak-2</i>	PRKAA2	NSP	AMPK	- Short-lived
AGD397	<i>aak-1(tm1944) II/aak-2(ok524) X</i>	<i>aak</i>	PRKAA1 PRKAA2	NSP	AMPK	- Short-lived
VC199	<i>sir-2.1(ok434) IV</i>	<i>sir-2.1</i>	SIRT1	NSP	Sirtuins	- Superficially WT
MQ1333	<i>nuo-6(qm200)</i>	<i>nuo-6</i>	NUDFB4	MITO	-	- Low oxygen consumption -Slow development - Long-lived
DA1113	<i>eat-2(ad1113) II</i>	<i>eat-2</i>	CHRFAM7	CR	-	- Decreased food intake -Reduced pharyngeal pumping - Long-lived





**ABSTRACT**





$\text{Ca}^{2+}$  is a second messenger that affects nearly every aspect of cellular life including muscle contraction, neuronal secretion and cell proliferation and differentiation. The dysregulation of the cellular toolkit that controls and maintains  $\text{Ca}^{2+}$  homeostasis has been linked to the physiopathology of the aging process including neurodegeneration. *Caenorhabditis elegans* has been proven to be an excellent model organism to study aging and neurodegeneration due to the conservation of numerous signaling pathways that have been proven to modulate aging, and the availability of several models of neurodegenerative diseases. Moreover, the interrelationship between aging and  $\text{Ca}^{2+}$  signaling can be studied in the worms because of their transparent cuticle that allows to perform *in vivo*  $\text{Ca}^{2+}$  dynamics studies throughout the whole life of the organisms.

The metabolic pathways that are known to regulate aging in *C. elegans* are the so called nutrient sensing pathways. All these pathways, that are conserved in mammals, are able to respond to changes in nutrient availability that, in the end, affect the longevity of the worms. These pathways are the insulin/insulin-like-growth factor (IGF-1) signaling pathway (IIS), the mechanistic target of rapamycin (mTOR) signaling pathway, the adenosine monophosphate-activated protein kinase (AMPK) pathway, and the sirtuins pathway. Although not much information about how intracellular  $\text{Ca}^{2+}$  regulates these pathways, there is some evidence that suggests that  $\text{Ca}^{2+}$  might be implicated in the modulation of nutrient sensing pathways activities.

This thesis has focused in the study of the interrelationship between  $\text{Ca}^{2+}$  signaling and nutrient sensing pathways, and its possible effects in the aging process through two different pharmacological approaches: the submaximal inhibition of sarco-endoplasmic reticulum calcium-ATPase (SERCA) using 2,5-BHQ and thapsigargin, and the submaximal inhibition of the mitochondrial  $\text{Na}^+/\text{Ca}^{2+}$  exchanger using CGP37157.

SERCA refills the endoplasmic reticulum (ER) with  $\text{Ca}^{2+}$  up to the millimolar range being the main controller of the ER [ $\text{Ca}^{2+}$ ] level, implicated in the modulation of cytosolic  $\text{Ca}^{2+}$  signaling and ER-mitochondria  $\text{Ca}^{2+}$  transfer. In this work it has been proven that the submaximal inhibition of SERCA with 2,5-BHQ and thapsigargin induced an increase in the lifespan of *C. elegans* worms and that this effect was mediated by the modulation of mTOR and AMPK signaling pathways. Moreover, it was also discarded that the effect was mediated by the activation of the ER stress response.

CGP37157 is a benzothiazepine with neuroprotective effects in several *in vitro* models of excitotoxicity involving dysregulation of intracellular  $\text{Ca}^{2+}$  homeostasis. CGP37157 has been used for decades as an inhibitor of the mitochondrial  $\text{Na}^+/\text{Ca}^{2+}$



exchanger (mNCX), although several off targets have been described. Throughout this thesis, the effects of CGP37157 in *C. elegans* healthspan, as well as its possible modulation of nutrient sensing pathways and  $\text{Ca}^{2+}$  dynamics, have been explored. Our results show that the treatment with CGP37157 is able to induce an increase in *C. elegans* life expectancy through the modulation of the mTOR and IIS signaling pathways. Moreover, it was proven that a functional electron transport chain activity was required for CGP37157 to exert its effects, and that CGP37157 treatment induced changes in intracellular  $\text{Ca}^{2+}$ , including cytosolic and mitochondrial  $\text{Ca}^{2+}$  dynamics changes in two different muscular systems, the pharynx and the vulva. Finally, the changes induced by CGP37157 also caused an improvement in worm's locomotion and muscle function delaying the sarcopenia process and improving mitochondrial integrity and organization in *C. elegans* body wall muscle cells.

In conclusion, this work has described two novel pharmacological interventions that improve *C. elegans* lifespan through the modulation of  $\text{Ca}^{2+}$  signaling in a different manner. These results outline the possible therapeutic effects of both SERCA inhibitors and CGP37157 in the aging process, and the importance of  $\text{Ca}^{2+}$  signaling in the regulation and evolution of aging related physiopathology.



# INTRODUCTION







## I. CAENORHABDITIS ELEGANS BIOLOGY

### I.1 *C. elegans* as a model organism

*Caenorhabditis elegans* is a free-living, non-parasitic nematode that was first introduced as a model organism by Sidney Brenner in 1963 as a new genetic tool to study development and neurodegeneration (Brenner, 1974). It is a small (1 mm length), transparent roundworm, with a short life cycle of around three days, and an overall lifespan of about two to three weeks. Despite its small size, *C. elegans* has many of the organ systems present in more complex organisms and exhibits complex behaviors. Moreover, the small size, its transparent nature and its invariant cell lineage characteristics led to an unprecedented view of development in this animal (Sulston et al., 1983; Sulston and Horvitz, 1977), and allowed to determine the entire wiring diagram of *C. elegans* nervous system (Varshney et al., 2011).

*C. elegans* has two sexual forms: self-fertilizing hermaphrodites and males (figure 1). Essentially, hermaphrodites are females whose gonads temporarily produce sperm before they produce oocytes. Hermaphrodites can produce around 300 eggs. When fertilized by males, they can produce up to 1.000 offspring individuals. The sexes differ in that hermaphrodites have two X chromosomes (XX) and males have a single X chromosome (XO). Only 0.1-0.2 % of the progeny of self-fertilized hermaphrodites are males. This sexual dimorphism characteristic provides several advantages including the maintenance of stocks in the laboratory, the tendency of the population to homozygosity, and the possibility to maintain paralyzed mutant populations.

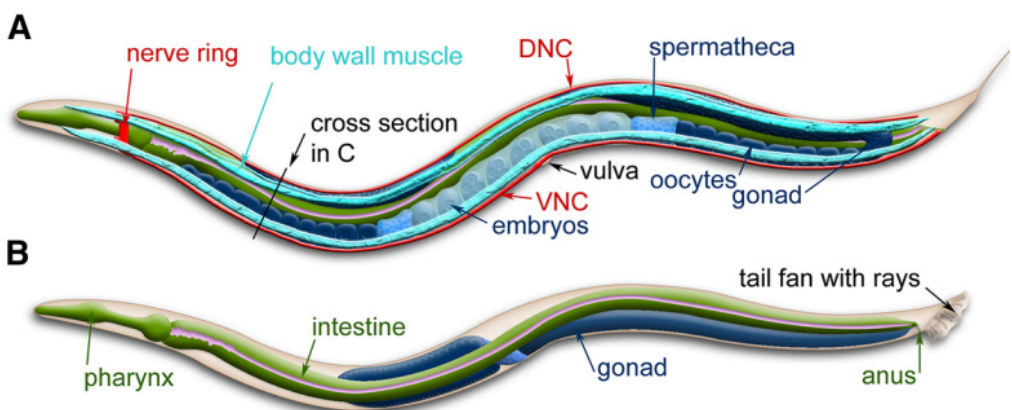


**Figure 1: Anatomical differences between *C. elegans* hermaphrodite and male. a) hermaphrodite reproductive system anatomy. b) male reproductive system anatomy. Modified from ©Wormatlas.**

There are several reasons that make *C. elegans* a really easy maintenance organism in the laboratory. In the wild, *C. elegans* eats a set of bacteria present in its environment (Samuel et al., 2016). In the laboratory, animals are normally grown on agar plates containing a lawn of *Escherichia coli* OP50 (Brenner, 1974), a nonpathogenic bacteria that serve as a food source for the population. Also, using a dissecting microscope, a certain number of worms can be moved from plate to plate using a “pick”, thus facilitating the isolation of individuals. Because of their small size and high hermaphrodites’ reproductive rate, hundreds or thousands of worms can be grown in an individual petri dish. Finally, different stocks can be stored frozen at -80°C or in liquid nitrogen for long periods of time (Apfeld and Alper, 2018).

Because *C. elegans* is transparent, whole independent cells and subcellular protein localizations are easily studied using differential interference contrast (DIC) optics. Even more detailed information can be obtained using fluorescent probes to tag proteins or subcellular compartments. Fluorescent proteins can also be used to study developmental processes, screen for mutants affecting cell development and function, isolate cells, and characterize protein interactions *in vivo* (Corsi et al., 2015).

The completion of its genome sequence was finished in 1998 (Consortium, 1998). All this effort lead to three notable discoveries that earned *C. elegans* researchers Noble Prizes including the award to Sidney Brenner, Robert Horvitz , and John Sulston in 2002 for their discoveries in the field of development and cell death (Ellis and Horvitz, 1986; Check, 2002; Marx, 2002); Andrew Fire and Craig Mello in 2006 for their discovery of RNA of interference (RNAi) (Fire et al., 1998); and Osamu Shimomura, Martin Chalfie and Roger Tsien in 2008 for the discovery of Green Fluorescent Protein (GFP), and the demonstration that it could be a useful tool in different organisms including *C. elegans* (Chalfie et al., 1994). Other important discoveries in *C. elegans* include the identification of microRNAs (Lee et al., 1993).

Around 30-60% of genes in *C. elegans* have orthologs or strong homologs in humans (Shaye and Greenwald, 2011; Kim et al., 2018). This fact, together with the forward (random mutations induced by mutagens) and reverse genetic tools available for *C. elegans* (RNAi, targeted transposon insertion, and CRISPR/Cas9 genome editing) (Kutscher and Shaham, 2014), have made *C. elegans* a premier model for several purposes, as the increased knowledge about gene function in *C. elegans* may be directly applied to human development and disease.

All the characteristics exposed above, make *C. elegans* a suitable model to perform drug discovery and screening. One of the biggest advantages of using the

worms as a drug discovery and screening model is the relatively easy and advantageous possibility to use genetic and physiological tractable markers to understand the effects of small molecules in a whole *in vivo* organism. Moreover, *C. elegans* is an important model used to understand the molecular mechanisms of aging and to identify pro-longevity compounds. Specifically, the study of a wide variety of mutant strains suggested that some drugs that induced an increase in the worms life expectancy were disrupting neurotransmission associated with food sensing and causing a perceived state of reduced nutrient intake, which completely agreed with the well-known fact that caloric restriction, and molecules that mimic it, extend *C. elegans* and other species lifespan. Last but not least, in the last decade the use of transgenic and mutant *C. elegans* strains to study neurodegenerative diseases has increased. Nowadays, mutant strains for Alzheimer's, Parkinson's and Huntington diseases are available and used for the discovery of potential therapeutics to treat these disorders (Strange, 2016).

The advance of the genetic and physiological techniques has made essential to establish a *C. elegans* nomenclature (table 1) that clarifies both the genotype, and phenotype of the different *C. elegans* strains available.

Nomenclature	Definition
<b>ZK154.3</b>	Systematic gene identification (3 <sup>rd</sup> ORF on cosmid ZK154)
<b><i>mec-7</i></b>	Gene name (the 7 <sup>th</sup> “mechanosensory abnormality” gene named)
<b><i>mec-7(e1506)</i></b>	Allele name (from the MRC Laboratory of Molecular Biology -e)
<b>MEC-7</b>	Protein name (product of <i>mec-7</i> gene)
<b>Mec</b>	Phenotype (Mechanosensory abnormal phenotype)
<b><i>e1506</i></b>	Homozygous allele
<b><i>e1506/+</i></b>	Heterozygous allele
<b><i>mnDp30</i></b>	Duplication (from the Herman Lab - <i>mn</i> )
<b><i>nDf6</i></b>	Deficiency/Deletion (from the Horvitz Lab - <i>n</i> )
<b><i>mulS35</i></b>	Integrated transgene (from the Kenyon Lab - <i>mu</i> )
<b><i>evEx1</i></b>	Extrachromosomal transgene array (from the Culotti Lab - <i>ev</i> )
<b>CB3270</b>	Strain name (from MRC Laboratory of Molecular Biology -CB)
<b><i>mec-7p::gfp</i></b>	GFP transcriptional fusion (using only the promoter of the gene)
<b><i>mec-7::gfp</i></b>	GFP translational fusion ( <i>gfp</i> is inserted in the coding sequence of the gene)
<b><i>ceh(pk33::Tc1)</i></b>	Transposon Tc1 insertion in <i>ceh-6</i> gene

**Table 1: *C. elegans* nomenclature.** Genetic nomenclature differs from species to species. The most common terms used in *C. elegans* research are gene names, allele designations, reporter genes, cosmids, proteins, phenotypes and strain names. Modified from Corsi et al., 2015.

## I.2 *C. elegans* life cycle

*C. elegans* life cycle is comprised of the embryonic stage, the larval stages and adulthood (figure 2). The end of each larval stage is marked with a molt, when a stage-specific cuticle is synthesized and the old one is shed. The embryonic stage is primarily divided in two stages, proliferation and organogenesis/morphogenesis, and happens before the hatching of the egg. Once the worm is out of the egg, its development is triggered by feeding and characterized by four larval stages until reaching the adult form. Out of 1090 somatic cells generated during an hermaphrodite development, during the four larval stages (L1-L4), 131 will undergo programmed cell death at characteristic times (Driscoll, 1995). The 959 remaining cells will form the organs of the worms. Interestingly, almost a third part of the cells, 302 are neurons, and 95 are body wall muscle cells (Altun and Hall, 2009e).

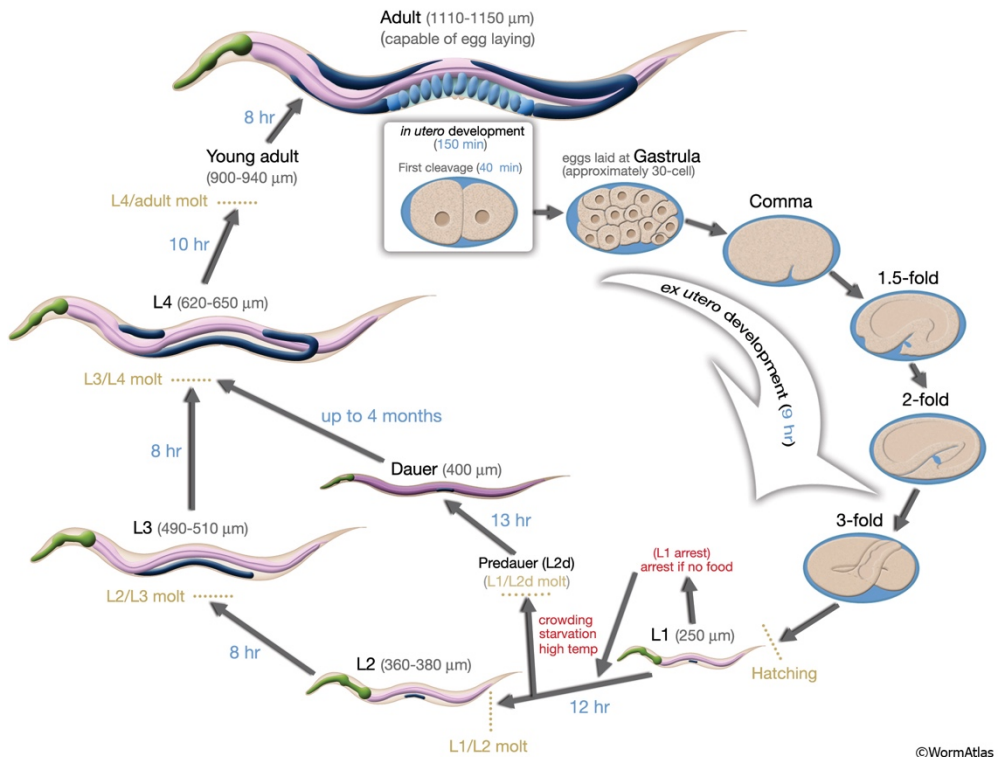


**Figure 2: *C. elegans* life cycle.** *C. elegans* life cycle is formed by three different periods. The embryonic stage, in which larva is developed inside the egg; The larval stages, L1-L4. During this four stages the worms develop and organs are formed. Finally, the individuals reach their invariable adult form being able to lay eggs. If environmental conditions are challenging, at the beginning of L2 stage, development shifts to a resistance stage called dauer. ©WormAtlas.

In the interphase between L1 and L2 larval stages the development process can be deviated to a resistance state called “dauer”. This shift to an arrested state is triggered by challenging environmental conditions. Among the environmental conditions that cause dauer formation are the absence of food, an increase in temperature, or an increase in the presence of pheromones that acts as an indicator of the density of the population. The dauer larva is defined as a non-aging state because the arrested individuals can stay in this larval stage until the environmental conditions are favorable without affecting their lifespan. Specifically, after one hour of food availability the animals exit the dauer stage and in about ten hours they molt to the L4 larval stage (Wolkow and Hall, 2015).

Approximately twelve hours after the L4 molt, hermaphrodites begin to produce eggs for a period of two to three days until they have utilized all of their self-produced sperm; after their fertile period, worms live for several more days until dying of senescence (Corsi et al., 2015).

### I.3 *C. elegans* adult hermaphrodite anatomy

Despite being a simple organism, *C. elegans* has a high degree of differentiation providing an excellent experimental system to study differentiation, cell biology and physiology. This fact is even more relevant when is taken into account that numerous physiological functions of mammals are present or have an analog in *C. elegans* (Strange, 2016).

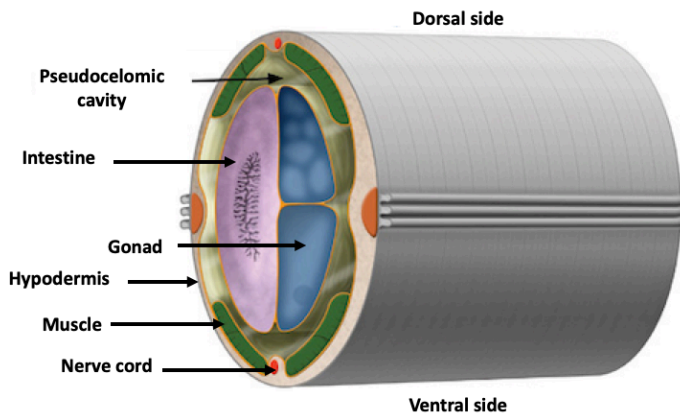


**Figure 3: *C. elegans* anatomical structure.** *C. elegans* is formed by two concentric tubes. The hypodermis, the nervous system, the excretory system and the muscles form the outer one. The intestine and the pharynx form the inner one. Both tubes are separated by the pseudocoelomic cavity. Modified from ©WormAtlas.

Nematodes, including *C. elegans* are organized in a basic anatomical structure based on unsegmented cylindrical bodies tapered at both ends. Their body is formed by an outer and an inner tube separated by an aqueous cavity called pseudocoelomic space. The outer tube, also called body wall, is integrated by different tissues including the cuticle, the hypodermis, the excretory system, the nervous system, and the locomotory system. The rest of the different organs, pharynx, intestine and gonads are found in the inner tube (figure 3). The pseudocoelomic space is osmoregulated and responsible of maintaining body shape by controlling the hydrostatic pressure (Riddle et al., 1997a).

### 1.3.1 Cuticle

The cuticle forms the outer surface of the worm. It is a tough and flexible extracellular covering that protects the worms from the environment and allows and helps movement acting as an external skeleton. It also contributes to maintain body shape (Lints and Hall, 2009b).

The cuticle consists of five layers and is approximately 0.5  $\mu\text{m}$  thick (Cox et al., 1981a; Cox et al., 1981b). It is composed of crossed-linked collagens, insoluble proteins named cuticlins, and associated glycoproteins and lipids (figure 4) (Xu et al., 2012). With aging, the thickness of the adult cuticle increases due to the expansion of the basal zone (Herndon et al., 2002).

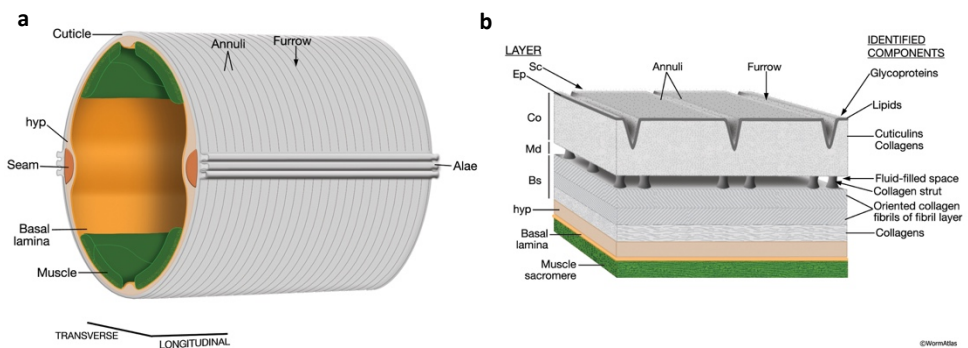


**Figure 4: *C. elegans* structure and composition of the adult cuticle. a)** the cuticle is the outer layer of the worms and its placed covering the hypodermis (hyp), the seam cells, and the body wall muscles (green). **b)** The cuticle is formed by five layers with different components. ©WormAtlas.

### I.3.2 Epithelial system

The epithelial system or epidermis of *C. elegans* is divided in two main types of cells: the hypodermis and specialized epithelial cells. The **hypodermis** is formed by a series of concentric rings of five small syncytial cells in the head and three mononucleate and one syncytial cell in the tail. The **specialized epithelial cells** are the seam cells, the interfacial epithelial cells, and the atypical epithelial cells (Altun and Hall, 2009c). All the epithelial cells are strongly connected to each other by junction wraps. This type of communication provides a seal and a mechanical link to adjacent cells and polarizes the cell membranes into an apical and basolateral side (Michaux et al., 2001). The apical side secretes the cuticle, and the basolateral side is in contact with the internal basal surface (Chisholm and Hsiao, 2012)

The epidermis plays several roles in the life of *C. elegans*. The main function, as all skin layers, is to act as a barrier epithelium. In the case of *C. elegans*, epidermis exhibits more functions including wound repairing, ionic homeostasis, metabolic storage, phagocytosis of cellular debris, innate immune responses to external pathogens, and the mediation of the communication between sensory neurons and the external environment (Chisholm and Xu, 2012).

### I.3.3 Nervous system

The nervous system is the most complex organ in *C. elegans*. It is formed by 302 neurons (divided in 118 different classes) and 56 glial cells. The neuronal network can be divided in two different and independent nervous systems: the somatic one, integrated by 282 neurons, and the pharyngeal one, formed by 20 neurons. Cell bodies of most neurons are clustered in ganglia in the head or tail (figure 5) (Sulston and Horvitz, 1977; Hobson et al., 2017).

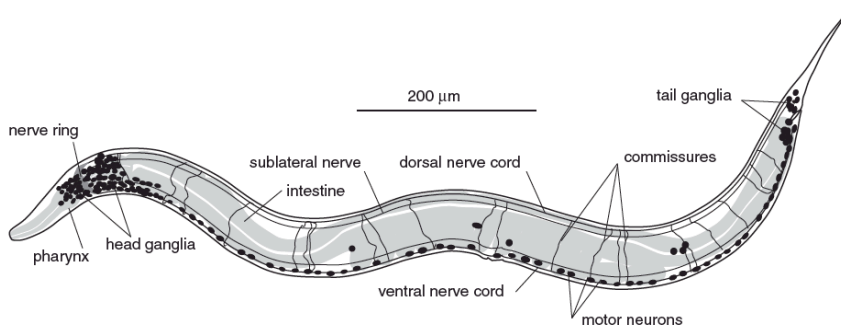


**Figure 5: *C. elegans* adult nervous system structure.** The nervous system of *C. elegans* is constituted by 302 neurons. Most of their cell bodies can be found in the head or tail ganglia, and distributed through all the ventral cord (Hobson, Yook and Jorgensen 2017).



Although *C. elegans* presents a simple and compact nervous system, it exhibits complex behaviors in addition to the basic ones such as locomotion, feeding, and defecation. For example, it can sense different environmental factors including chemicals, odorants, temperature, and food sources, moving towards or away from them. It can also exhibit social behaviors reacting to pheromones or changes in oxygen levels (Golden and Riddle, 1982; Cheung et al., 2004; Gray et al., 2004; Barr and Garcia, 2006). Finally, it is remarkable that all these complex behaviors are plastic, meaning that nematodes responses can be modified by learning and memory (Giles et al., 2006).

One of the most striking features of *C. elegans* nervous system is the fact that it does not generate sodium-based action potentials (Goodman et al., 1998). However, it uses  $\text{Ca}^{2+}$  signaling as a way to propagate electrical signals through the nervous system (Hobert, 2013), as it was demonstrated when action potentials driven by calcium were described in the body wall muscle (Gao and Zhen, 2011).

Finally, *C. elegans* nervous system uses a plethora of classical neurotransmitters including acetylcholine, GABA, dopamine, serotonin, and glutamate. This variety of neurotransmitters approximates *C. elegans* nervous system complexity to vertebrates (Riddle et al., 1997b).

### 1.3.4 Muscular system

Musculature in *C. elegans* can be divided in two different systems: the somatic muscle system, formed by the striated body wall muscle; and the nonstriated muscle system, that is part of the pharynx, intestine, anus, and the hermaphrodite uterus, gonad sheath, and vulva.

The **somatic muscle system**, the most numerous muscle group in the worms, is integrated by multiple sarcomere muscle cells arranged in longitudinal bands along the body wall responsible for locomotion. These muscles present evenly distributed attachment points to the hypodermis and cuticle and are separated from the hypodermis and nervous tissue by a thin basal lamina (figure 6) (Strange, 2006; Altun and Hall, 2009g; Moerman and Williams, 2006). The body wall muscle is obliquely striated allowing to create an evenly distributed muscle force resulting in a smooth bending of the worm (Burr and Gans, 1998).

The **nonstriated muscle system** is formed by muscle cells with one or a few well-structured sarcomeres or myofilaments that are less organized than the striated muscles (Altun and Hall, 2009f). These muscles are responsible for



pharyngeal pumping, defecation, ovulation and fertilization, and egg-laying (Strange, 2006).

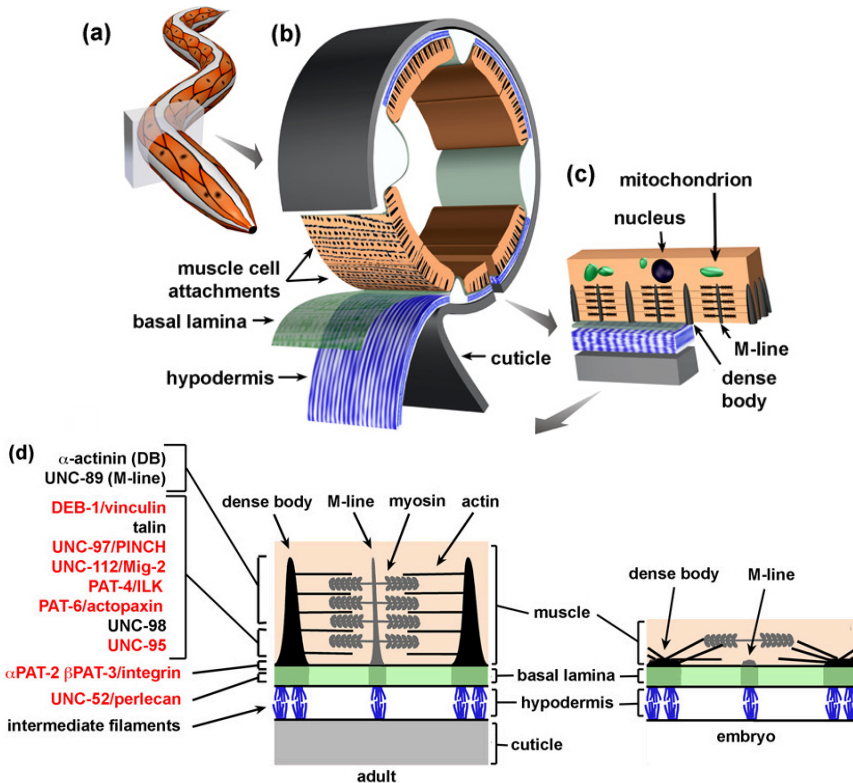


**Figure 6: *C. elegans* body wall muscle structure.** **a, b)** adult worm's body wall muscle. The cross section shows the disposition of the cuticle, hypodermis, basal membrane and two body wall muscle cells. **c)** The longitudinal section of a body wall muscle cell show that dense bodies attach to actin filaments, while M-lines attach to myosin filaments. **d)** Location of some attachment proteins. Modified from (Moerman and Williams 2006).

### 1.3.5 Excretory system

*C. elegans* excretory system is a very simple tubular organ that is integrated by three unicellular tubes (canal or excretory cell, duct, and pore) and a fused pair of gland cells connected in tandem to form a continuous lumen (figure 7) (Nelson et al., 1983). This system seems to have at least two different functions: osmoregulation and secretion (Sundaram and Buechner, 2016). The excretory cell is a single-cell that appears to secrete salt, water, and waste products into the excretory canal (Strange, 2006). This system, presumably then, empties the collected material outside via the excretory duct and pore (Altun and Hall, 2009d).

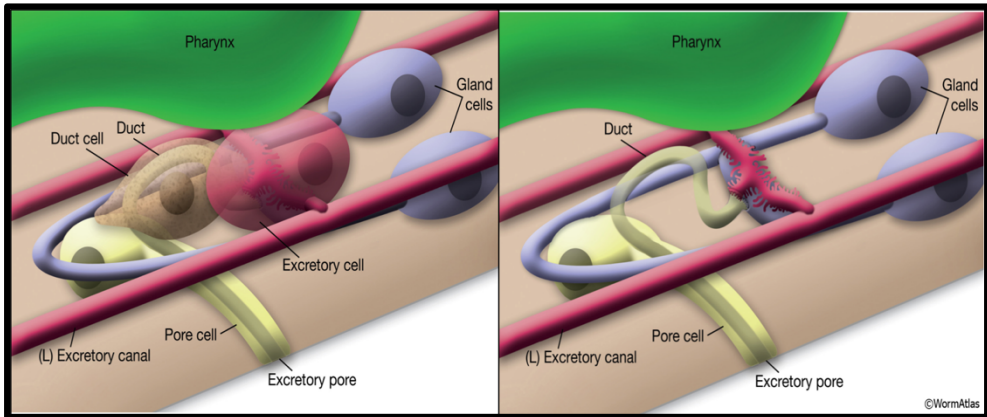


**Figure 7: *C. elegans* excretory system structure.** This system consists of the excretory cell (red), the duct cell (brown), the pore cell (yellow), and the gland cells (blue). The excretory, duct, and pore cells are joined at an intercellular junction called the secretory-excretory junction, where glandular secretions and excreted material are conducted to the duct to be transported outside the body. Modified from (Altun and Hall 2009g). ©WormAtlas

### 1.3.6 Reproductive system

Due to the sexual dimorphism of *C. elegans*, the reproductive system is the most differing organ between hermaphrodites and males. The reproductive system of the hermaphrodites is integrated by three different parts: the somatic gonad, the germ line, and the egg-laying apparatus (figure 8a). These three components of the reproductive system allow the production of gametes, the fertilization, and the egg-laying.

The **somatic gonad** is formed by the non-germline components of the two gonad arms. It consists of five different tissues with critical roles in development, organization, and function of the germline in the adult.

The **germline** of the hermaphrodite is composed by male and female gametes, oocytes and sperm respectively. During the L4 stage, germ cells differentiate into approximately 150 spermatids per gonad arm. These spermatids develop into mature sperm that is stored in the spermatheca. In adult worms, germ cells differentiate into oocytes (Strange, 2006; Lints and Hall, 2009a).

The **egg-laying apparatus** is formed by the uterus, the uterine muscles, the vulva, the vulval muscles, and a local neuropil formed by the egg-laying neurons (figure 8b). The vulval and uterine nonstriated muscles conform the sex muscles. Only four of the sixteen muscles receive inputs from the egg-laying neurons. The remaining ones are electrically coupled to the innervated muscles. It is believed

that this disposition allows the coordinated contraction of the uterus and the vulva (Altun and Hall, 2009f).

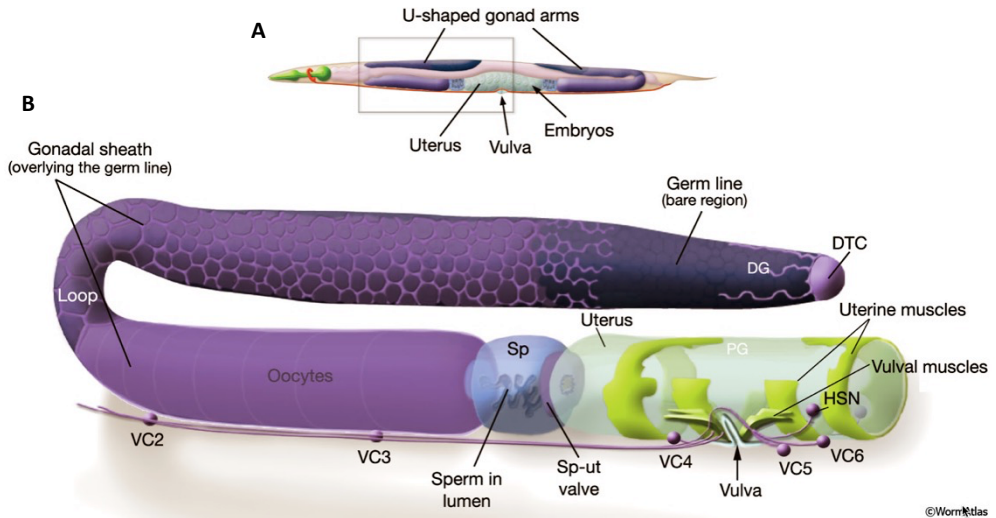


**Figure 8: *C. elegans* reproductive system structure.** **a)** The reproductive system consists of two U-shaped gonad arms joined to a common uterus. The reproductive system opens to the environment via the vulva, located in the ventral midbody. **b)** One half of the reproductive system, enlarged and separated from other body parts. (DTC) Distal tip cell; (DG) distal gonad; (PG) proximal gonad; (Sp) spermatheca; (Sp-ut) spermathecal-uterine valve; VC1-6 and HSNL/R are motor neurons that control egg-laying. Modified from (Lints and Hall, 2009a) ©WormAtlas

### 1.3.7 Digestive system

The digestive tract of *C. elegans* consists of a pharynx, intestine, rectum and anus (figure 9). These organisms consume liquid media with OP50 in suspension being considered filter feeders. The **pharynx** is a muscular organ that pumps food into the pharyngeal lumen, grinds it up, and then moves it into the intestine. The entrance of the grinded food into the intestine is done by the pharyngeal-intestinal valve.

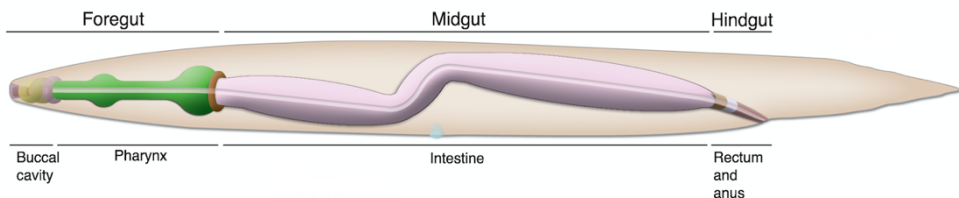


**Figure 9: *C. elegans* digestive system.** The alimentary system of *C. elegans* is divided in three parts: the foregut (buccal cavity and pharynx), the midgut (intestine) and the hindgut (rectum and anus). Modified from Altun and Hall 2009a. ©WormAtlas

The **intestine** is one of the major organs in *C. elegans* and is largely responsible for food digestion and assimilation, and the synthesis and storage of macromolecules. This organ is formed by twenty epithelial cells with profuse apical microvilli that secrete digestive enzymes and absorb nutrients. Interestingly, intestine is emerging as an experimental system to study numerous biological processes including vesicular trafficking, biochemical blocks, stress responses, and aging.

The **rectum** is formed by five epithelial cells and connected to the intestine by the intestinal-rectal valve that opens through the action of the sphincter muscle. This muscle together with the anal depressor muscle and two more muscle cells control defecation (McGhee, 2007; Strange, 2006; Altun and Hall, 2009a).

## 1.4 *C. elegans* pharynx

The pharynx is the feeding organ of *C. elegans*. It is an encapsulated, bilobed organ with a simple anatomy: twenty neurons, and eight gap-junction connected muscles. Therefore, the pharynx is a neuromuscular pump that has similarities to the vertebrate and invertebrate heart. As properly defined hearts, the pharynx pumps throughout the life of the worm, but its action potentials are driven by the activity of L and T-Type  $\text{Ca}^{2+}$  channels (Mango, 2007). It can also respond to neurotransmitters and neuromodulators (Trojanowski et al., 2016; Mango, 2007).

### 1.4.1 Pharynx anatomy

The pharynx is a linear tube covered by a basement membrane. It is formed by six subdivisions: the buccal cavity, the procorpus, the metacarpus, the isthmus, the terminal bulb and the pharyngeal-intestinal valve (figure 10). It contains nine epithelial cells, twenty muscle cells, nine marginal cells, four gland cells, and twenty neurons. It is about 100  $\mu\text{m}$  long and has a diameter of 20  $\mu\text{m}$  in its wider region, the terminal bulb (Altun and Hall, 2009b).

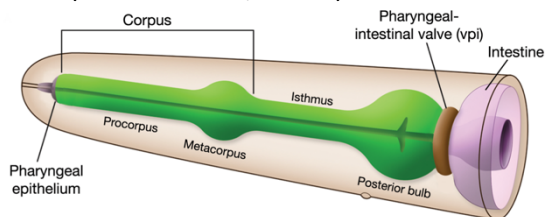


**Figure 10: *C. elegans* pharynx anatomy.** The pharynx is divided in six different parts: the buccal cavity, the corpus (procorpus and metacarpus), the isthmus, and the terminal bulb or grinder.  
©WormAtlas

The **muscle cells** of the pharynx are grouped into eight circular segments (pm1-pm8). Most of the pharyngeal rings are composed by three syncytial cells organized in a radial orientation that allows the lumen to close and open during the contraction/relaxation cycles. The three muscle cells of each segment are separated from the other segments by three marginal cells, although gap-junctions between contiguous segment muscle cells allow the electrical and chemical communication (figure 11).

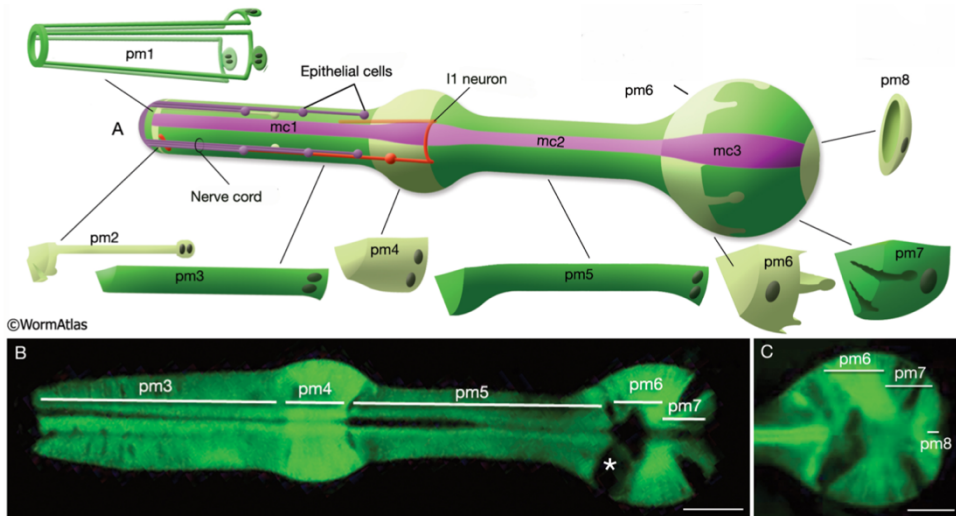


**Figure 11: *C. elegans* pharynx muscular anatomy.** a) Pharynx has eight muscle segments (pm1-pm8) represented in green. Marginal cells (mc), in pink, are situated between the pharyngeal muscle cells (pm). The pharyngeal nerve cords are positioned in the grooves within the muscle cells. b) fluorescence image of the pharynx. ©WormAtlas

#### 1.4.2 Pharyngeal nervous system

The pharyngeal nervous system is formed by twenty neurons divided in fourteen different types. All the neuronal bodies are located in the anterior or posterior bulb. Also, all of them form a small plexus, the pharyngeal ring, at the anterior bulb where they decussate to the other side. The neurons extend processes forming the pharyngeal nerve cords (dorsal and right and left ventral cords) and form synapses with the other neurons in the nerve ring. Some of the neurons present in the nerve ring are linked to the extrapharyngeal nervous system by gap-junctions between pharyngeal neurons and RIP neurons (White et al., 1986; Dalli ere et al., 2019).

Among the different neurons that are included in the pharyngeal nervous system there are motoneurons (M1-M5), Interneurons (I1-I5), MC neurons (MCs), MI neuron, and neurosecretory motor neurons (NSM) (figure 12), (White et al., 1986). All of these neurons release at least one of the classical neurotransmitters including acetylcholine (ACh), glutamate, and serotonin. Moreover, they can express receptors for neuromodulators that the pharyngeal neurons are unable to synthesize, as dopamine (Sugiura et al., 2005), suggesting that a probable neurohormonal communication between the pharyngeal and somatic nervous system of *C. elegans* is possible, as it has been demonstrated with an external serotonin treatment (Cunningham et al., 2012; Flavell et al., 2013).

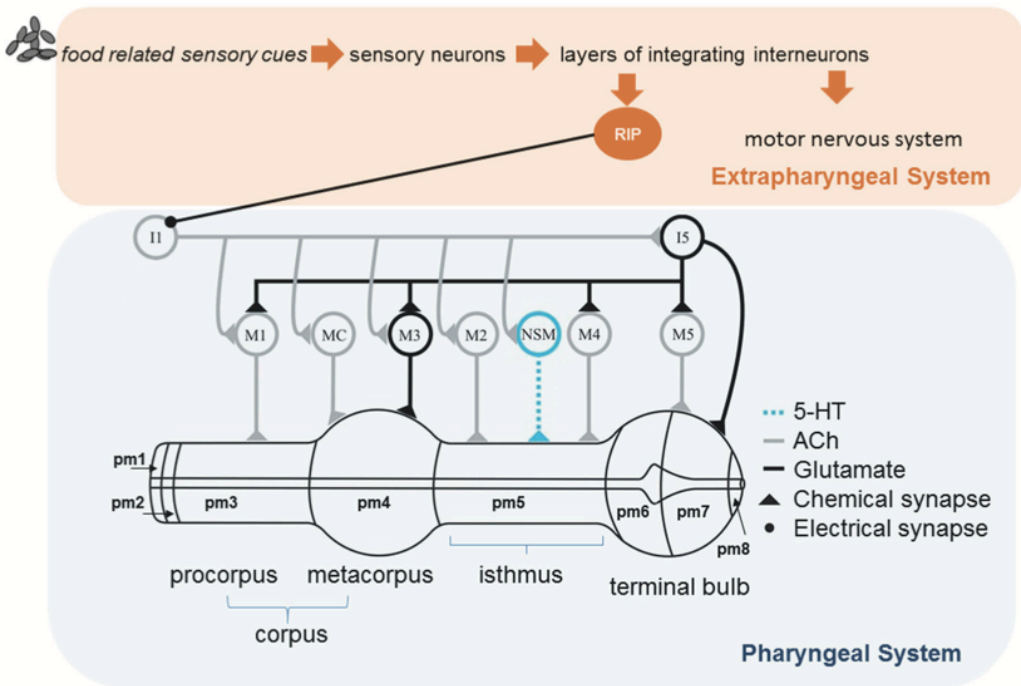


**Figure 12: Organization of pharyngeal nervous system.** The pharyngeal interneurons and motor neurons that regulate the contraction-relaxation cycle of the pharyngeal muscle, are encapsulated within the pharyngeal basal membrane. A subset of the 20 pharyngeal neurons is depicted along with their major neurotransmitter phenotype. The pharyngeal nervous system is connected to the extrapharyngeal system by a gap junction linking RIP to I1. In addition, neurotransmitters released from neurons either within the pharyngeal system, or by the extrapharyngeal system, may act in a neurohormonal fashion to exert effects that do not require neural connectivity. (Dallière et al. 2019).

Three pharyngeal motoneurons (M3s and M4), and MCs play an important role in the regulation of the pumping rate. While M4 and MCs are cholinergic, M3s are glutamatergic. M3 motoneurons synapse with pm4 controlling the duration



of the pumping by initiating the relaxation of the muscle (Avery, 1993). MCs also synapse with pm4 and are responsible of controlling the pumping rate (Avery and Horvitz, 1989). There is evidence that the ablation of pharyngeal motoneurons does not stop pharyngeal pumping (Avery and Horvitz, 1989), suggesting that it is also under the regulation of a myogenic component (Trojanowski et al., 2016).

Finally, the neurosecretory-motor neurons (NSMs) are serotonergic neurons that may have neurosecretory and motor activities, communicating the presence of food to the rest of the body. Exogenous stimulation of serotonin stimulates pumping, decreases locomotion and stimulates egg-laying (Altun and Hall, 2009b). Regarding how NSMs control locomotion in *C. elegans* it has been demonstrated that this neuron can promote adaptative behaviors of the organisms in response to food ingestion through the activity two different acid-sensing ion channels (ASICs), DEL-7 and DEL-3 (Rhoades et al., 2019).

### **I.4.3 Pharyngeal action potentials**

The resting membrane potential in *C. elegans* depends on  $K^+$  permeability and an ouabain-sensitive electrogenic pump (Franks et al., 2002). As discussed before, pharyngeal action potentials are mostly driven by T and L-type voltage gated  $Ca^{2+}$  channels that open after the activation of MCs and M3 neurons. Specifically, MC firing starts an excitatory post-synaptic potential (EPSP), resulting in the depolarization of pharyngeal muscle cells and contraction. During contraction, M3 fires causing small notch hyperpolarizations (IPSPs) allowing the repolarization of the membrane (Shtonda and Avery, 2005).

There are several ionic channels that take an active part in the generation, propagation, and repolarization of each action potential (figure 13). EAT-2 nicotinic acetylcholine receptor, CCA-1 T-type  $Ca^{2+}$  channel, and EGL-19 L-type  $Ca^{2+}$  channels are responsible for the depolarization and subsequent contraction of pharyngeal muscle cells. The restoration of membrane potential to the basal state is mediated by the glutamate chloride channel AVR-15, and the potassium channel EXP-2. Finally, the propagation of the action potential through all the muscular cells is possible because of the presence of gap-junctions that connect all the pharyngeal muscle cells (Avery and You, 2012).

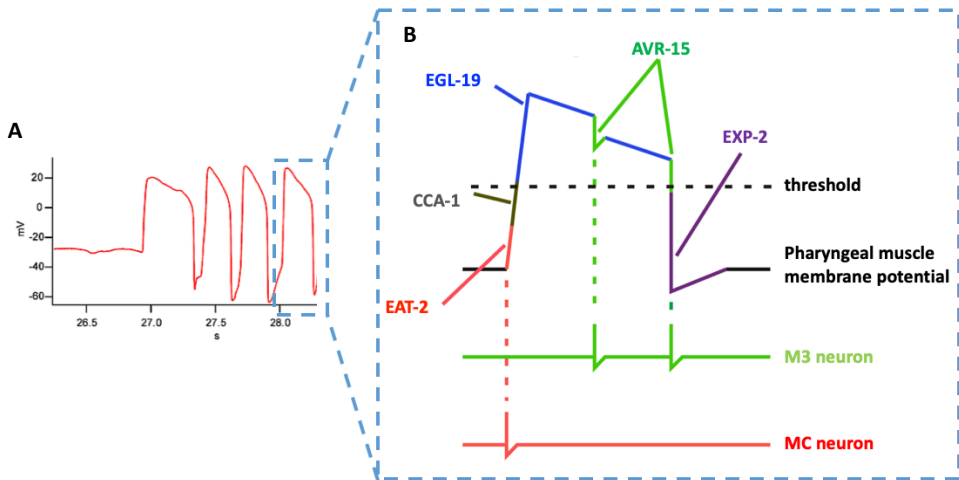


**Figure 13. Pharyngeal muscle action potential. a)** Train of pharyngeal action potentials. **b)** main ionic channels and its role in pharyngeal pumping. EAT-2, nicotinic acetylcholine receptor; CCA-1, T-type  $\text{Ca}^{2+}$  channel; EGL-19, L-Type  $\text{Ca}^{2+}$  channel; AVR-15, Glutamate gated chloride channel; EXP-2, potassium channel. Modified from Avery and You 2012.

#### I.4.3.1 Nicotinic acetylcholine receptor: EAT-2 and EAT-18

The EPSP caused by the firing of the MC neurons arrives to the pharyngeal muscle neuromuscular junction (NMJ) by the activation of nicotinic receptors mediated by acetylcholine. *eat-2* encodes a subunit of the nicotinic receptor expressed only in the pharynx. *eat-18* encodes a small single-pass transmembrane protein necessary for EAT-2 activity (Avery and You, 2012).

#### I.4.3.2 T-type calcium channel: CCA-1

*cca-1* encodes the pore-forming  $\alpha_1$  subunit of a T-type  $\text{Ca}^{2+}$  channel that is active at the beginning of the pharyngeal muscle action potential (Steger et al., 2005). CCA-1 boosts the excitatory effect of the MCs EPSP allowing the rapid depolarization and contraction of pharyngeal muscles (Avery and You, 2012).

#### I.4.3.3 L-Type calcium channel: EGL-19

*egl-19* codes for the  $\alpha_1$  subunit of an homolog of vertebrate L-type voltage-activated  $\text{Ca}^{2+}$  channels, with a deciding role in the regulation of



muscle excitation and contraction in *C. elegans* (Avery and You, 2012). EGL-19 is a major player in the generation and maintenance of the high voltage activated current (HVA) in the pharynx conforming the action potential plateau phase (Shtonda and Avery, 2005)

#### **I.4.3.4 Glutamate gated chloride channel: AVR-15**

AVR-15 is a member of the family of ligand-gated chloride channels necessary to respond to M3 neuron IPSPs. *avr-15* encodes two alternatively spliced channel subunits included in the family of glutamate-activated chloride channel subunits (Avery and You, 2012).

#### **I.4.3.5 Potassium channel: EXP-2**

EXP-2 is a potassium channel of the Kv family that opens when the membrane depolarizes. This is a really particular channel as it behaves oppositely to the rest of the Kv family. EXP-2 activates rather slowly but is inactivated very rapidly and mediates a fast regenerative negative-going current. Because its properties, EXP-2 can remain dormant during an action potential of unpredictable length, and yet efficiently return the muscle cell to its resting potential when the membrane potential drops below a threshold after M3 firing (Shtonda and Avery, 2005; Avery and You, 2012).

### **I.4.4 Pharyngeal motility**

All the fine regulation of pharyngeal muscles is needed for the optimal uptake of bacteria from the environment, and its proper assimilation. That is why pharyngeal muscles exhibit two different types of movements: the pharyngeal pumping and the isthmus peristalsis.

The **pharyngeal pumping** consists of a coordinated muscle contraction and a posterior relaxation of the corpus. It allows the entrance of the bacteria in the digestive system and stores them in the anterior isthmus while grinding bacteria for further digestion.

The **isthmus peristalsis** is a peristaltic contraction that happens in the posterior isthmus to transport bacteria to the terminal bulb, specifically to the grinder, where they are crushed (Song and Avery, 2013).



## II. AGING

Aging is broadly defined as a time-dependent decline that affects most living organisms. According to the World Health Organization (WHO), at a biological level, aging results from the impact of the accumulation of a wide variety of molecular and cellular damage over time leading to a decrease in physical and mental capacity, a growing risk of disease and ultimately death (López-Otín et al., 2013; Organization, 2018).

Nowadays the pace of population aging is much faster than in the past, being expected that the proportion of people over sixty years by 2050 will double reaching the 22% of the population. This fact together with the comorbidities associated to aging have made aging research to experience a great advance in the last 30 years since the first *Caenorhabditis elegans* long-lived mutant strain was isolated (Klass, 1983), as it was a proof that aging had a genetic component that could be regulated.

One of the major reasons for aging research development is that aging is the predominant risk factor for most diseases and conditions that limit healthspan, including cancer, diabetes, cardiovascular disorders and neurodegeneration. Lifespan extensions in model organisms are accompanied by a delay or prevention of several chronic diseases. All these findings made the scientific community to establish the term **Geroscience**, defined as an interdisciplinary field that seeks to define the biological mechanisms of aging that give rise to numerous age related diseases and disorders (Kennedy et al., 2014; Kaeberlein, 2017).

Although significant progress has been made at treating or preventing specific diseases associated with aging, the treatment approach is individual for each pathology, even if application of discoveries from basic biology of aging research has the potential for much larger increases in both life expectancy and **healthspan**. Perhaps, more important than lifespan extension is the improvement of population's healthspan, defined as the period of life free from chronic disease and disability (Kaeberlein, 2017). The main focus of Geroscience is to understand the molecular mechanisms of aging in order to improve population's healthspan.

### II.1 Theories of aging

As new findings in the aging research field have been revealed, many theories have appeared, that fall into two categories. One of the categories includes all the theories that support the idea that aging is a programmed process. On the other hand, the second category is formed by theories that state that aging is a result of

biological error accumulation. Although several theories have been proposed, none of them is able to fully explain aging as they may interact with each other in complex ways (Jin, 2010; Sergiev et al., 2015) .

The **programmed theories** state that aging follows a biological timetable, perhaps after the one that regulates childhood, growth, and development. This regulation would depend on changes in gene expression that affect the systems responsible for maintenance, repair, and defense response. Depending on the systems that change their expression, three theories can be defined. The **programmed longevity theory** states that aging is a result of a sequential switching on and off of different genes causing senescence. The **endocrine theory** defends that there is a biological clock regulated by hormones that control the pace of aging. The last theory is the **immunological theory** stating that the immune system is programmed to be downregulated with age increasing the vulnerability of aged organisms to external insults (Jin, 2010).

The **damage or error theories** defend that environmental assaults to living organisms lead to cumulative damage, in different levels, promoting aging. Among the theories that can be found in this group are the wear and tear theory, the rate of living theory, the cross-linking theory, the free radicals theory, and the somatic DNA damage theory. The **wear and tear theory** states that in almost every existing organism, different parts of cells and tissues are wear out with the pass of the years that result in aging. The **rate of living theory** postulates that there is an inverse relationship between the rate of oxygen basal metabolism and longevity. This means that as the basal oxygen metabolism increases, the lifespan of the individuals decreases. The **cross-linking theory** says that cross-linked proteins accumulation is harmful for cells and tissues slowing down body processes. The **free radical theory**, one of the most studied, proposes that superoxide and other free radicals are responsible for the accumulation of damage inside the cells at a macromolecular level causing that cells stop functioning. Finally, the **somatic DNA damage theory** defends that accumulative genetic damage, as a consequence of the inability of the cell machinery to repair some of the defects that are continuously occurring in DNA of living organisms, is the cause of aging (Jin, 2010; Sergiev et al., 2015).

## II.2 Cellular and molecular hallmarks of aging

Due to the advances in aging research and the amount of different theories that have been proposed through the years to try to explain aging, in 2013 Lopez-Otín and collaborators proposed nine candidate **cellular and molecular hallmarks of aging** instead of trying to explain aging as an event caused just by one

mechanism. All these hallmarks should meet the following criteria: they should manifest during normal aging, its experimental aggravation should accelerate aging, and its experimental amelioration should retard normal aging increasing healthspan. All these hallmarks can be divided into three different categories: primary hallmarks, antagonistic hallmarks, and integrative hallmarks (figure 14).



**Figure 14. Hallmarks of aging.** Nine different hallmarks of aging are represented in the figure. They can be distributed in three different categories according to their effects. The primary hallmarks include genomic instability, telomere attrition, epigenomic alterations and the loss of proteostasis; the antagonistic hallmarks have a dual effect depending on the level of activity. At low levels, they are beneficial, while at high levels they become dangerous. Included in this group are nutrient-sensing pathways, mitochondrial dysfunction, and cellular senescence. Finally, the integrative hallmarks are the stem cell exhaustion, and altered intracellular communication. Modified from López-Otín et al. 2013.

The group of alterations that form the **primary hallmarks** is characterized by their negative nature. This group includes genomic instability, telomere attrition, epigenetic alterations and the loss of proteostasis.

The **antagonistic hallmarks** exhibit different behaviors depending on their intensity. At low levels, they have beneficial effects for the individuals, but when their intensity increases, they become harmful. Deregulated nutrient-sensing pathways, mitochondrial dysfunction, and cellular senescence form this group.

Finally, the last category is formed by the **integrative hallmarks**. This group is formed by stem cell exhaustion, and altered intracellular communication leading to a dysregulation of tissue homeostasis and function (López-Otín et al., 2013).

Because of the nature of this work, the loss of proteostasis as a primary hallmark, and the antagonistic hallmarks nutrient-sensing pathways and mitochondrial dysfunction will be discussed in more detail.

### II.3 Loss of proteostasis as an aging promoter

Proteostasis can be defined as the maintenance of the protein state within the cell through protein elimination and repair. The folding state of a protein is determined by the balance between its translation, folding, and elimination. This balance is regulated in a coordinated way by the heat-shock family of proteins, and the degradation of proteins by the proteasome or lysosome (figure 15), preventing the accumulation of damaged components and assuring the continuous renewal of intracellular proteins (López-Otín et al., 2013; Song et al., 2018; Grandi and Bantscheff, 2019).

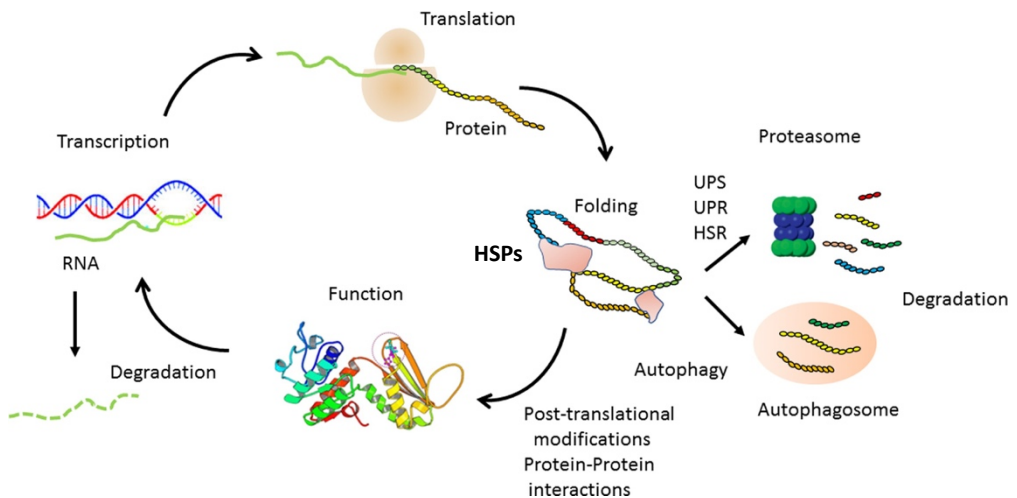


**Figure 15. Protein homeostasis maintenance.** The main mechanisms that have the ability of maintaining protein homeostasis are the heat shock proteins (HSP) in charge of the proper folding of new proteins and the refolding of denatured proteins, the ubiquitin/proteasome system and autophagy. The last two mechanisms are proteolytic systems able to dispose damaged or misfolded proteins. From Grandi and Bantscheff 2019.



### II.3.1 The stress response

**Heat shock proteins (HSPs)** are molecular chaperones involved in the regulation of the proteome maintenance, protecting cells from proteotoxic stress, and processing of immunogenic agents. Specifically, HSPs are able to facilitate the folding of newly synthesized polypeptides and refold denatured proteins (Murshid et al., 2013). These proteins are constitutively expressed and their expression is induced by different types of stress including heat, and oxidative stress (Murshid et al., 2013). When misfolded proteins accumulate in the cytosol, heat shock factor 1 (HSF-1), the main member of the HSF family of transcription factors responsible for the expression of HSPs, is activated regulating the heat shock protein family.

Aging cells undergo a decline in numerous transcriptional pathways, including HSF-1 potency, thus reducing the ability of the cells to synthesize HSPs. This event causes a time-dependent loss of protein quality control contributing to protein aggregate formation. Moreover, there is evidence that an increased expression of HSPs in numerous organisms including *C. elegans* and *Drosophila melanogaster* increase individuals lifespan (Murshid et al., 2013; Alavez, 2017).

Beside the activity of HSPs, the accumulation of misfolded proteins in the ER lumen and cytoplasm induces ER stress. Due to the importance of the maintenance of proteostasis, ER has developed diverse mechanisms to degrade unfolded proteins including the **ER unfolded protein response (UPR<sup>ER</sup>)**. The UPR<sup>ER</sup> is a conserved pathway from yeast to mammals that tries to restore or maintain cell function through the reduction of the protein folding workload, the enforcement of the cellular protein-folding capacity, and the removal and degradation of unfolded proteins (Xu and Park, 2018). This system is divided in three different branches represented by three ER transmembrane proteins: the inositol-requiring kinase-1 (IRE-1), protein kinase RNA-like endoplasmic reticulum kinase (PERK), and activating transcription factor-6 (ATF-6). These regulatory proteins are bound to BiP, a chaperone, in the absence of ER stress, and rapidly get activated when dissociated from it, as it preferentially binds to misfolded proteins in the presence of ER stress leading to the activation of the transcription factors X-box binding protein 1 (XBP-1), and ATF-4 (Estébanez et al., 2018).

Regarding the importance of this process in *C. elegans* aging, numerous studies have demonstrated that UPR<sup>ER</sup> plays a fundamental role by adjusting the organismal proteostasis, and that the ability of aged worms to respond to this stress is significantly reduced independently of the nature of the stress that activates it (Ben-Zvi et al., 2009). Moreover, it has been proven that lifespan extension driven by XBP-1 expression is dependent on the Insulin like signaling

pathway by a parallel interaction between XBP1 and the FoXO transcription factor DAF-16 modifying the expression of longevity related genes (Henis-Korenblit et al., 2010; Martínez et al., 2017).

### II.3.2 The degradation system: Ubiquitin/Proteasome (UPS)

Proteins that need to be removed from the cells are normally processed by the degradation system UPS. Damaged or obsolete proteins are covalently marked with several ubiquitin proteins so they can be degraded by an ATP-dependent process in the proteasome (Alavez, 2017). The UPS is how the cells degrade most of their cytosolic and nuclear proteins as well as aberrant proteins (Bustamante et al., 2018).

Proteasome system experiences a decline with age altering the proteome state of aging cells and tissues that translates in a detrimental metabolic outcome. On the contrary, there is evidence that the increase of the proteasomal activity has a beneficial effect. This effect has been associated with deregulation of the AMPK signaling pathway in yeasts (Yao et al., 2015). Moreover, increased proteasomal activity has also been associated with an elevation of respiratory activity, and an increased oxidative stress response (López-Otín et al., 2016).

### II.3.3 The disposal system: Autophagy

Autophagy can be defined as a catabolic process that controls the quality of the cytoplasm facilitating lysosomal degradation and recycling of intracellular macromolecules and organelles.

Different types of autophagy have been described depending on the mechanism that delivers the cargo into the lysosomes: **microautophagy** refers to the process that consist in a direct delivery of the cargo to the lysosome from the cytoplasm; in **chaperone-mediated autophagy** the cargo is marked by a selective chaperone allowing its recognition and delivery to the lysosome. This mechanism activates in response to stress, and is present in every cell. Finally, **macroautophagy** refers to the process that involves the sequestration of the cargo in a double membrane vesicle called autophagosome that will eventually fuse with the lysosomes for cargo degradation (Hansen et al., 2018). This last type of autophagy is the most studied one and has been related to the appearance of numerous diseases including cancer, neurodegenerative, and metabolic diseases (Mizushima et al., 2008).

The macroautophagy process, from now on referred as autophagy, is mediated by several **autophagy related proteins (ATG)** and occurs at a basal rate in most cells. Briefly, the process starts with the formation of the double-membrane vesicles called autophagosomes. Once formed, the autophagosomes are transported to the proximity of the lysosomes facilitating their fusion, enabling the degradation of autophagic cargos, and the recycling of nutrients and membranes (Rubinsztein et al., 2012).

Autophagy is an evolutionarily conserved process regulated by multiple mechanisms that involve several signaling pathways including nutrient starvation, hypoxia, oxidative stress, pathogen infection, and ER stress. Among the stimuli that can increase autophagic activity is nutrient deprivation. When an organism is exposed to stress and starvation, mechanistic/mammalian target of rapamycin (mTOR) is inhibited initiating the autophagy process. Other signaling pathway involved in autophagy regulation is intracellular  $\text{Ca}^{2+}$  homeostasis. When  $\text{Ca}^{2+}$  is mobilized by the stimulation of IP3 receptors, the autophagy process is inhibited by the stimulation of calmodulin and ERK pathways. Moreover,  $\text{Ca}^{2+}$  also inhibits autophagy by increasing mitochondrial ATP levels and inhibiting the AMPK pathway, known as a promoter of autophagy via the inhibition of mTOR. (Khandia et al., 2019).

At a molecular level, autophagy can be divided in several steps including the autophagosome formation (induction, cargo selection and packaging, vesicle nucleation, vesicle expansion and completion, and retrieval), and vesicle targeting, docking and fusion. For the autophagosome formation the activity of four enzymatic complexes is required (figure 16).

First, the **induction** of the process is mediated by a serine/threonine protein kinase complex that responds to upstream inhibitory signals as mTOR (figure 16a). For the **vesicular nucleation** a class III phosphatidylinositol 3-kinase (PI3K) enzymatic complex needs to be activated allowing the localization of other autophagy proteins that are involved in autophagosome formation (figure 16b). The **vesicle elongation** step is performed by two novel ubiquitin-like conjugation pathways (figure 16c). Finally, the retrieval system is formed by a protein complex (figure 16d). Fusion of the autophagosome vesicle involves proteins common to all types of autophagy that terminate in the vacuole/lysosome (Meléndez and Levine, 2009).



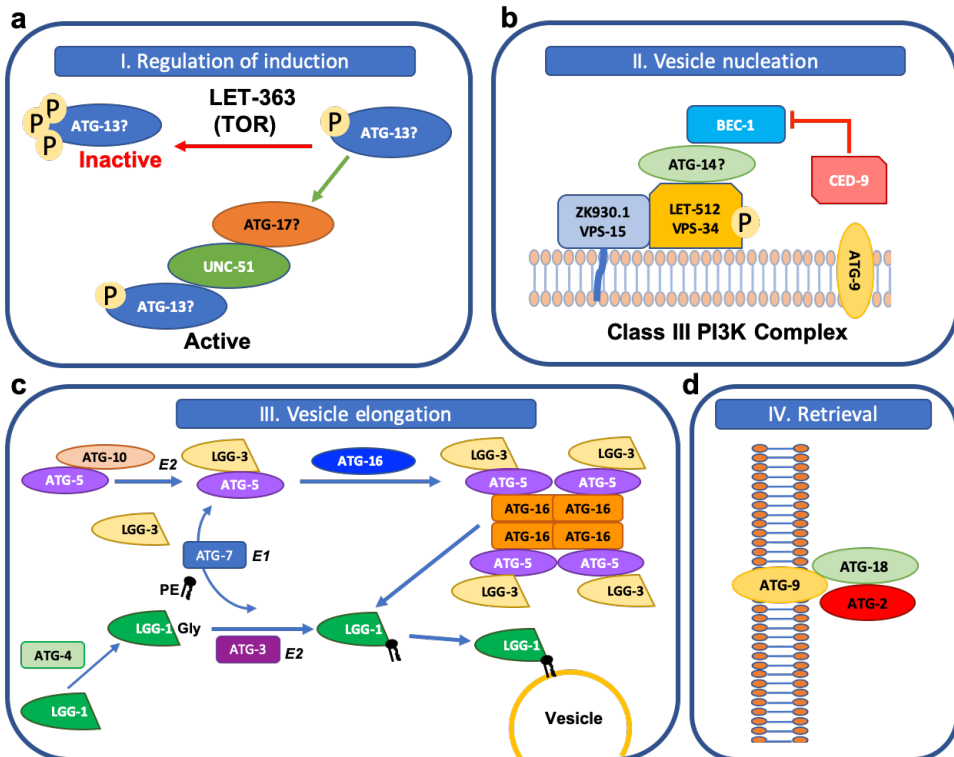


**Figure 16. Molecular pathways that regulate autophagosome formation in *C. elegans*.** **a)** the induction of the autophagic process is driven by TOR kinase and its effectors. **b)** The vesicle nucleation step requires a lipid kinase complex, the Class III PI3K Complex. The activation of class III phosphatidylinositol 3-kinase (PI3K) requires of the presence of binding partners including BEC-1. The interaction between BEC-1 and the antiapoptotic protein CED-9 is conserved in *C. elegans* inhibiting autophagy in a similar way to the interaction observed in mammals between Bcl-2 and Beclin 1. **c)** the vesicle elongation process requires the action of two novel ubiquitin-like conjugation pathways, the LGG-3 conjugation system and the LGG-1 lipidation system. In the conjugation system, LGG3-ATG5 oligomerize with ATG-16 to allow the formation of a multimeric complex. The formation of LGG3-ATG5 complex requires the activity of ATG-10, an E2-like ubiquitin conjugating enzyme. The lipidation system consists of two posttranslational processing events of LGG-1 required for its conjugation with phosphatidylethanolamine (PE) and its recruitment to the phagophore assembly site (PAS). ATG-4 is a cysteine protease, ATG-7 is an E1 ubiquitin activating enzyme required for the activation of LGG-1, and ATG-3 is an E2-like ubiquitin conjugating enzyme. Remarkably, LGG-1 seems to remain in the completed autophagosome and thus is an excellent marker for early and late autophagosomal structures. **d)** The last step is the retrieval for ATG-9 to the PAS. In this step the activity of two interacting peripheral proteins, ATG-18, and ATG-2 is required. Modified from Melendez and Levine 2009.

It has been reported that multiple orthologs for some autophagy genes are present in *C. elegans*. Moreover, the key signaling mechanisms for autophagy

regulation in other eukaryotic organisms seem to be conserved in *C. elegans*. Interestingly, autophagy genes in *C. elegans* are required for lifespan extension in different conserved longevity paradigms including the inhibition of mTOR, reduced insulin/IGF-1 signaling, germline ablation, and reduced mitochondrial respiration (Chang et al., 2017).

There is substantial evidence from multiple organisms that confirms a decrease in gene expression and protein levels of autophagy machinery with age. For example, levels of lysosomal protease activity, and autophagic activity in whole-body extracts decline with age in *C. elegans* (Sarkis et al., 1988; Wilhelm et al., 2017; Hansen et al., 2018). Although it is known that the atophagic activity decreases with age, it is still unclear if the increases or decreases of this process are related to age-associated impairment of cellular function and organismal health (Chang et al., 2017).

## II.4 Nutrient sensing pathways and aging regulation

The ability of almost every organism to respond to nutrient availability in the environment, and modify its metabolism according to changes in their energetic state is essential for organismal survival. Nutrient scarcity is a selective pressure that has led to the existence of different signaling pathways that are able to detect changes in intracellular and extracellular levels of sugars, amino acids, lipids, and surrogate metabolites. This signaling pathways are known as **nutrient sensing pathways** and include the insulin/insulin-like growth factor 1 (IGF-1) signaling pathway, the mechanistic target of rapamycin (mTOR) pathway, the adenosine monophosphate-activated protein kinase (AMPK) pathway, and the sirtuins pathway. All these metabolic pathways play an important role in the regulation of physiological decisions to reproduce, grow, and age. Moreover, it has been demonstrated that mutations in all of these pathways are able to modify life expectancy in numerous organisms including *C. elegans* (Efeyan et al., 2015; Templeman and Murphy, 2018).

### II.4.1 IIS: Insulin/insulin-like growth factor (IGF-1) signaling pathway

IIS Pathway (figure 17) is one of the main coordinators of the response to nutrient availability with energy homeostasis and metabolic processes across numerous invertebrate and vertebrate species, and has been deeply investigated in *C. elegans*. Particularly, insulin/IGF-1 signaling is a key regulator of metabolism that coordinates food intake and cellular energy homeostasis by stimulating glucose uptake and by driving anabolic processes.

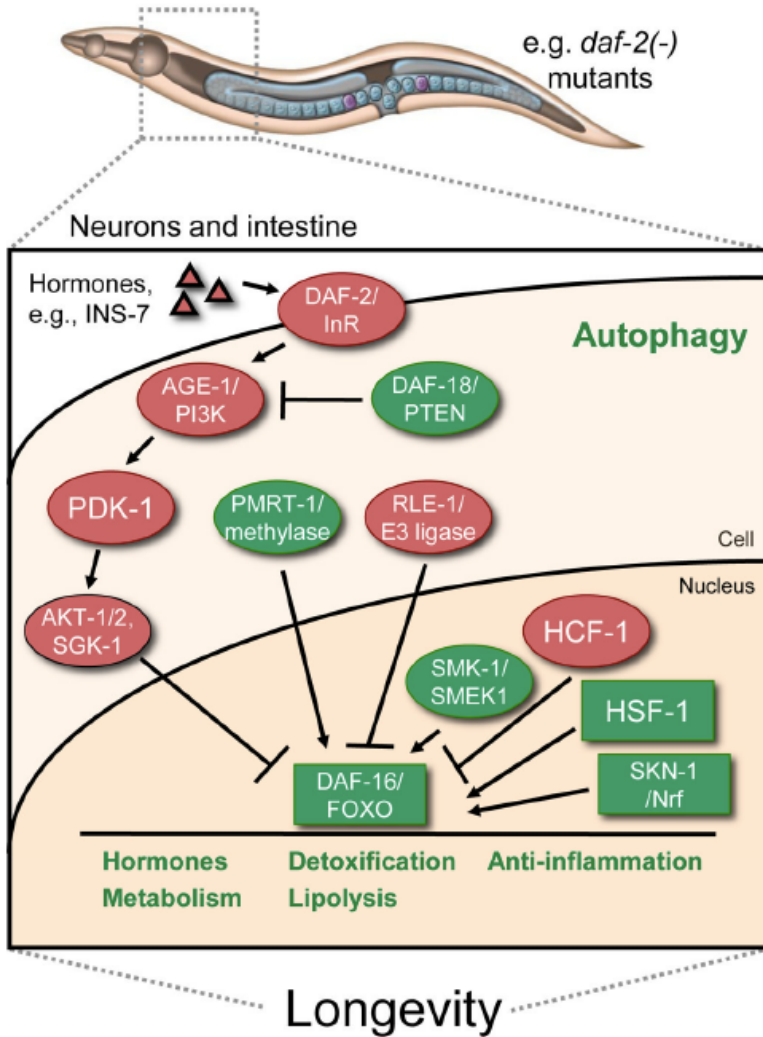


**Figure 17. Insulin/IGF-1 signaling in *C. elegans* regulation of aging.** When ILPs reach intestinal cells trigger the IIS pathway preventing the DAF-16 translocation to the nucleus. There are other molecules that can regulate DAF-16 activity: in the cytoplasm RLE-1, an ubiquitination protein, and PMRT-1, an arginine methylase, have opposite effects. While PMRT-1 promotes translocation of DAF-16 to the nucleus, RLE-1 prevents it. There are also molecules that can regulate DAF-16 in the nucleus: SMK-1 and HSF-1 enhance DAF-16 function, while HCF-1 inhibits it. As it seems that DAF-16 translocation to the nucleus is the main reason of lifespan extension in numerous species including *C. elegans*, reduction of function mutations of the pathway, such as *daf-2* mutants, experiment a decrease in IIS pathway activity promoting DAF-16 translocation to the nucleus. This activates processes such as detoxification, lipolysis, anti-inflammation, metabolic and endocrine changes that lead to an increased longevity (Modified from Lapierre and Hansen 2012).

This pathway is activated and modulated by peptide hormones called insulin-like peptide ligands (ILPs) that bind to the DAF-2/InR membrane receptor with tyrosine kinase activity. Approximately, around 40 genes in *C. elegans* encode for ILPs (Pierce et al., 2001), including both agonists and antagonists of the DAF-2 receptor, and are able to interact in several ways comprising complex networks that exert different effects on various physiological processes (Templeman and Murphy, 2018).

When an ILP binds to the DAF-2 receptor its tyrosine kinase activity is activated leading to the activation of the phosphoinositide 3-kinase AGE-1/PI3K kinase. The next steps in the phosphorylation cascade are carried out by PDK-1, AKT-1, and AKT-2, that are serine/threonine kinases that regulate the activity of FoXO transcription factor DAF-16 by preventing its translocation to the nucleus, blocking the transcription of target genes. As a counterpart to DAF-16 inactivation, DAF-18/PTEN activity lipid phosphatase inactivates AGE-1 allowing the translocation of DAF-16 to the nucleus. (Lapierre and Hansen, 2012; Murphy and Hu, 2013). DAF-2 receptor does not only exert its function by regulating DAF-16. Transcription factors HSF-1 and SKN-1 are also under the control of the IIS pathway. Together, these three transcription factors regulate numerous processes that act accumulatively increasing lifespan. This regulation includes the stress-response genes, as well as genes encoding antimicrobial peptides, chaperones, apolipoproteins, and channels (Kenyon, 2010).

DAF-16 is a member of the FoXO family of Forkhead transcription factors, that are key regulators of growth, metabolism, stress response, cell cycle control, and longevity in many organisms (Accili and Arden, 2004). Gene expression profiling of *C. elegans daf-2* mutants have confirmed that numerous genes related with the stress response including oxidative stress, detoxification, and immunity as proteostasis and metabolism genes are regulated by DAF-16. For example, the expression of HSP *hsp16* protein family and the cytochrome P450 enzymes is increased in *daf-2* long-lived mutants.

Regarding the effects of this pathway in longevity regulation of *C. elegans*, it is important to remark that the process is tissue specific being the effect mediated mainly by neuronal and intestinal cells (Wolff and Dillin, 2006). At a molecular level, basal levels of expression are important, since extreme down regulation or deletion of IIS is detrimental for invertebrates and mammals. However, the reduction-of-function mutations of different components of DAF-2 signaling pathway lead to an extension of lifespan in numerous species including *C. elegans*, seeming to be the regulation of DAF-16 activity and translocation to the nucleus the main factor influencing longevity. For instance, this mutations can result in an increase of lifespan around 1.000% in *C. elegans* (Ayyadevara et al., 2008), of 40-

80% in *D. melanogaster*, and 6-33% in mice (Lapierre and Hansen, 2012; Templeman and Murphy, 2018). Finally, this pathway activity has also been linked to changes in human longevity. For example, centenarians of a human population had lower fasting insulin levels than 78 year old comparison group (Paolisso et al., 1996), and reduced activity of IIS pathway has been associated with reduced mortality in women (van Heemst et al., 2005).

#### **II.4.2 Mechanistic target of rapamycin (mTOR) signaling pathway**

mTOR (mechanistic target of rapamycin) pathway is one of the main nutrient sensing intracellular pathways, and controls numerous processes including reproduction, growth, and metabolism depending on the availability of amino acids and growth factors.(Lapierre and Hansen, 2012; Templeman and Murphy, 2018).

mTOR is a serine/threonine kinase that belongs to the phosphoinositide 3-kinase (PI3K) related protein family that conforms the catalytic subunit of two different complexes, mTORC1 and mTORC2, that mainly differ in their binding proteins, RAPTOR and RICTOR respectively, their downstream signaling effects and their sensitivity to the inhibitory drug rapamycin (Antikainen et al., 2017). These two complexes are able to respond to a broad array of unique molecular signals including mTORC1 activation through amino acid sensing at the lysosome mediated by the Ragulator complex (Kim and Kim, 2016) inhibition as a result of a low cellular ATP/ADP ratio mediated by AMPK, or low oxygen levels (Vadysirisack and Ellisen, 2012), and ribosome capacity sensing by mTORC2 (Zinzalla et al., 2011) (figure 18). Interestingly, although mTOR complexes are critical as a consequence of the importance of the processes that they regulate, reductions in mTOR activity can also have important consequences leading to the activation of different mechanisms that have been proven to promote the protection of cells and organisms from stress (Blackwell et al., 2019).

*C. elegans* has made major contributions to understand mTOR biology as a consequence of the existence of numerous orthologs for mTOR, RAPTOR, RICTOR, and other conserved regulators of TORC1 and TORC2 complexes. The ortholog of mTOR in *C. elegans* is LET-363, and was named based on the lethal phenotype of its mutant (Howell AM et al., 1987) before being described as the mTOR homolog in worms (Long et al., 2002). The two orthologs for RAPTOR and RICTOR are DAF-15 and RICT-1 respectively. DAF-15 was named as a result of an abnormal dauer formation as a consequence of its loss-of-function mutation (Albert and Riddle, 1988). The availability of RNAi for both proteins described before, has led to the discovery that the exposure of worms to both of RNAi's results in identical

phenotypes in *C. elegans* consistent with the predicted association of LET-363 and DAF-15 to form the TORC1 complex in *C. elegans*. Finally, the RICTOR homolog was named RICT-1 and the loss-of-function of *rict-1* gene did not caused a delay in larval development but affected life span after diet restrictions and other conditions. This fact supports the idea that both complexes, TORC1 and TORC2 display different functions, and that TORC1 complex is essential for the correct development of *C. elegans* while TORC2 does not affect this process (Blackwell et al., 2019).

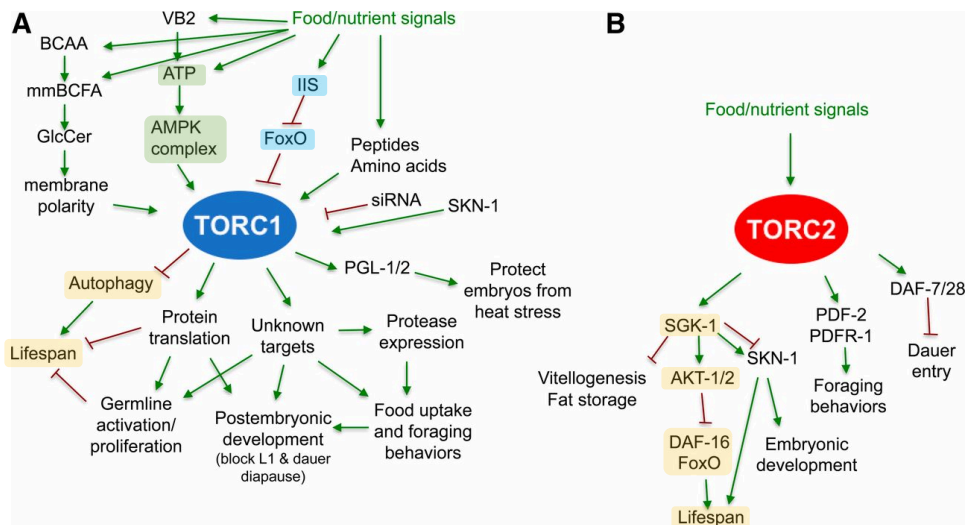


**Figure 18. Upstream and downstream regulation of TORC1/2 complexes in *C. elegans*.** Changes in food availability or nutrient signals are able to stimulate TORC1 (A), and TORC2 (B) signaling pathways involved in numerous processes including lifespan and development. TORC1 complex is able to respond to numerous upstream signaling molecules including the ADP/ATP ratio through its regulation by AMPK. Also, it can be inhibited by DAF-16 after the IIS pathway is activated. As downstream effectors of TORC1 signaling autophagy machinery is included. TORC2 signaling can also affect longevity by modulating DAF-16 activity through SGK-1-AKT1/2 pathway. Modified from Blackwell et al. 2019.

There are numerous downstream targets of mTOR that have been described in *C. elegans*. For example, TORC1 complex directly phosphorylates S6K/RSKS-1, the ribosomal protein S6 kinase in mammals. Functional studies with *rsk-1* mutants, have shown that not all the phenotypes associated to LET-363 are present in *rsk-1* mutants. However, some of the phenotypes can be observed including lifespan extension, translation regulation, and germline proliferation (Blackwell et al., 2019). Another pathway that is highly affected by downstream regulation of mTOR signaling is autophagy. TORC1 is able to inhibit autophagy (Hansen et al., 2008) and its effects are at least partly mediated by the

transcription factor HLH-30/TFEB as the phosphorylation of HLH-30 by TORC1 controls its subcellular localization (Lapierre et al., 2013; Napolitano and Ballabio, 2016). As for the TORC2 complex, the main downstream target is SGK-1, the *C. elegans* ortholog of the serum and glucocorticoid induced kinase 1, that was first characterized as a player in the stress response and lifespan regulation (Hertweck et al., 2004). Posterior studies have shown that SGK-1 activity is regulated by RICT-1 and is involved in diverse processes including the regulation of fat metabolism in the intestine (Blackwell et al., 2019), the regulation of mesodermal embryonic development (Ruf et al., 2013), and longevity (Mizunuma et al., 2014; Zhou et al., 2019).

mTOR signaling reduction has been linked to lifespan regulation in several organisms including *C. elegans* (Vellai et al., 2003), *D. melanogaster* (Kapahi and Zid, 2004), and when combined with LST8 subunit knockdown of TORC1 complex, in mice (Lamming et al., 2012). Pharmacological inhibition of TORC1 complex using rapamycin also exhibits pro-longevity effects in numerous species including *C. elegans* (Robida-Stubbs et al., 2012) and mice, even when the treatment is started at late adulthood (Harrison et al., 2009; Templeman and Murphy, 2018), and has been described as a major mediator of the beneficial dietary restriction (DR) effects on longevity. As indicated in figure 18, TORC1/2 complexes have different downstream effectors thus their effects on longevity are driven through different processes. TORC1 mainly extends lifespan through the reduction of mRNA translation and protein synthesis, and regulation of autophagy (figure 19). The lifespan extension driven by a reduced translation seems to be evolutionary conserved (Johnson et al., 2013). Also, it has been described that reduced translation pro-longevity effects depend on the function of two different transcription factors, DAF-16 (Henderson et al., 2006) and SKN-1 (Wang et al., 2010), being critical for lifespan extension after TORC1 inhibition. As for the autophagy regulation, TORC1 inhibition increases the autophagy process through different transcription factors including HLH-30 and PHA-4. Finally, TORC2 role in aging and stress resistance is less known, but three different mechanisms have been detected in *C. elegans* that modulate lifespan through TORC2 activity (figure 19). First, TORC2 through SGK-1 is able to activate TRPA-1 channel at low temperature conditions promoting an increase in longevity through DAF-16 activation. Also through SGK-1, TORC2 inhibits the formation of the mitochondrial permeability transition pore (mPTP) preventing the harmful effects of an excessive mitochondrial permeability. On the other hand, TORC2 activity is able to limit lifespan and stress response by impeding nuclear localization of SKN-1 (Blackwell et al., 2019).



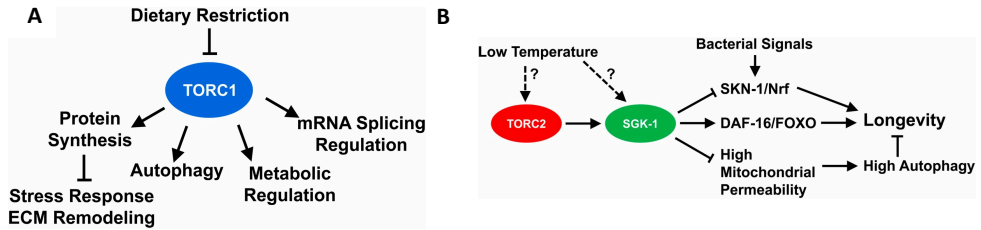


**Figure 19. Effects of TORC1 and TORC2 in *C. elegans* aging.** **a)** TORC1 inhibition extends lifespan in *C. elegans* mainly through the reduction of protein synthesis and promotion of autophagy. Its inhibition can be achieved either by caloric restriction or pharmacologically by rapamycin. **b)** TORC2 regulation of aging is not that clear, although three different mechanisms have been described to affect aging. In one hand, low temperatures can activate SGK-1 by its phosphorylation mediated by TORC2 complex. SGK-1 can induce longevity through the activation of two different transcription factors, SKN-1 and DAF-16. On the other hand, TORC2 inhibits the formation of the mPTP, decreasing mitochondrial permeability causing a harmful elevation of the autophagy process. Modified from Blackwell et al. 2019.

### II.4.3 Adenosine monophosphate-activated protein kinase (AMPK) pathway

5' AMP-activated protein kinase (AMPK) is a highly conserved heterotrimeric serine/threonine protein kinase formed by three different subunits: the catalytic  $\alpha$  subunit, and two regulatory ones,  $\beta$  and  $\gamma$ . AMPK acts as an energy status sensor that activates when cellular energy is depleted inducing catabolic pathways and inhibiting anabolism (Hardie et al., 2012). Importantly, AMPK is conserved in several species including *C. elegans* (Beale, 2008). As AMPK acts as an energy sensor, it activates when ATP/AMP levels decrease in response to cellular ATP hydrolysis, activating the ATP producing pathways and inhibiting the ATP consuming ones. Energy homeostasis and its impairment has been established as an important factor to develop numerous diseases including type 2 diabetes, obesity, and cancer; that is why understanding AMPK pathway and its regulation is a promising target to treat metabolic syndrome diseases and cancer (Carling, 2017).

There are numerous upstream regulators of AMPK including several kinases such as  $\text{Ca}^{2+}$ /calmodulin-dependent protein kinase kinase  $\beta$  (CaMKK $\beta$ ), serine/threonine kinase 11 (LKB1) and transforming growth factor- $\beta$ -activated kinase 1 (TAK1). All these kinases phosphorylate the catalytic  $\alpha$  subunit at Thr172 in response to different stimulus. The canonical activation of AMPK is driven by adenine nucleotides levels inside the cells, that will activate LKB1, allowing the phosphorylation of AMPK. There is also a non-canonical activation of AMPK in response to hormones that increase intracellular  $\text{Ca}^{2+}$ . When  $\text{Ca}^{2+}$  concentration



increases inside the cells, CaMKK $\beta$  is activated, and therefore AMPK is phosphorylated. As AMP can directly bind to AMPK  $\gamma$  subunit allowing its phosphorylation, both canonical and non-canonical phosphorylation can act synergistically (Hardie et al., 2016). AMPK is then deactivated by several phosphatases including PP2A, PP2C $\alpha$ , and Ppm1E (figure 20) (Slack and Tullet, 2018).

As other nutrient sensing pathways, AMPK signaling can be increased by numerous stimulus including oxidative stress and exercise leading to an increase in metabolic stress that activates AMPK. On the other hand, the excessive storage of essential nutrients, glucose, fatty acids or amino acids have a detrimental effect on AMPK activity contributing to insulin resistance (Coughlan et al., 2013). All these evidences have led to associate AMPK activity to the regulation of numerous processes including glucose/lipid homeostasis, body weight, food intake, insulin signaling and mitochondrial biogenesis. Besides these effects, AMPK activation has been associated with a decrease of tumor proliferation progression; evidence of this effect is the description of LKB1 as a tumor suppressor, and the observation that different pharmacological activators of AMPK delay tumorigenesis *in vivo* (Kim et al., 2016).

*C. elegans* organism model has been used to study the participation of AMPK signaling pathway in the aging process. For that purpose, AMPK  $\alpha$  subunit (*aak-2*) mutants were studied revealing that *aak-2* is an essential gene for lifespan extension mediated by AMPK (Apfeld et al., 2004). Basically, AAK-2 protein is activated by a decrease of the ATP/AMP ratio derived from environmental stressors or normal aging in the worm, linking cellular energy availability to the aging process (Curtis et al., 2006). Also, in *C. elegans* has been demonstrated that CRTC-1, a cytoplasmic co-activator of CREB, is a direct phosphorylation target of AAK-2, that inactivates it by blocking its translocation to the nucleus, promoting lifespan extension in the nematodes (Mair et al., 2011). CRTC-1 dephosphorylation, thus activation, can be mediated by calcineurin allowing its translocation to the nucleus where it binds to CREB factors (Screaton et al., 2004). This fact was also proved in *C. elegans* as the mutation of TAX-6, ortholog of calcineurin also extends its lifespan (Mair et al., 2011). Moreover calcineurin deficiency promotes the autophagic pathway extending lifespan in *C. elegans* (Dwivedi et al., 2009) which agrees with the idea that Ca<sup>2+</sup> dysregulation is associated with accelerated aging (Foster et al., 2001).

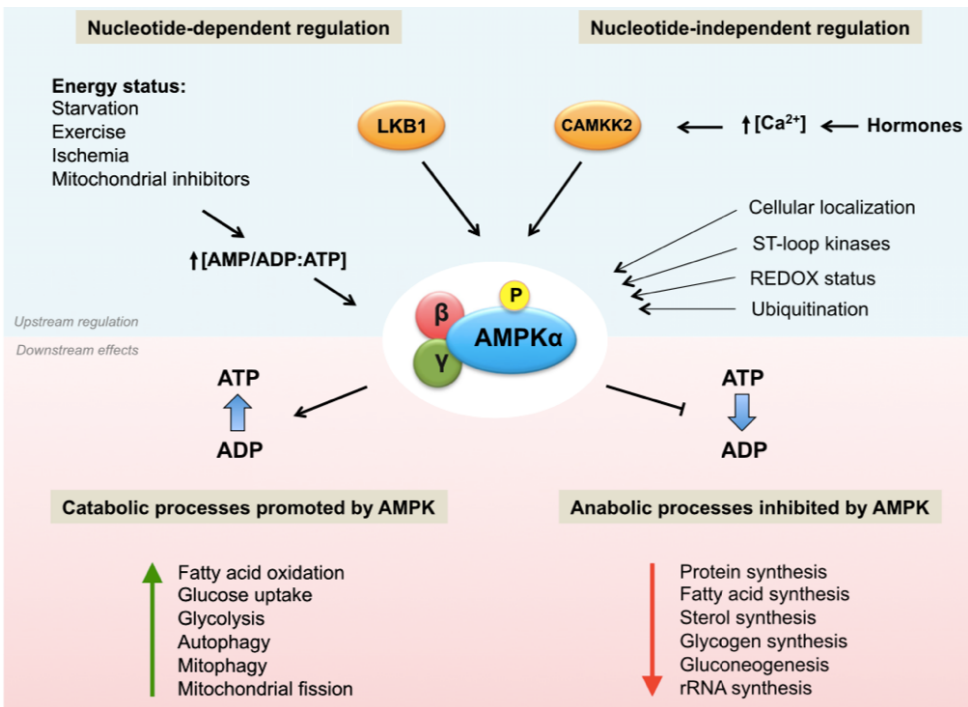


**Figure 20. AMPK upstream regulators and downstream effects.** AMPK is a serine/threonine kinase that is activated by the phosphorylation of its  $\alpha$  catalytic subunit in the Thr172. There are a few kinases that can phosphorylate AMPK in response to different stimulus. For example, an increase in intracellular  $Ca^{2+}$  activates CaMKK $\beta$ , that then phosphorylates AMPK. Also AMP/ADP increased ratio activates LKB1 kinase leading also to AMPK phosphorylation. Finally the allosteric activation of the kinase is achieved by direct binding of AMP to AMPK  $\gamma$  subunit. To deactivate AMPK, several phosphatases are activated when ATP levels increase. The activation of AMPK causes a metabolic modulation that consists in a decrease of anabolic pathways activity and an increase of the catabolic ones (García and Shaw 2017)

Besides AMPK pro-longevity effects mediated by CRTC-1 activity regulation, it can regulate the function of several pathways including the rest of nutrient sensing pathways (discussed in more detail in section II.6, p59) forming an integrated network that result in the modulation of autophagy and oxidative stress, two metabolic hallmarks of the aging process (Salminen and Kaarniranta, 2012; Garcia and Shaw, 2017).

#### II.4.4 Sirtuins pathway

Sirtuins (silent information regulator proteins, SIRT) are conserved protein NAD<sup>+</sup>-dependent deacylases that act as energy sensors by reacting to changes in the ratio of NAD<sup>+</sup>/NADH, favoring the oxidized form. SIRTs have diverse functions,

studied more in detail in the case of SIRT1, as it can sense energy balance changes in different cellular locations including the nucleus, the cytoplasm and the mitochondria, playing a critical role in maintaining metabolic homeostasis (Chang and Guarente, 2014). As in all the pathways described before, SIRT's function is correlated with the nutritional balance of the organisms (Burkewitz et al., 2016).

The anti-aging functions of sirtuins were first proposed in yeast, as a response to caloric restriction, promoting healthy aging and longevity (Kaeberlein et al., 1999). Since that moment, sirtuins regulation of longevity has been studied in different model organisms including *C. elegans*. In this regard, the overexpression of *sir-2.1* has been proven to significantly increase lifespan in a DAF-16 dependent manner (Berdichevsky et al., 2006).

## II.5 Mitochondrial dysfunction

One of the first aging theories that was proposed to explain the aging phenomena was the free radical theory of aging, stating that mitochondrial dysfunction associated with aging caused a deleterious effect on organisms due to the accumulation of metabolic damage because of the increased amount of free radicals in the cells (Harman, 1956).

Since then, numerous studies have described some of the mitochondrial alterations that happen with age from model organisms, as worms and flies, to humans. Mitochondrial changes that can be observed with age include a gradual decline in respiratory chain capacity, decreased activities of electron transport chain (ETC) complexes, elevated oxidative damage, decreased mitochondrial content, morphological abnormalities in mitochondrial structure, and increased fragility of aged mitochondria (Wang and Hekimi, 2015). Besides the important knowledge of mitochondrial changes with age, it is also clear for the scientific community that the impairment of mitochondrial function is related to the physiological process of aging (figure 21) and age related diseases including diabetes, neurodegeneration, and cancer (Raffaello and Rizzuto, 2011).

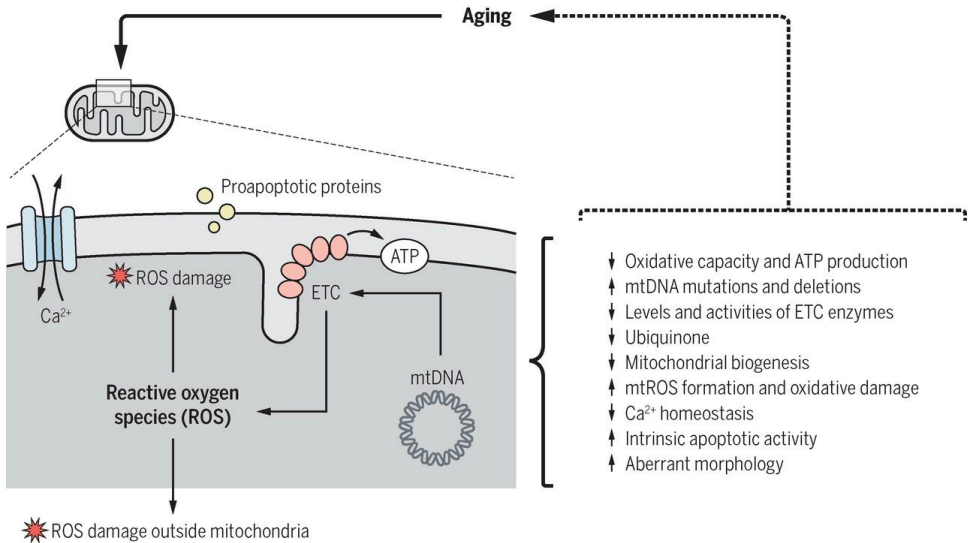


**Figure 21. Mitochondrial dysfunction with age.** As organisms age, mitochondrial function starts to be impaired causing an excess of oxidative stress by the production of radical oxygen species (ROS). This impairment leads to reduced mitochondrial capacity, increased apoptotic activity, and reduced Ca<sup>2+</sup> homeostasis affecting the aging process. From Wang and Hekimi 2015.

One of the main focuses on the field for a while has been the pursue of the idea that if mitochondrial dysfunction effects on aging were caused by an excess of reactive oxygen species (ROS), the treatment with antioxidants should be enough to slow aging. However, the experimental evidence for this statement is mixed; while it has been proven that the reduction of mitochondrial oxidative stress can impact aging in mice, several trials threw inconclusive results when antioxidants were dietarily supplemented. That is why the **mitohormesis model** has been proposed. It states that the final effect on longevity of mitochondrial dysfunction and increased oxidative stress depends on the level of stress induced. While low levels can promote the activation of beneficial stress responses and signaling pathways, higher levels are damaging causing frailty and premature death (Bennett and Kaerberlein, 2014).

The mitochondrial unfolded protein response (UPR<sup>mt</sup>) is a mitochondrial stress signaling pathway that activates when mitochondrial proteotoxicity increases involving mitochondrial-nucleus communication. Although first discovered in mammalian cells, *C. elegans* has been really useful in understanding this process. The induction of mitochondrial stress in *C. elegans* results in the activation of the UPR<sup>mt</sup> pathway leading to an increased transcription of the mitochondrial chaperone genes *hsp-6* and *hsp-60* mainly mediated by the transcription factor ATFS-1 (Qureshi et al., 2017). As for its regulation of the aging

process, it is still unclear how this pathway really affects longevity, although several interventions that increase *C. elegans* lifespan by disrupting mitochondrial function induce fluorescent reporters of mitochondrial chaperones, like *hsp-6* (Bennett and Kaeberlein, 2014).

## II.6 Delaying aging: the intricate network machinery of Caloric Restriction

Dietary or caloric restriction (DR/CR), understood as a moderate reduction in calorie intake without causing malnutrition is the most robust environmental manipulation known to increase active and healthy lifespan in many species extending their lifespan and delaying many age-related diseases including cancer, diabetes, and cardiovascular disorders (Dilova et al., 2007; Kapahi et al., 2017). Initially, DR was thought to extend lifespan just by reducing the rate at which cellular damage accumulates over time as a result of nutrient metabolism. However, further investigation shed light to the effects of DR showing that lowering nutrient intake did not just reduce the accumulation of cellular damage, but also counteracts the effects of aging in an acute manner. Nowadays, it is well established that DR effects on aging are regulated by a coordinated response of the nutrient signaling pathways, although the importance of each pathway depends on the regimen of dietary restriction, at least in *C. elegans* (figure 22) (Kenyon, 2010).

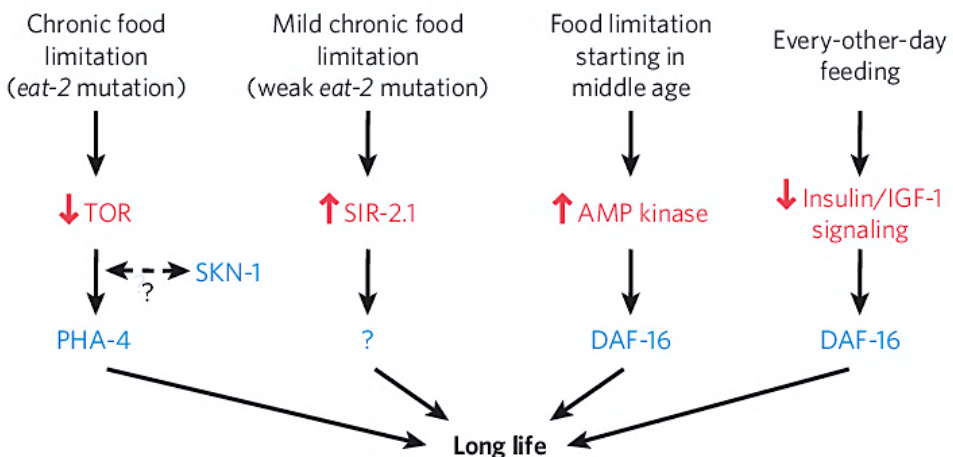


**Figure 22. Different regimes of dietary restriction activate different signaling pathways.** *eat-2* mutants, which reduce calorie intake through the whole life of the worms have been used to study the activity of nutrient signaling pathways depending on the nutrient deprivation nature. Different sensors activate depending on the amount of nutrients available, and also on the moment the DR regime starts. Kenyon 2010.

Every nutrient signaling pathway described before can modulate each other activity at some level (figure 23). While IIS and mTOR have detrimental effects on the aging process, AMPK and SIRT1 pathways exhibit the opposite effect, being reasonable that this pathways regulate each other's activity to promote longevity. IIS and mTOR pathways are linked to each other through multiple connections. IIS can activate mTOR pathway by the activation of AKT, and mTORC1 can negatively regulate IIS through S6K. Although these two pathways seem to be highly interconnected, studies in *C. elegans* have shown that mTOR signaling pathway can modulate aging either in a dependent or in an independent manner of IIS signaling (Johnson et al., 2013). One of the major interconnections between all the pathways is AMPK by itself. Under DR conditions, AMPK increases its activity causing the activation of SIRT1 pathway by increasing NAD<sup>+</sup> levels. Also, SIRT1 pathway can modulate AMPK activity through the activation of LKB1. Finally, AMPK can modulate mTORC activity at different levels by reducing its activity. AMPK can directly phosphorylate raptor or inhibit its upstream regulators TSC1/2, resulting in mTORC1 decreased activity (Pan and Finkel, 2017).

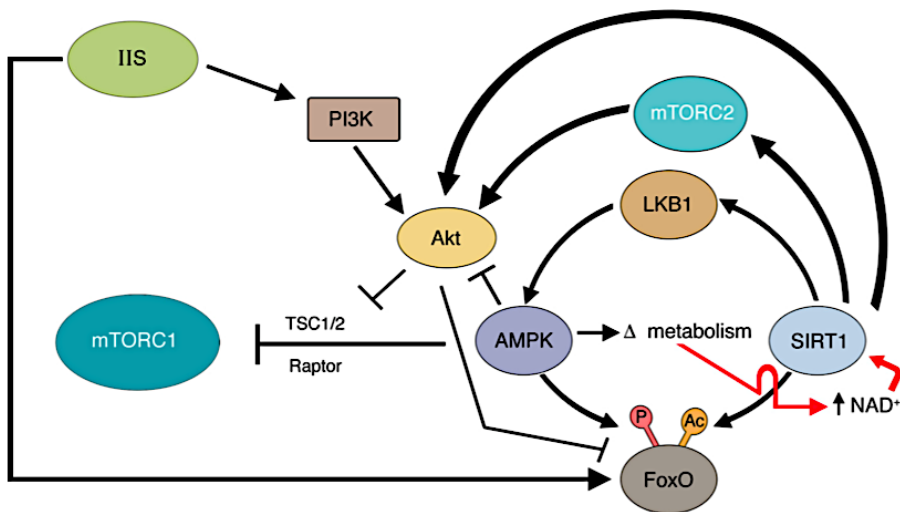


**Figure 23. Interaction between nutrient signaling pathways.** Nutrient signaling pathways interact with each other at different levels. IIS can modulate mTOR pathway by the activation of AKT. One of the key regulators of all these pathways is AMPK. AMPK activity promotes longevity by inhibiting IIS and mTORC signaling and stimulating SIRT1 activity. Interestingly, SIRT1 also activates AMPK through LKB1. From Pan and Finkel 2017.

Besides their biochemical interactions, nutrient signaling pathways have more global and physiological effects. One of the main examples is the regulation of autophagy mainly by regulating DAF-16/FoxO activity, which appears to regulate

the expression of numerous autophagic genes. IIS can inhibit the process in two different manners. The activation of AKT induces the activation of mTOR phosphorylating ATG1 in yeast or ULK-1 in mammals and impeding the autophagophore formation (Kim et al., 2011), and also negatively regulates DAF-16/FoXO activity (Zhao et al., 2007). Additionally, AMPK, SIRT6 and mTOR pathways can directly modulate the autophagic process (Pan and Finkel, 2017; Templeman and Murphy, 2018).

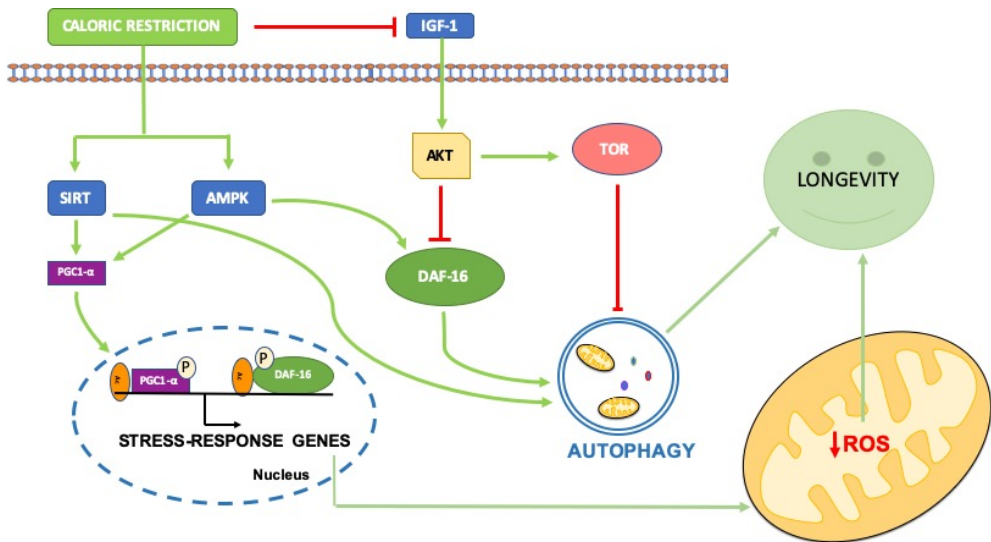


**Figure 24. Caloric restriction signaling pathways.** nutrient signaling pathways modify their activity after nutrient deprivation causing the translocation to the nucleus of DAF-16/FoXO. DAF-16 regulates the expression of the stress-response genes reducing ROS production. The promotion of autophagy and the amelioration of mitochondrial oxidative stress lead to a promotion of longevity. Based on Raffaello and Rizzuto 2011.

Finally, it is important to mention that CR has a beneficial impact on mitochondrial function causing a significant reduction of mitochondrial ROS production and oxidative damage, as well as increased biogenesis. It has been seen that nutrient signaling pathways modulation by CR also modulate mitochondrial function leading to the discovery of interrelationships between these pathways and mitochondria (figure 24). For example, *daf-2* mutants in *C. elegans* show increased oxidative stress resistance, suggesting that at least some of the pro-longevity effects observed in this mutant is related to effects on mitochondrial protection from oxidative damage. As explained before, one of the key points that is at least in part shared by all nutrient signaling pathways is the regulation of DAF-16 activity. It has been shown that DAF-16/FoXO can induce the expression of several antioxidant enzymes, and that its overexpression is enough

to extend lifespan in flies and mice (Sun et al., 2002; Hu et al., 2007). Basically, nutrient signaling pathways modulation is able to promote mitochondrial oxidative stress amelioration, being at least in part the cause of their pro-longevity effects (Raffaello and Rizzuto, 2011).

To conclude this section, it is evident that aging is a highly regulated process which involves the activity of numerous metabolic pathways and physiological events (figure 25). Longevity assays in *C. elegans* have outlined the participation of nutrient signaling pathways (IIS, AMPK, mTOR, and SIRT6) in the regulation of not just organisms lifespan, but also all the decline associated with aging, including diseases such as cancer, diabetes, and neurodegeneration. It is also well established that mitochondrial function and the stress response play a key role in the aging process. Although it has been described that these two processes can regulate longevity in a separate manner, more and more evidence is supporting the idea that all this mechanisms involved in lifespan regulation interact with each other to promote healthy aging opening a new line of interventions to delay aging and related diseases that focus directly in the modulation of this intricated network.

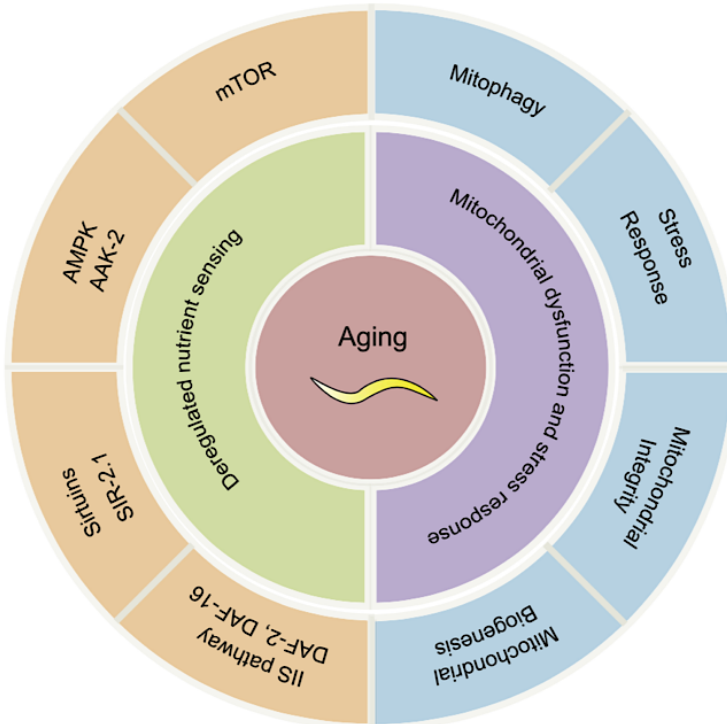


**Figure 25. Metabolic regulation of aging in *C. elegans*.** Aging is a multifactorial process regulated by numerous signaling pathways, the nutrient signaling pathways (IIS, AMPK, SIRT, and mTOR). Also, mitochondrial function and the stress response can modulate longevity in numerous species. From Gao et al 2018.



### III. CALCIUM SIGNALING PATHWAY

Calcium ( $\text{Ca}^{2+}$ ) is the most common signal transduction element in cells ranging from bacteria to specialized neurons. Unlike other second-messenger molecules,  $\text{Ca}^{2+}$  is required for life, and its dysregulation contributes to cell death (Clapham, 1995).  $\text{Ca}^{2+}$  operates throughout the life history of typical cells: it triggers new life at fertilization, it controls many developmental processes, and once cells have differentiated, it functions to control processes as diverse as contraction, secretion, metabolism, proliferation, learning and memory (Berridge et al., 1999).

$\text{Ca}^{2+}$  signaling is characterized by its speed and effectiveness because of the 20.000 fold gradient between the extracellular and intracellular media maintained at resting state. Normally, free  $\text{Ca}^{2+}$  concentration inside the cells is around 100 nM, while at the extracellular space  $\text{Ca}^{2+}$  reaches a concentration of around 2 mM. Moreover,  $\text{Ca}^{2+}$  cannot be chemically altered, so the control and regulation of  $\text{Ca}^{2+}$  homeostasis relies on its chelation, compartmentalization, and extrusion from cells by a complex protein machinery. That is why cells invest much of their energy to produce changes in  $\text{Ca}^{2+}$  concentration ( $[\text{Ca}^{2+}]$ ) (Clapham, 2007). Finally, each cell type expresses a unique set of components from the  $\text{Ca}^{2+}$  signaling machinery conforming its own  $\text{Ca}^{2+}$  signaling system with different spatial and temporal properties (Berridge et al., 2003).

#### III.1 Calcium signaling dynamics

$\text{Ca}^{2+}$  signaling has several properties including its dynamic nature, its spatial location and a wide temporal range (Berridge, 2012). Its dynamic nature relies on the balance of two different processes: the **ON reactions**, and the **OFF reactions**. The first ones refer to the activation of all the channels and proteins that facilitate an increase of intracellular  $\text{Ca}^{2+}$  after a stimulus reaches the cells. On the other hand, the OFF reactions involve the activation of pumps and exchangers that restore basal levels of free  $\text{Ca}^{2+}$  in the cytoplasm (Berridge et al., 2003). These two phases in  $\text{Ca}^{2+}$  signaling are fast and coordinated allowing to describe a  $\text{Ca}^{2+}$  transient (figure 26). The sources of  $\text{Ca}^{2+}$  are the extracellular media and certain intracellular organelles, such as sarcoplasmic reticulum (SR) in striated muscle cells, and the endoplasmic reticulum (ER) in other cells. The ER acts as an intracellular store of  $\text{Ca}^{2+}$  reaching  $[\text{Ca}^{2+}]$  of 0,5 to 2 mM (Montero et al., 1997; de la Fuente et al., 2013).

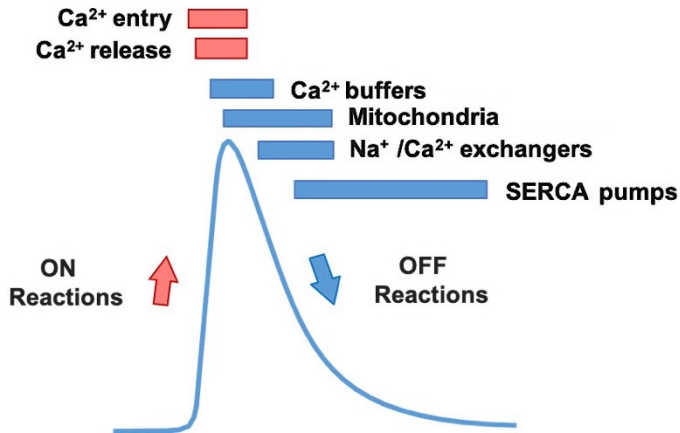


**Figure 26. Calcium transient.** When a stimulus arrives to the cell, ON reactions are responsible for the entrance of  $\text{Ca}^{2+}$  from the extracellular space, and its release from the intracellular stores. When  $\text{Ca}^{2+}$  reaches a threshold concentration, OFF reactions are activated to restore basal  $[\text{Ca}^{2+}]$  in the cytosol where  $\text{Ca}^{2+}$  uptake by the ER plays a significant role. Based on Berridge 2012.

An important aspect of  $\text{Ca}^{2+}$  signaling is its spatial location. One example of this feature is the ER/mitochondrial  $\text{Ca}^{2+}$  interconnection, where changes in  $[\text{Ca}^{2+}]$  in the ER are closely linked to those in the mitochondria. Another example is that ON reactions are often closely associated with the effector systems that respond to  $\text{Ca}^{2+}$ . Finally, intracellular  $\text{Ca}^{2+}$  can operate over a wide time domain lasting from microseconds to hours. When cells need to be stimulated for a long period of time  $\text{Ca}^{2+}$  transients are repeated at set intervals leading to a pattern of  $\text{Ca}^{2+}$  oscillations (Berridge, 2012).

### III.1.1 Cytosolic $\text{Ca}^{2+}$ concentration increase (ON reactions)

As described before,  $\text{Ca}^{2+}$  signalosome can vary from cell type to cell type, although all of them base their  $\text{Ca}^{2+}$  homeostasis toolkit in different channels that get activated after a stimulus arrives to the cell, both in the plasma membrane and in the endoplasmic reticulum.

$\text{Ca}^{2+}$  entry to the cell from the extracellular space is one of the main components of the ON reactions. This phenomenon is driven by the presence of an electrochemical gradient across the plasma membrane. When a stimulus arrives to the cell a plethora of channels present in the plasma membrane with different properties get activated (figure 27). Among the channels that take part in  $\text{Ca}^{2+}$  signaling we can find the **voltage operated channels (VOCs)**, found in

excitable cells which generate rapid  $\text{Ca}^{2+}$  fluxes that control processes such as muscle contraction and exocytosis in synaptic endings; the **receptor operated channels (ROCs)**, such as NMDA receptors that respond to glutamate; the **second-messenger operated channels (SMOCs)**, controlled by internal messengers; and the **store-operated channels (SOCs)** that can respond to  $\text{Ca}^{2+}$  depletion of the stores; and **transient receptor potential channels (TRPC)** that respond to numerous stimuli including temperature and stretch activation (Berridge et al., 2003). All these channels are opened for a short period of time, but it is enough to cause significant cytosolic  $\text{Ca}^{2+}$  concentration  $[\text{Ca}^{2+}]_{\text{cyt}}$  changes, mainly in the proximity of the channels conforming microdomains (Rizzuto and Pozzan, 2006).

The second main component of the ON reactions is the release of  $\text{Ca}^{2+}$  to the cytoplasm from the ER. The channels responsible for this release are the **inositol-1,4,5-trisphosphate receptors ( $\text{IP}_3\text{R}$ )**, and the **ryanodine receptors (RyRs)**. Both of these channels can be activated by  $[\text{Ca}^{2+}]$  increases in a process known as calcium induced calcium release (CICR). Besides this common regulatory mechanism, both channels activities can be modulated by different signals. The  $\text{IP}_3\text{R}$  can be activated by  $\text{IP}_3$ . When  $\text{IP}_3$  binds to the receptor it increases its sensitivity to  $\text{Ca}^{2+}$  having a dual effect: it functions as an activator at low  $[\text{Ca}^{2+}]_i$ , and as an inhibitor at high concentrations. Also,  $\text{IP}_3\text{R}$  can be modulated by different kinases including  $\text{Ca}^{2+}/\text{CaM}$ -dependent kinase II (CaMKII), cGMP-dependent protein kinase (PKG), protein kinase C (PKC), and cAMP-dependent protein kinase (PKA) (Berridge et al., 2003). **Ryanodine receptors (RyRs)** are also regulated by a variety of small proteins and phosphorylation. They can respond to several molecules including caffeine, ATP, or heparin, and be activated by voltage channels in the absence of  $\text{Ca}^{2+}$  during excitation-contraction coupling (Rios and Brum, 1987).

### III.1.2 Restoration of cytosolic $\text{Ca}^{2+}$ concentration (OFF reactions)

After the ON reactions have allowed the increase of  $[\text{Ca}^{2+}]_{\text{cyt}}$ , the cells need to return to their basal state so they can respond to new stimuli. To achieve this goal different pumps, channels and buffers get activated. The main component of the OFF reactions is the activity of different pumps that remove  $\text{Ca}^{2+}$  from the cytoplasm against the electrochemical gradient, with an energetic cost to the cells. Mainly, there are two different types of pumps in the cells, the plasma membrane  $\text{Ca}^{2+}$  ATPase (PMCA), and the **sarco-endoplasmic reticulum  $\text{Ca}^{2+}$  ATPase (SERCA)**. Both are P type ATPases that transport  $\text{Ca}^{2+}$  with different equilibriums. While PMCA transports 1  $\text{Ca}^{2+}$  per ATP hydrolyzed, SERCA transports two  $\text{Ca}^{2+}$  ions per ATP hydrolyzed (Clapham, 1995).

Pumps are not the only mechanism that cells have developed to restore  $[Ca^{2+}]_{\text{cyt}}$ . The other participants in the OFF reactions are  **$Na^+/Ca^{2+}$  exchangers (NCX)**,  $Ca^{2+}$ -binding proteins, like calmodulin, and mitochondria. The NCX are transporters from the SLC8 protein family that can be found in the plasma membrane and the mitochondria (will be discussed in more detail in section III.3, p67). All these proteins transport  $Ca^{2+}$  to the extracellular media in an electrogenic way. In the case of the NCX it transports three  $Na^+$  ions to the cytoplasm and extrudes one  $Ca^{2+}$  ion. Interestingly, as the gradient of  $[Na^+]$  between the intracellular and extracellular space regulate NCX activity, the exchanger can act in reverse, meaning that it may shift ion transport direction when  $[Na^+]_c$  increases (Brini and Carafoli, 2011).

All these mechanisms have different thresholds for activity as indicated in figure 23. ATPases have lower transport rates but high affinities being able to sense modest elevations in  $[Ca^{2+}]_{\text{cyt}}$  and being responsible for the maintenance of resting  $Ca^{2+}$  concentration levels. The NCX and other channels in mitochondria, have bigger transport rates and can regulate  $Ca^{2+}$  transients over a wider dynamic range. For example, the optimal mitochondrial  $Ca^{2+}$  uptake is achieved when cytosolic  $Ca^{2+}$  reaches concentrations of several  $\mu\text{M}$  (Berridge et al., 2003).

### III.2 Mitochondrial $Ca^{2+}$ dynamics

Mitochondria are double-membrane-bounded organelles that are able to respond rapidly and efficiently to changes in  $[Ca^{2+}]_c$  thanks to the electrochemical gradient provided by the action of the Electron Transport Chain (ETC) that generates the driving force necessary to accumulate cations in the mitochondrial matrix (Granatiero et al., 2017). The two membranes that delimitate mitochondria have different permeabilities to ions and small peptides. The most exterior one, the outer mitochondrial membrane (OMM) allows its entrance to the intermembrane space through the **voltage-dependent anion channels (VDAC)**. The inner mitochondrial membrane (IMM) is considered impermeable to ions being necessary the activity of ETC to create an electrochemical gradient that allows the entrance of ions to the mitochondrial matrix. The accumulation of  $Ca^{2+}$  in the mitochondria is possible due to the existence of the **mitochondrial calcium uniporter (MCU)** that gets activated by an increase in  $[Ca^{2+}]_c$ , allowing the uptake of  $Ca^{2+}$  by mitochondria using the electrochemical gradient. As should be expected, there are also mechanisms to extrude  $Ca^{2+}$  from this organelle.  $Ca^{2+}$  efflux to the cytoplasm can be driven through two different exchangers, the **mitochondrial  $Na^+/Ca^{2+}$  exchanger (mNCX)**, and the mitochondrial  $H^+/Ca^{2+}$  exchanger (mHCX). Both exchangers are responsible of maintaining the electrochemical gradient (Rimessi et al., 2008).

### III.3 *C. elegans* Ca<sup>2+</sup> signaling toolkit

If not every protein, channel, and exchanger described before, almost all of them are present in its homolog form in *C. elegans*. This fact is reasonable if it is taken into account that as mentioned before, these nematodes do not have Na<sup>+</sup> based action potentials, thus relying its control in Ca<sup>2+</sup> signaling. There are numerous homologs for all the machinery complex (figure 27), although the amount of homologs per channel can vary between mammals and nematodes.

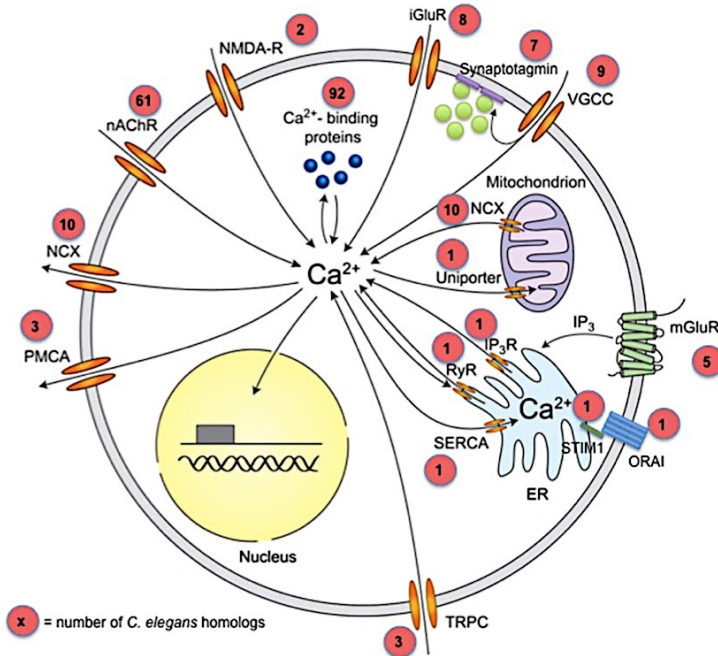


**Figure 27. Neuronal Ca<sup>2+</sup> signaling toolkit in *C. elegans*.** Due to the importance of neuronal Ca<sup>2+</sup> signaling in *C. elegans*, its machinery has been studied in neurons. In this image are represented all the proteins implicated in Ca<sup>2+</sup> influx and efflux. In the red circles are indicated the amount of homologs present in *C. elegans* for each protein. Ca<sup>2+</sup> influx to the cytoplasm is driven by channels present in the plasma membrane including voltage gated Ca<sup>2+</sup> channels (VGCC), and ligand operated channels (NMDAR, AChR, iGluR). The extrusion of Ca<sup>2+</sup> from the ER is performed by ITR-1, the only homolog of the IP<sub>3</sub> receptor, and UNC-68, the homolog for the RyR. As for mitochondria there is only one homolog for MCU thought to introduce Ca<sup>2+</sup> to the mitochondrial matrix. The efflux mechanisms include the three PMCA homologs (*mca-1*, *mca-2* and *mca-3*), and the SERCA homolog SCA-1. To maintain [Ca<sup>2+</sup>]<sub>c</sub> ten different isoforms of Na<sup>+</sup>/Ca<sup>2+</sup> exist in *C. elegans* present in the plasma membrane and the mitochondria (From Hobert 2012).

There is just one SERCA homolog in *C. elegans* named *sca-1* that codes for two different SCA-1 isoforms that show differential functional characteristics and expression patterns. The alternative splicing needed for the second isoform

happens at a homologous position in the worm transcript as in vertebrates. As for their expression pattern, SCA-1a is expressed in head muscles, pharynx, and intestine, while SCA-1b can be found in the reproductive system organs and vulva muscles. Both isoforms are expressed in body wall muscle. Finally, it is important to mention that it has been proven that thapsigargin is able to inhibit irreversibly SCA-1 proteins (Zwaal et al., 2001).

The case of NCX exchangers family is different. There are ten different isoforms in *C. elegans* (*ncx-1* – *ncx-10*) that are widely expressed in different tissues and cell types (table 2) and exhibit different properties. The first group of this protein family is formed by the three first isoforms (*ncx-1* – *ncx-3*), which belong to the NCX family of exchangers. *ncx-1* is the most closely related NCX transporter to the human orthologs, although all of them are structurally similar to mammalian NCX exchangers presenting two Na<sup>+</sup>/Ca<sup>2+</sup> exchanger domains and an intracellular loop containing two Ca<sup>2+</sup>-binding domains. The second group is formed by *ncx-4* and *ncx-5*, which encode for proteins that belong to the NCKX exchangers. Finally, the rest of isoforms (*ncx-6* – *ncx-10*) belong to the CCX exchanger family (Sharma et al., 2013).

Gene	Sequence	Expression pattern in adult hermaphrodites
<i>ncx-1</i>	Y113G7A.4	AIY neurons
<i>ncx-2</i>	C10G8.5	Pharyngeal muscle including procorpus, metacarpus, isthmus, and terminal bulb, body-wall muscle, enteric muscle, and vulval muscle.
<i>ncx-3</i>	ZC168.1	Head neurons, dorsal/ventral nerve cord and commissures, phasmid neurons
<i>ncx-4</i>	F35C12.2	AWC, ASE, two pairs of labial neurons, ventral/dorsal nerve cord and commissures, faint expression on one pair of nondye-filling posterior neurons
<i>ncx-5</i>	Y32F6B.2	URX, AQR, and BAG anterior neurons and PQR phasmid neurons
<i>ncx-6</i>	C07A9.4	ADL neuron, intestine
<i>ncx-7</i>	C07A9.11	ADL neuron, intestine, one pair of posterior cells
<i>ncx-8</i>	C13D9.7	Pharyngeal muscle including procorpus, metacarpus, isthmus and terminal bulb; intestine
<i>ncx-9</i>	C13D9.8	Very faint expression in neurons
<i>ncx-10</i>	Y97E10B.7	Pharyngeal muscle, mainly in the terminal bulb

**Table 2: *C. elegans* *ncx* genes and their expression pattern.** AWC: Amphid wing “C” cells; ASE: Amphid neurons; URX: nonciliated dendritic endings in nose; AQR, BAG, PQR: oxygen sensory neurons. Modified from Sharma et al. 2013.

### III.4 Mitochondria-ER Associated Membranes (MAMs)

One of the main properties of  $\text{Ca}^{2+}$  signaling is its spatial location, in the sense that there are highly regulated spots in the cells that conform cellular microdomains. Among this type of  $\text{Ca}^{2+}$  signaling regulation, Mitochondria-ER Associated Membranes (MAMs) have been gaining interest in the last decades as more and more physiological and pathological events seem to be regulated by these structures.

MAMs are defined as a physical association between ER and mitochondria membranes that conform an entity with a defined structure and architecture, fundamental for the maintenance of  $\text{Ca}^{2+}$  homeostasis. This physical proximity between membranes provides a direct, selective transmission of physiological and pathological  $\text{Ca}^{2+}$  signals (Patergnani et al., 2011; Marchi et al., 2017). MAMs are highly specialized subcellular compartments shaped by ER subdomains juxtaposed to mitochondria but biochemically different from both organelles (Morciano et al., 2018).

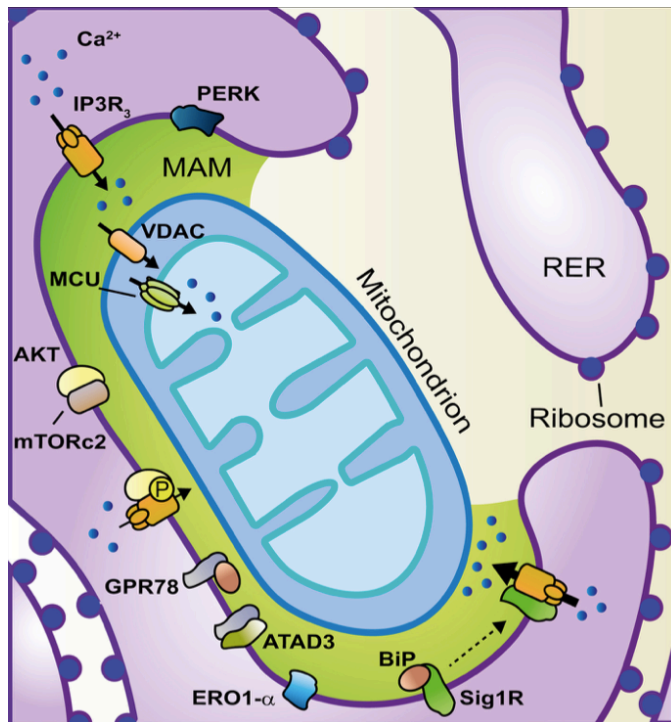


**Figure 28. MAM-resident proteins.** MAMs conform a cellular microdomain by establishing tight interactions between mitochondria and ER membranes. These are highly regulated structures in the cells, where numerous proteins and pathways interplay with each other. Modified from Morciano et al. 2018.

These structures are formed by numerous molecular components (figure 28), being enriched in several proteins including  $\text{Ca}^{2+}$  channels and pumps as SERCA,  $\text{IP}_3\text{R}$ , and the  $\text{Ca}^{2+}$ -binding mitochondrial carrier SLC25A12 (Sala-Vila et al., 2016). Besides the enrichment in  $\text{Ca}^{2+}$  homeostasis related proteins, MAMs are also formed by different chaperones, as calnexin and sigma-1 receptors (Sig1R) (Hayashi and Su, 2007). Sig1R seem to be involved in the response to ER stress. At basal conditions the receptor is forming a complex with BiP. When  $[\text{Ca}^{2+}]_{\text{ER}}$  drops by  $\text{IP}_3\text{R}$  activation, the complex is dissociated activating the chaperone activity of BiP (Mendes et al., 2005). Finally, there has also been described a link between MAMs, nutrient signaling pathways, and autophagy. MAMs are enriched in the promyelocytic leukemia protein (PML) which is able to modulate the autophagic process by the regulation of AMPK/mTOR/Ulk1 pathway (Missiroli et al., 2016; Marchi et al., 2017).

### III.5 $\text{Ca}^{2+}$ signaling and nutrient signaling pathways

There is not too much evidence about the interplay between  $\text{Ca}^{2+}$  signaling and nutrient signaling pathways, although some recent studies have shown that at least two of the four pathways are regulated at some level by changes in intracellular  $\text{Ca}^{2+}$  (figure 29).

AMPK can be activated by numerous stimulus described in section II.4.3, p54. Among the canonical mechanisms of activation of AMPK its phosphorylation by  $\text{Ca}^{2+}$ -calmodulin protein kinase  $\beta$  after an increase of  $[\text{Ca}^{2+}]_c$  allows the modulation of this pathway by  $\text{Ca}^{2+}$  signaling (Woods et al., 2005; Jeon, 2016). Also, as the main energy sensor in the cells, AMPK responds to changes in ATP/AMP ratio, which conforms another regulatory spot for  $\text{Ca}^{2+}$  signaling since ATP production by mitochondria is controlled by mitochondrial  $\text{Ca}^{2+}$  uptake. Also, to increase ATP production AMPK is able to activate the MCU (Zhao et al., 2019). Besides its effects in mitochondrial  $[\text{Ca}^{2+}]$ , AMPK is also able to modulate ER  $\text{Ca}^{2+}$  signaling by inhibiting  $\text{IP}_3\text{R}$  (Arias-Del-Val et al., 2019) and/or RyR (Yavari et al., 2017) leading to a decreased  $\text{Ca}^{2+}$  release by the ER, which may also contribute to modulate mitochondrial metabolism and autophagy through MAMs  $\text{Ca}^{2+}$  transfer regulation (Gomez-Suaga et al., 2017; Ahumada-Castro et al., 2019).

The other pathway that is known to be regulated by  $\text{Ca}^{2+}$  signaling is the mTOR pathway, although much less about its regulation has been elucidated. On one hand, it is reasonable to assume that  $\text{Ca}^{2+}$  signalling should modulate mTOR activity through AMPK activation, as these two pathways interplay with each other (Pan and Finkel, 2017) (see section II.6, p59). In addition, a direct activation of mTOR by  $\text{Ca}^{2+}$  has been described in response to amino acids (Carroll et al.,



2015) and physical exercise (Ito et al., 2013). Finally, mTOR is able to modulate by itself  $\text{Ca}^{2+}$  signalling by activating plasma membrane store-operated  $\text{Ca}^{2+}$  channels (Ogawa et al., 2012; Peng et al., 2013), and  $\text{IP}_3\text{R}$  in the ER (MacMillan et al., 2005; Régimbald-Dumas et al., 2011), thus contributing to generate a larger increase in  $[\text{Ca}^{2+}]_{\text{cyt}}$ .

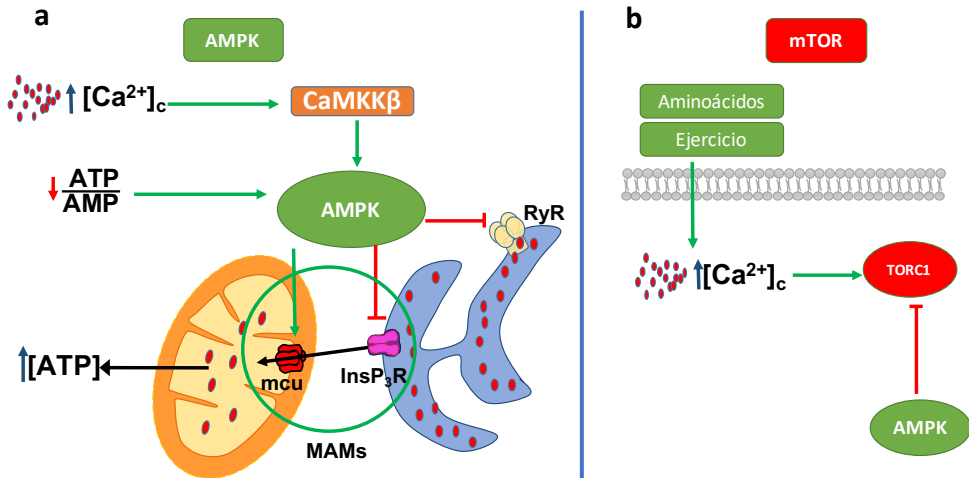


**Figure 29. Regulation of AMPK and mTOR signaling pathways by  $\text{Ca}^{2+}$  signaling.** a) one of the canonical ways of activation of AMPK is through its phosphorylation by  $\text{CaMKK}\beta$ , activated by an increase in intracellular  $\text{Ca}^{2+}$ . Besides this regulation, AMPK is able to modulate  $\text{Ca}^{2+}$  signaling by modulating  $\text{Ca}^{2+}$  dynamics in mitochondria and the ER. It is able to activate MCU increasing  $[\text{Ca}^{2+}]$  in mitochondria, and it also inhibits  $\text{Ca}^{2+}$  release channels in the ER,  $\text{IP}_3\text{R}$ , and RyR, which seems to be an important way of regulation of  $\text{Ca}^{2+}$  transfer from the ER to the mitochondria in MAMs. b) mTOR regulation by  $\text{Ca}^{2+}$  is less clear, although it is known that it gets activated by an increase of intracellular  $\text{Ca}^{2+}$  in response to amino acids and physical exercise. Also, as AMPK and mTOR pathways interplay, AMPK activation by  $\text{Ca}^{2+}$  causes mTOR inhibition.

Although little knowledge about the regulation of nutrient sensing pathways by  $\text{Ca}^{2+}$  signaling has been elucidated, it seems clear that cytosolic and mitochondrial  $[\text{Ca}^{2+}]$  act as intracellular modulators of AMPK and mTOR activity, depending on the ER  $[\text{Ca}^{2+}]$  levels, ER  $\text{Ca}^{2+}$  release and ER to mitochondria  $\text{Ca}^{2+}$  transfer, especially in MAMs.

## IV. AGING AND CALCIUM SIGNALING

### IV.1 Dysregulation of Ca<sup>2+</sup> signaling in aging and neurodegeneration

It has been clear for several decades that Ca<sup>2+</sup> homeostasis dysregulation is one of the common features that appears as the organisms age. This observation led to the postulation of the so called “**Calcium hypothesis of Alzheimer’s disease and brain aging**” nearly 40 years ago (Khachaturian, 1984). This theory sustains the idea that a continuous disruption of some of the mechanisms that regulate intracellular Ca<sup>2+</sup> homeostasis trigger adverse changes in the function of neurons leading to neuronal dysfunction and chronic brain disorders in aging. The loss of the fine regulation of Ca<sup>2+</sup> homeostasis seems to be a consequence of numerous upstream events including metabolic, oxidative, and proteotoxic stress causing changes in several Ca<sup>2+</sup> signaling players including ion channels, buffers, and ATP-dependent ion pumps (Workgroup, 2017). As the aging research field has evolved, the underlying mechanisms of Ca<sup>2+</sup> dysregulation in aging and neurodegenerative diseases that support the *Calcium hypothesis* have been described including energy-generating deficits and accumulation of oxidative damage (Carafoli, 2003; Starkov and Beal, 2008); impaired lysosomal function and autophagic mechanisms (Colacurcio and Nixon, 2016); diminished ability to respond to metabolic challenges or cellular stress (Mattson, 2004; Bezprozvanny and Mattson, 2008); increased protein aggregation (Mrak and Griffin, 2007; Wyss-Coray and Rogers, 2012); and activation of immune responses (Workgroup, 2017).

Regarding the involvement of Ca<sup>2+</sup> homeostasis dysregulation in the development and prevalence of Alzheimer’s disease (AD) it is now known that A $\beta$  oligomers and tau, two main pathological indicators of the disease, can induce increases of [Ca<sup>2+</sup>]<sub>cyt</sub> mediated by several mechanisms, including an increase in Ca<sup>2+</sup> entry to the cytosol through voltage or receptor-operated Ca<sup>2+</sup> channels, and the inhibition of its extrusion through the plasma membrane by PMCA or the Na<sup>+</sup>/Ca<sup>2+</sup> exchanger (Wang and Zheng, 2019). Additionally, Alzheimer’s disease has also been linked to changes in ER Ca<sup>2+</sup> dynamics linked with an increased sensitivity or expression level of IP<sub>3</sub>R and RyR induced by A $\beta$  oligomers and presenilins mutations. There is also evidence that MAMs are important for the development of the disease as some of the proteins known to cause it, like presenilins and APP, are preferentially located in this structures, increasing Ca<sup>2+</sup> transfer from ER to mitochondria in MAMs (Rossi et al., 2019; Vallese et al., 2020).

The *Calcium hypothesis* has been revised several times (Berridge, 2010; Workgroup, 2017) due to the increased knowledge in Ca<sup>2+</sup> signaling and aging, extending the theory to other neurodegenerative diseases including Parkinson’s (PD) and Huntington’s diseases. In PD has also been described an increased [Ca<sup>2+</sup>]<sub>c</sub>

(Post et al., 2018; Ludtmann and Abramov, 2018) preceded by a transitory  $\text{Ca}^{2+}$  decrease caused by  $\alpha$ -synuclein aggregates activation of SERCA pumps that seems to be important in the cell damage response, as the treatment with SERCA inhibitors in *C. elegans* increase cell viability (Betzer et al., 2018).

ER  $\text{Ca}^{2+}$  dynamics in aging and neurodegeneration cannot be taken into account in an isolated manner since this organelle establishes tight connections with mitochondria, so it is not rare that mitochondrial dysfunction has been known to be a common feature in aging and neurodegeneration, being the opening of MPTP and altered  $\text{Ca}^{2+}$  handling the main events prior to cell death (Lin and Beal, 2006; Wojda et al., 2008; Cali et al., 2012). Specifically, in AD disease A $\beta$  oligomers can be transported to the mitochondrial matrix reducing the activity of the ETC (Caspersen et al., 2005). This fact, together with the increased  $\text{Ca}^{2+}$  release promoted by A $\beta$  oligomers induce mitochondrial  $\text{Ca}^{2+}$  overload and cell death (Ferreiro et al., 2008; Sanz-Blasco et al., 2008).

#### **IV.2 C. elegans: insights in $\text{Ca}^{2+}$ signaling, aging, and neurodegeneration**

The availability of numerous mutants for proteins and channels related with  $\text{Ca}^{2+}$  signaling, as well as models for most neurodegenerative diseases has made *C. elegans* a model of choice to study the relationship between  $\text{Ca}^{2+}$  dyshomeostasis, aging, and neurodegeneration.

Particularly, using loss-of-function mutants for IP $_3$ R (*itr-1*), RyR (*unc-68*), and calreticulin (*crt-1*) the implication of  $\text{Ca}^{2+}$  signaling in neurodegenerative diseases, has been shown in *C. elegans*. For example, the phenotype caused by defective dopaminergic neurons in worms was suppressed by loss-of-function mutations for *itr-1*, *unc-68*, and *crt-1* (Nagarajan et al., 2014). Additionally, the effects of SERCA inhibition in neurodegeneration have also been explored, observing different outcomes for different diseases. While in some models the treatment with thapsigargin induced neurodegeneration, in other models including AD (Griffin et al., 2019) and PD (Betzer and Jensen, 2018), SERCA inhibition exerts a neuroprotective effect, which correlates with the fact that the SERCA homolog in *C. elegans*, *sca-1*, undergoes a large expression decrease during aging (Copes et al., 2015). All this evidence suggests that reduced ER  $\text{Ca}^{2+}$  release might be an important intervention to promote longevity and neuroprotection.





## **MOTIVATION AND AIMS**







Aging is one of the main risk factors known for the development of a complex onset of diseases including cardiovascular diseases, cancer, and neurodegeneration. This is the reason that has motivated the scientific community to search for interventions that delay this process in a way that the healthspan of the individuals gets improved.

The model organism *Caenorhabditis elegans* has been established as a genetic model to study the aging process helping to untangle the molecular mechanisms that regulate aging. Among them, four metabolic pathways, called nutrient sensing pathways, have been deeply investigated in this model organism revealing that the modulation of their activity leads to changes in the aging process. This group is formed by the insulin/IGF-1 signaling pathway, the mTOR signaling pathway, the AMPK signaling pathway, and the sirtuins pathway. All of them establish complex interconnections between them, and recent studies have revealed that  $\text{Ca}^{2+}$  signaling might be one of the main regulatory mechanisms that control their activity.

Due to the lack of information about how  $\text{Ca}^{2+}$  signaling modulates the activity of nutrient sensing pathways, the main objective of this thesis is to investigate the interrelationship between  $\text{Ca}^{2+}$  signaling and nutrient sensing pathways regulation in the model organism *Caenorhabditis elegans*. To address this goal, this work has been structured in two main axes based on the modulation of  $\text{Ca}^{2+}$  signaling by two different pharmacological interventions:

**Aim 1: Study the effects of SERCA inhibitors in *C. elegans* lifespan and its possible modulation of nutrient sensing pathways.**

To achieve this goal the following experiments have been carried out in the presence or absence of two different SERCA inhibitors: 2,5-BHQ and thapsigargin.

- Survival assays in wildtype worms to study the effects of SERCA inhibitors in *C. elegans* lifespan.
- Survival assays in long-lived *C. elegans eat-2* mutants to evaluate the possible induction of a caloric restriction response after the treatments.
- Survival assays in short and long lived nutrient sensing pathways *C. elegans* mutants to investigate the interrelationship between  $\text{Ca}^{2+}$  signaling modulators activity and these pathways including:
  - IIS mutants *daf-2* and *daf-16*
  - mTOR mutants *daf-15* and *rsk-1*
  - AMPK mutants *aak-2* and *aak-1;aak-2*
  - Sirtuins mutant *sir-2*



- Survival assays in the long-lived ETC mitochondrial mutant *nuo-6* to evaluate the importance of mitochondrial activity in  $\text{Ca}^{2+}$  modulation effects.
- ER stress assessment to investigate the possible effect of SERCA inhibitors in the ER stress response pathway.

**Aim 2: Study the effects of the mitochondrial  $\text{Na}^+/\text{Ca}^{2+}$  exchanger (mNCC) inhibitor CGP37157 in *C. elegans* healthspan and its possible modulation of nutrient sensing pathways.**

To achieve this goal the following experiments have been carried out in the presence or absence of the mNCC inhibitor CGP37157:

- Survival assays in wildtype *C. elegans* worms.
- Survival assays in long-lived *C. elegans eat-2* mutants to evaluate the possible induction of a caloric restriction response after the treatment.
- Survival assays in short and long-lived nutrient sensing pathways *C. elegans* mutants to investigate the interrelationship between  $\text{Ca}^{2+}$  signaling modulators activity and these pathways including:
  - IIS mutants *daf-2* and *daf-16*
  - mTOR mutants *daf-15* and *rsk-1*
  - AMPK mutants *aak-2* and *aak-1;aak-2*
  - Sirtuins mutant *sir-2*
- Survival assays in the long-lived ETC mitochondrial mutant *nuo-6* to evaluate the importance of mitochondrial activity in CGP37157 effects.
- Assessment of CGP37157 effects on  $\text{Ca}^{2+}$  dynamics studying:
  - cytosolic  $\text{Ca}^{2+}$  oscillatory patterns in the pharynx
  - mitochondrial  $\text{Ca}^{2+}$  oscillatory patterns in the pharynx
  - cytosolic transients in vulva body wall muscle cells.
- Electropharyngeograms to evaluate possible changes of the electrophysiological properties of pharyngeal pumping after the treatment with CGP37157.
- Assessment of CGP37157 effects in several biomarkers of aging in *C. elegans* including:
  - locomotion
  - egg laying rate
  - *hsp-16.2* expression
  - mitochondrial activity through the evaluation of ATP production in treated and untreated worms.
- Assessment of CGP37157 effects in the evolution of sarcopenia and mitochondrial distribution and morphology during aging.





**METHODS AND  
MATERIALS**





## I. C. ELEGANS STRAINS

### I.1 C. elegans control strains

#### I.1.1 Wildtype strain (N2)

Wildtype strain. Known as the Bristol strain of *C. elegans*, was described for the first time by Sydney Brenner in 1963 (Brenner, 1974). Normally used by most laboratories as the control *C. elegans* strain providing a single genetic background.

#### I.1.2 Control strains with fluorescent indicators

##### I.1.2.1 Strains with cytosolic Ca<sup>2+</sup> probes

- **AQ2038 (*pmyo2::YC2.1*):** This strain has been used in this work as the control strain to perform lifespan assays as well as to study cytosolic Ca<sup>2+</sup> dynamics in the pharynx. It is an integrated strain that expresses the fluorophore cameleon YC2.1 (Miyawaki et al., 1997; Nagai et al., 2004) in the pharyngeal muscle cells driven under the promoter *myo2*. Moreover, it has been demonstrated that the expression of the probe does not modify the expectancy of *C. elegans* population (Alvarez-Illera et al., 2016; García-Casas et al., 2018).
- **AQ2121 (*pmyo3::YC2.1*):** Integrated strain that expresses cameleon YC2.1 in the body wall muscle cells. It has been used as the control strain to perform motility assays, to study cytosolic Ca<sup>2+</sup> dynamics in the muscular cells of the vulvae, and to evaluate the effects of CGP37157 in sarcopenia.

##### I.1.2.2 Strains with mitochondrial Ca<sup>2+</sup> probes

- **AQ3055 (*pmyo-2::2mt8::YC3.60*):** Strain that expresses mitochondrial yellow cameleon 3.60 (YC3.60) as an extrachromosomal array on pharynx muscular cells, under the *myo-2* promoter. This strain has been used to study the effects of the treatments in mitochondrial Ca<sup>2+</sup> dynamics of pharynx muscular cells (Alvarez-Illera et al., 2017).
- **SJ4103 (*zcls14[myo-3::GFP(mit)]*):** Wildtype strain that expresses GFP at high levels in mitochondria of body wall muscle cells. It has been used



to study the possible effects of CGP37157 in mitochondria distribution and morphology by confocal microscopy (Benedetti et al., 2006).

### 1.1.3 Strains with stress reporters

- **SJ4005 (*zcls4[hsp-4::GFP]*):** Stable transgenic line expressing GFP when the *hsp-4* gene is transcribed. *hsp-4* is the *C. elegans* ortholog of the mammalian ER-localized Hsp70 chaperone BiP, that is upregulated in response to ER stress. That is why we have used this strain as a way to study ER stress in *C. elegans*. (Kapulkin et al., 2005)
- **TJ375 (*gpls1[hsp-16.2p::CFP]*):** Stable transgenic line that induces GFP expression when *hsp-16.2* is transcribed. *hsp-16.2* is the *C. elegans* ortholog of human CRYAA (crystallin alpha A), CRYAB (crystallin alpha B), and HSPB1 (heat shock protein family B (small) member 1) that localizes in the cytoplasm and has a role in the unfolded protein response. Therefore we have used this strain to evaluate cytoplasmic stress (Link et al., 1999).

<i>C. elegans</i> control strains					
STRAIN	GENOTYPE	PROBE	GROUP	METHOD	ORTHOLOG
N2	Wild type	-	-	Transcriptomics RT-PCR	-
AQ2038	<i>pmyo2::YC2.1</i>	Cameleon YC2.1	Cytosolic Ca <sup>2+</sup> probe	Lifespan Ca <sup>2+</sup> dynamics	-
AQ2121	<i>pmyo3::YC2.1</i>	Cameleon YC2.1	Cytosolic Ca <sup>2+</sup> probe	Ca <sup>2+</sup> dynamics Motility assay	-
AQ3055	<i>pmyo-2::2mt8::YC3.60</i>	Cameleon YC3.6	Mitochondrial Ca <sup>2+</sup> probe	Ca <sup>2+</sup> dynamics	-
SJ4103	<i>zcls14[myo3::GFP(mit)]</i>	GFP	Mitochondrial GFP	Confocal imaging	-
SJ4005	<i>zcls4[hsp-4::GFP]</i>	GFP	ER stress reporter	Stress induction	BiP
TJ375	<i>gpls1hsp-16.2p::GFP]</i>	GFP	Cytosolic stress reporter	Stress induction	CRYAA CRYAB HSPB1

**Table 3: *C. elegans* control strains.** The table summarizes all the control strains used in this work, indicating the genotype of the strain, if it has a fluorescent reporter, the methods where the strain has been used and the human ortholog in case the strain has a reporter gene.

## I.2 *C. elegans* mutant strains

### I.2.1 Nutrient sensitive pathways mutants

#### I.2.1.1 IGF-1 signaling pathway mutants

- **CB1370 (*daf-2(e1370) III*):** This strain has a mutation in the *daf-2* (abnormal DAuer formation) gene that causes a long-lived temperature sensitive phenotype having to maintain the strain at 15°C. *daf-2* gene codes for the insulin-like growth factor receptor (IGFR-1). Multiple studies in *C. elegans* have concluded that this gene is essential in the regulation of development, oxidative stress resistance, temperature, hypoxia and aging regulation (Kenyon, 2011).
- **CF1038 (*daf-16(mu86) I*):** *daf-16* (abnormal DAuer formation) is the ortholog gene of human FoXO1, FoXO3 and FoXO4. Mutant worms with a loss of function in *daf-16* exhibit Dauer defective forms and are short lived. *daf-16* transcription factor accumulates in the nucleus when *daf-2* is inactive, regulating the transcription of several genes involved in numerous processes including stress resistance, fat metabolism, and lifespan, among others (Tullet, 2015).

#### I.2.1.2 mTOR signaling pathway mutants

- **DR412 (*daf-15(m81)/unc24(e138)IV*):** *daf-15* (abnormal DAuer formation) gene encodes the *C. elegans* ortholog of Raptor. As Raptor is required for maturation to the adult state, the worms are heterozygous for the mutation, being enough to present a long-lived phenotype. Moreover, *daf-15* transcription is regulated by *daf-2* insulin/IGF signaling indicating that DAF-15 is a point of integration of nutrient sensitive pathways to regulate larval development, metabolism and longevity (Jia et al., 2004).
- **RB1206 (*rsk-1(ok125)*):** *rsk-1* (RSK-p70kinase homolog) is an ortholog of human S6K (ribosomal protein S6 kinase). S6K is a highly conserved signaling molecule that promotes cell growth and cell cycle progression in humans when is phosphorylated by TORC1. In *C. elegans* this mutation generates a long-lived population and the mutant gene has been implicated in numerous processes including metabolism, lifespan regulation and associative learning (Hansen et al., 2007; Sakai et al., 2017; Roy et al., 2018).



### I.2.1.3 AMPK signaling pathway mutants

- **RB754 (*aak-2(ok524) X*):** *aak-2* (AMP-Activated kinase 2) is an ortholog of human PRKAA2 (protein kinase AMP-activated catalytic subunit alpha 2). This gene is involved in several processes including the determination of adult lifespan. *aak-2* mutants exhibit a phenotype characterized by accelerated aging and reduced lifespan (Apfeld et al., 2004), and oxidative stress hypersensitivity (Lee et al., 2008).
- **AGD397 (*aak-1(tm1944) III; aak-2(ok524) X*):** *aak* (AMP activated kinase) has two catalytic subunits, alpha 1 and alpha 2. Therefore, we have used a model that has deletion for both of the catalytic subunits that would allow us to conclude if AMPK is required for lifespan extension. Like RB754 mutants, AGD397 worms exhibit reduced lifespan (Mair et al., 2011).

### I.2.1.4 Sirtuins signaling pathway mutants

- **VC199 (*sir-2.1(ok434) IV*):** *sir-2.1* (yeast SIR related) gene is an ortholog of human SIRT1 (sirtuin-1). This gene is involved in numerous processes including cellular protein modification, dauer larval development and adult lifespan. Although the VC199 does not express SIR-2.1, the phenotype has been described as superficially wildtype (Consortium, 2012).

### I.2.2 Mitochondrial mutants

- **MQ1333 (*nuo-6(qm200)*):** *nuo-6* (NADH Ubiquinone Oxidoreductase) gene is an ortholog of the human conserved subunit of mitochondrial complex I (NUDFB4). This mutation reduces the function of complex I leading to low oxygen consumption, slow growth, slow behavior, and increased lifespan (Yang and Hekimi, 2010).

### I.2.3 Caloric restriction mutants

- **DA1113 (*eat-2(ad1113) II*):** *eat-2* (EATing: abnormal pharyngeal pumping) is an ortholog of human CHRFA7, a selective acetylcholine gated cation-selective channel. Involved in several processes including action potential, regulation of eating behavior, and regulation of gene expression. It is

localized in the acetylcholine-gated channel complex and the neuromuscular junction of *pm4* and *pm5*. *eat-2* mutants phenotype is characterized by a decreased food intake, slower pharyngeal pumping and increased lifespan (Lakowski and Hekimi, 1998; McKay et al., 2004).

<i>C. elegans</i> mutant strains						
STRAIN	GENOTYPE	MUTATED GENE	ORTHOLOG	GROUP	PATHWAY	PHENOTYPE
CB1370	<i>daf-2(e1370) III</i>	<i>daf-2</i>	IGF1R INSR	NSP	IGF-1	- Temperature sensitive - Long-lived
CF1038	<i>daf-16(mu86) I</i>	<i>daf-16</i>	FOXO1 FOXO3 FOXO4	NSP	IGF-1	- Dauer defective - Short-lived
DR412	<i>daf-15(m81)/unc-24(e138) IV</i>	<i>daf-15</i>	RAPTOR	NSP	mTOR	- Long-lived
RB1206	<i>rsk-1(ok125)</i>	<i>rsk-1</i>	S6K	NSP	mTOR	- Long-lived
RB754	<i>aak-2(ok524) X</i>	<i>aak-2</i>	PRKAA2	NSP	AMPK	- Short-lived
AGD397	<i>aak-1(tm1944) II/aak-2(ok524) X</i>	<i>aak</i>	PRKAA1 PRKAA2	NSP	AMPK	- Short-lived
VC199	<i>sir-2.1(ok434) IV</i>	<i>sir-2.1</i>	SIRT1	NSP	Sirtuins	- Superficially WT
MQ1333	<i>nuo-6(qm200)</i>	<i>nuo-6</i>	NUDFB4	MITO	-	-Low oxygen consumption - Slow development - Long-lived
DA1113	<i>eat-2(ad1113) II</i>	<i>eat-2</i>	CHRFAM7	CR	-	- Decreased food intake -Reduced pharyngeal pumping - Long-lived


**Table 4: *C. elegans* mutant strains.** The table summarizes all the mutant strains used in this work, indicating the genotype of the strain, the group it belongs to (NSP: nutrient sensitive pathway; MITO: mitochondrial mutant; CR: caloric restriction mutant), the signaling pathway affected, and the resulting phenotype.

## II. C. ELEGANS LABORATORY MAINTENANCE

*C. elegans* strains were maintained and handled as it has been described by Stiernagle (Stiernagle, 2006) and kept at all times at 20°C unless otherwise indicated in the strain CGC specifications.

### II.1 Nematode Growth Medium (NGM)

The Nematode Growth Medium was described for the first time by Sydney Brenner (Brenner, 1974) and it is still the preferred way to maintain worms in the laboratory. NGM agar is prepared in 500 ml autoclavable bottles adding NaCl, agar, peptone and double distilled water. Then it is autoclaved for 20 minutes at 121°C and tempered in a hot water bath at 55° for at least 20 minutes. Once the medium has cooled to 55°C, and under sterile conditions, Cholesterol, CaCl<sub>2</sub>, MgSO<sub>4</sub> and KPO<sub>4</sub> buffer are incorporated to the medium, and the bottle is stirred to avoid the formation of precipitates.

NGM	Amount			Solution	Volume
NaCl	1,5 g		→	Cholesterol 5 mg/ml	500 µl
Peptone	1,25 g			CaCl <sub>2</sub> 1 M	500 µl
Agar	8,5 g			MgSO <sub>4</sub> *	500 µl
ddH <sub>2</sub> O	500 ml			KPO <sub>4</sub> Buffer (pH=6,00)**	500 ml

**Table 5: Nematode Growth Medium (NGM) composition:** compounds and solutions needed to prepare NGM. \* solutions were prepared in advance and autoclaved before being added to the media. \*\* KPO<sub>4</sub> buffer was also prepared in advance by adding 108,3 g KH<sub>2</sub>PO<sub>4</sub>, 35,6 g K<sub>2</sub>HPO<sub>4</sub>, and 1 liter of double distilled H<sub>2</sub>O. pH was adjusted to pH=6,00 before being autoclaved.

Once the NGM medium is ready, it is poured on the petri dishes at a constant volume, using a pipette controller. The volume poured into the plates depends on the petri dishes diameters. During this work we have used three different agar plates sizes, 35 mm, 60 mm and 100 mm Ø that contain 4 ml, 10 ml and 20 ml of NGM medium respectively.



### II.1.1 NGM FuDR agar plates

There are certain assays in this work that require the avoidance of the worm's progeny. Specifically, any population of worms involved in an assay that requires a synchronized adult population needs to be treated to avoid the progeny. To do that, is necessary to incorporate into the NGM plates 5-fluoro-2'-deoxyuridine (FuDR). This compound is a thymidylate synthase inhibitor that affects cell division, allowing the treatment to stop cell division inside the eggs or in larvae laid by the initial population of worms, without affecting the adults since their cells, once reached the adult state, do not divide again (Mitchell et al., 1979).

When needed FuDR was used at a final concentration of 15  $\mu$ M by adding 250  $\mu$ l of FuDR 30 mM to the 500 ml of liquid NGM medium before pouring the agar into the plates.

### II.1.2 NGM agar plates for pharmacological treatments

The main goal of this study pretends to elucidate the effects of different intracellular  $Ca^{2+}$  modulators on *C. elegans* lifespan and  $Ca^{2+}$  dynamics. One way to administer the drugs is to incorporate them at the effective concentration in the NGM agar plates. As in the case of the FuDR, the drugs 2,5-BHQ and CGP37157 solved in DMSO were incorporated to the NGM medium at the desired concentration before pouring the plates. For thapsigargin treatment, the drug solved in DMSO was added on top of the OP50 lawn the same day the experiment starts.

## II.2 *E. coli* OP50: worm's bacterial food source

### II.2.1 Active OP50 culture

OP50 *E. coli* strain has been used as *C. elegans* food source since it was described by Brenner in 1974. From a first culture, colonies are isolated on a streak plate prepared with LB agar medium and grown 8 hours at 37°C. A single colony is aseptically inoculated in 100 ml of sterile 2xYT medium. Then, the culture is allowed to grow to the saturation point another 8 hours at 37°C, or overnight at room temperature. Once the culture is ready, is stored at 4°C.



## II.2.2 Heat-inactivated OP50 culture

To really understand the effect of the different treatments on *C. elegans* lifespan, and to rule out any possible effect on lifespan as a result of the metabolization of the drugs by the bacterial culture, lifespan assays were performed using heat-inactivated OP50 cultures. To inactivate bacteria, the cultures were grown as indicated in point 4.2 and then incubated in a thermostatic bath at 65°C for 30 minutes. The result of the incubation is a batch of metabolic inactivated OP50 *E. coli*, without destroying the bacteria structural integrity (Gruber et al., 2007).

## II.3 Seeded NGM plates

After the plates are poured with the NGM, and dried for at least 12 hours, they are seeded with the OP50 culture that is needed for a particular assay. Three different plate sizes have been used in this work: small, medium, and large plates (35, 60 mm and 100 Ø respectively). For small and medium plates 250 µl of OP50 culture are added. The 100 Ø were seeded with 1 ml of OP50. Preferably, the food needs to stay in the center of the plates trying not to reach the edges, so the worms do not desiccate by crawling up the edges of the plates, as they tend to spend the majority of their time on the OP50 lawn (Stiernagle, 2006).

### III. PHARMACOLOGICAL TREATMENTS

#### III.1 Intracellular Ca<sup>2+</sup> modulators

##### III.1.1 Sarco-Endoplasmic Reticulum Ca<sup>2+</sup> ATPase inhibitors

###### III.1.1.1 Thapsigargin

Thapsigargin was isolated from the Mediterranean plant *Thapsia garganica* L. It belongs to a group of related, naturally occurring hexaoxygenated guianolides (Doan et al., 2015).

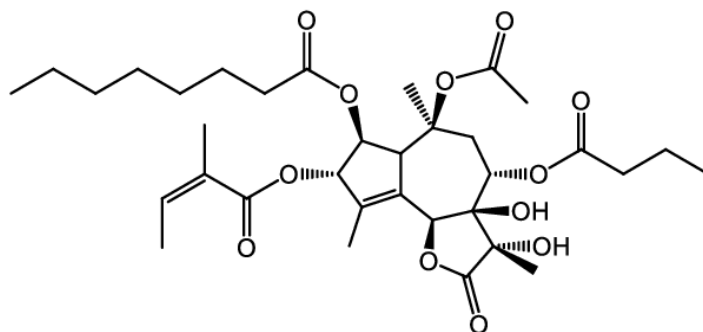


Figure 30: Thapsigargin molecule structure.

This molecule (figure 30) acts as an irreversible inhibitor of the Sarco-Endoplasmic Reticulum Ca<sup>2+</sup> ATPase in the subnanomolar range (Thastrup et al., 1990) which was first observed in cells in 1995 (Davidson and Varhol, 1995) and in *C. elegans* in 2001 (Zwaal et al., 2001). The binding of thapsigargin to SERCA prevents the conformational changes in the pump needed for its proper function. Consequently, the pump is not able to remove Ca<sup>2+</sup> ions from the cytosol and introduce them in the ER. Moreover, Ca<sup>2+</sup> can efflux from the ER to the cytosol. As a consequence, the SERCA is unable to maintain a high Ca<sup>2+</sup> concentration in the ER (Doan et al., 2015).

The potential medical benefits of thapsigargin have been discussed in the literature for a few years now. For example, it has become clear that application of this drug activates apoptosis in several cell types indicating that it could be a potential anti-cancer drug (Treiman et al., 1998).

### III.1.1.2 2,5-di-tert-butylhydroquinone (2,5-BHQ)

2,5-BHQ is an hydroquinone-type antioxidant (figure 31a) that acts as an inhibitor of SERCA, elevating intracellular  $\text{Ca}^{2+}$  concentration in several culture systems (Kass et al., 1989). The difference between thapsigargin and 2,5-BHQ is that while thapsigargin is a natural compound that inhibits SERCA irreversibly, 2,5-BHQ is a molecule that inhibits SERCA in a reversible way.

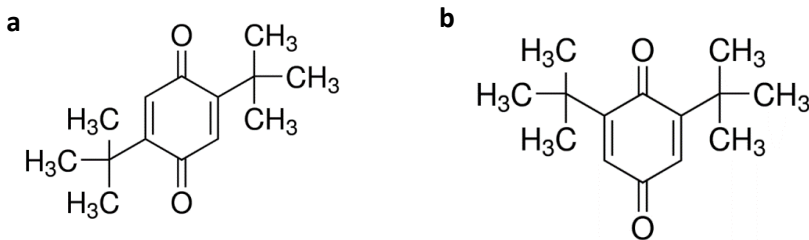


**Figure 31: 2,5-BHQ and 2,6-BHQ molecule structures. (a)** 2,5-Di-tert-butylhydroquinone is an antioxidant molecule with the ability to reversibly inhibit SERCA pumps. **(b)** 2,6-Di-tert-butylhydroquinone. Control treatment to evaluate the effects of 2,5-BHQ.

Because of the antioxidant properties of 2,5-BHQ a control treatment became necessary to be able to clarify if the effects of the treatment with 2,5-BHQ were due to the antioxidant effect or the SERCA inhibition properties of the molecule. For that purpose, **2,6-Di-tert-butylhydroquinone** (2,6-BHQ) an isomer that shows similar antioxidant properties (figure 31b) but not SERCA inhibitory action (García-Casas et al., 2018) has been used in this study as a control treatment for 2,5-BHQ.

## III.1.2 Mitochondrial $\text{Na}^+/\text{Ca}^{2+}$ exchanger (mNCX) inhibitor

### III.1.2.1 CGP37157

7-Chloro-5-(2-chlorophenyl)-1,5-dihydro-4,1-benzothiazepin-2(3H)-one (CGP37157, figure 32) is a cell-permeable benzothiazepine derivative of clonazepam that acts as an inhibitor of the mitochondrial  $\text{Na}^+/\text{Ca}^{2+}$  exchanger (mNCX), the main mitochondrial efflux pathway. Nevertheless, a series of off-target effects of the molecule have been described. They include the inhibition of L-type VDCC (Baron and Thayer, 1997), plasma membrane  $\text{Na}^+/\text{Ca}^{2+}$  exchangers (Cyz and Kiedrowski, 2003) or  $\text{Ca}^{2+}$  homeostasis modulator 1 (CALMH1)  $\text{Ca}^{2+}$  channels (Moreno-Ortega et al., 2015). Many of

these additional effects happen at the same concentration range being difficult to attribute the effects of the drug to a particular one.

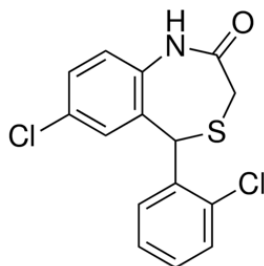
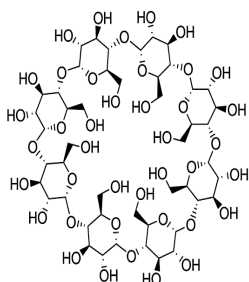


**Figure 32: molecular structure of CGP37157**

CGP37157 has been described as a neuroprotectant in several experimental models of neurotoxicity (Nicolau et al., 2009; Nicolau et al., 2010; González-Lafuente et al., 2012; Martínez-Sanz et al., 2015). However, it is remarkable that CGP37157 was not able to protect chromaffin cells or rat hippocampal slices against the combination of oxidative phosphorylation inhibitors oligomycin A and rotenone (Nicolau et al., 2010; González-Lafuente et al., 2012).

### III.2 $\gamma$ -cyclodextrin inclusion compounds

Due to the lipophilic nature of all the intracellular  $\text{Ca}^{2+}$  modulators, the question of how efficient the drug delivery is when the drug is incorporated in the NGM media came up. To answer it, we decided to include all these compounds in  $\gamma$ -cyclodextrin ( $\gamma$ -CD).



**$\gamma$ -CYCLODEXTRIN**

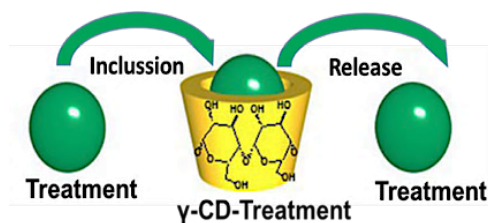


**Figure 33:  $\gamma$ -CD inclusion compounds.** Molecular structure of gamma-cyclodextrin showing the internal cavity with the ability to host lipophilic substances and take them to their place of action.



$\gamma$ -cyclodextrin is a cyclic oligosaccharide with the ability to include lipophilic substances on its cavity increasing the water solubility of the molecules included in it (figure 33). Moreover, the inclusion of the drugs in this molecule not only increases their solubility, but also limits the intake of the drug to oral administration (Kashima et al., 2012).

To obtain the inclusion compounds all the drugs were dissolved in DMSO at an initial concentration of 50mM. Briefly, a 230 mg/ml  $\gamma$ -CD sterile water solution was mixed 10:1 with the 50 mM DMSO solutions of each compound, stirred in a shaker at 1200 rpm for 20 hours and centrifuged at 12.500 rpm for 10 minutes. The supernatant was discarded and the resulting pellet (inclusion compounds) were dried in the hood. After the compounds are dried, they are weighted and solved at the desired concentration in M9 Buffer (table 6, p107). The resulting inclusion compounds were mixed with the OP50 culture to obtain the final desired concentration and added to the plate as indicated in the seeded NGM plates section.



#### IV. WORM'S POPULATION SYNCHRONIZATION

Worms synchronization is essential for almost every *in vivo* *C. elegans* assay. The method used to synchronize a population is the isolation of eggs so the larvae that will come from them will start developing almost at the same time (figure 34). To obtain the eggs, first is necessary to have a few plates containing adult worms carrying a lot of eggs inside of them. Once we have enough worms (2-3 plates) they are treated with a chemical (bleach-NaOH solution) and mechanical procedure (Stiernagle, 2006) as follows:

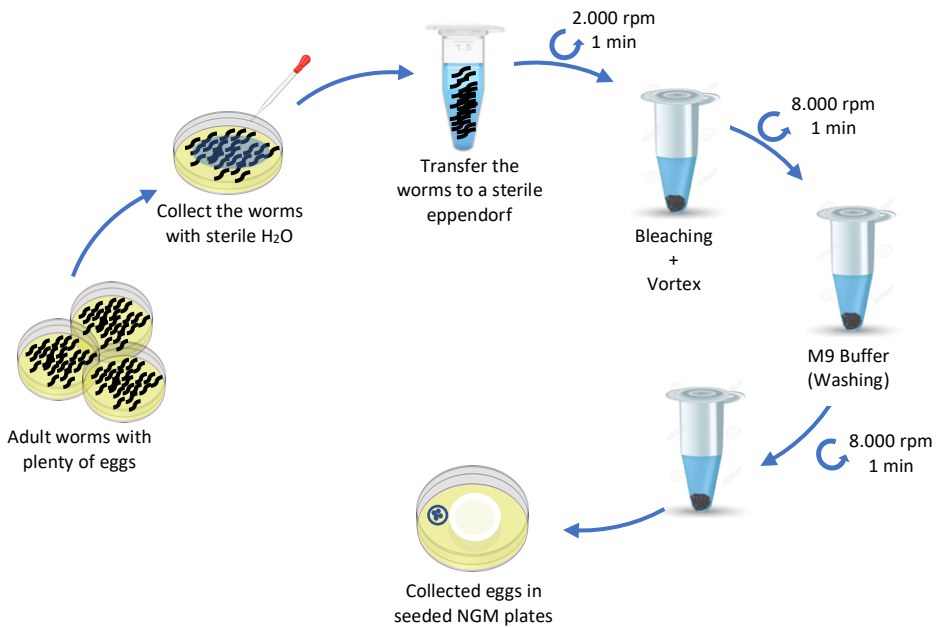


**Figure 34: worms population synchronization.** Representative scheme of the main steps of the protocol followed to obtain eggs.

Adult worms are collected with 1 ml sterile distilled H<sub>2</sub>O with a glass Pasteur pipette and transferred to a sterile eppendorf. To precipitate the worms, the sample is centrifuged at 2,000 rpm for 1 minute. The supernatant is carefully discarded. The next step is the chemical and mechanical treatment of the worms. To do that, we add to the eppendorf 250  $\mu$ l of M9 buffer (table 6, p107) and 150  $\mu$ l of bleaching solution (table 7, p107). Simultaneously, and for the next 10 minutes, the worms are vortexed for 10 seconds every 2 minutes. Then, the sample is centrifuged again at 8,000 rpm for 1 minute precipitating the eggs. The supernatant is carefully discarded and 1 ml of M9 Buffer is added to the eggs.



Finally, the sample is centrifuged again at 7200 g for 1 min. The resulting pellet contains the clean eggs. For the larvae to develop, the eggs are suspended in the M9 Buffer and transferred to NGM seeded plates. Once the M9 buffer has dried, the plates are placed in the incubator at 20°C.

Once the worms reach the young adult stage (day 1), a certain number of worms is transferred to the seeded FuDR NGM plates corresponding to the assay that needs to be done.



## V. IN VIVO *C. ELEGANS* ASSAYS

### V.1 *C. elegans* lifespan assay

When the synchronized population reaches the young adult stage (around 56 hours after egg laying for wildtype worms), 100 to 150 worms are transferred to either control or treatment 35 mm FuDR plates. There are different plates settings depending on the lifespan assay that is going to be performed:

- Control plates:
  - **NGM FuDR plates:** control plates for lifespan assays where the drugs are incorporated in the liquid NGM.
  - **NGM FuDR plates +  $\gamma$ -CD-Cholesterol:** control plates for lifespan assays where the drugs are delivered by inclusion compounds
- Treatment plates:
  - **Treatment NGM FuDR plates:** in this case the NGM poured in the plates already has the drug at the desired concentration.
  - **NGM FuDR plates +  $\gamma$ -CD-Drug:** inclusion compounds are incorporated to the plates with the OP50 at the desired concentration.

Around 15 worms are placed in each plate using a platinum wire, and 10 plates per condition are prepared. Control and treatment assays are always kept close together in a temperature controlled incubator at 20°C and performed in parallel. From that day on, all the plates are scored for alive, dead (worms that did not respond to touch with a platinum wire) and censored worms until the last worm is dead. There are several reasons for censorship that were established before starting the experiments:

- Fungal or bacterial contamination: plates with fungal contamination in the first days of experiment were excluded from the assay. If the contamination appears later on the worms remaining in the plate are censored.
- Missing worms
- Gonad extrusion
- Internal egg hatching
- Paralysis or uncoordinated movements

Finally, statistics are made with SPSS software using the Kaplan-Meier estimator and the log-rank routine for significance.

## V.2 C. elegans Ca<sup>2+</sup> dynamics assay

### V.2.1 Cameleons

Cameleons are genetically encoded Ca<sup>2+</sup> indicators. Specifically, they are fluorescence resonance-energy transfer (FRET) based indicators that consist of tandem fusions of a blue (or cyan) emitting mutant of the green fluorescent protein (GFP), calmodulin, the calmodulin-binding peptide M13, and an enhanced green (or yellow) emitting GFP (figure 35). Binding of Ca<sup>2+</sup> makes calmodulin wrap around the M13 domain, increasing the fluorescence resonance energy transfer (FRET) between the flanking GFPs. Calmodulin mutations can tune the Ca<sup>2+</sup> affinities to measure free Ca<sup>2+</sup> concentrations in the range 10<sup>-8</sup> to 10<sup>-2</sup> M (Miyawaki et al., 1997; Palmer and Tsien, 2006).

In FRET applications, spectral imaging can be considered a variation of the sensitized emission technique that relies on excitation of the donor alone, followed by acquisition of the entire emission spectrum of both the donor and acceptor fluorescence. This way the cameleon constructs allow to do **ratiometric measurements** (Miyawaki et al., 1997; Rainey and Davidson, 2019).

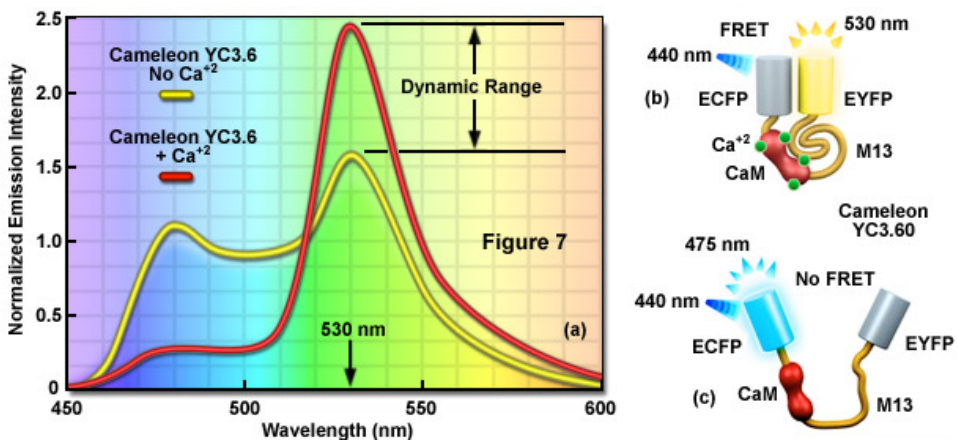


**Figure 35: ratiometric imaging of cameleon YC3.6.** **a)** absence (yellow curve) of Ca<sup>2+</sup> demonstrate the high dynamic range of the probe at 530 nm. **b)** cameleon sensor in the presence of Ca<sup>2+</sup> showing its conformational change. **c)** cameleon biosensor in the absence of Ca<sup>2+</sup>. Modified from Rainey and Davidson 2019.

This fluorescent probe has several advantages over the usual covalent labelling fluorescent probes. First, the indicator is generated *in situ* by gene transfer. Second, the sites of fusions are defined exactly, giving a molecularly



homogenous product. Third, the chromophore of GFP is fixed in the protein (Miyawaki et al., 1997).

## V.2.2 Sample preparation and equipment

To evaluate the effects of the different drugs in either pharyngeal and vulvae muscular  $\text{Ca}^{2+}$  cytosolic dynamics (**AQ2038** and **AQ2121** respectively, Table 3, p82), or mitochondrial pharyngeal muscular  $\text{Ca}^{2+}$  dynamics (**AQ3055**, table 3, p82), around 50 worms are transferred on day 1 of adulthood to a control or treatment plate. At day 5,  $\text{Ca}^{2+}$  imaging experiments are performed for both conditions in parallel. During the treatment time is essential to ensure that the worms do no run out of OP50, as caloric restriction changes  $\text{Ca}^{2+}$  dynamics (Alvarez-Illera et al., 2016). In case there is not enough food in the plate for the 5 days, the worms are transferred with a pick to new plates.

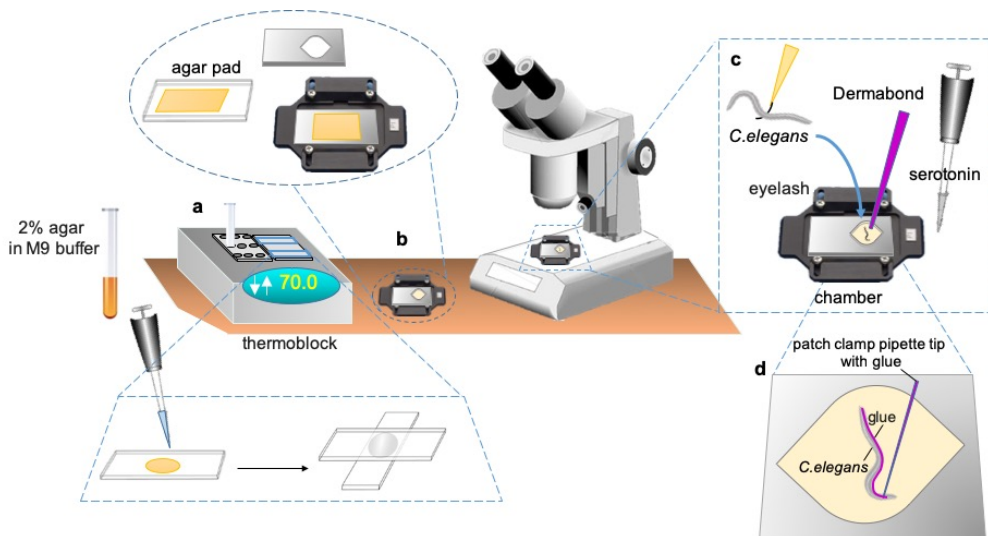


**Figure 36:  $\text{Ca}^{2+}$  imaging sample preparation.** **a)** a 2% agarose solution is heated at  $70^{\circ}\text{C}$  and a drop is placed in a 22x40 coverslip. **b)** the agar pad is placed in a Warner chamber **c,d)** a single worm is placed in the center of the agar pad with an eyelash and glued using Dermabond®, without reaching the mouth, using a patch clamp pipette.

At **day 5**, a single worm is transferred, with an eyelash, to a 2% agarose pad made in a 22x40 coverslip that is mounted in a Warner Instrument RC-25 chamber (figure 36 a,b). Carefully, the worm is glued from the tail to the mouth without reaching the opening of the mouth using Dermabond® glue. Next,  $300\mu\text{l}$  of **0.5 mM serotonin in M9 buffer solution** (for pharyngeal recordings) or just **M9 buffer**



(for vulvae recordings) are added to the chamber (figure 36 c,d), and the sample is placed on a Zeiss Axiovert inverted microscope.

### V.2.3 Recording settings

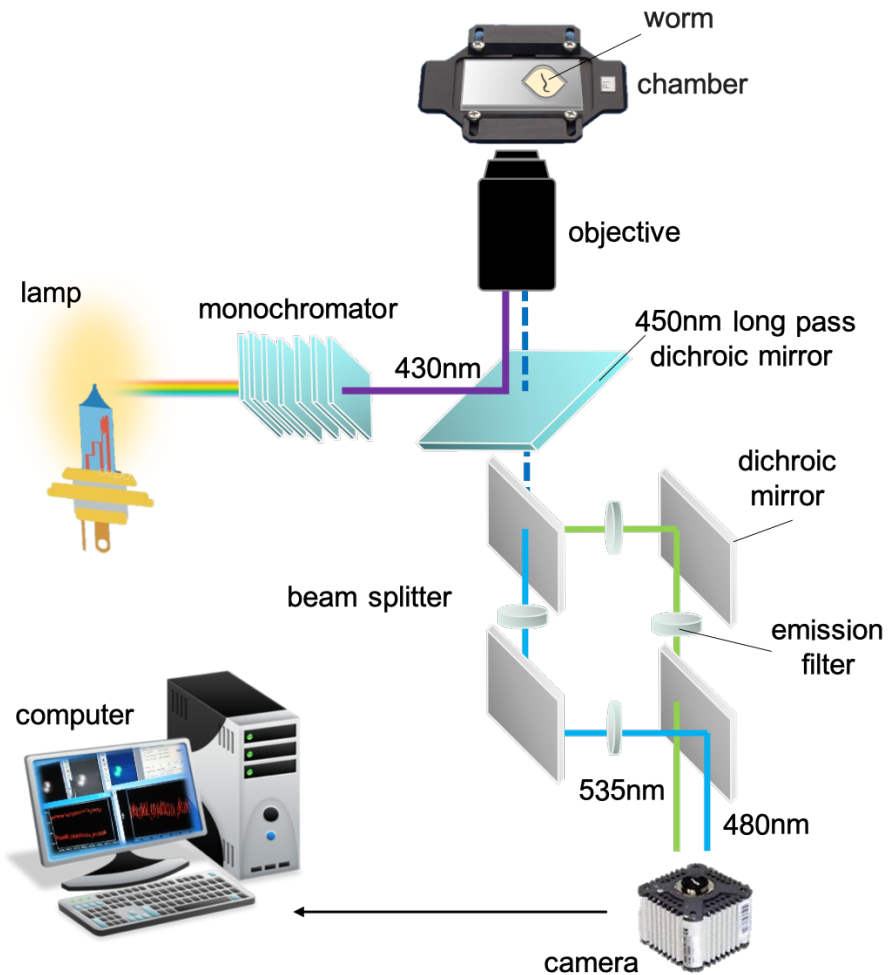


**Figure 37: Zeiss Axiovert configuration for  $\text{Ca}^{2+}$  measurements.** Representative scheme of the internal organization of the Zeiss microscope.

As all the strains used to register intracellular  $\text{Ca}^{2+}$  dynamics express cameleon probes, the samples are excited at 430 nm using a Cairn monochromator (10 nm bandwidth, continuous excitation) and the images of the emission fluorescence,

obtained with a Zeiss C-apochromat 40x1,2W objective, are directed to a 450 nm long pass dichroic mirror. A Cairn Optosplit II emission image splitter separates the 480 nm and 535nm emission images. The splitter has two emission filters, DC/ET480/40m and DC/ET535/30m, and the dichroic mirror FF509-FDi01-25x36, all from Chroma Technology (figure 37).

Simultaneous 200 ms images for the two emission wavelengths are recorded continuously for 30 minutes (2,5 Hz image rate) by a Hamamatsu ORCA-ER camera and the MetaFluor software (Universal Imaging). Using MetaFluor, ratio image is obtained dividing the 535 nm emission to the 480 nm emission images (figure 38).

All the experiments are carried out at 20°C . For the pharyngeal recordings, the region of interest is limited to the terminal bulb of the pharynx, for the vulvae the whole fluorescent cells are selected.

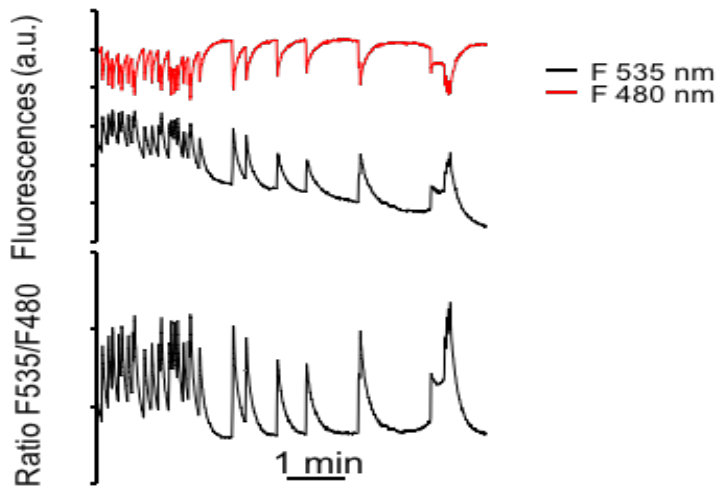


**Figure 38: representative traces of a  $\text{Ca}^{2+}$  recording with a cameleon probe.** Cameleons allow to make ratiometric measurements increasing the fluorescence at 535 nm when the probe is bound to  $\text{Ca}^{2+}$ . The opposite effect is observed at 480 nm. By dividing both emission wavelengths the ratio is obtained (lower trace).

#### V.2.4 Statistical analysis

MetaFluor numerical results of both wavelength recordings are carefully revised to ensure that all the peaks included in the final ratio values correspond to inverted changes in the individual fluorescence emission wavelengths. Then, fluorescence intensities and ratio changes are analyzed with a specific algorithm designed to calculate the width at mid-height, expressed in seconds; the height as



percentage of ratio change, and the frequency of every  $\text{Ca}^{2+}$  peak. For each peak the frequency value refers to 9 divided by the distance among the previous and posterior 4 peaks. The mean frequency is expressed as the mean of all the individual frequencies higher than 5 peaks/min.

Finally, differences between groups were analyzed using an ANOVA test between the means of each parameter.

### V.3 Electropharyngeogram (EPG)

EPG is a non-invasive electrophysiological readout of neuromuscular function in *C. elegans*. The assay monitors the activity of the nematode's pharynx, a muscular pump that contracts rhythmically to draw liquid nutrients into the digestive tract during feeding. As in the vertebrate heart, the pattern of rhythmic contractions of the pharynx is mainly generated by the pharyngeal muscles, being each contraction associated with an action potential, a large voltage transient that can be recorded by electrodes placed on the surface of the body. Moreover, EPG also registers the activity of neurons that regulate the rate of pharyngeal pumping in a similar way as the autonomic nervous system regulates the vertebrate heart. Therefore, EPG can be used to study drug effects in both pharyngeal neurons and muscles (Lockery et al., 2012).

Interestingly, it has been known for a while that pharyngeal pumping rate declines during aging. And that this decline can be used as a measurement of *C. elegans* healthspan. Consequently, pharyngeal pumping is a screening method to determine *C. elegans* aging rate (Huang et al., 2004).

The measurement of the electrical activity of the pharyngeal muscle during pumping allows to perform an exhaustive analysis of the activity of the underlying neuro-muscular circuitry. In an EPG recording the pharyngeal pump is characterized by a stereotypical waveform (figure 39) composed by five electrical transients appearing in the following order: **e**, a small positive spike that corresponds to the activity of the cholinergic motorneuron MC; **E**, an upwards spike representing muscle depolarization; **P**, plateau phase with multiple negative spikes through the action of M3 motorneuron; **R**, large downwards spike that corresponds to the relaxation and repolarization of the corpus; and **r**, smaller repolarization spike representing the relaxation of the terminal bulb (Dillon et al., 2009).

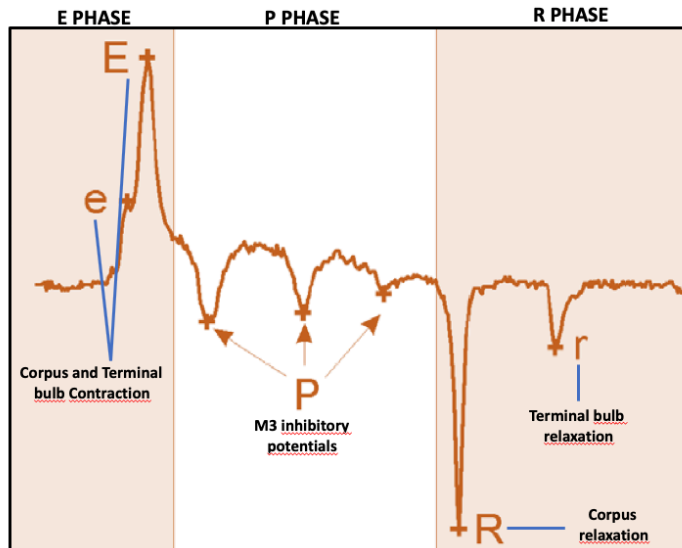


**Figure 39: EPG recording stereotypical wave.** Five different electrical spikes integrate an EPG wave. First two upward spikes (e, E) represent the contraction of the Corpus and the Terminal bulb through the action of MC motoneurons. Then, a plateau phase (P) appears characterized by several downward spikes caused by M3 motorneuron inhibitory potentials. Finally the relaxation of the corpus and the terminal bulb is represented by two downward spikes (R,r). Modified from Dillon et al., 2009.

### V.3.1 Sample preparation and equipment

EPG assays are performed at **day 5** of adulthood of the worms. As in  $\text{Ca}^{2+}$  dynamics assays, young adult **N2** worms are transferred to FuDR control or treatment plates and left in the incubator at  $20^{\circ}\text{C}$  for 5 days making sure that they are not food deprived. The day of the experiment, around 100 worms are transferred from the plates to M9 buffer and washed one time. For the next washing steps, a solution of M9 Buffer and Tween 0,1% is used to eliminate possible remaining eggs or OP50. Finally, the worms are incubated in serotonin 2.3 mM solution for 20 minutes before being loaded in the EPG equipment.

The equipment used to register EPGs is the ScreenChip™ System from NemaMetrix. This system is a microfluidics platform for recording EPGs that allows to investigate the electrophysiological effects of specific drugs in pharyngeal pumping (NemaMetrix, 2019). The ScreenChip™ System is mounted in a Zeiss Axiovert 200 microscope using the 20X objective to the recordings. In order to minimize interfering electrical noise during the recordings, we use the system grounding shield. Baseline noise was typically between 10 and  $40\ \mu\text{V}$ . The experiments were performed at  $20^{\circ}\text{C}$ .



For each experiment, 100 worms were collected and washed in 1.5ml of 0.2  $\mu\text{m}$  filtered M9 Buffer + 0.1% Tween. The worms were then washed 4X with 0.2 filtered M9 Buffer via low speed centrifugation, and finally 1 more time in 2.3 mM 5-HT in M9 buffer. Then they were suspended in 1 ml of 2.3 mM 5-HT containing medium and were allowed to settle for 15 min. All the experiments were performed between 15 and 120 min of initial serotonin exposure.

First, using the NemAcquire software the basal power line noise is recorded, and then the worms are vacuum-loaded onto the Nemamatrix Screen Chip SC40 and the experiment is initiated. To view acquisition EGPs the 1 Hz high-pass and 50 Hz notch filter settings were selected. A 300 s EPG recording was made for each animal. Among 20-25 animals were recorded for each replicate.

To extract measurements of different physiological events from the EPG recordings, NemAnalysis v0.2 software is used. The data is then filtered according to the following conditions: Minimum E SNR 1.4, Minimum R SNR 2.0, E highpass cutoff 15 Hz, R highpass cutoff 20 Hz, Minimum absolute threshold 15  $\mu\text{V}$ . The following parameters were analyzed for each 300 seconds recording: worm orientation, number of pumps, recording duration (s), mean frequency (Hz), mean pump duration (ms), median pump duration (ms), pump duration standard deviation (ms), mean amplitude ( $\mu\text{V}$ ), amplitude standard deviation ( $\mu\text{V}$ ), mean inter-pump interval duration (ms), median inter-pump interval duration (ms), inter-pump interval duration standard deviation (ms), baseline noise amplitude ( $\mu\text{V}$ ), pump duration coefficient of variation (%), mean signal-to-noise. The recordings whose pump duration coefficient of variation was higher to 50% were discarded (figure 40). Finally, data was exported into Excel for an ANOVA statistical analysis.

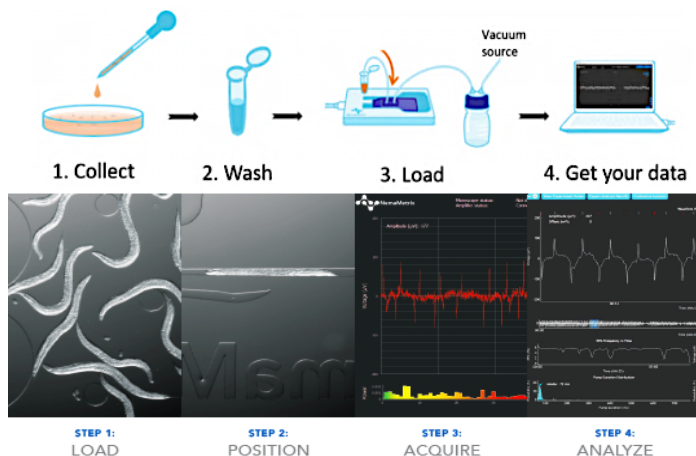


Figure 40: Schematic representation of an EPG assay (NemaMetrix 2019)



## V.4 Confocal imaging

Among the possible effects of CGP37157, is to produce changes in sarcopenia and mitochondrial physiology or distribution. To study these possible changes, treated and untreated AQ2121 for sarcopenia evaluation, and SJ4103 for mitochondrial organization (table 3, p82), were studied by confocal imaging. Specifically, around 200-300 synchronized worms in the young adult stage are transferred to control or treatment 55 mm  $\emptyset$  plates.

From day 2 until day 12, worms are transferred to a 2% agarose pad containing a drop of sodium azide 50 mM, that acts as a worm anesthetic. Then, a coverslip is used to cover the drop. Images are taken in a Leica SP5 confocal microscope. The excitation-emission windows used for GFP are 488 nm excitation and 500-554 nm emission.

Finally, images are processed and analyzed using ImageJ software.

## V.5 Evaluation of drug induced stress assay

To evaluate if the different treatments induce ER, in the case of SERCA inhibitors, or cytosolic stress, for CGP37157 treatment, *C. elegans* strains that express a fluorescent reporter when the stress in one of the different cellular compartments increases are used. Specifically, the ER stress is reported by SJ4005 and cytosolic stress by TJ375 (see table 3, p82).

Briefly, around 100 young adult synchronized worms are transferred to control and treatment 55 mm  $\emptyset$  plates and incubated at 20°C. 10-15 worms are imaged after 3 days of treatment. To use as a positive control, around 20 worms at day 3 of adulthood are transferred to plates containing stress inducers. To induce ER stress 20 worms are transferred to plates containing Tunicamycin 10  $\mu$ g/ml and incubated for 6 hours; cytosolic stress was induced by 2 hour heat shock treatment at 37°C and a posterior O/N recovery of the worms at 20°C . To evaluate changes in GFP expression, around 15 worms per treatment are anesthetized using 50 mM NaN<sub>3</sub> and imaged using a Leica microscope.

Finally, the images are analyzed using ImageJ software. The mean fluorescence of the total area of each worm is calculated, and the mean of at least 20 worms values are compared using an ANOVA test.



## V.6 *C. elegans* tracking assay

The tracking assays were performed from day 5 to day 15 of *C. elegans* AQ2121 adult worms to evaluate possible effects of CGP37157 in worm's motility. Basically, as previously described, day 1 synchronized adult worms were placed in control or treatment 35 mm  $\emptyset$  plates and kept at 20°C. 2 minute videos were taken every day from day 5 until day 15 of control and treated populations, and afterwards analyzed using ImageJ plugin "wrMTrck" as described in (Nussbaum-Krammer et al., 2015)

## V.7 Fertility assay

To perform fertility assays, seeded control and CGP37157 50  $\mu$ M 35 mm  $\emptyset$  plates are prepared in the absence of FuDR. Using a synchronized population, one L4 stage larva is transferred to each plate and the number of eggs laid is counted every 24 hours. The worm in each plate is transferred to a new plate every 24 hours. At least 10 plates per condition are scored.

## VI. BIOCHEMICAL ASSAYS

### VI.1 Measurement of CGP37157 in *C. elegans* worms

When inclusion compounds are formed, the amount of CGP37157 that finally gets to the worms is unknown. For that reason, we decided to measure the CGP37157 in a known number of worms so we could interpolate the concentration of CGP37157.

#### VI.1.1 Sample preparation

Around 4.000 **AQ2038** worms are transferred at day 1 of adulthood to treatment 100 mm Ø NGM plates containing 1 µg of CGP37157  $\gamma$ -CD inclusion compounds per 20 worms mixed with OP50. At day 8 of treatment, worms are collected and washed by centrifugation at 2.000 rpm with cold water. The supernatant is removed and 500 µl of cold methanol are added. Worms are resuspended and sonicated for 50 cycles (5 sec on/5 sec off). The suspension obtained was centrifuged at 5.000 rpm for 5 minutes. The supernatant was collected and stored at -80°C until its analysis by high-performance liquid chromatography-tandem mass spectrometry (HPLC-MS/MS).

#### VI.1.2 HPLC-MS/MS

CGP37167 quantification was performed by a collaboration with Cristobal de los Ríos group at the Hospital Universitario La Princesa, Universidad Autónoma de Madrid. The instrument consisted of HPLC, 1200 Series separation module (Agilent Technologies, Santa Clara, CA, USA) coupled to triple quadrupole mass spectrometer (MS/MS, 6410 series) equipped with an electrospray ionization source (ESI). HPLC-MS/MS system is controlled by Agilent Mass Hunter Workstation Data Acquisition software. The MS/MS was operating in positive multiple reaction monitoring mode and the conditions were set as followed: desolvation gas (N<sub>2</sub>) flow 12 L/min, nebulizer pressure 60 psi, drying gas temperature 300°C and capillary voltage 4.000 V. The *m/z* ratios for the CGP37157 quantifier and qualifier ions were 324.1 > 214.1 and 324.1 > 179.1 respectively. The HPLC separation was carried out at 25°C in a reversed-phase C18 column (ZORBAX Eclipse XDB, 4.6 mm x 150 mm and 5 µm particle size; Agilent Technologies, Santa Clara, CA, USA) protected by a 0.2 µm on-line filter. 0.2% formic acid in water, pH=3.0 (A) and 0.2% formic acid in CAN (B; 30:70, v/v) were used as the mobile phase. The chromatogram was run under gradient conditions



at a flow rate of 0.8 mL/min. The following gradient program was used for CGP37157 separation: 70% of B at 0.0-0.5 min; gradually increasing phase B to 100% at 0.5-1.0 min; 100% of B at 1.0-2.0 min; returning to the initial conditions (30% of A and 70% of B) at 2.0-2.5 min; followed by a re-equilibration time of 2.5 min, to give a total run of 5 min. 5  $\mu$ l of CGP were injected into the chromatographic system.

Three different extractions from different populations have been used to calculate the final concentration of CGP37157 per worm.

## **VI.2 ATP assessment in *C. elegans* worms**

To assess possible changes in ATP levels in the worms after the treatment with CGP37157, day 5 control and treated worms were pelleted and boiled for 15 min in 100  $\mu$ l double distilled sterile water to obtain the samples. This treatment allows the liberation of ATP and the inactivation of the ATPases. The quantification of ATP levels in the samples was performed using the Invitrogen™ Molecular Probes™ ATP Determination Kit, a luminescence based detection kit.

Finally, the ATP concentration of each sample was normalized to the total protein content of the sample, evaluated by a Pierce™ BCA™ protein assay, and then the ratios [ATP]/[Total protein] were compared using an ANOVA test.



## VII. SOLUTIONS AND REAGENTS

### VII.1 Solutions

#### VII.1.1 M9 Buffer

REAGENT	AMOUNT
$\text{KH}_2\text{PO}_4$	3 g
$\text{Na}_2\text{HPO}_4$	6 g
NaCl	5 g
$\text{MgSO}_4$ 1M	1 ml
$\text{H}_2\text{O}$	Add to 1 L

**Table 6: M9 buffer composition.** Reagents and amounts needed to prepare M9 Buffer

#### VII.1.2 Bleaching solution

REAGENT	AMOUNT
Bleach	300 $\mu\text{l}$
NaOH 5N	150 $\mu\text{l}$

**Table 7: Bleaching solution composition.** Reagents and amounts needed to prepare bleaching solution for worm's synchronization.

#### VII.1.3 $\text{KPO}_4$ Buffer 1M

REAGENT	AMOUNT
$\text{KH}_2\text{PO}_4$	108.3 g
$\text{K}_2\text{HPO}_4$	35.6 g
$\text{H}_2\text{O}$	1 L

**Table 8:  $\text{KPO}_4$  Buffer composition.** Buffer included in NGM liquid medium. Before autoclaving the solution, pH is adjusted to 6.00.



## VII.2 Materials

- *C. elegans* strains: RB754 (*aak-2*), CB1370 (*daf-2*), CF1038 (*daf-16*), DR412 (*daf-15/unc-24*), RB1206 (*rsk-1*), AGD397 (*aak-1/aak-2*), VC199 (*sir 2.1*), MQ1333 (*nuo-6*), DA1113 (*eat-2*), and SJ4103 (*pmyo3::GFP(mit)*) were obtained from the Caenorhabditis Genetics Center (CGC), University of Minnesota, USA.
- *C. elegans* strains AQ2038 (*pmyo-2::YC2.1*), and AQ2121 (*pmyo3::YC2.1*), were kindly provided by Drs. Robyn Branicky and W. Schafer (MRC Laboratory of Molecular Biology, Cambridge, UK). AQ3055 (*pmyo-2::2mt8::YC3.6*) was obtained by Dr. Mayte Montero in Schafer's Lab (LMB-MRC).
- *C. elegans* strains SJ4005 (*zcls4[hsp-4::GFP]*), and TJ375 (*gpls[hsp16.2::GFP]*) were kindly provided by Dr. Malene Hansen (Sandford Burnham Prebys Medical Discovery Institute, San Diego, CA, USA).
- cholesterol, sodium phosphate dibasic ( $\text{Na}_2\text{HPO}_4$ ), magnesium sulphate ( $\text{MgSO}_4$ ), dimethylsulfoxide (DMSO), 2,5-di-tert-butylhydroquinone (2,5-BHQ), 2,6-di-tert-butylhydroquinone (2,6-BHQ), sodium azide ( $\text{NaN}_3$ ), CCCP, and tunicamycin were supplied by Sigma, Missouri, USA.
- sodium chloride ( $\text{NaCl}$ ), dipotassium hydrogenophosphate ( $\text{K}_2\text{HPO}_4$ ), potassium dihydrogenophosphate ( $\text{KH}_2\text{PO}_4$ ), absolut ethanol (EtOH), methanol for HPLC (MeOH) and other salts and substrates were supplied by Merck, Darmstadt, Germany.
- thapsigargin was supplied by abCam, Cambridge, UK.
- gamma-cyclodextrin ( $\gamma$ -CD) was obtained from PanReac Applichem, Chicago, USA.
- 5-fluoro-2'-deoxyuridine (FuDR) and serotonin hydrochloride were acquired from Alfa-Aesar, Kandel, Germany.
- agar was obtained from Calbiochem, San Diego, USA.
- bacteriological peptone was supplied by Pronadisa, Madrid, Spain.
- 2xYT (LB Broth) and pasteur pipettes 230-250 were purchased to FisherBrand, Pittsburgh, USA.
- 55 and 100 mm  $\varnothing$  petri dishes were supplied by Deltalab, Barcelona, Spain .
- 35 mm petri dishes, tunicamycin, Invitrogen™ Molecular Probes™ ATP Determination Kit (A22066), and Pierce™ BCA™ protein assay kit were supplied by Thermo Fisher Scientific, Pittsburgh, USA.



**RESULTS**







During the introduction of this work, the interrelationship between nutrient signaling pathways and longevity modulation has been explained. It is now clear that aging is a biological process genetically regulated. What is not so clear is the role of  $\text{Ca}^{2+}$  signaling in the regulation of this process, although it has already been demonstrated that at least some of the nutrient sensing pathways activities are affected by  $\text{Ca}^{2+}$  signaling.

Due to the increasing importance of the nutrient sensing pathways in the modulation of aging and the lack of information about its regulation by  $\text{Ca}^{2+}$  this work has focused in the study of the effects of different drugs that affect  $\text{Ca}^{2+}$  signaling, specifically, SERCA inhibitors 2,5-BHQ and thapsigargin, and  $\text{Na}^+/\text{Ca}^{2+}$  exchanger inhibitor CGP37157 in *C. elegans* lifespan and its relationship with nutrient sensing pathways.

## I. SERCA INHIBITION AND AGING IN *C. ELEGANS*

As mentioned before, two different SERCA inhibitors have been used during the development of this work, 2,5-BHQ and thapsigargin (Tg). Even though both molecules can inhibit the same  $\text{Ca}^{2+}$  pump, they do not behave in the same manner; while Tg inhibits SERCA irreversibly with a really high specificity, 2,5-BHQ inhibits it in a reversible way. This difference in their SERCA inhibitory nature has led us to study the effects of both pharmacological treatments in *C. elegans*.

### I.1 2,6-BHQ: inactive isomer of 2,5-BHQ

Besides its inhibitory SERCA activity, 2,5-BHQ, due to its molecular nature, also has antioxidant properties. This fact has made necessary to search for a control molecule that has the same molecular nature without exerting SERCA inhibition. To this end, 2,6-BHQ effects in SERCA activity were studied by aequorin in HeLa cells. As shown in figure 41, stimulation of HeLa cells with 2,5-BHQ 10  $\mu\text{M}$  causes a rapid decrease in  $[\text{Ca}^{2+}]_{\text{ER}}$  as expected, while the stimulation with 2,6-BHQ at the same concentration did not cause changes in  $[\text{Ca}^{2+}]_{\text{ER}}$ . This result led us to use 2,6-BHQ as a control molecule for the effects of 2,5-BHQ in *C. elegans* allowing us to differentiate if the effects of 2,5-BHQ in *C. elegans* are caused by SERCA inhibition or not.

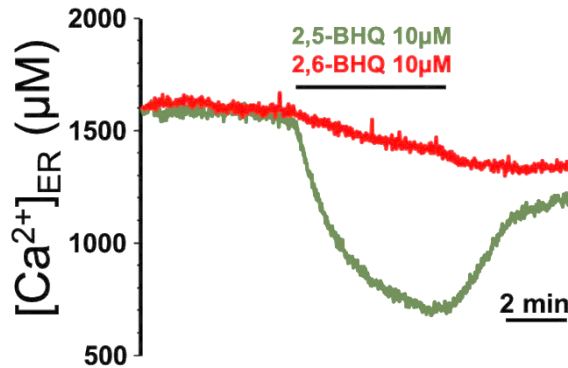


**Figure 41: Effects of 2,5-BHQ and 2,6-BHQ in ER  $[Ca^{2+}]$  of HeLa cells.** HeLa cells expressing double mutated aequorin targeted to the ER (de la Fuente et al.2013) were reconstituted with coelenterazine i, placed in the perfusion chamber and perfused with external medium prior to the stimuli with both drugs.

## I.2 Effects of SERCA inhibitors in *C. elegans* lifespan

### I.2.1 2,5-BHQ extends *C. elegans* lifespan

#### I.2.1.1 Oral administration of 2,5-BHQ extends *C. elegans* lifespan

One of the main physical characteristics of SERCA inhibitors is their lipophilic nature, which can challenge the delivery of this compound to the worms as they live in an aqueous medium. To minimize this possible complications, the drugs were included in  $\gamma$ -CD forming inclusion compounds, increasing their water solubility, and restricting drug uptake to just oral administration (Kashima et al., 2012).

There was no data available about the effective concentration of this compounds in *C. elegans*, as they had never been used in this model organism. To study the possible effects of 2,5-BHQ in *C. elegans* a dose response experiment was designed to find the most effective concentration of 2,5-BHQ in *C. elegans*. To explore the effects of the reversible inhibition of SERCA in *C. elegans* the strain AQ2038 that expresses the  $Ca^{2+}$  probe cameleon YC2.1 in pharynx muscle cells was used as it has been demonstrated that the expression of the probe does not modify its phenotype compared to the control strain N2 (Alvarez-Illera et al., 2016). Finally, to be able to attribute the effects of 2,5-BHQ to SERCA inhibition, 2,6-BHQ parallel experiments at the same concentration were performed. All the experiments were at least performed three times (table 9, p114).

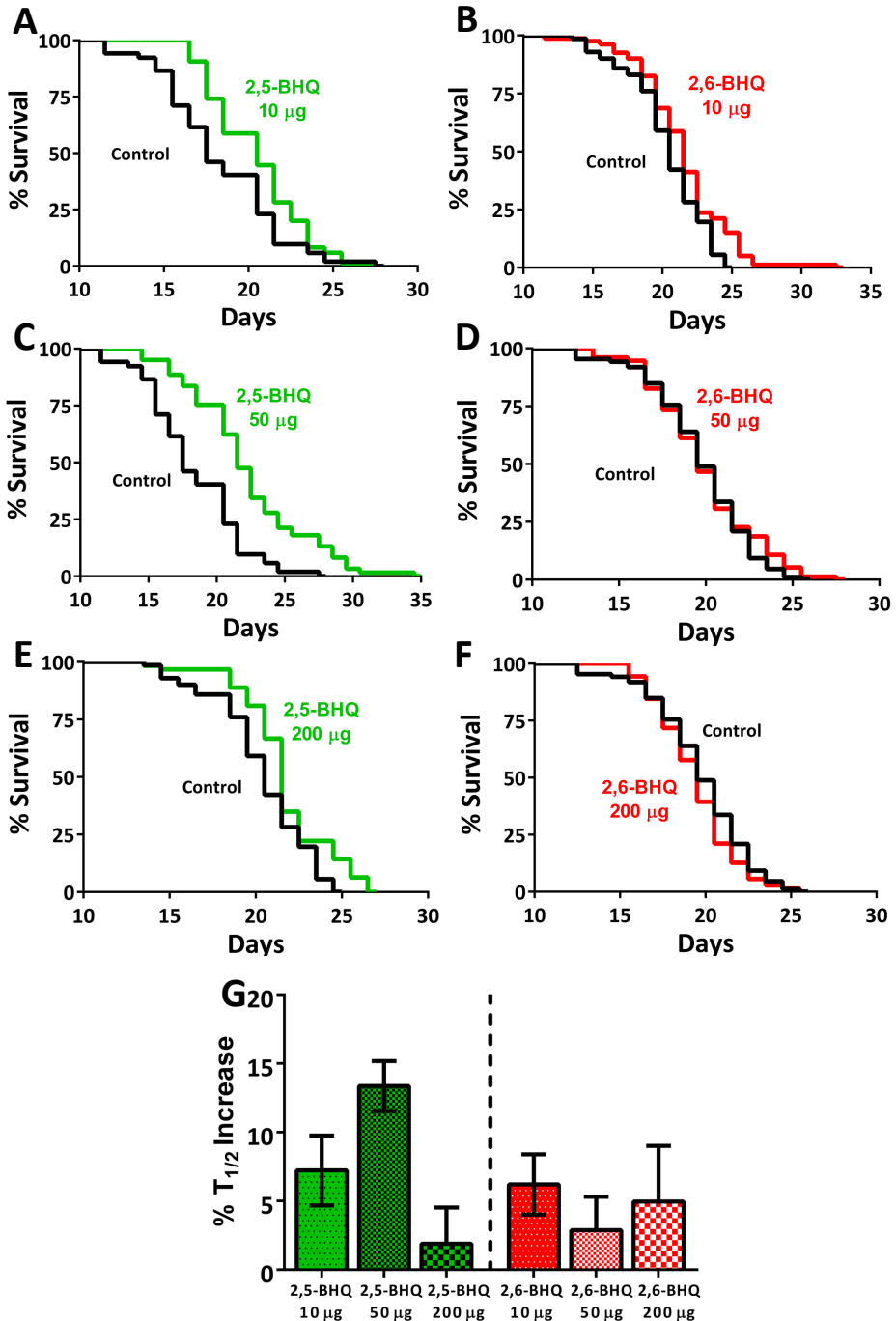


**Figure 42: Effects of 2,5-BHQ and 2,6-BHQ inclusion compounds in AQ2038 *C. elegans* lifespan.** The effects of 2,5-BHQ in *C. elegans* lifespan (in green) were studied at three different concentrations (A, C, E), always in parallel to 2,6-BHQ treatments (B, D, F) in red. In figure G the mean % of lifespan increase is shown for each treatment.

Drug	T <sub>1/2</sub> drug (days)	N drug	T <sub>1/2</sub> control (days)	N Control	% T <sub>1/2</sub> increase	P value	Mean % T <sub>1/2</sub> increase
<b>AQ2038 + <math>\gamma</math>-CD-2,5-BHQ</b>							
<b>2,5-BHQ 10 <math>\mu</math>g</b>	<b>18,516</b>	<b>76/97</b>	<b>16,997</b>	<b>69/81</b>	<b>8,936871213</b>	<b>&lt; 0,0001</b>	
	22,164	45/60	20,054	52/64	10,5215917	<0,018	
	21,499	77/105	20,416	86/109	5,304663009	<0,006	<b>8,59 <math>\pm</math> 1,52</b>
	22,432	73/100	21,043	71/95	6,600769852	<0,0001	
	21,121	85/106	18,928	52/62	11,58601014	<0,001	
<hr/>							
<b>2,5-BHQ 50 <math>\mu</math>g</b>	18,391	69/82	16,997	69/81	8,201447314	<0,0001	
	<b>23,51</b>	<b>42/60</b>	<b>20,054</b>	<b>52/64</b>	<b>17,23346963</b>	<b>&lt; 0,0001</b>	
	22,579	63/80	20,416	86/109	10,59463166	<0,0001	<b>13,86 <math>\pm</math> 2,4</b>
	23,563	81/98	21,043	71/95	11,97547878	<0,0001	
	22,96	61/80	18,928	52/62	21,30177515	<0,0001	
<hr/>							
<b>2,5-BHQ 200 <math>\mu</math>g</b>	16,603	77/101	16,997	69/81	-2,318056128	0,193	
	21,293	63/82	20,054	52/64	6,17831854	0,099	
	19,908	60/82	20,416	86/109	-2,488244514	0,171	<b>3,30 <math>\pm</math> 2,4</b>
	<b>22,279</b>	<b>63/80</b>	<b>21,043</b>	<b>71/95</b>	<b>5,873687212</b>	<b>&lt;0,005</b>	
	20,68	59/80	18,928	52/62	9,256128487	<0,015	
<hr/>							
<b>AQ2038 + <math>\gamma</math>-CD-2,6-BHQ</b>							
<b>2,6-BHQ 10 <math>\mu</math>g</b>	17,7	62/80	16,997	69/81	4,136024004	0,046	
	22,45	63/84	20,054	52/64	11,9477411	<0,001	
	20,226	78/101	20,416	86/109	-0,930642633	0,421	<b>6,03 <math>\pm</math> 2,3</b>
	<b>22,147</b>	<b>80/99</b>	<b>21,043</b>	<b>71/95</b>	<b>5,246400228</b>	<b>&lt;0,006</b>	
	20,77	71/85	18,928	52/62	9,731614539	<0,01	
<hr/>							
<b>2,6-BHQ 50 <math>\mu</math>g</b>	18,291	68/84	16,997	69/81	7,613108196	<0,0001	
	18,44	53/60	18,88	52/64	-2,330508475	0,265	<b>3,82 <math>\pm</math> 2,5</b>
	<b>20,783</b>	<b>75/102</b>	<b>20,416</b>	<b>86/109</b>	<b>1,797609718</b>	<b>0,289</b>	
	20,479	57/81	18,928	52/64	8,194209637	<0,022	
<hr/>							
<b>2,6-BHQ 200 <math>\mu</math>g</b>	19,372	45/59	16,997	69/81	13,97305407	<0,0001	
	18,057	53/60	20,054	52/64	-9,958113095	<0,001	
	<b>20,216</b>	<b>71/98</b>	<b>20,416</b>	<b>86/109</b>	<b>-0,979623824</b>	<b>0,314</b>	<b>4,64 <math>\pm</math> 4,4</b>
	23,071	53/64	21,043	71/95	9,637409115	<0,0001	
	20,923	59/83	18,928	52/62	10,53994083	<0,007	
<hr/>							

**Table 9: Lifespan assays performed with 2,5-BHQ and 2,6-BHQ inclusion compounds in AQ2038 worms.** The table shows the amount of drug used; the half-life (T<sub>1/2</sub>) of the control and treated worms obtained from the Kaplan-Meier analysis for survival; the number of worms in the experiment (final/total); the % increase in the half-life of treated worms; the statistical significance of the effect of the drug in each case; and the mean  $\pm$  s.e of the T<sub>1/2</sub> increase in treated worms. In bold, are indicated the survival assays plotted in figure 42.

Figure 42, shows that the effects of the treatment with 2,5-BHQ in *C. elegans* are dose dependent, being the most effective concentration 50  $\mu$ g of  $\gamma$ -CD-2,5-BHQ. Besides its dose dependent nature, the treatment was able to extend *C. elegans* lifespan around a 14% in the most effective concentration as a consequence of SERCA inhibition, as the parallel treatments with the same concentrations of  $\gamma$ -CD-2,6-BHQ did not mimic the effects of the treatment with 2,5-BHQ (table 9).

### 1.2.1.2 *C. elegans* lifespan extension of 2,5-BHQ is not dependent on its method of administration or the presence of active OP50.

Once the effect of 2,5-BHQ in *C. elegans* was demonstrated, the importance of the delivery method was tested. For this purpose, the drugs were added in the NGM media, before pouring the plates, at the desired concentration.

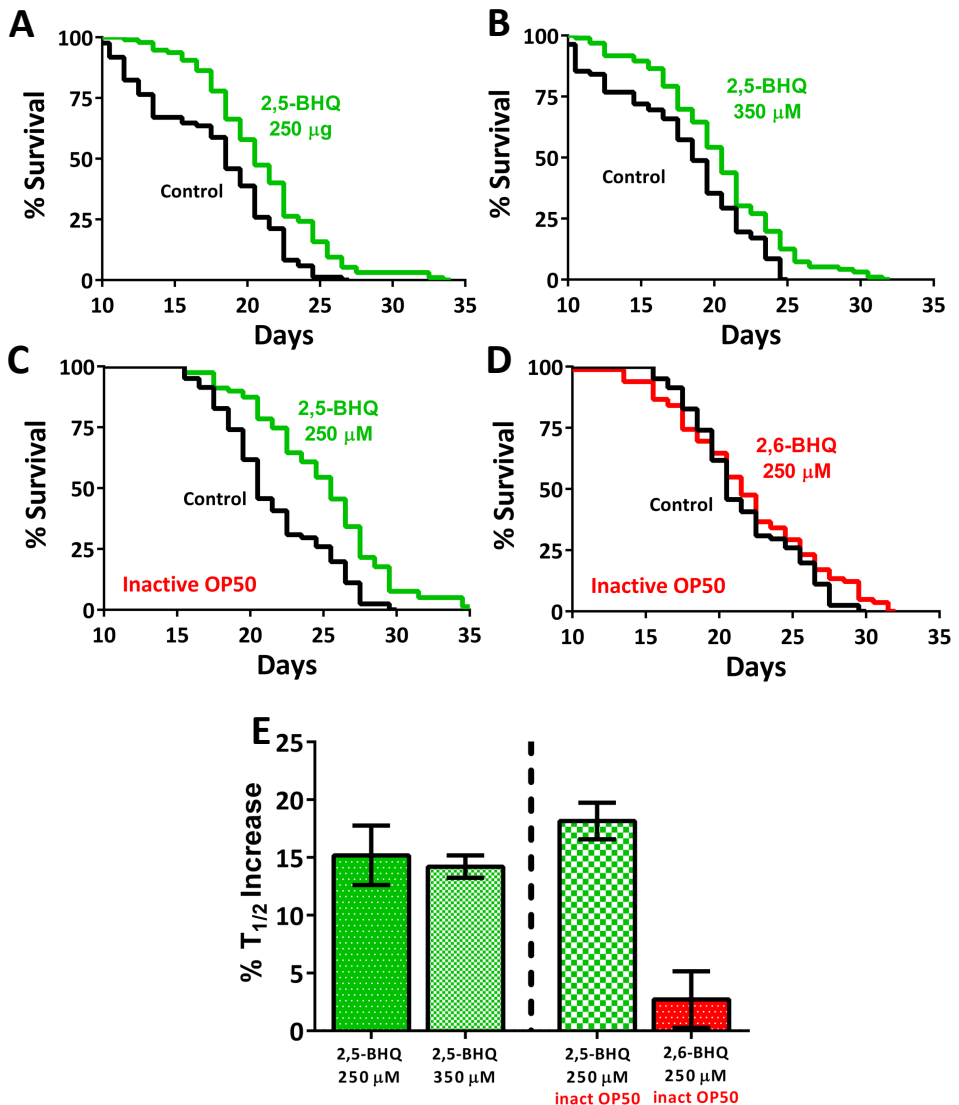


**Figure 43: Effects of 2,5-BHQ and 2,6-BHQ incorporated in the NGM media in AQ2038 *C. elegans* lifespan.** The effects of 2,5-BHQ in *C. elegans* lifespan (in green) were studied at two different concentrations (A,B). In figures C,D the possible participation of OP50 in the effects were explored. In figure E the mean % of lifespan increase is shown for each treatment.

Drug	T <sub>1/2</sub> drug (days)	N drug	T <sub>1/2</sub> control (days)	N Control	% T <sub>1/2</sub> increase	P value	Mean % T <sub>1/2</sub> increase
<b>AQ2038 + 2,5-BHQ</b>							
<b>2,5-BHQ 250 μM</b>	25,279	85/97	22,596	82/100	11,87378297	< 0,0001	<b>15,19 ± 2,6</b>
	<b>21,605</b>	<b>95/105</b>	<b>18,523</b>	<b>85/103</b>	<b>16,63877342</b>	<b>&lt;0,0001</b>	
	20,466	96/108	18,535	82/90	10,41812787	<0,006	
	22,39	80/94	18,381	74/80	21,81056526	<0,0001	
<b>2,5-BHQ 350 μM</b>	<b>25,889</b>	<b>96/111</b>	<b>22,596</b>	<b>82/100</b>	<b>14,57337582</b>	<0,0001	<b>14,21 ± 1,0</b>
	20,817	99/106	18,523	85/103	12,38460293	<0,002	
	20,963	96/109	18,535	82/90	13,09954141	<0,001	
	21,463	71/84	18,381	74/80	16,76731407	<0,0001	
<b>AQ2038 treated with INACTIVATED OP50</b>							
<b>2,5-BHQ 250 μM</b>	25,991	79/102	22,360	81/107	16,24	<0,0001	<b>18,15 ± 1,7</b>
	25,793	74/100	21,266	84/100	21,29	<0,0001	
	<b>22,481</b>	<b>69/81</b>	<b>19,229</b>	<b>85/103</b>	<b>16,91</b>	<b>&lt;0,001</b>	
<b>2,6-BHQ 250 μM</b>	<b>22,782</b>	<b>82/101</b>	<b>22,360</b>	<b>81/107</b>	<b>1,89</b>	<b>0,156</b>	<b>2,71 ± 2,4</b>
	21,043	87/100	21,266	84/100	-1,05	0,681	
	20,630	83/93	19,229	85/103	7,29	<0,005	

**Table 10: Lifespan assays performed with 2,5-BHQ and 2,6-BHQ incorporated in the NGM media in AQ2038 worms.** The table shows the amount of drug used; the half-life (T<sub>1/2</sub>) of the control and treated worms obtained from the Kaplan-Meier analysis for survival; the number of worms in the experiment (final/total); the % increase in the half-life of treated worms; the statistical significance of the effect of the drug in each case; and the mean ± s.e of the T<sub>1/2</sub> increase in treated worms. In bold, are indicated the survival assays plotted in figure 43.

As shown in figure 43, the effects of the treatment with 2,5-BHQ in the NGM media are also dose dependent, being the most effective concentration 250 μM. Besides its dose dependent nature, the treatment was able to extend *C. elegans* lifespan around a 15% in the most effective concentration, and this effect was not dependent on the presence of active OP50 in the plates as can be seen in graphs C and D of figure 42 where the treatment with the SERCA inhibitor was able to extend *C. elegans* lifespan even when the OP50 culture is heat-inactivated, while 2,6-BHQ was still ineffective (figure 43, table 10).

### I.2.2 Thapsigargin (Tg) extends *C. elegans* lifespan

The effects of thapsigargin in *C. elegans* were performed using the same protocol as the one used for 2,5-BHQ. In this case the drug was also delivered in two different ways, included in a  $\gamma$ -CD inclusion compound, or added in the plate coating the OP50 culture. Besides the study of the delivery methods and the dose dependent response, the possible effect of the OP50 culture in the resulting effects were discarded using inactivated OP50 cultures (figure 44).

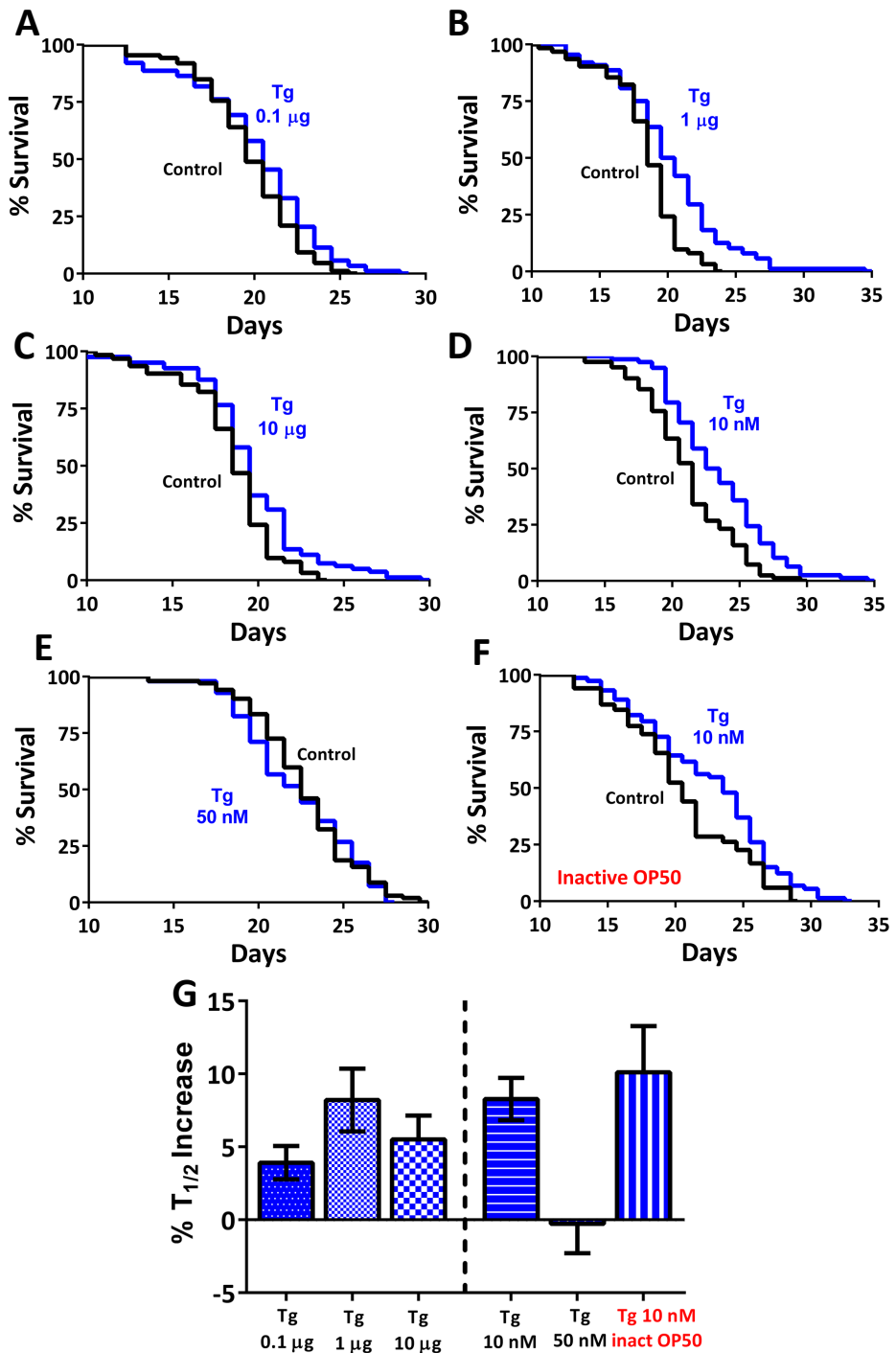


**Figure 44: Effects of thapsigargin in AQ2038 *C. elegans* lifespan.** The effects of thapsigargin (Tg) in *C. elegans* lifespan (in blue) were studied with two delivery methods:  $\gamma$ -CD (A, B,C), and NGM (D,E). In graph F the possible participation of OP50 in the effects were explored. In figure G the mean % of lifespan increase is shown for each treatment.

Drug	T <sub>1/2</sub> drug (days)	N drug	T <sub>1/2</sub> control (days)	N Control	% T <sub>1/2</sub> increase	P value	Mean % T <sub>1/2</sub> increase
<b>AQ2038 + <math>\gamma</math>-CD-Thapsigargin</b>							
Thapsigargin 0,1 $\mu$ g	17,024	80/96	16,997	69/81	0,158851562	0,89	<b>3,21 <math>\pm</math> 1,4</b>
	19,925	69/82	19,305	62/80	3,211603212	0,107	
	21,437	61/82	20,054	52/64	6,896379775	0,057	
	<b>20,938</b>	<b>88/106</b>	<b>20,416</b>	<b>86/109</b>	<b>2,556818182</b>	<b>&lt;0,038</b>	
Thapsigargin 1 $\mu$ g	<b>21</b>	<b>88/102</b>	<b>19,305</b>	<b>62/80</b>	<b>8,78010878</b>	<0,0001	<b>8,01 <math>\pm</math> 0,3</b>
	21,545	70/80	20,054	52/64	7,434925701	<0,028	
	18,319	80/93	16,997	69/81	7,777843149	<0,0001	
	22,061	60/81	20,416	86/109	8,057405956	<0,004	
Thapsigargin 10 $\mu$ g	18,19	89/102	16,997	69/81	7,018885686	<0,0001	<b>3,71 <math>\pm</math> 1,7</b>
	<b>20,392</b>	<b>81/99</b>	<b>19,305</b>	<b>62/80</b>	<b>5,630665631</b>	<b>&lt;0,014</b>	
	20,619	79/101	20,054	52/64	2,817393039	0,37	
	20,29	90/109	20,416	86/109	-0,617163009	0,974	
<b>AQ2038 + Thapsigargin in plate</b>							
Thapsigargin 10 nM	<b>24,182</b>	<b>78/103</b>	<b>21,868</b>	<b>82/101</b>	<b>10,58167185</b>	<b>&lt;0,0001</b>	<b>9,59 <math>\pm</math> 2,1</b>
	21,494	50/60	21,043	71/95	2,143230528	0,207	
	23,407	53/82	21,652	70/102	8,105486791	<0,005	
	25,246	96/108	22,235	102/115	13,54171351	<0,0001	
	25,705	67/80	22,634	73/84	13,56808341	<0,0001	
Thapsigargin 50 nM	20,562	86/103	21,868	82/101	-5,972196817	<0,002	<b>-0,45 <math>\pm</math> 2,2</b>
	22,015	70/100	21,652	70/102	1,67651949	0,927	
	<b>22,851</b>	<b>97/107</b>	<b>23,235</b>	<b>102/115</b>	<b>-1,652679148</b>	0,616	
	23,577	85/101	22,634	73/84	4,166298489	0,15	
	<b>AQ2038 treated with inactivated OP50</b>						
Thapsigargin 10 nM	23,326	75/105	22,360	81/107	4,32	0,055	<b>10,10 <math>\pm</math> 3,17</b>
	<b>23,553</b>	<b>73/89</b>	<b>21,266</b>	<b>84/100</b>	<b>10,75</b>	<b>&lt;0,002</b>	
	22,159	78/101	19,229	85/103	15,24	<0,0001	

**Table 11: Lifespan assays performed with thapsigargin in AQ2038 worms.** The table shows the amount of drug used; the half-life (T<sub>1/2</sub>) of the control and treated worms obtained from the Kaplan-Meier analysis for survival; the number of worms in the experiment (final/total); the % increase in the half-life of treated worms; the statistical significance of the effect of the drug in each case; and the mean  $\pm$  s.e of the T<sub>1/2</sub> increase in treated worms. In bold, are indicated the survival assays plotted in figure 44.

As shown in figure 44 and table 11, the effects of the treatment with thapsigargin behave in a dose dependent manner with both methods of administration being the most effective concentrations 1  $\mu$ g for  $\gamma$ -CD-thapsigargin reaching a mean increase of 8%, and 10 nM for direct delivery with a 9,6% mean lifespan increase. As in the case of 2,5-BHQ treatment, it seems to be more effective the direct delivery method than the inclusion compounds. Finally, the possible effect of the metabolism of the drug by OP50 in lifespan extension was explored repeating the lifespan assays in the presence of heat-inactivated OP50.

After studying the results, it was decided that the following experiments were going to be performed delivering the drug to the worms through the NGM as it seemed more effective. The only exception is the delivery of the drugs to the *eat-2* mutants as they have reduced food intake and the oral administration of the drug was more suitable for the purpose of the work.



### I.3 SERCA inhibitors do not extend lifespan inducing caloric restriction

As SERCA inhibitors modulate intracellular  $Ca^{2+}$  signaling, there was a possibility that its effects on *C. elegans* lifespan were caused by the induction of caloric restriction (CR) by the reduction of pharyngeal pumping. To investigate this question, the mutant strain DA1113 (see table 4, p85) was treated with both inhibitors. This strain has a loss of function of *eat-2*, an acetylcholine receptor of pharyngeal muscular cells causing defective pumping, reducing worm's food intake, and increasing their lifespan.

Because this mutant shows a decrease in pharyngeal pumping, limiting the drugs intake to oral administration could give a more conclusive result on the induction of caloric restriction by SERCA inhibitors. This is the reason to treat this mutant with the drugs in the form of inclusion compounds.

Drug	$T_{1/2}$ drug (days)	N drug	$T_{1/2}$ control (days)	N Control	% $T_{1/2}$ increase	P value	Mean % $T_{1/2}$ increase
<b><i>eat-2 + <math>\gamma</math>-CD-2,5-BHQ</i></b>							
<b>2,5-BHQ 10 <math>\mu</math>g</b>	<b>33,144</b>	<b>84/102</b>	<b>30,217</b>	<b>48/60</b>	<b>9,686600258</b>	<b>&lt;0,035</b>	<b>8,28 <math>\pm</math> 1,8</b>
	29,225	59/71	27,892	87/96	4,779148143	<0,038	
	28,247	50/61	25,589	61/65	10,38727578	<0,010	
<b>2,5-BHQ 50 <math>\mu</math>g</b>	32,733	77/103	30,217	48/60	8,32643876	0,129	<b>10,85 <math>\pm</math> 1,3</b>
	<b>31,047</b>	<b>83/96</b>	<b>27,892</b>	<b>87/96</b>	<b>11,31148716</b>	<b>&lt;0,0001</b>	
	28,8946	61/67	25,589	61/65	12,91805072	<0,001	
<b><i>eat-2 + <math>\gamma</math>-CD-2,6-BHQ</i></b>							
<b>2,6-BHQ 10 <math>\mu</math>g</b>	31,382	56/78	30,217	48/60	3,85544561	0,9	<b>5,94 <math>\pm</math> 1,7</b>
	<b>29,21</b>	<b>63/68</b>	<b>27,892</b>	<b>87/96</b>	<b>4,725369282</b>	<b>&lt;0,044</b>	
	27,952	71/87	25,589	61/65	9,234436672	<0,006	
<b>2,6-BHQ 50 <math>\mu</math>g</b>	29,272	26/104	30,217	48/60	-3,127378628	0,153	<b>5,89 <math>\pm</math> 5,9</b>
	<b>29,683</b>	<b>105/116</b>	<b>27,892</b>	<b>87/96</b>	<b>6,421196042</b>	<b>&lt;0,002</b>	
	29,268	35/43	25,589	61/65	14,37727148	<0,0001	
<b><i>eat-2 + <math>\gamma</math>-CD-Thapsigargin</i></b>							
<b>Thapsigargin 1 <math>\mu</math>g</b>	28,402	56/68	27,892	87/96	1,828481285	0,9	<b>6,08 <math>\pm</math> 1,8</b>
	<b>27,405</b>	<b>73/83</b>	<b>25,589</b>	<b>61/65</b>	<b>7,096799406</b>	<b>&lt;0,028</b>	
	23,408	57/85	21,414	64/95	9,311665266	<0,001	
<b>Thapsigargin 10 <math>\mu</math>g</b>	<b>27,425</b>	<b>57/63</b>	<b>25,589</b>	<b>61/65</b>	<b>7,17495799</b>	<b>&lt;0,039</b>	<b>7,79 <math>\pm</math> 0,6</b>
	23,213	70/101	21,414	64/95	8,401046045	<0,007	

**Table 12: Lifespan assays performed with SERCA inhibitors in DA113 (*eat-2*) worms.** The table shows the amount of drug used; the half-life ( $T_{1/2}$ ) of the control and treated worms obtained from the Kaplan-Meier analysis for survival; the number of worms in the experiment (final/total); the % increase in the half-life of treated worms; the statistical significance of the effect of the drug in each case; and the mean  $\pm$  s.e of the  $T_{1/2}$  increase in treated worms. In bold, are indicated the survival assays plotted in figure 45.

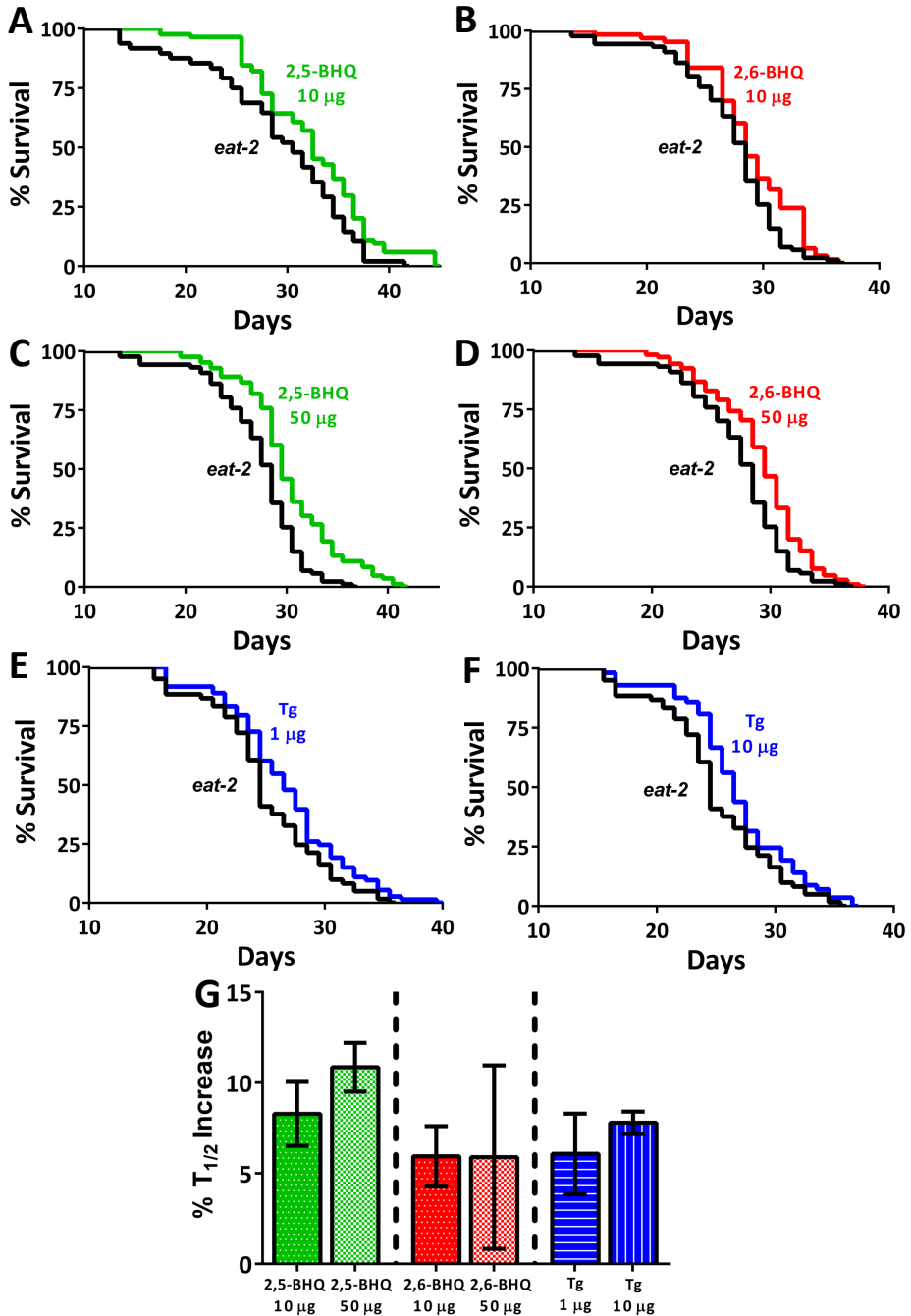


**Figure 45: Effects of SERCA inhibitors in DA1113 (*eat-2*) mutants lifespan.** The effects of both SERCA inhibitors, 2,5-BHQ (A,C) (in green), and Tg (E,F) (in blue) were studied in DA1113 mutants. Parallel experiments with 2,6-BHQ (C,D) are in red. In figure G the mean % of lifespan increase is shown for each treatment.

As shown in figure 45 and table 12, both 2,5-BHQ and Tg were able to increase DA1113 lifespan a 10,85% and 7,79% respectively highlighting that the treatments were efficient enough to induce changes in life expectancy, thus SERCA inhibitors do not extend lifespan by the induction of caloric restriction.

#### I.4 SERCA inhibitors require functional mitochondria to extend *C. elegans* lifespan

It has already been discussed in the introduction that SERCA and mitochondria establish physical connections between each other forming cellular microdomains called MAMs. As more and more evidence has come up in the last years implicating these structures in the aging process and its regulation by  $\text{Ca}^{2+}$  signaling, it seemed appropriate to study the effects in *C. elegans* mutants that are characterized by dysfunctional mitochondria.

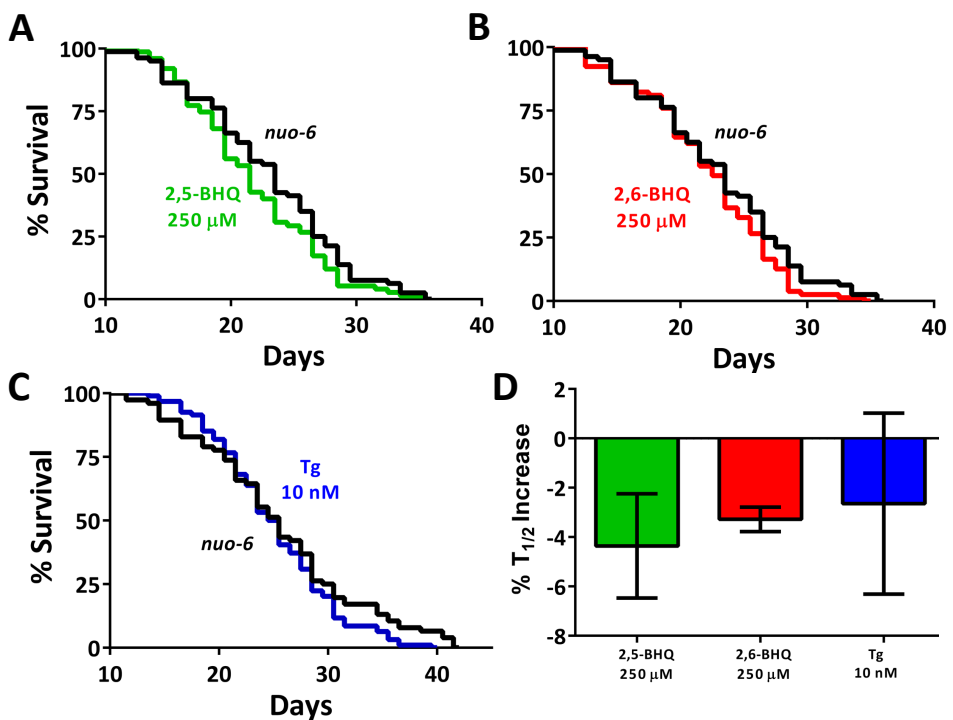


**Figure 46: Effects of SERCA inhibitors in MQ1333 (*nuo-6*) mutants lifespan.** The effects of both SERCA inhibitors, 2,5-BHQ (A) (in green), and Tg (C) (in blue) were studied in MQ1333 mutants. Parallel experiments with 2,6-BHQ (B) are in red. In graph D the mean % of lifespan increase is shown for each treatment.

Drug	T <sub>1/2</sub> drug (days)	N drug	T <sub>1/2</sub> control (days)	N Control	% T <sub>1/2</sub> increase	P value	Mean % T <sub>1/2</sub> increase
<b><i>nuo-6</i> + 2,5-BHQ</b>							
<b>2,5-BHQ 250 μM</b>	24,518	90/103	26,39	76/102	-7,093596059	< 0,013	
	25,055	83/92	25,107	70/89	-0,207113554	0,098	<b>-4,36 ± 2,1</b>
	<b>22,433</b>	<b>75/93</b>	<b>23,808</b>	<b>80/104</b>	<b>-5,775369624</b>	<b>0,071</b>	
<b><i>nuo-6</i> + 2,6-BHQ</b>							
<b>2,6-BHQ 250 μM</b>	25,434	88/104	26,39	76/102	-3,622584312	0,08	
	24,529	79/103	25,107	70/89	-2,302146812	0,814	<b>-3,28 ± 0,5</b>
	22,876	79/100	23,808	80/104	-3,914650538	0,102	
<b><i>nuo-6</i> + Thapsigargin</b>							
<b>Thapsigargin 10 nM</b>	25,678	94/105	26,39	76/102	-2,697991664	0,138	
	26,044	89/101	25,107	70/89	3,732026925	0,878	<b>-2,64 ± 3,7</b>
	21,673	90/100	23,808	80/104	-8,967573925	<0,001	

**Table 13: Lifespan assays performed with SERCA inhibitors in MQ1333 (*nuo-6*) worms.** The table shows the amount of drug used; the half-life (T<sub>1/2</sub>) of the control and treated worms obtained from the Kaplan-Meier analysis for survival; the number of worms in the experiment (final/total); the % increase in the half-life of treated worms; the statistical significance of the effect of the drug in each case; and the mean ± s.e of the T<sub>1/2</sub> increase in treated worms. In bold, are indicated the survival assays plotted in figure 46.

In this case, the chosen mutant is MQ1333 (*nuo-6*) (see table 4, p85). This strain is defective in the NADH Ubiquinone Oxidoreductase resulting in the impaired function of the complex I of the electron transport chain. This strain shows increased lifespan. After the treatment with SERCA inhibitors of MQ1333 mutants no effects in lifespan were observed (see figure 46, table 13). This fact highlights the necessity of functional mitochondria for the drugs to be effective and extend *C. elegans* lifespan.

## 1.5 Effect of SERCA inhibitors in nutrient sensing pathways *C. elegans* mutants

Nutrient signaling pathways are able to respond to changes in nutrient availability and have been linked to changes in life expectancy for several years. There are mainly four different pathways including IIS pathway, AMPK pathway, mTOR pathway and Sirtuins pathway. Although they are included in the same group, not all of them show the same effect on life expectancy: while AMPK and Sirtuins increased activity cause beneficial effects on lifespan, IIS and mTOR produce the opposite effect. Although the regulation of this pathways by Ca<sup>2+</sup> signaling is not totally clear yet, it has been demonstrated that both AMPK and mTOR activities can be modulated by intracellular Ca<sup>2+</sup> (see introduction, section III.5, p70). Conveniently, mutant strains for the four pathways are available allowing to study the implication of all these pathways in SERCA inhibitors lifespan extension induction.

### I.5.1 DAF-2 is not required for SERCA inhibitors lifespan extension

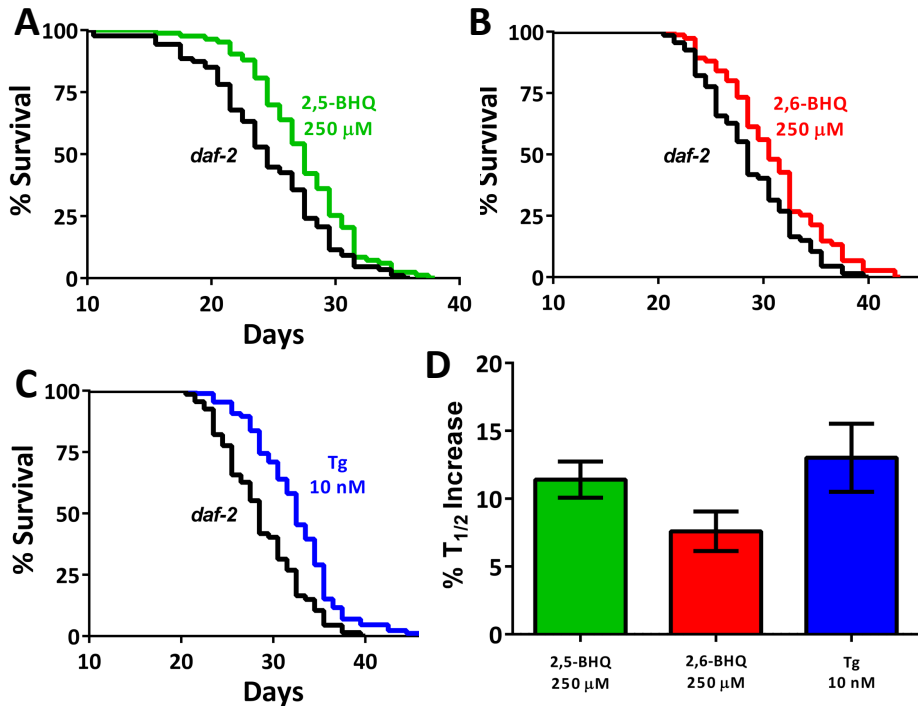


**Figure 47: Effects of SERCA inhibitors in CB1370 (*daf-2*) mutants lifespan.** The effects of both SERCA inhibitors, 2,5-BHQ (A) (in green), and Tg (C) (in blue) were studied in CB1370 mutants. Parallel experiments with 2,6-BHQ (B) are in red. In graph D the mean % of lifespan increase is shown for each treatment.

Drug	$T_{1/2}$ drug (days)	N drug	$T_{1/2}$ control (days)	N Control	% $T_{1/2}$ increase	P value	Mean % $T_{1/2}$ increase
<i>daf-2</i> + 2,5-BHQ							
2,5-BHQ 250 $\mu$ M	<b>27,984</b>	<b>83/108</b>	<b>25,284</b>	<b>87/99</b>	10,68	<b>&lt;0,001</b>	<b>11,41 <math>\pm</math> 1,3</b>
	32,180	77/103	29,371	67/91	9,56	<0,0001	
	29,336	100/143	25,736	75/146	13,99	<0,0001	
<i>daf-2</i> + 2,6-BHQ							
2,6-BHQ 250 $\mu$ M	<b>26,614</b>	<b>107/113</b>	<b>25,284</b>	<b>87/99</b>	5,26	<b>0,128</b>	<b>7,60 <math>\pm</math> 1,46</b>
	31,499	75/102	29,371	67/91	7,25	<0,01	
	28,384	93/144	25,736	75/146	10,29	<0,0001	
<i>daf-2</i> + Thapsigargin							
Thapsigargin 10 nM	<b>27,464</b>	<b>98/110</b>	<b>25,284</b>	<b>87/99</b>	8,62	<0,051	<b>13,03 <math>\pm</math> 2,51</b>
	<b>33,23</b>	<b>86/107</b>	<b>29,371</b>	<b>67/91</b>	<b>13,14</b>	<b>&lt;0,0001</b>	
	30,192	108/145	25,736	75/146	17,31	<0,0001	

**Table 14: Lifespan assays performed with SERCA inhibitors in CB1370 (*daf-2*) worms.** The table shows the amount of drug used; the half-life ( $T_{1/2}$ ) of the control and treated worms obtained from the Kaplan-Meier analysis for survival; the number of worms in the experiment (final/total); the % increase in the half-life of treated worms; the statistical significance of the effect of the drug in each case; and the mean  $\pm$  s.e. of the  $T_{1/2}$  increase in treated worms. In bold, are indicated the survival assays plotted in figure 47.

The effect of SERCA inhibitors and its link to IIS pathway was explored using the CB1370 mutant (see table 4, p85), that has a loss-of-function mutation of *daf-2*, orthologue to the insulin receptor in mammals. As shown in figure 47 and table 14 both 2,5-BHQ and Tg were able to increase the worm's lifespan with a mean value of 11,41% and 13,03% respectively, indicating that the effect of SERCA inhibitors is not achieved through the modulation of IIS signaling pathway in a direct manner.

### I.5.2 AMPK is required for SERCA inhibitors lifespan extension

AMPK is the main energy sensor in the cells responding to changes in the ATP/AMP ratio. Besides its activation by changes in the energy balance, AMPK is also activated by changes in intracellular  $[Ca^{2+}]$  through CaMKK $\beta$ . In *C. elegans* AMPK homologue, AAK has two catalytic subunits *aak-1* and *aak-2* although their particular regulation is not well established. To study the possible implication of AAK in SERCA inhibitors lifespan extension two different mutants have been used: RB754 (*aak-2*), and AGD397 (*aak-1; aak-2*).

Drug	$T_{1/2}$ drug (days)	N drug	$T_{1/2}$ control (days)	N Control	% $T_{1/2}$ increase	P value	Mean % $T_{1/2}$ increase
<b><i>aak-2</i></b>							
2,5-BHQ 250 $\mu$ M	16,496	76/100	15,423	64/101	6,96	<0,003	6,26 $\pm$ 1,37
	13,845	76/93	12,934	47/61	7,04	<0,005	
	14,360	98/112	14,033	85/95	2,33	0,756	
	16,547	93/111	15,221	92/107	8,71	<0,0001	
2,6-BHQ 250 $\mu$ M	15,778	69/90	15,423	64/101	2,30	0,393	4,57 $\pm$ 1,93
	14,084	83/94	12,934	47/61	8,89	<0,001	
	14,088	101/105	14,033	85/95	0,39	0,964	
	16,242	97/111	15,221	92/107	6,71	<0,004	
Thapsigargin 10 nM	18,19	89/102	16,997	69/81	7,018885686	<0,0001	3,71 $\pm$ 1,69
	20,392	81/99	19,305	62/80	5,630665631	<0,014	
	20,619	79/101	20,054	52/64	2,817393039	0,37	
	20,29	90/109	20,416	86/109	-0,617163009	0,974	
<b><i>aak-1;aak-2</i></b>							
2,5-BHQ 250 $\mu$ M	15,311	99/154	15,579	93/156	-1,72	0,222	-0,96 $\pm$ 1,02
	14,520	105/122	14,447	101/112	0,51	0,957	
	14,446	102/118	14,970	102/121	-3,50	<0,016	
	13,714	98/115	13,594	86/109	0,88	<0,698	
2,6-BHQ 250 $\mu$ M	15,863	101/151	15,579	93/156	1,82	0,649	0,31 $\pm$ 1,6
	14,407	118/137	14,447	101/112	-0,28	0,771	
	14,410	86/101	14,970	102/121	-3,74	<0,006	
	14,061	96/117	13,594	86/109	3,44	0,16	
Thapsigargin 10 nM	14,786	89/112	14,970	102/121	-1,23	0,399	0,25 $\pm$ 1,49
	13,83	86/117	13,594	86/109	1,74	0,563	

**Table 15: Lifespan assays performed with SERCA inhibitors in RB157 (*aak-2*) and AGD397 (*aak-1;aak-2*) worms.** The table shows the amount of drug used; the half-life ( $T_{1/2}$ ) of the control and treated worms obtained from the Kaplan-Meier analysis for survival; the number of worms in the experiment (final/total); the % increase in the half-life of treated worms; the statistical significance of the effect of the drug in each case; and the mean  $\pm$  s.e of the  $T_{1/2}$  increase in treated worms. In bold, are indicated the survival assays plotted in figure 48.

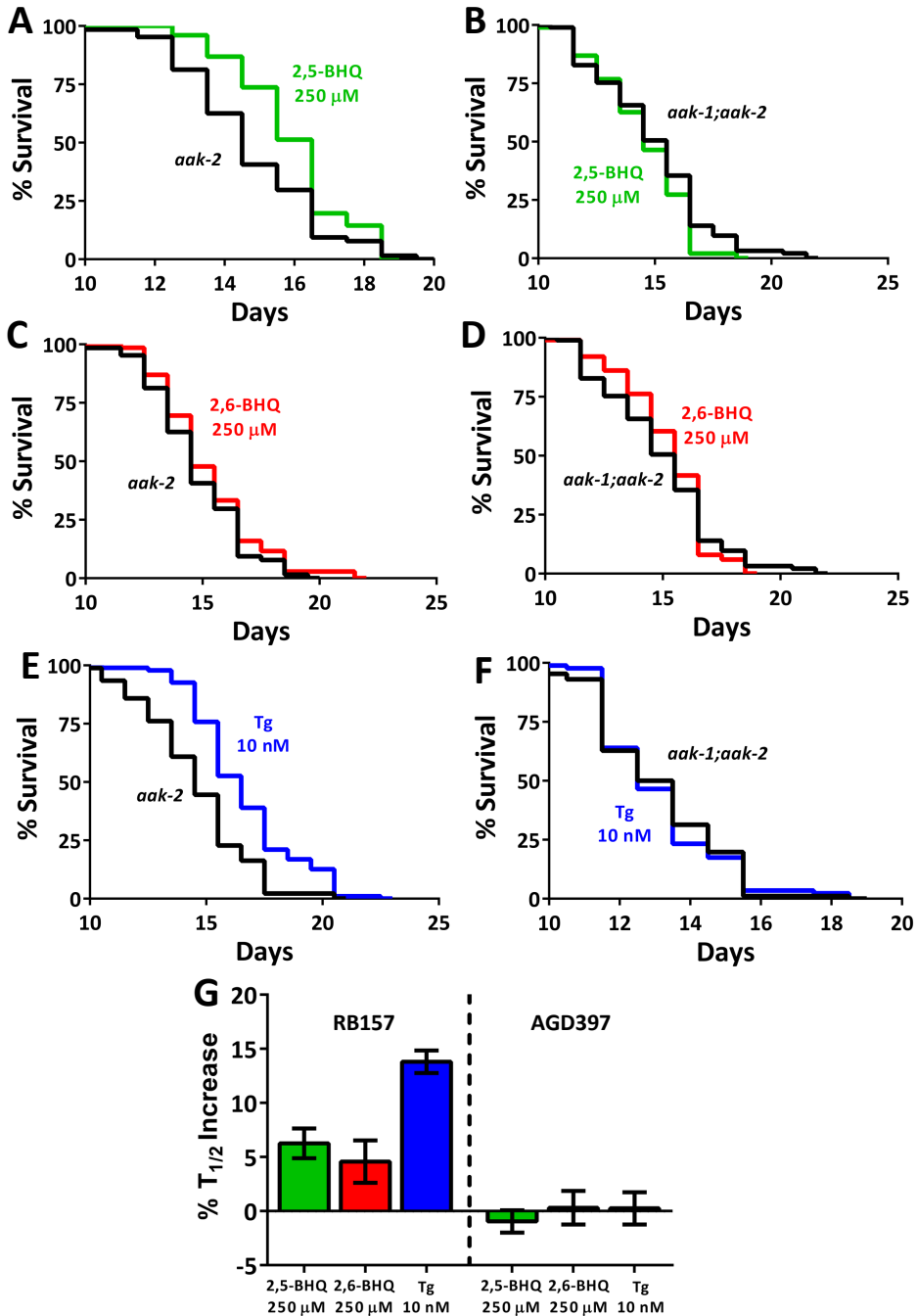


**Figure 48: Effects of SERCA inhibitors in RB157 (*aak-2*) and AGD397 (*aak-1;aak-2*) mutants lifespan.** The effects of both SERCA inhibitors, 2,5-BHQ (A,B) (in green), and Tg (C) (in blue) were studied in RB157 and AGD397 mutants. Parallel experiments with 2,6-BHQ (C) are in red. In graph G the mean % of lifespan increase is shown for each treatment.

Figure 48 shows that SERCA inhibitors behave differently in the two mutants used to explore the role of AMPK in lifespan extension through SERCA inhibition. While RB157 mutants, that are defective only in the *aak-2* catalytic subunit, exhibit lifespan extension after the treatment with 2,5-BHQ and Tg, the lack of both catalytic subunits abolishes the observed effects (figure 48, table 15). As no specific regulation of AAK by its two subunits is well established, this differential behavior can just be interpreted by saying that although loss of function of one of AAK catalytic subunits, *aak-2*, is not enough to abolish SERCA inhibitors effects, the lack of function of both subunits suppresses the lifespan extension, suggesting that AMPK plays a role in this phenomena.

### I.5.3 mTOR is required for SERCA inhibitors lifespan extension

mTOR, mechanistic target of rapamycin, is a serine/threonine involved in the response to changes in amino acids availability. mTOR pathway has multiple downstream effects through the formation of two different complexes and the activation of multiple cascades (see introduction, section II.4.2, p51).

Drug	T <sub>1/2</sub> drug (days)	N drug	T <sub>1/2</sub> control (days)	N Control	% T <sub>1/2</sub> increase	P value	Mean % T <sub>1/2</sub> increase
<i>daf-15 (+/-)</i>							
2,5-BHQ 250 μM	17,718	85/103	18,226	81/100	-2,79	0,377	-1,72 ± 1,2
	19,748	77/100	19,620	69/91	0,65	0,819	
	19,559	79/96	20,171	82/93	-3,03	0,172	
2,6-BHQ 250 μM	18,950	87/102	18,226	81/100	3,97	0,082	0,96 ± 1,8
	19,827	80/101	19,620	69/91	1,06	0,833	
	19,737	89/107	20,171	82/93	-2,15	0,321	
Thapsigargin 10 nM	19,877	71/90	19,62	69/91	1,31	0,745	-4,77 ± 6,1
	17,981	89/104	20,171	82/93	-10,86	<0,000	
<i>rsk-1</i>							
2,5-BHQ 250 μM	24,757	142/155	19,840	135/146	24,78	<0,0001	24,92 ± 2,2
	30,135	134/155	24,163	116/146	24,72	<0,0001	
	28,903	152/159	22,154	116/143	30,46	<0,0001	
	26,672	133/141	22,276	146/155	19,73	<0,0001	
2,6-BHQ 250 μM	24,730	143/151	19,840	135/146	24,65	<0,0001	24,90 ± 3,3
	29,241	126/143	24,163	116/146	21,02	<0,0001	
	29,720	154/160	22,154	116/143	34,15	<0,0001	
	26,684	153/158	22,276	146/155	19,79	<0,0001	
Thapsigargin 10 nM	19,857	139/155	17,575	132/154	12,98	<0,0001	10,15 ± 2,1
	24,667	117/153	22,154	116/143	11,34	<0,001	
	23,643	144/151	22,276	146/155	6,14	<0,012	

**Table 16: Lifespan assays performed with SERCA inhibitors in DR412 (*daf-15*) and RB1206 (*rsk-1*) worms.** The table shows the amount of drug used; the half-life (T<sub>1/2</sub>) of the control and treated worms obtained from the Kaplan-Meier analysis for survival; the number of worms in the experiment (final/total); the % increase in the half-life of treated worms; the statistical significance of the effect of the drug in each case; and the mean ± s.e of the T<sub>1/2</sub> increase in treated worms. In bold, are indicated the survival assays plotted in figure 49.



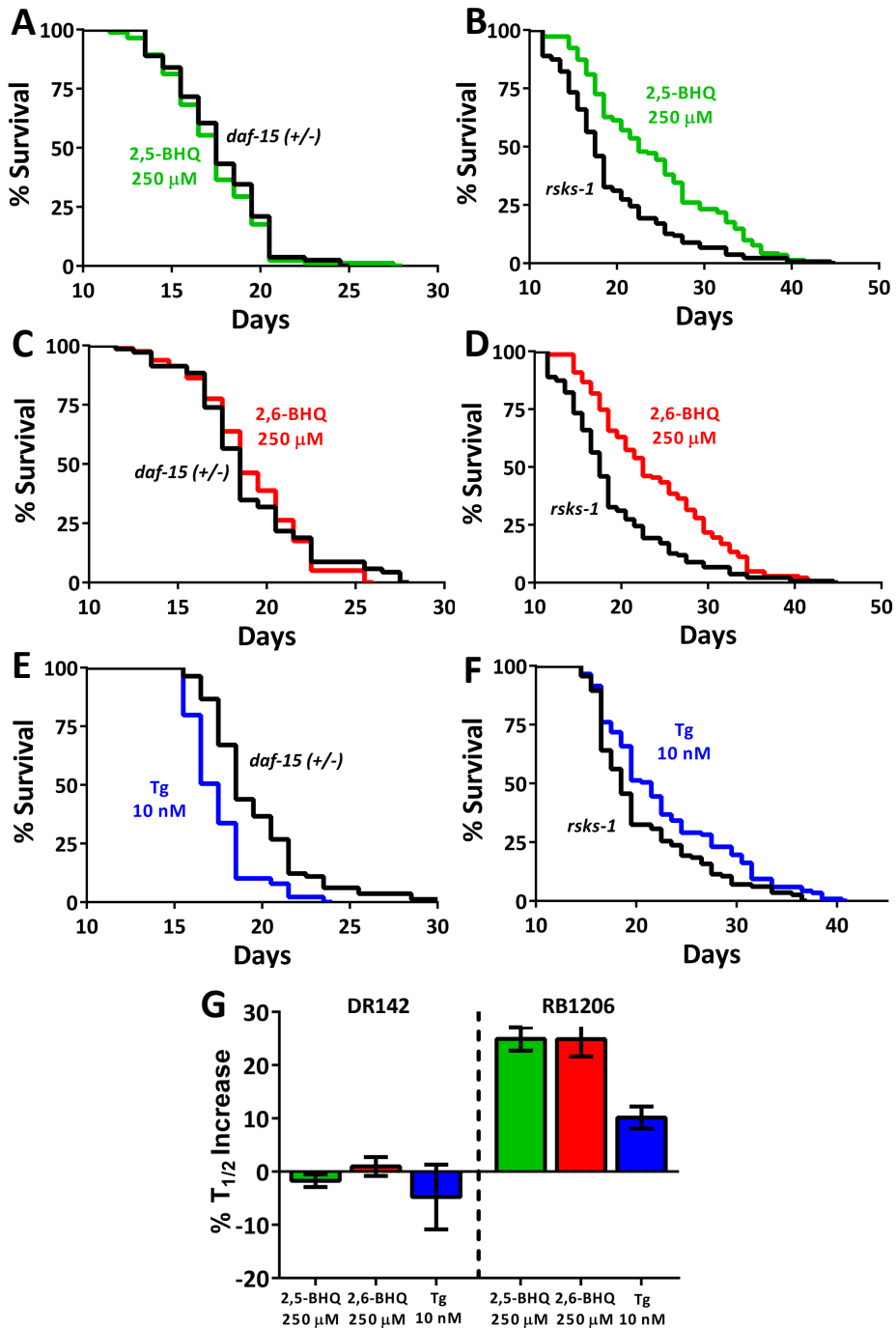


**Figure 49: Effects of SERCA inhibitors in DR142 (*daf-15*) and RB1206 (*rsk-1*) mutants lifespan.** The effects of both SERCA inhibitors, 2,5-BHQ (A,B) (in green), and Tg (E,F) (in blue) were studied in DR142 and RB1206 mutants. Parallel experiments with 2,6-BHQ (C,D) are in red. In graph G the mean % lifespan increase is shown for each treatment.

There are *C. elegans* strains with mutations in proteins involved in the mTOR pathway including the heterozygous *daf-15* mutant (DR142), the orthologue of RAPTOR, and *rsk-1* mutant (RB1206), the orthologue of S6K in mammals (see table 4, p85). Using this two loss of function mutants the participation of mTOR pathway in lifespan extension induced by SERCA inhibitors has been investigated. In figure 49 and table 16 are shown the effects of SERCA inhibitors in the mTOR pathway mutants. As it happens in AMPK pathway mutants, the effect of the treatments in both mutants are different. While DR142 mutants are not affected by the treatment with 2,5-BHQ, with a mean lifespan of -1,72%, or even the effects observed are detrimental in the case of thapsigargin (-4,77%), in RB1206 mutants the lifespan extension is really large in the case of 2,5-BHQ with a mean increase in lifespan around the 25%. It has to be noted that the same effect can be observed with the treatment with 2,6-BHQ indicating that this increase in lifespan is not caused by SERCA inhibition. On the other hand, the treatment with thapsigargin was able to produce a mean lifespan increase of 10%, meaning that RSKS-1 is not essential for SERCA inhibitors effect in lifespan. Considering all this data together, it is clear that mTOR pathway activity is needed for the induction of lifespan extension, but this effect is not driven through RSKS-1 activity.

#### I.5.4 Sirtuins pathway is not required for SERCA inhibitors lifespan extension

Sirtuins (silent information regulator proteins) conform a pathway that responds to changes in NAD<sup>+</sup>/NAHD favoring the oxidized form (see introduction, section II4.4, p56). To study the implication of this pathway in SERCA inhibitors lifespan extension, the *sir-2.1* mutant has been used.

Drug	T <sub>1/2</sub> drug (days)	N drug	T <sub>1/2</sub> control (days)	N Control	% T <sub>1/2</sub> increase	P value	Mean % T <sub>1/2</sub> increase
<i>sir-2.1</i> + 2,5-BHQ							
2,5-BHQ 250 μM	17,956	100/103	17,924	88/101	0,18	0,931	
	<b>23,875</b>	<b>98/107</b>	<b>21,737</b>	<b>81/90</b>	<b>9,84</b>	<b>&lt;0,016</b>	<b>10,19 ± 5,8</b>
	19,305	90/98	16,014	83/86	20,55	<0,0001	
<i>sir-2.1</i> + 2,6-BHQ							
2,6-BHQ 250 μM	16,386	99/09	17,924	88/101	-8,58	<0,011	
	<b>24,252</b>	<b>95/103</b>	<b>21,737</b>	<b>81/90</b>	<b>11,57</b>	<b>&lt;0,004</b>	<b>5,60 ± 7,1</b>
	18,228	105/118	16,014	83/86	13,83	<0,0001	
<i>sir-2.1</i> + Thapsigargin							
Thapsigargin 10 nM	19,792	97/107	17,924	88/101	10,42	<0,011	
	23,375	90/104	21,737	81/90	7,54	0,053	<b>9,37 ± 0,9</b>
	<b>17,638</b>	<b>97/108</b>	<b>16,014</b>	<b>83/86</b>	<b>10,14</b>	<b>&lt;0,001</b>	

**Table 17: Lifespan assays performed with SERCA inhibitors in VC199 (*sir-2.1*) worms.** The table shows the amount of drug used; the half-life (T<sub>1/2</sub>) of the control and treated worms obtained from the Kaplan-Meier analysis for survival; the number of worms in the experiment (final/total); the % increase in the half-life of treated worms; the statistical significance of the effect of the drug in each case; and the mean ± s.e of the T<sub>1/2</sub> increase in treated worms. In bold, are indicated the survival assays plotted in figure 50.

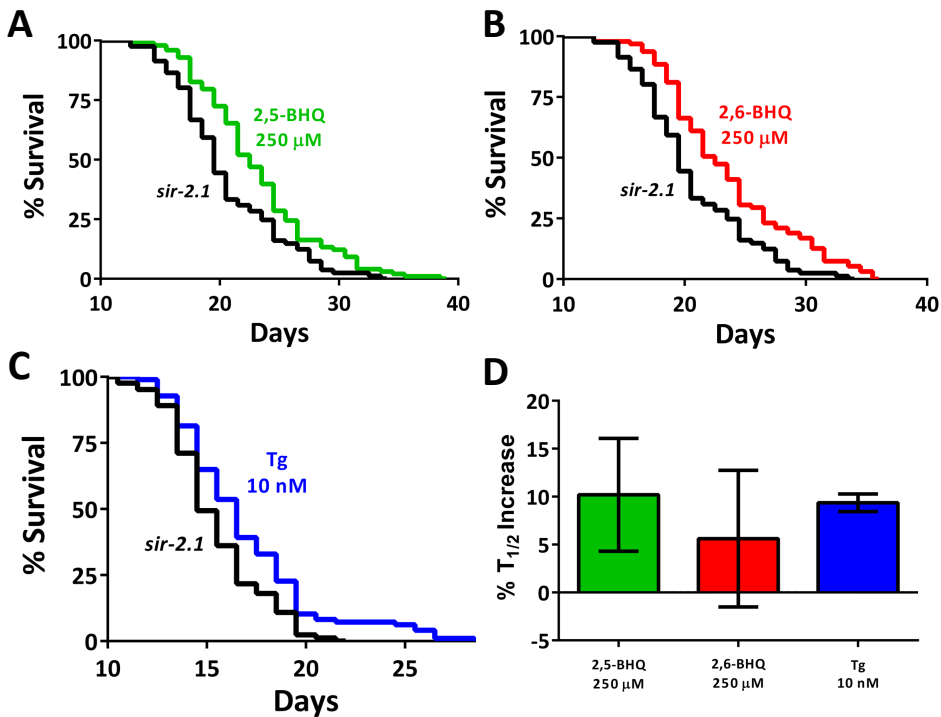


**Figure 50: Effects of SERCA inhibitors in VC199 (*sir-2.1*) mutants lifespan.** The effects of both SERCA inhibitors, 2,5-BHQ (A) (in green), and Tg (C) (in blue) were studied in VC199 mutants. Parallel experiments with 2,6-BHQ (B) are in red. In graph D the mean % lifespan increase is shown for each treatment.

Figure 50 and table 17 show that both 2,5-BHQ and thapsigargin induced and increase in *sir-2.1* worm's lifespan indicating that this pathway is not required for the pro longevity effect driven by SERCA inhibitors.

### I.5.5 DAF-16 is required for SERCA inhibitors lifespan extension

DAF-16 is the FoXO orthologue, and acts as a pro longevity nuclear effector in response to numerous stimulus including the activation of AMPK and the inhibition of mTOR. There is available a *C. elegans* mutant, CF1038 (see table 4, p85), that has been used to investigate the importance of DAF-16 in the lifespan extension induced by SERCA inhibitors.

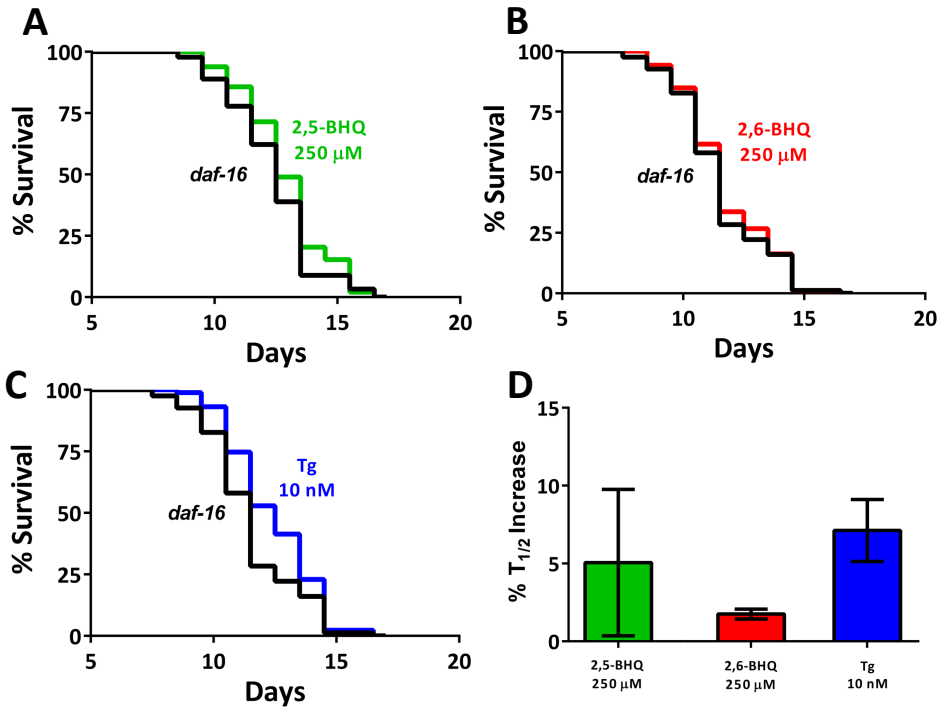


**Figure 51: Effects of SERCA inhibitors in CF1038 (*daf-16*) mutants lifespan.** The effects of both SERCA inhibitors, 2,5-BHQ (A) (in green), and Tg (C) (in blue) were studied in CF1038 mutants. Parallel experiments with 2,6-BHQ (B) are in red. In graph D the mean % lifespan increase is shown for each treatment.

Drug	$T_{1/2}$ drug (days)	N drug	$T_{1/2}$ control (days)	N Control	% $T_{1/2}$ increase	P value	Mean % $T_{1/2}$ increase
<b><i>daf-16</i> + 2,5-BHQ</b>							
2,5-BHQ 250 $\mu$ M	11,814	<b>76/82</b>	12,165	<b>81/101</b>	-2,89	0,128	
	13,512	98/114	12,909	90/103	4,67	<0,04	<b>5,05 <math>\pm</math> 4,7</b>
	16,966	80/95	14,964	0,889	13,38	<0,0001	
<b><i>daf-16</i> + 2,6-BHQ</b>							
2,6-BHQ 250 $\mu$ M	12,379	86/102	12,165	81/101	1,76	0,577	
	13,063	<b>101/107</b>	<b>12,909</b>	<b>90/103</b>	1,19	0,83	<b>1,75 <math>\pm</math> 0,32</b>
	15,308	103/117	14,964	0,889	2,30	0,193	
<b><i>daf-16</i> + Thapsigargin</b>							
Thapsigargin 10 nM	13,01	87/104	12,165	81/101	6,95	<0,014	
	13,394	<b>96/111</b>	<b>12,909</b>	<b>81/101</b>	3,76	0,118	<b>7,12 <math>\pm</math> 2,0</b>
	16,558	97/118	14,964	0,889	10,65	<0,0001	

**Table 18: Lifespan assays performed with SERCA inhibitors in CF1038 (*daf-16*) worms.** The table shows the amount of drug used; the half-life ( $T_{1/2}$ ) of the control and treated worms obtained from the Kaplan-Meier analysis for survival; the number of worms in the experiment (final/total); the % increase in the half-life of treated worms; the statistical significance of the effect of the drug in each case; and the mean  $\pm$  s.e of the  $T_{1/2}$  increase in treated worms. In bold, are indicated the survival assays plotted in figure 51.

Figure 51 and table 18 show the effects of SERCA inhibitors in *daf-16* loss-of-function mutants. SERCA inhibitors 2,5-BHQ and thapsigargin are able to induce a moderate lifespan extension of 5% and 7% respectively which implies that even loss-of-function of *daf-16* is not enough to completely abolish the effect of the treatments, this effects are less effective than in wild-type worms.

## I.6 Effects of SERCA inhibitors in the ER stress response

### I.6.1 SERCA inhibitors do not trigger ER stress response

ER stress response activation has been linked to the promotion of longevity, which could be taking part in the prolongevity effects observed with SERCA inhibitors treatment. Moreover, thapsigargin, at higher doses than the ones used in this work, has been described to highly activate the ER stress response being harmful for different organisms. All this reasons led us to explore the possibility that this stress response pathway was being activated by the treatments.

ER stress response in *C. elegans* is induced by the activation of numerous proteins including the chaperone *hsp-4*, the *C. elegans* orthologue of BiP. That is why the transgenic strain SJ4005 (see table 3, p82) has been used to explore the effects of SERCA inhibitors in *C. elegans*. Briefly, this strain has GFP under the promoter of *hsp-4* inducing increases of fluorescence when the ER stress response is activated.

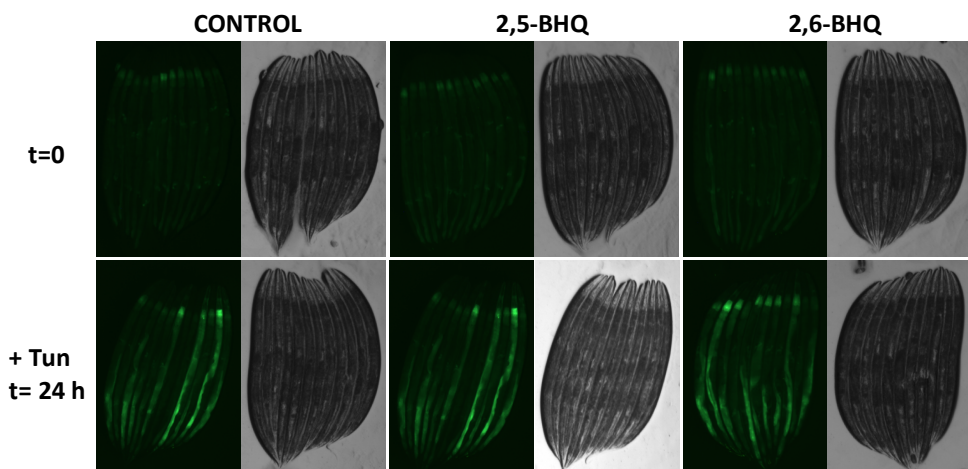


**Figure 52: Effects of 2,5-BHQ and 2,6-BHQ 250  $\mu$ M in SJ4005 GFP expression.** The figure shows the changes in GFP expression of SJ4005 worms after 72 hrs of treatment with 2,5-BHQ and 2,6-BHQ, and 24 hrs later after the induction of the ER stress response using tunicamycin in the presence of the treatment.

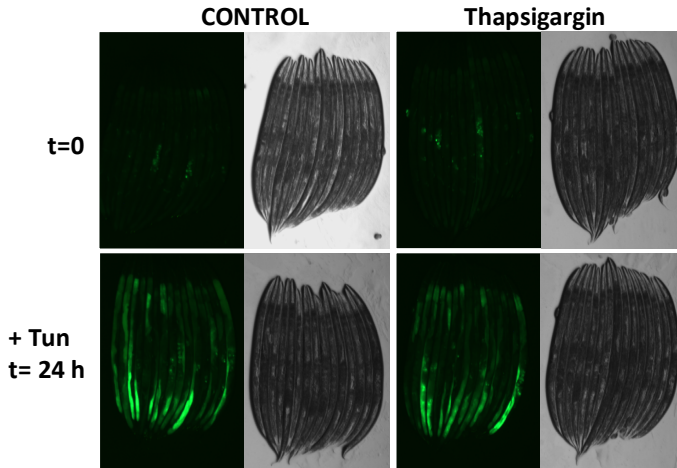


**Figure 53: Effects of thapsigargin 10 nM in SJ4005 GFP expression.** The figure shows the changes in GFP expression of SJ4005 worms after 72 hrs of treatment with 2,5-BHQ and 2,6-BHQ and 24 hrs later after the induction of the ER stress response using tunicamycin in the presence of the treatment.

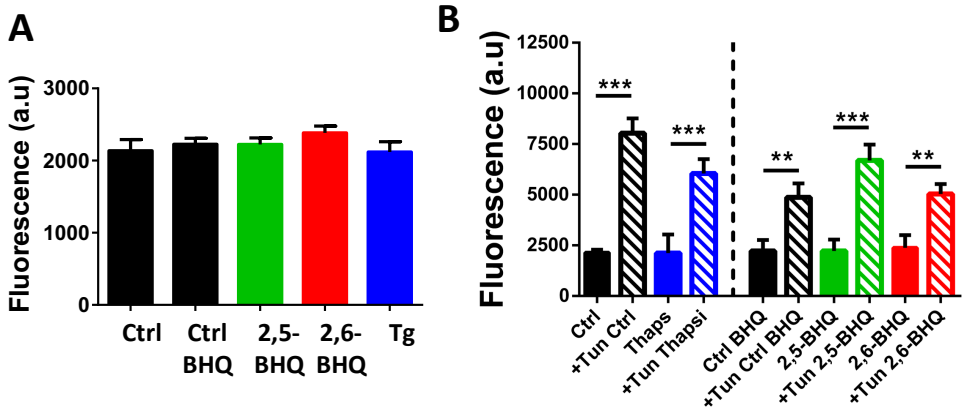


**Figure 54: ER stress response is not induced by SERCA inhibition.** The figure shows the changes in GFP expression of SJ4005 worms after 72 hrs of treatment with 2,5-BHQ and 2,6-BHQ and Tg (A) and 24 hrs later after the induction of the ER stress response using tunicamycin in the presence of the treatment (B). At least 40-42 worms per condition were analyzed.

Figure 52 is composed by representative images of the effects of 2,5-BHQ and 2,6-BHQ on the ER stress response. It shows that none of treatments stimulate the activation of the ER stress response. In a similar way, figure 53 shows that Tg does not induce the overexpression of *hsp4*. In all the cases mentioned above, the induction of ER stress by tunicamycin at a concentration of 10  $\mu\text{g}/\text{ml}$  was able to induce it. Finally, figure 54 summarizes the changes of GFP expression in control and tunicamycin conditions for all the treatments showing that although the SERCA inhibitors do not cause the initiation of the ER stress response, the treatment with tunicamycin initiated it in every condition.

## II. $\text{Na}^+/\text{Ca}^{2+}$ EXCHANGER INHIBITION AND AGING IN *C. ELEGANS*

During the development of this work, the inhibition of the  $\text{Na}^+/\text{Ca}^{2+}$  exchanger has been achieved by the treatment of the worms with CGP37157. This molecule is a permeable benzothiazepine mainly described as an inhibitor of the mitochondrial  $\text{Na}^+/\text{Ca}^{2+}$  exchanger with neuroprotectant properties.

### II.1 Effects of CGP37157 in *C. elegans* lifespan

#### II.1.1 CGP37157 extends *C. elegans* lifespan

Equally to the case of SERCA inhibitors, CGP37157 has a lipophilic nature, which can challenge the delivery of this compound to the worms as they live in an aqueous medium. To minimize this possible complications CGP37157 was also included in  $\gamma$ -CD forming inclusion compounds, increasing their water solubility, and restricting drug uptake to just oral administration (Kashima et al., 2012).

There was no data available about the effective concentration of this compound in *C. elegans*, as it had never been used in this model organism. To study the possible effects of CGP37157 in *C. elegans* a dose response experiment was designed to find the most effective concentration using the *C. elegans* strain AQ2038 that expresses the  $\text{Ca}^{2+}$  probe cameleon 2.1 in pharynx muscle cells as it has been demonstrated that the expression of the probe does not modify the phenotype compared to the control strain N2 (Alvarez-Illera et al., 2016) and was later going to be used to study the effects of the drug in pharyngeal  $\text{Ca}^{2+}$  signaling.

Finally, it was also tested if the method of administration of the drug could be influencing the results observed in lifespan extension. To that purpose, CGP37157 was added to the NGM before pouring the plates at different concentrations to find the most effective dose and evaluate the effects of the drug in *C. elegans* lifespan. Lastly, the possible interference of active OP50 culture in the results obtained was evaluated by the study of lifespan extension of CGP37157 using as a food source a heat-inactivated OP50 culture.

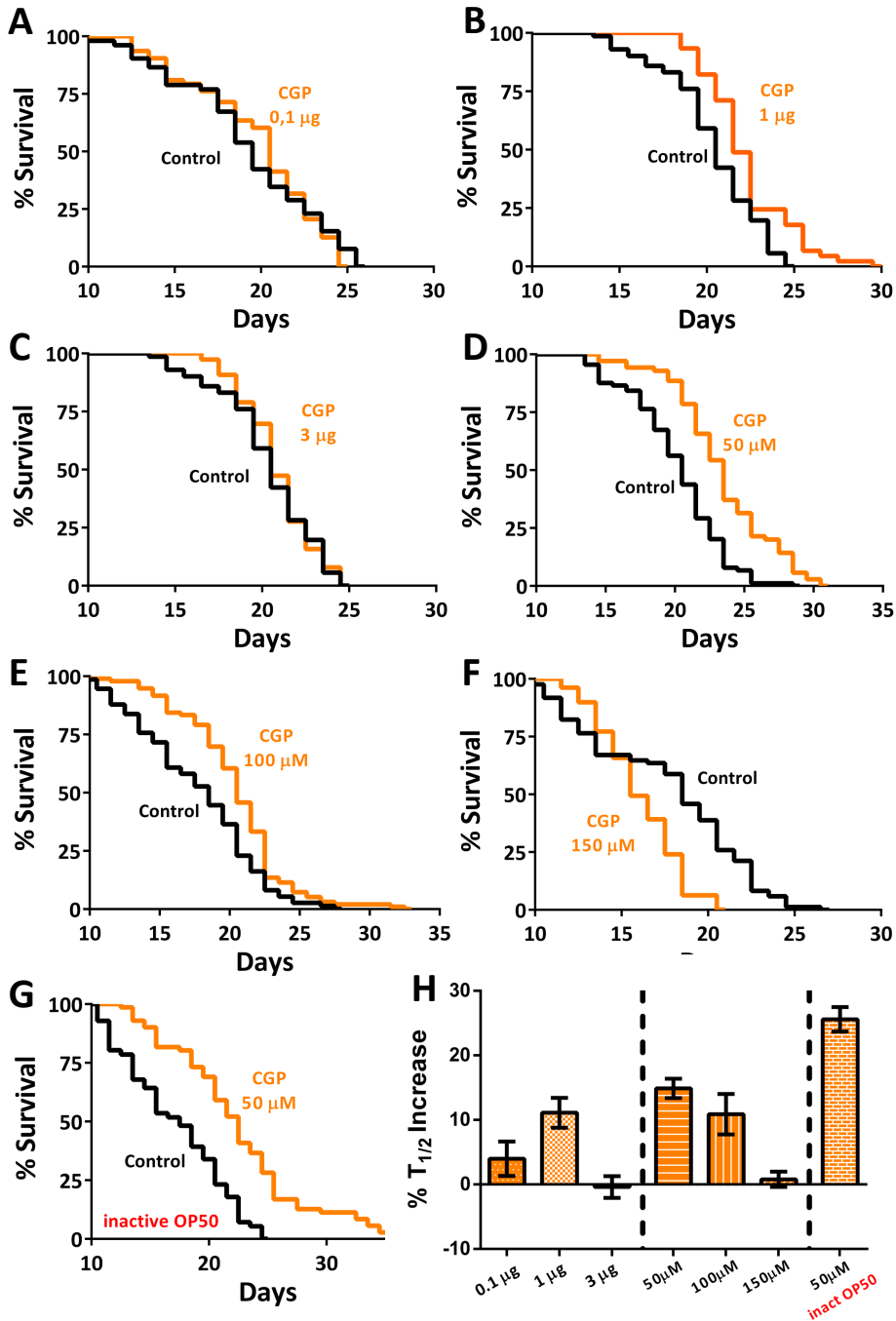


**Figure 55: Effects of CGP37157 in AQ2038 *C. elegans* lifespan.** The effects of CGP37157 were studied using two different methods of administration, including it in  $\gamma$ -CD (A, B, C) or adding it to the NGM (D, E, F). Graph G shows the effect of CGP37157 when OP50 is inactive. Finally, graph H summarizes the % mean lifespan increase for each treatment condition.



Drug	T <sub>1/2</sub> drug (days)	N drug	T <sub>1/2</sub> control (days)	N Control	% T <sub>1/2</sub> increase	P value	Mean % T <sub>1/2</sub> increase
<b>AQ2038 + <math>\gamma</math>-CD-CGP3757</b>							
<b>CGP37157 0,1 <math>\mu</math>g</b>	18,6	63/76	17,0	69/81	9,6	<0,0001	<b>2,7 <math>\pm</math> 2,5</b>
	20,5	78/100	19,3	62/80	6,4	<0,003	
	<b>20,7</b>	<b>63/80</b>	<b>20,1</b>	<b>52/64</b>	<b>3,0</b>	<b>0,636</b>	
	20,7	78/98	21,0	71/95	-1,7	0,668	
	21,4	45/60	22,3	78/103	-3,9	<0,024	
<b>CGP37157 1 <math>\mu</math>g</b>	19,3	88/101	17,0	69/81	13,4	<0,0001	<b>9,1 <math>\pm</math> 1,2</b>
	20,9	72/83	19,3	62/80	8,4	<0,001	
	21,9	48/61	20,1	52/64	9,4	0,092	
	<b>22,8</b>	<b>45/52</b>	<b>21,0</b>	<b>71/95</b>	<b>8,4</b>	<b>&lt;0,001</b>	
	23,7	79/103	22,3	78/103	6,0	<0,0001	
<b>CGP37157 3 <math>\mu</math>g</b>	17,6	73/99	17,0	69/81	3,8	0,112	<b>0,0 <math>\pm</math> 2,0</b>
	20,0	51/62	19,3	62/80	3,4	0,367	
	19,6	49/61	20,1	52/64	-2,2	0,962	
	<b>21,4</b>	<b>76/101</b>	<b>21,0</b>	<b>71/95</b>	<b>1,6</b>	<b>0,86</b>	
	20,9	49/62	22,3	78/103	-6,6	<0,008	
<b>AQ2038 + CGP37157</b>							
<b>CGP37157 50 <math>\mu</math>M</b>	25,628	90/107	22,908	82/100	11,87	<0,0001	<b>14,88 <math>\pm</math> 1,5</b>
	<b>24,110</b>	<b>70/96</b>	<b>20,690</b>	<b>89/106</b>	<b>16,53</b>	<b>&lt;0,0001</b>	
	21,368	105/114	18,381	74/80	16,25	<0,0001	
<b>CGP37157 100 <math>\mu</math>M</b>	<b>24,686</b>	<b>94/104</b>	<b>22,908</b>	<b>82/100</b>	<b>7,76</b>	<b>&lt;0,0001</b>	<b>10,90 <math>\pm</math> 3,1</b>
	20,960	96/105	18,381	74/80	14,03	<0,0001	
<b>CGP37157 150 <math>\mu</math>M</b>	16,590	79/90	16,399	85/92	1,16	0,994	<b>0,80 <math>\pm</math> 1,2</b>
	16,721	99/104	17,087	85/104	-2,14	0,073	
	<b>15,185</b>	<b>95/101</b>	<b>15,108</b>	<b>94/103</b>	<b>0,51</b>	<b>0,98</b>	
	15,953	94/103	15,390	96/101	3,66	0,348	
<b>AQ2038 treated with inactivated OP50</b>							
<b>CGP37157 50 <math>\mu</math>M</b>	23,149	71/98	17,669	56/74	31,01	<0,0001	<b>25,58 <math>\pm</math> 1,9</b>
	25,412	69/100	20,470	80/100	24,14	<0,0001	
	18,832	66/100	15,415	75/100	22,17	<0,0001	
	<b>21,296</b>	<b>63/80</b>	<b>17,037</b>	<b>46/60</b>	<b>25,00</b>	<b>&lt;0,0001</b>	

**Table 19: Lifespan assays performed with CGP37157 in AQ2038 wild type worms.** The table shows the amount of drug used; the half-life (T<sub>1/2</sub>) of the control and treated worms obtained from the Kaplan-Meier analysis for survival; the number of worms in the experiment (final/total); the % increase in the half-life of treated worms; the statistical significance of the effect of the drug in each case; and the mean  $\pm$  s.e of the T<sub>1/2</sub> increase in treated worms. In bold, are indicated the survival assays plotted in figure 55.

Represented in figure 55 and table 19 are the effects of CGP37157 in AQ2038 lifespan using two different methods of administration: the inclusion compounds and added to the NGM media. In both cases the treatment with CGP37157 succeeded to extend *C. elegans* lifespan in a dose dependent manner being the most effective doses 1  $\mu$ g in the case of the treatment with  $\gamma$ -CD-CGP37157 reaching a mean lifespan extension of 9,1%, and 50  $\mu$ M when the drug is added to the NGM causing a mean increase of *C. elegans* lifespan of 14,9%, seeming to be more effective this mode of drug administration. Finally, the effect of OP50 activity in the results observed was studied by feeding the worms with heat-inactivated OP50 cultures resulting even in a bigger lifespan increase of around

25.6% indicating that if OP50 has any effect in CGP37157 effect is by reducing its effect.

After the obtention of this results, it was decided to use the direct method of administration, adding the drug to the NGM, as the preferred one for the rest of the survival experiments except for the ones studying the effect of the drug in *eat-2* mutants as in the case of the SERCA inhibitors.

### II.1.2 CGP37157 does not extend *C. elegans* lifespan inducing caloric restriction

CGP37157, as many other  $\text{Ca}^{2+}$  signaling modulators could influence the muscular function of *C. elegans* affecting its pharyngeal pumping activity that could result in a caloric restriction induction. To explore if the effects of this treatment are caused by the induction of CR, the effect of the treatment in DA1113 mutants (see table 4, p79) was studied, as they have a mutation in the acetylcholine receptor EAT-2, that results in a decrease of pharyngeal activity, thus the CR response is already active. The reason to treat the worms with inclusion compounds is already explained in previous results (see section I.3, p119).

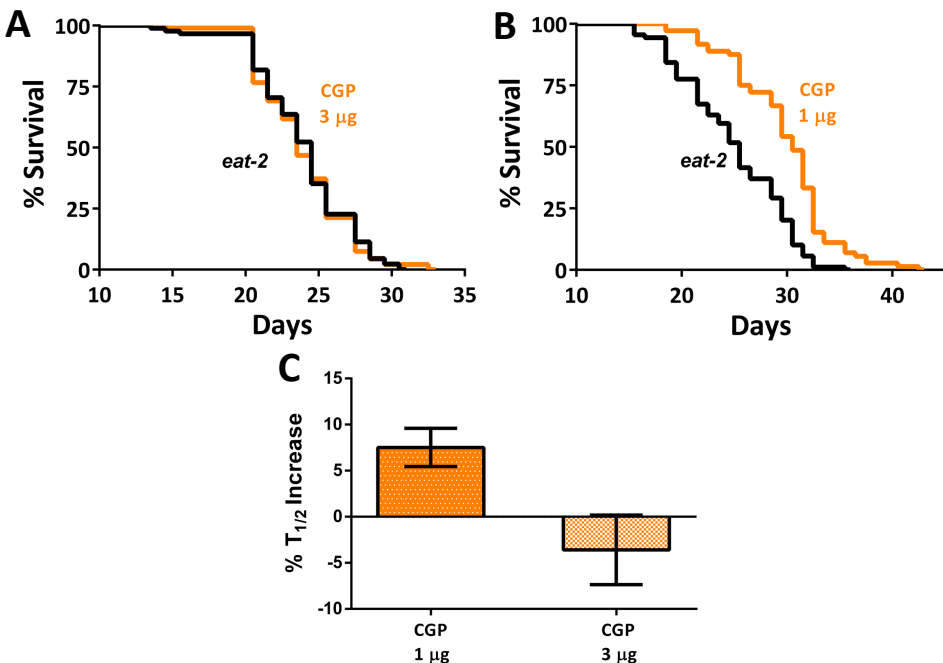


**Figure 56: Effects of CGP37157 in DA1113 (*eat-2*) *C. elegans* lifespan.** The effects of CGP37157 were studied using two different concentrations of  $\gamma$ -CD-CGP37157 (A, B). Graph C summarizes the % mean lifespan increase for each treatment condition.

Drug	T <sub>1/2</sub> drug (days)	N drug	T <sub>1/2</sub> control (days)	N Control	% T <sub>1/2</sub> increase	P value	Mean % T <sub>1/2</sub> increase
<b><i>eat-2 + ψ-CD-CGP3757</i></b>							
<b>CGP37157 1 μg</b>	30,4	72/93	25,9	89/107	17,6	<0,0001	<b>13,0 ± 2,7</b>
	26,8	67/101	24,7	88/121	8,3	<0,0001	
	<b>26,1</b>	<b>110/123</b>	<b>23,1</b>	<b>79/84</b>	<b>13,1</b>	<b>&lt;0,0001</b>	
<b>CGP37157 3 μg</b>	26,6	57/97	25,9	89/107	2,9	0,696	<b>1,4 ± 0,9</b>
	24,7	94/124	24,7	88/121	-0,1	0,832	
	<b>23,5</b>	<b>89/105</b>	<b>23,1</b>	<b>79/84</b>	<b>1,5</b>	<b>0,453</b>	

**Table 20: Lifespan assays performed with CGP37157 in DA1113 (*eat-2*) worms.** The table shows the amount of drug used; the half-life (T<sub>1/2</sub>) of the control and treated worms obtained from the Kaplan-Meier analysis for survival; the number of worms in the experiment (final/total); the % increase in the half-life of treated worms; the statistical significance of the effect of the drug in each case; and the mean ± s.e of the T<sub>1/2</sub> increase in treated worms. In bold, are indicated the survival assays plotted in figure 56.

As shown in figure 56 and table 20, CGP37157 was able to increase DA1113 lifespan a 13% when worms were treated with 1 μg of inclusion compound, while 3 μg caused no change in DA1113 expectancy having a mean increase in lifespan of 1,4%. This fact shows that this compound does not extend lifespan by inducing caloric restriction, which is even more evident when there is no need to use higher doses of the drug in a population that already has pharyngeal pumping reduced.

### II.1.3 CGP37157 requires functional mitochondria to increase *C. elegans* lifespan

CGP37157 is mainly known as an inhibitor of the mNCX. That is why it seemed appropriate to study if this treatment was able to induce lifespan extension in mitochondrial mutants that have the ETC activity impaired. To that end, the MQ1333 (*nuo-6*) was used. (see table 4, p85).

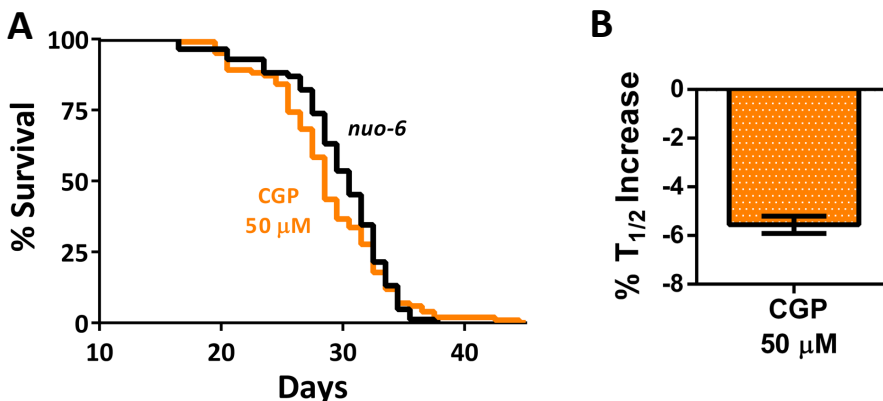


**Figure 57: Effects of CGP37157 in MQ1333 (*nuo-6*) *C. elegans* lifespan.** Graph A shows the effects of CGP37157 MQ1333 mutants. Graph B summarizes the % mean lifespan increase after the treatment.

Drug	T <sub>1/2</sub> drug (days)	N drug	T <sub>1/2</sub> control (days)	N Control	% T <sub>1/2</sub> increase	P value	Mean % T <sub>1/2</sub> increase
<b><i>nuo-6 + γ-CD-CGP3757</i></b>							
<b>CGP37157 1 μg</b>	34,8	117/140	32,7	115/151	6,3	<0,021	
	<b>30,0</b>	<b>101/141</b>	<b>31,0</b>	<b>84/115</b>	<b>-3,3</b>	<b>0,166</b>	<b>-1,2 ± 3,8</b>
	33,1	52/100	35,4	27/55	-6,6	0,197	

**Table 21: Lifespan assays performed with CGP37157 in MQ1333 (*nuo-6*) worms.** The table shows the amount of drug used; the half-life (T<sub>1/2</sub>) of the control and treated worms obtained from the Kaplan-Meier analysis for survival; the number of worms in the experiment (final/total); the % increase in the half-life of treated worms; the statistical significance of the effect of the drug in each case; and the mean ± s.e of the T<sub>1/2</sub> increase in treated worms. In bold, are indicated the survival assays plotted in figure 57.

MQ1333 mutants are not affected by the treatment with CGP37157 showing a mean lifespan increase of -1,2%. This means, that functional mitochondria, and more specifically, functional ETC is necessary for CGP37157 to be effective and extend *C. elegans* lifespan.

### II.1.4 Effects of CGP37157 in nutrient sensing pathways *C. elegans* mutants lifespan

As explained in results, section I.5, p122, nutrient sensing pathways are IIS, AMPK, mTOR and sirtuins signaling pathways. All of them are able to change their activity in response to changes in nutrient availability or the organisms energy balance. All this pathways have been described to regulate aging, but not much information about how Ca<sup>2+</sup> signaling regulates this process is known. That is why we decided to investigate the possible effects of CGP37157 in *C. elegans* mutant strains for this four pathways.

#### II.1.4.1 Effects of CGP37157 in IIS, AMPK, and Sirtuins pathways mutants longevity.

The effect of CGP37157 and its link to IIS pathway was explored using the CB1370 (*daf-2*) mutant, that has a loss-of-function mutation of *daf-2*, the orthologue of the insulin receptor in mammals. As this pathway activation has detrimental effects for lifespan, this mutation causes an increase in survival of *C. elegans* worms. For the AMPK implication in lifespan extension induced by CGP37157 two different mutants were used, the RB754 (*aak-2*) and the AGD397 (*aak-1;aak-2*) mutants, both of them with mutations in the catalytic subunits of AMPK. Sirtuins pathway requirement was investigated using the VC199 (*sir-2.1*) mutant, and DAF-16 activity implication was studied using the CF1038 (*daf-16*) mutant. For more information see table 4, p85.

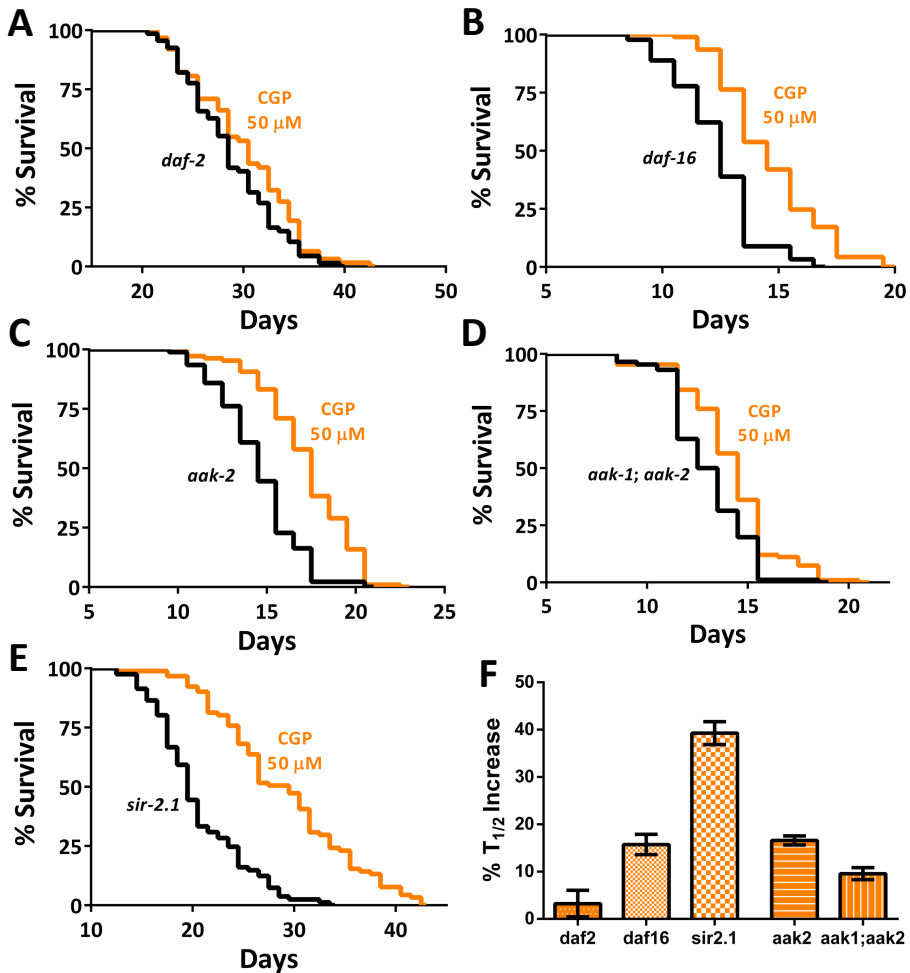


**Figure 58: Effects of CGP37157 in CB1370 (*daf-2*), CF1038 (*daf-16*), RB754 (*aak-2*), AGD397 (*akk-1;aak-2*), VC199 (*sir-2.1*), and CF1038 (*daf-16*) *C. elegans* mutants lifespan. Graph A shows the effects of CGP37157 in *daf-2* mutants. Graph B shows the effect of CGP37157 in *daf-16* mutants. Graphs C and D show the effects of the treatment in AMPK pathway mutants, and graph E shows the effects of CGP37157 in *sir-2.1* mutants. Finally graph F summarizes the % mean lifespan increase after each mutant treatment.**

Drug	T <sub>1/2</sub> drug (days)	N drug	T <sub>1/2</sub> control (days)	N Control	% T <sub>1/2</sub> increase	P value	Mean % T <sub>1/2</sub> increase
<b><i>daf-2</i></b>							
CGP37157 50 μM	31,148	62/101	29,371	67/91	6,05	<0,024	<b>3,23 ± 2,9</b>
	25,844	92/148	25,736	75/146	0,42	0,628	
<b><i>daf-16</i></b>							
CGP37157 50 μM	14,365	87/100	12,165	81/101	18,08	<0,0001	<b>15,74 ± 2,7</b>
	<b>15,19</b>	<b>93/111</b>	<b>12,909</b>	<b>90/103</b>	<b>17,67</b>	<b>&lt;0,0001</b>	
	16,68	82/98	14,964	0,889	11,47	<0,0001	
<b><i>aak-2</i></b>							
CGP37157 50 μM	17,675	73/90	15,423	64/101	14,60	<0,0001	<b>16,60 ± 0,96</b>
	14,955	80/105	12,934	47/61	15,63	<0,0001	
	16,698	99/111	14,033	85/95	18,99	<0,0001	
	<b>17,838</b>	<b>107/116</b>	15,221	92/107	<b>17,19</b>	<b>&lt;0,0001</b>	
<b><i>aak-1; aak-2</i></b>							
CGP37157 50 μM	17,391	119/156	15,579	93/156	11,63	<0,0001	<b>9,57 ± 1,3</b>
	16,087	104/125	14,447	101/112	11,35	<0,0001	
	15,887	109/121	14,970	102/121	6,13	<0,001	
	<b>14,841</b>	<b>108/119</b>	<b>13,594</b>	<b>86/109</b>	<b>9,17</b>	<b>&lt;0,0001</b>	
<b><i>sir-2.1</i></b>							
CGP37157 50 μM	24,381	96/109	17,924	88/101	36,02	<0,0001	<b>39,27 ± 2,4</b>
	<b>29,954</b>	<b>91/107</b>	<b>21,737</b>	<b>81/90</b>	<b>37,80</b>	<b>&lt;0,0001</b>	
	23,058	105/115	16,014	83/86	43,99	<0,0001	

**Table 22: Lifespan assays performed with CGP37157 in CB1370 (*daf-2*), CF1038 (*daf-16*), RB754 (*aak-2*), AGD397 (*akk-1;aak-2*), VC199 (*sir-2.1*), and CF1038 (*daf-16*) mutant worms.** The table shows the amount of drug used; the half-life (T<sub>1/2</sub>) of the control and treated worms obtained from the Kaplan-Meier analysis for survival; the number of worms in the experiment (final/total); the % increase in the half-life of treated worms; the statistical significance of the effect of the drug in each case; and the mean ± s.e of the T<sub>1/2</sub> increase in treated worms. In bold, are indicated the survival assays plotted in figure 58.

Shown in figure 58 and table 22 are the effects of the treatment with CGP37157 in multiple nutrient sensing pathways mutants. *daf-2* IIS pathway mutants showed a mean lifespan extension of 3,63% while the one of *daf-16* mutants reached a 15,7%; AMPK mutants exhibited a mean lifespan extension of 16.6% for *aak-2* mutants and 9.57% for *aak-1;aak-2* mutants; sirtuins pathway mutants showed an impressive 39,3% mean increase in life expectancy. This results indicate that AMPK and the sirtuins pathways are not required for the prolongevity effects of CGP37157 in *C. elegans*. On the contrary, IIS pathway, and specifically DAF-2 seems to be required for CGP37157 to be effective in *C. elegans*. Finally, DAF-16 mutants were able to respond to the treatment which could be indicating that the effects of CGP37157 in DAF-2 activity are enough to promote *C. elegans* longevity even with a reduction of DAF-16 expression.

#### II.1.4.2 mTOR pathway is required for CGP37157 *C. elegans* lifespan extension

mTOR, mechanistic target of rapamycin, is a serine/threonine involved in the response to changes in amino acids availability. mTOR pathway has multiple

downstream effects through the formation of two different complexes and the activation of multiple cascades (see introduction, section II.4.2, p51). There are *C. elegans* strains with mutations in proteins involved in mTOR pathway including the heterozygous *daf-15* mutant (DR142), the homologue of RAPTOR, and *rsk-1* mutant (RB1206), the homologue of S6K in mammals. Using this two loss of function mutants the participation of mTOR pathway in lifespan extension induced by CGP37157 has been investigated.

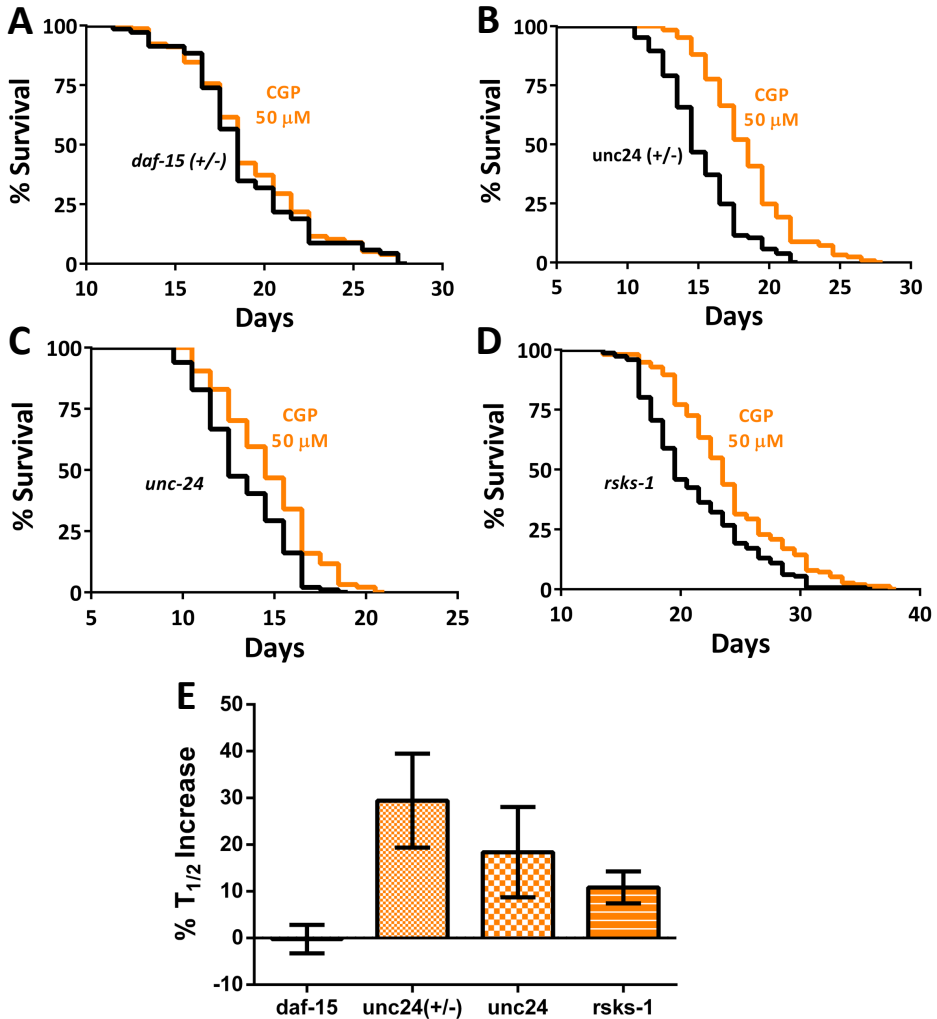


**Figure 59: Effects of CGP37157 in DR142 (*daf-15*) and RB1206 (*rsk-1*) *C. elegans* mutants lifespan.** Graph A shows the effects of CGP37157 in *daf-15* mutants. Graphs B,C shows the effect of CGP37157 in heterozygous and homozygous *unc-24* mutants respectively. Graph D shows the effects of the treatment in *rsk-1* mutants. Finally graph E summarizes the % mean lifespan increase after each mutant treatment.

Drug	T <sub>1/2</sub> drug (days)	N drug	T <sub>1/2</sub> control (days)	N Control	% T <sub>1/2</sub> increase	P value	Mean % T <sub>1/2</sub> increase
<b><i>daf-15 (+/-)</i></b>							
CGP37157 50 μM	18,96	82/101	18,226	81/100	4,03	0,069	<b>-0,2 ± 3,0</b>
	<b>19,893</b>	<b>78/90</b>	<b>19,62</b>	<b>69/91</b>	<b>1,39</b>	<b>0,701</b>	
	18,942	82/101	20,171	82/93	-6,09	<0,031	
<b><i>unc-24 (+/-)</i></b>							
CGP37157 50 μM	25,042	86/96	16,747	62/75	49,53	<0,0001	<b>29,44 ± 10,1</b>
	18,693	89/99	15,718	81/97	18,93	<0,0001	
	<b>18,965</b>	<b>125/140</b>	<b>15,824</b>	<b>105/126</b>	<b>19,85</b>	<b>&lt;0,0001</b>	
<b><i>unc-24</i></b>							
CGP37157 50 μM	19,844	89/99	14,407	70/85	37,74	<0,0001	<b>18,39 ± 9,6</b>
	18,868	91/104	17,473	91/105	7,98	<0,003	
	<b>15,297</b>	<b>94/112</b>	<b>13,975</b>	<b>99/117</b>	<b>9,46</b>	<b>&lt;0,0001</b>	
<b><i>rsks-1</i></b>							
CGP37157 50 μM	20,651	144/151	19,840	135/146	4,09	0,386	<b>10,83 ± 3,4</b>
	25,876	155/163	24,163	116/146	7,09	<0,015	
	26,519	160/165	22,154	116/143	19,70	<0,0001	
	<b>25,046</b>	<b>153/153</b>	<b>22,276</b>	<b>146/155</b>	<b>12,43</b>	<b>&lt;0,0001</b>	

**Table 23: Lifespan assays performed with CGP37157 in DR142 (*daf-15*) and RB1206 (*rsks-1*) mutant worms.** The table shows the amount of drug used; the half-life (T<sub>1/2</sub>) of the control and treated worms obtained from the Kaplan-Meier analysis for survival; the number of worms in the experiment (final/total); the % increase in the half-life of treated worms; the statistical significance of the effect of the drug in each case; and the mean ± s.e of the T<sub>1/2</sub> increase in treated worms. In bold, are indicated the survival assays plotted in figure 59.

The behavior of mTOR pathway mutants in response to CGP37157 treatment is quite similar to the one found for the effects of SERCA inhibitors. Shown in figure 59 and table 23 are the effects of this drug in two different mutants, the DR142 (*daf-15*) mutant and the RB1206 (*rsks-1*) mutant. In this case the effect of the treatment is different for both mutants. *daf-15* heterozygous mutants are not able to respond to CGP37157 treatment with a final mean lifespan extension of -0,2%. Moreover, this lack of activity is not caused by the *unc-24* mutation since both the heterozygous and the homozygous mutants show a mean increase in life expectancy of 29,4% and 18,4% respectively. Contrarily to DR142, in RB1206 mutants CGP37157 treatment is able to increase worms lifespan around a 10.9%. This results, highlight the importance of mTOR pathway for CGP37157 to be effective, although this effect does not require the activity of RSKS-1.

## II.2 Effective concentration of CGP37157 per worm

One of the most challenging aspects to determine while treating *C. elegans* populations is to know the effective concentration of the drug used in the worms. To try to elucidate this point, as well as to validate the inclusion compound method of administration, and the stability of the drugs in the plate along the days



of treatment an HPLC-MS study was performed using day 8 treated worms samples.

Sample 1 $\mu\text{g}$ Y-CD-CGP37157 per 20 worms	Final concentration (ng/mL)	Mean concentration (ng/mL)	3200 worms weight ( $\mu\text{g}$ )	Sample volume (mL)	ng CGP37157 per 1 $\mu\text{g}$ inclusion compound (ng/ $\mu\text{g}$ )	ng CGP37157 per 1 worm (ng/5 $\mu\text{g}$ )
<b>SAMPLE 1</b>						
Sample 1.1	15,26					
Sample 1.2	14,91	15,45	16000	0,50	0,000483	0,00241
Sample 1.3	16,18					
<b>SAMPLE 2</b>						
Sample 2.1	21,01					
Sample 2.2	22,49	21,92	16000	0,50	0,000685	0,00342
Sample 2.3	22,25					
<b>SAMPLE 3</b>						
Sample 3.1	6,34					
Sample 3.2	7,42	7,42	16000	0,50	0,000232	0,00116
Sample 3.3	8,49					

**Table 24: HPLC-MS determination of CGP37157 in a known size sample of worms.** The table shows the final concentration in ng/ml of CGP37257 in each sample triplicates; the mean concentration of CGP37157 in each sample; the weight of the sample size in  $\mu\text{g}$ , the sample volume (mL), the ng of CGP37157 per 1  $\mu\text{g}$  of inclusion compound; and the ng of CGP37157 per worm.

With all the data collected from the HPLC-MS studies shown in table 24, we were able to estimate a final concentration per cell in *C. elegans* of 1,48  $\mu\text{M}$  which is a really close concentration to the  $\text{IC}_{50}$  of CGP37157 inhibition of the mNCX. Finally, this study provided information about the viability of the treatments with inclusion compounds: in one hand it shows that worms are able to ingest the compounds and metabolize CGP37157, and in the other it shows that molecules included in inclusion compounds are stable for long periods of time.

### II.3 Effects of CGP37157 treatment on in vivo *C. elegans* $\text{Ca}^{2+}$ dynamics

As mentioned before, CGP37157 causes changes in the activity of multiple  $\text{Ca}^{2+}$  channels, being commonly used to inhibit the mNCX. As its main action mechanism is the modification of  $\text{Ca}^{2+}$  homeostasis, the study of possible changes in  $\text{Ca}^{2+}$  dynamics in *C. elegans* seemed necessary. The possible changes in  $\text{Ca}^{2+}$  dynamics as a consequence of the treatment with CGP37157 in *C. elegans* were explored in two different tissues: the pharynx (see introduction, section I.4, p34) and the vulva, both belonging to the nonstriated muscle system. The rationale to study two different muscular cells is their differential innervation system and the magnitude of  $\text{Ca}^{2+}$  changes that can be observed in each organ. While pharyngeal  $\text{Ca}^{2+}$  dynamics are characterized by small, and fast  $\text{Ca}^{2+}$  oscillations, vulva muscle cells behave in a different manner being characterized by larger and bigger  $\text{Ca}^{2+}$

peaks much more spaced in time. In the pharynx, measurements were made in cytosol and mitochondria, while in vulva it was only possible to study cytosolic changes.

### II.3.1 Effects of CGP37157 in pharyngeal $\text{Ca}^{2+}$ dynamics

#### II.3.1.1 CGP37157 induces changes in the pharyngeal cytosolic $\text{Ca}^{2+}$ oscillations

CGP37157 effects in pharyngeal cytosolic  $\text{Ca}^{2+}$  dynamics were studied using the AQ2038 (see table 3, p82) after 5 days of treatment. The day of the experiment, parallel recordings of control and treated worms were performed to study  $\text{Ca}^{2+}$  dynamics in pharynx muscular cells cytosol.

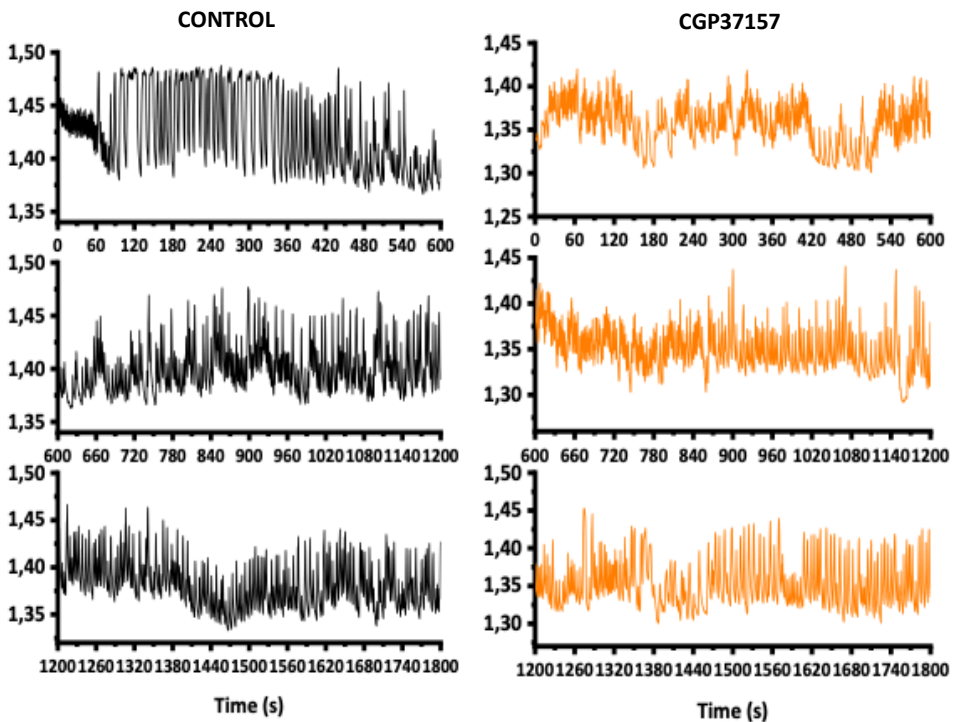


**Figure 60: Representative pharyngeal cytosolic  $\text{Ca}^{2+}$  traces of untreated, and treated with CGP37157, AQ2038 worms.** Cytosolic  $\text{Ca}^{2+}$  recordings were always done for 30 minutes in each worm under the stimulation of 0,5 mM of serotonin. Control traces are represented in black, and treated ones in orange. At least 20 worms per condition were studied.

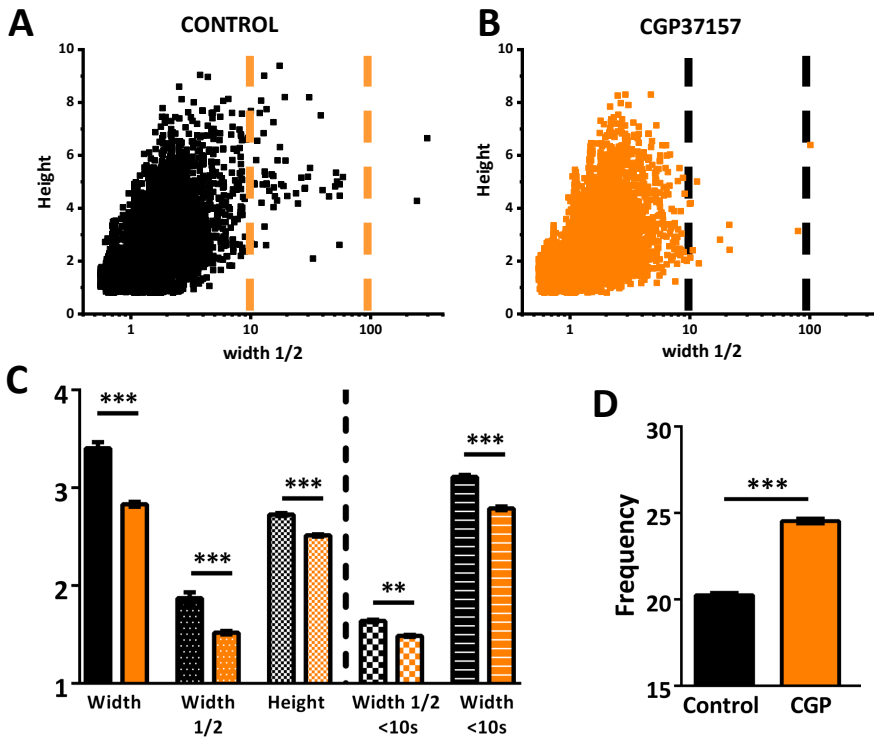


**Figure 61: Changes in height, width and frequency of pharyngeal cytosolic  $\text{Ca}^{2+}$  peaks at day 5 of treatment with CGP37157.** Graphs A and B show the distribution of every peak included in each group by its height and medium width. Graph C represents the changes in height and width after the treatment with CGP37157. Graph D shows the changes in the frequency of the oscillations. Control values are represented in black and CGP37157 values in orange.

After the study of cytosolic  $\text{Ca}^{2+}$  oscillations of muscular pharyngeal cells it can be concluded that the treatment of AQ2038 worms with CGP37157 induces changes in the morphology and the frequency of the peaks. Specifically, in figure 61 it is shown that the distribution of the peaks changes after the treatment, observing less long lasting peaks of more than 10 seconds in the treated group. It also shows that the cytosolic peaks are characterized by a decrease in the width, regardless if the total or medium width is studied, and the height. Finally, it is also possible to see changes in the frequency of the pumping being increased in the treated group.

### II.3.1.2 CGP37157 induces changes in the pharyngeal mitochondrial $\text{Ca}^{2+}$ oscillations

The possible changes in mitochondrial  $\text{Ca}^{2+}$  dynamics induced by CGP37157, were studied using the *C. elegans* strain AQ3055 (see table 3, p82) after five days of treatment, and under the stimulation with 0,5 mM serotonin. The day of the experiment parallel experiments of control and treated worms were performed to study  $\text{Ca}^{2+}$  dynamics in mitochondria of pharyngeal muscle cells.

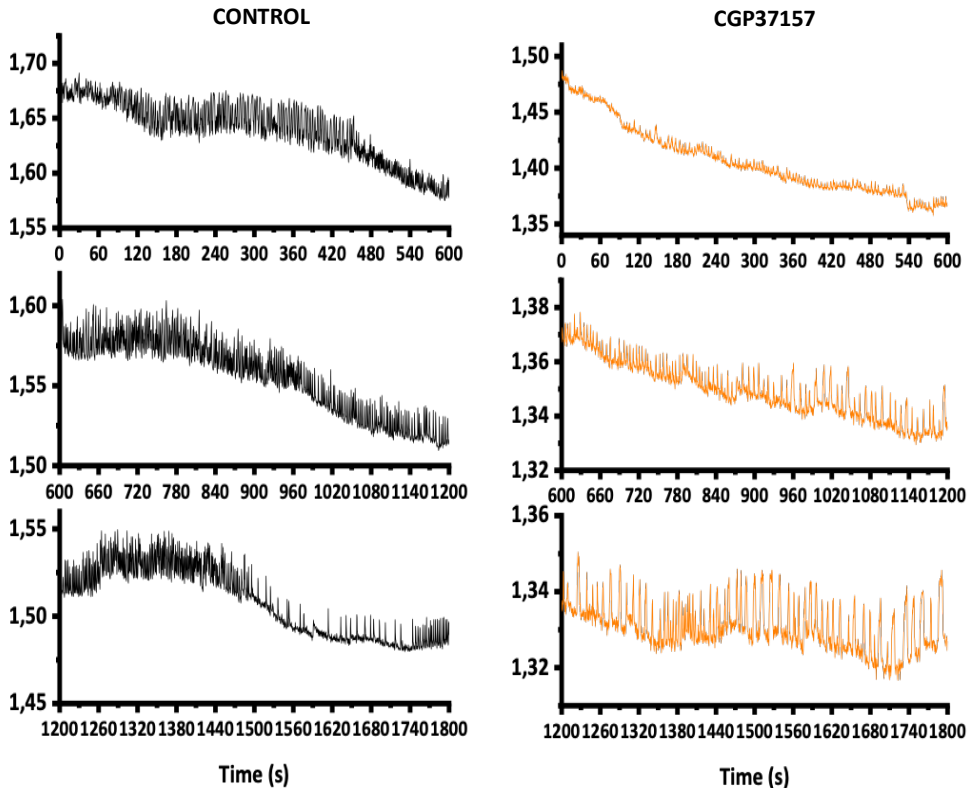


**Figure 62: Representative mitochondrial  $\text{Ca}^{2+}$  traces of untreated and treated with CGP37157 AQ3055 worms in pharyngeal muscle cells.** Mitochondrial  $\text{Ca}^{2+}$  recordings were always done for 30 minutes in each worm under the stimulation of 0,5 mM of serotonin. Control traces are represented in black, and treated ones in orange. At least 20 worms per condition were studied.

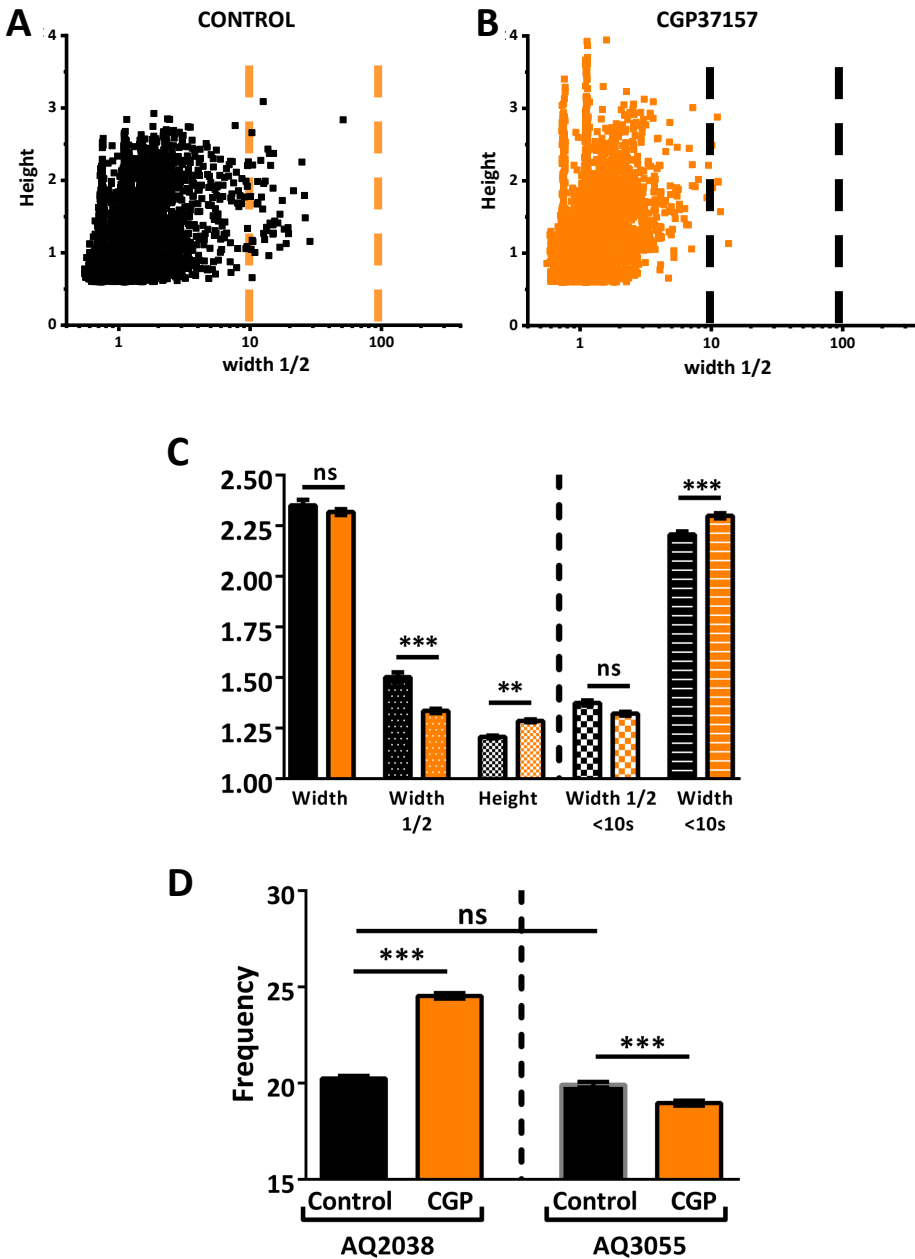


**Figure 63: Changes in height, width and frequency of pharyngeal mitochondrial  $\text{Ca}^{2+}$  peaks at day 5 of treatment with CGP37157.** Graphs A and B show the distribution of every peak included in each group by its height and medium width. Graph C represents the changes in height and width after the treatment with CGP37157. Control values are represented in black and CGP37157 values in orange. Graph D shows the changes in the frequency of the oscillations and its comparison with the changes in frequency of AQ2038 worms.

The study of mitochondrial  $\text{Ca}^{2+}$  oscillations of muscular cells in the pharynx, shows that the treatment of AQ3055 worms with CGP37157 induces changes in the morphology and the frequency of the peaks. Specifically, in figure 63 it is shown that the distribution of the peaks changes after the treatment, observing less long lasting peaks of more than 10 seconds in the treated group. It also shows that the mitochondrial peaks are characterized by a reduction of the medium width, while the total width is not affected when all the peaks are considered in the analysis. In this case the height is also affected by the treatment being higher in the treated worms. When only the peaks that last less than 10 seconds are considered in the analysis, the variation of the parameters changes, disappearing the difference between groups regarding the medium width and being significantly different the total width. This phenomena might be caused by the differential distribution of the peaks of each group. Finally, and interestingly, the frequency of mitochondrial pumping is reduced in the treated worms, which is totally opposite to the effects of the drug in the cytosolic  $\text{Ca}^{2+}$  dynamics, which could be indicating the action of the drug in mitochondrial  $\text{Ca}^{2+}$  homeostasis.

### II.3.2 Effects of CGP37157 in vulva $\text{Ca}^{2+}$ dynamics

Pharyngeal musculature is quite particular regarding its regulation by *C. elegans* nervous system since it has its own regulatory circuitry (see introduction, section I.4.2, p35). Furthermore, pharynx is constitutively contracting, being compared its activity with a heart. Due to this particularities, we decided to study the changes in  $\text{Ca}^{2+}$  dynamics in a different muscular system, the vulva. Although belonging to the same muscle group as pharynx, vulva contractility properties allow to make measurements without having to stimulate the muscle cells with serotonin, and its  $\text{Ca}^{2+}$  peaks are characterized for being much bigger than the pharyngeal ones, which could be beneficial to study the changes induced by CGP37157.

For vulva recording the experimental design was different to the one established for pharyngeal measurements. In this case, the recordings were made at day 2 and day 12 of treatment to be able to see if the changes in  $\text{Ca}^{2+}$  transients in vulva were maintained during aging. Also, two different concentrations of CGP37157 were used, 50 and 150  $\mu\text{M}$ .

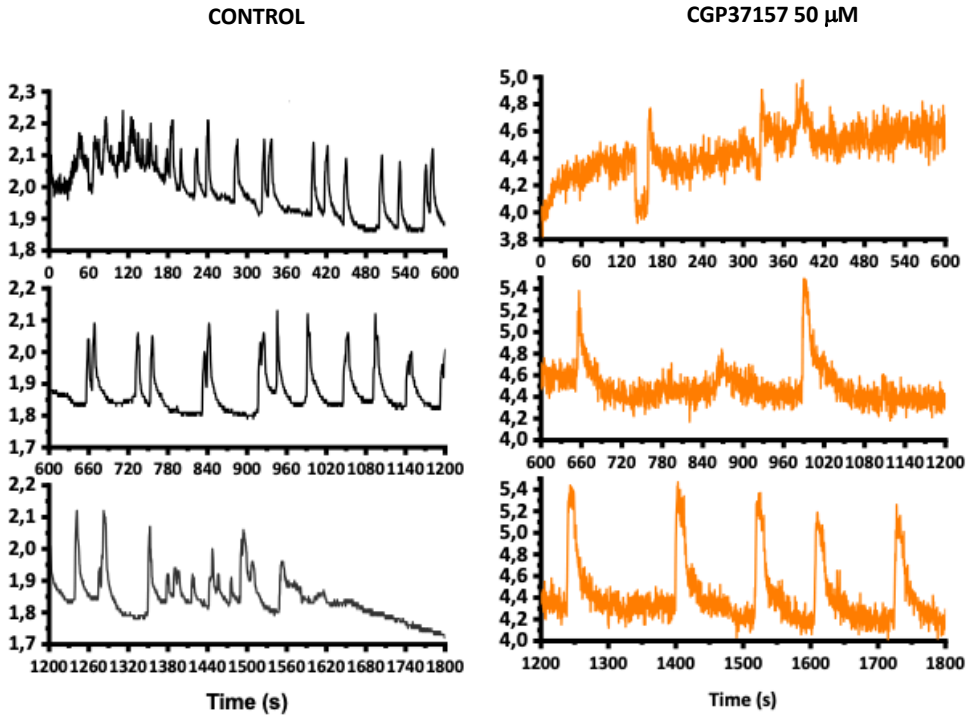


**Figure 64: Representative cytosolic vulva  $\text{Ca}^{2+}$  transients traces of untreated, and treated with CGP37157, AQ2121 worms.** Cytosolic  $\text{Ca}^{2+}$  recordings were always done for 30 minutes in each worm. Control traces are represented in black, and treated ones in orange. At least 20 worms per condition were studied.

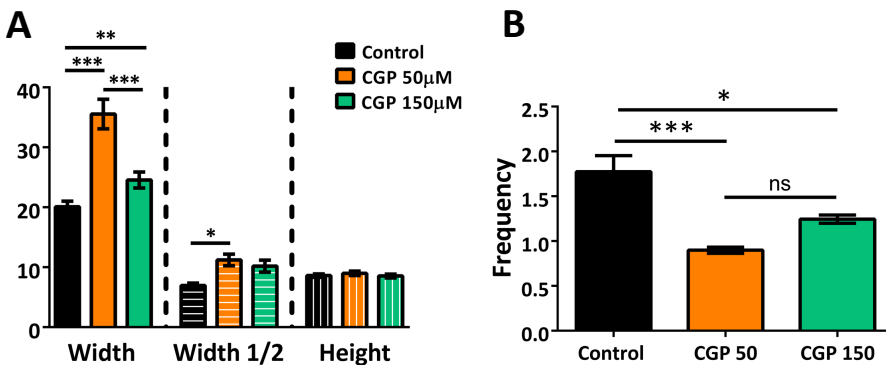


**Figure 65: Changes in height, width and frequency of cytosolic vulva  $\text{Ca}^{2+}$  transients at day 2 of treatment with CGP37157.** Graph A represents the changes in height and width after the treatment with CGP37157. Control values are represented in black, CGP37157 50  $\mu\text{M}$  in orange, and CGP37157 150  $\mu\text{M}$  in green. Graph B shows the changes in the frequency of the transients and its comparison between groups.

Represented in figure 65 are the mean changes in  $\text{Ca}^{2+}$  dynamics in vulva muscle cells of control, and two different treated groups, 50 and 150  $\mu\text{M}$  of CGP37157. In graph A are shown the changes in the total and medium width, and the height of the peaks. While no difference could be seen in the height of the peaks, the total and medium width were increased in the group treated with 50  $\mu\text{M}$  of CGP37157. As for the group of worms treated with 150  $\mu\text{M}$  of CGP37157, no changes appeared in the medium width, and as in the case of the 50  $\mu\text{M}$  group the total width was increased although the magnitude of the effect was lower than the one observed with lower doses of CGP37157. Graph B represents the changes in the frequency of the transients, being lower in both treatments.

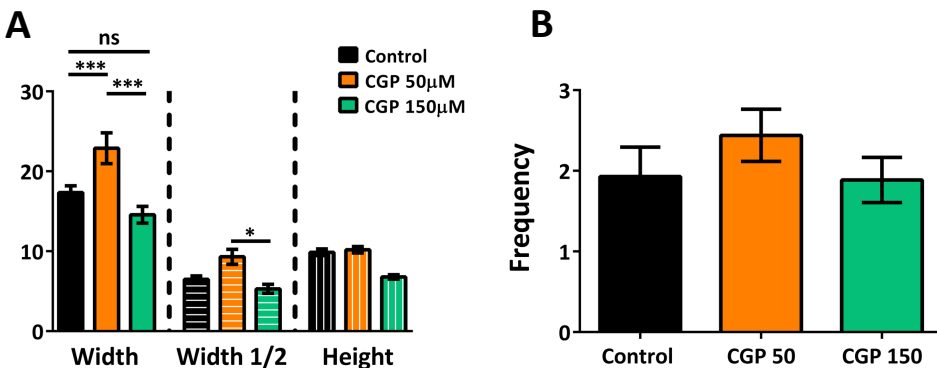


**Figure 66: Changes in height, width and frequency of cytosolic vulva  $\text{Ca}^{2+}$  transients at day 12 of treatment with CGP37157.** Graph A represents the changes in height and width after the treatment with CGP37157. Control values are represented in black, CGP37157 50  $\mu\text{M}$  in orange, and CGP37157 150  $\mu\text{M}$  in green. Graph B shows the changes in the frequency of the transients and its comparison between groups.

Figure 66 represents the effects of two different concentrations of CGP37157 treatments in cytosolic vulva  $\text{Ca}^{2+}$  transients after 12 days of treatment. Graph A represents the magnitude of the total and medium width and the height in the control and both treated groups. As it is shown, total width is still increased in the case of the worms treated with 50  $\mu\text{M}$  of CGP37157, while in the group of worms treated with a higher dose this effect disappears. Medium width effects disappear in both treated groups, and the height is still equal to the one of the control group. The maintenance of effects in the group treated with lower doses of the drug, and the disappearance of the effects in the higher dose group, agrees with the results obtained in the survival assays (figure 55, p134) where 50  $\mu\text{M}$  CGP37157 treatment was highly effective extending worms lifespan, while the 150  $\mu\text{M}$  CGP37157 treatment showed detrimental or no effects.



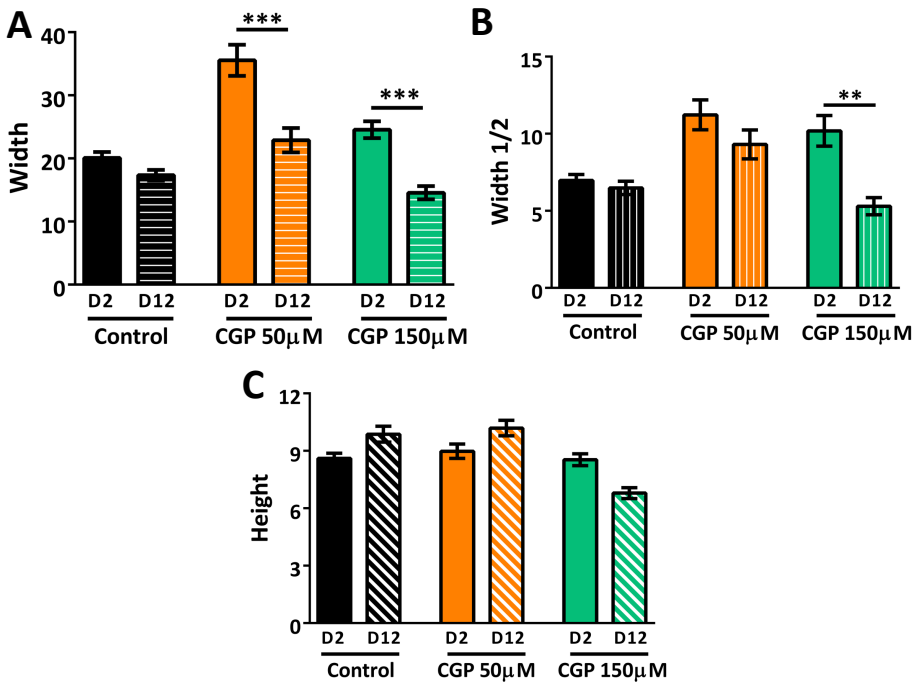


**Figure 67: Comparison of the changes observed in height, width and frequency of cytosolic vulva  $\text{Ca}^{2+}$  transients between day 2 and day 12 of treatment with CGP37157.** Graph A represents the changes in width. Graph B shows the changes in the medium width. Graph C shows the differences in the height. Control values are represented in black, CGP37157 50  $\mu\text{M}$  in orange, and CGP37157 150  $\mu\text{M}$  in green.

Finally, the comparison of the values for total and medium width and height between day 2 and day 12 of treatment were studied and represented in figure 67. Graph A shows the changes in the total width of the peaks observing that in the control group it does not change with age, while worms treated with 50  $\mu\text{M}$  of CGP37157 have larger total widths that are maintained with age, although, as in the control group, this value decreases with time. The effects observed in the 150  $\mu\text{M}$  CGP37157 treated group differ a little to the ones observed in the other treated group. In this case the increases in the total width at day 2, although significant, are lower in this group, and at day 12 no effect is observed. In graph B changes with age in the medium width are shown. In this case the treatment with 50  $\mu\text{M}$  of CGP37157 did not cause any changes in the medium width, while the 150  $\mu\text{M}$  treatment seemed to diminish the value of this parameter. Finally, graph C shows that the height of the peaks is not affected by the age of the worm or any of the treatments.

## II.4 Effects of CGP37157 in the electrophysiological properties of pharyngeal muscle

One of the main characteristics of action potentials in *C. elegans* is that they are driven by  $\text{Ca}^{2+}$  instead of  $\text{Na}^{+}$ . This fact led us to investigate if the treatment with CGP37157 could modify the electrophysiological properties of pharyngeal muscle cells. To this end, electropharyngeograms (EPGs) of control and treated worms were performed at day 5 of treatment.

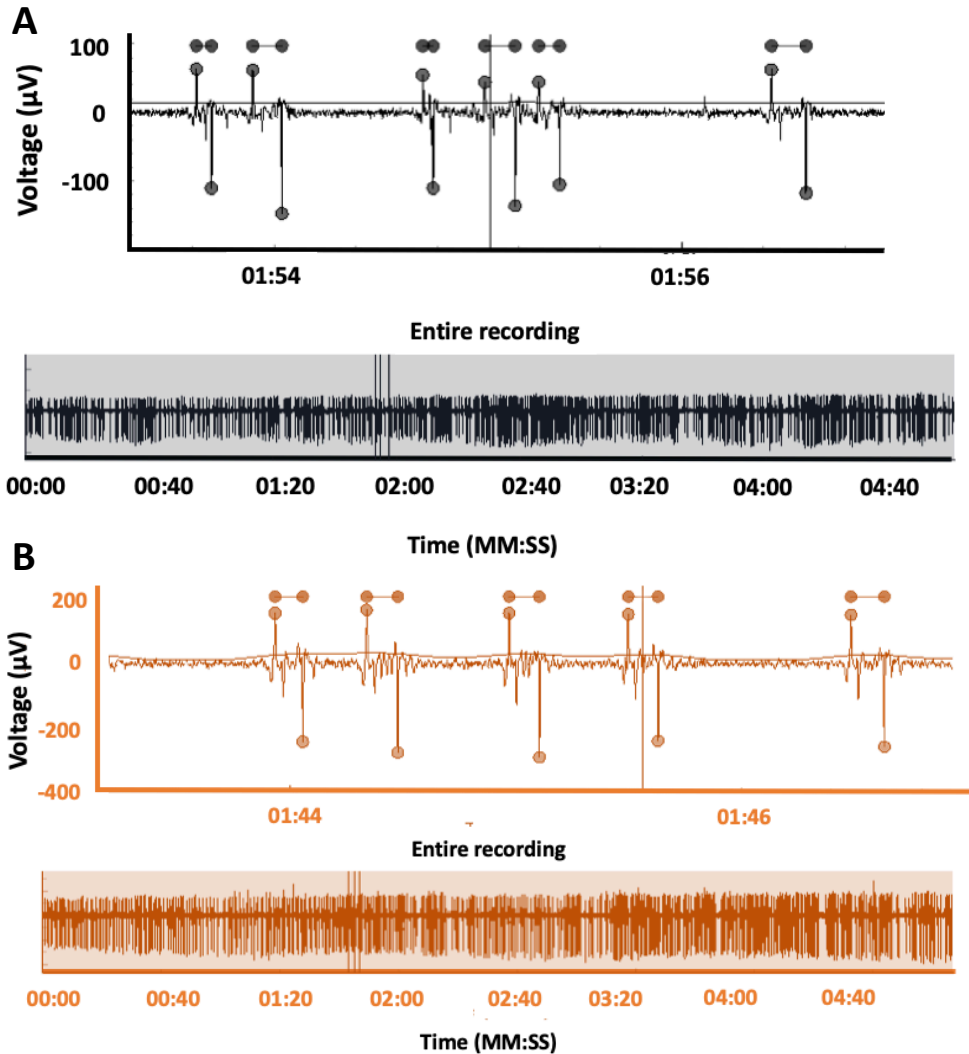


**Figure 68: Representative traces of EPGs from control and treated worms.** EPGs were done in control and treated worms in a parallel form for 5 minutes under the stimulation of 2,3 mM serotonin. Graph A represents a representative trace of the control group; Graph B represents a representative trace of CGP37157 50  $\mu\text{M}$  treated worms.

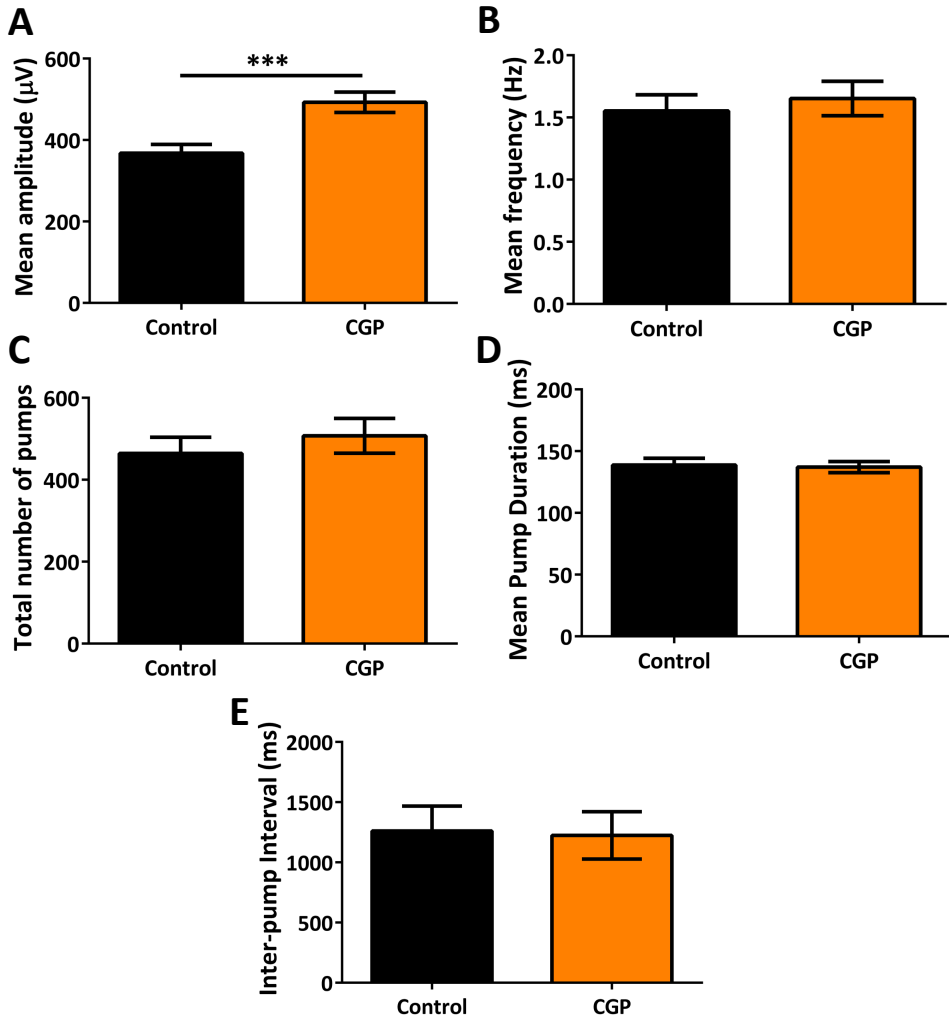


**Figure 69: Effects of CGP37157 in the electrophysiological properties of pharyngeal muscle cells.** Graph A represents the mean amplitude of the pumps in  $\mu\text{V}$ ; graph B represents the mean frequency in Hz; graph C shows the total number of pumps; graph D shows the mean pump duration in ms; and graph E shows the effects of CGP37157 in the inter-pump interval in ms.

Represented in figure 69 are the main parameter values obtained from the EPGs recordings in control and treated worms. Studying this values, it can be concluded that most of them are not modified by the treatment with CGP37157, only the mean amplitude of the depolarizations is increased, which indicates that CGP37157 does not limit the propagation or duration of pharyngeal muscle contraction.

## II.5 Effects of CGP37157 in several biomarkers of *C. elegans* aging

During the last years several biomarkers of aging have been described in *C. elegans*. All of them indicate the physiological and functional age of the organisms and can even be used to predict lifespan extensions. Included in this group of physiological indicators are the progeny number, locomotion, *hsp-16.2* expression after a temporary heat stress, and mitochondrial activity. While the first three biomarkers correlate in a positive manner with lifespan, mitochondrial function correlates negatively (Son et al., 2019).

### II.5.1 Effects of CGP37157 in *C. elegans* fertility

It has been known for several years now that when germline of *C. elegans* is removed, life expectancy of the adult worms can be increased up to a 60% when compared with intact controls (Berman and Kenyon, 2006). That is why we decided to explore if the treatment with CGP37157 modifies the egg laying rate in control and treated populations.

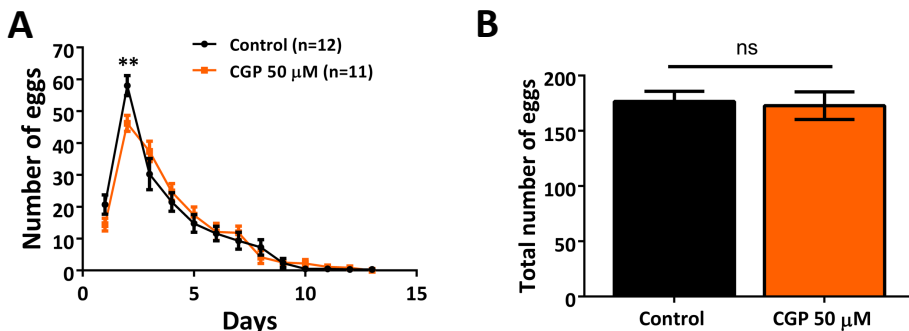
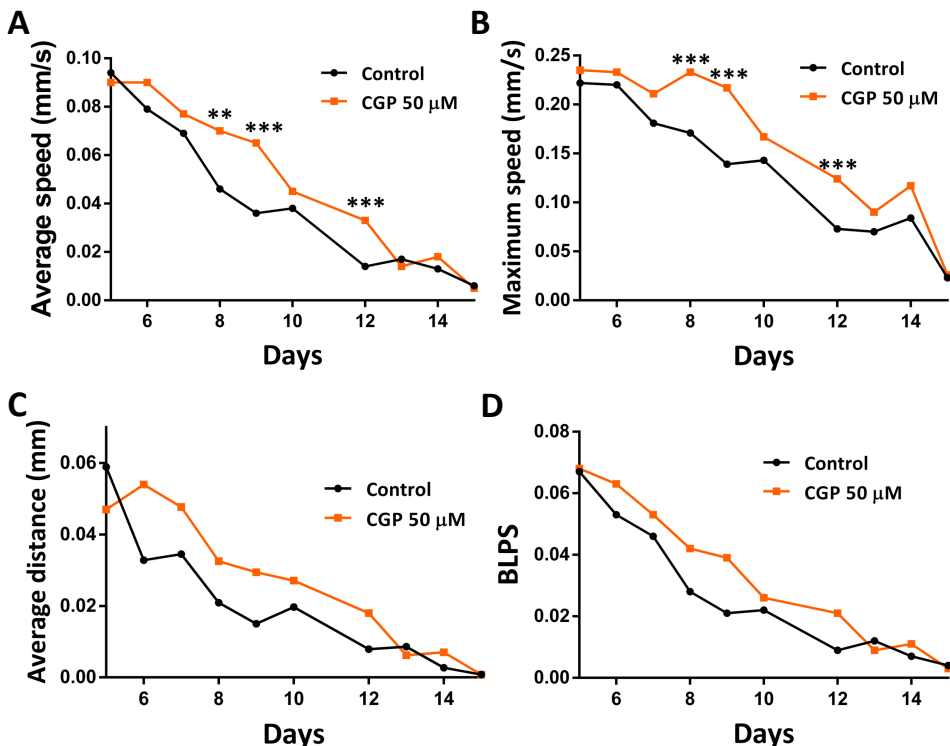


**Figure 70: Effects of CGP37157 in *C. elegans* fertility.** Graph A represents the number of eggs laid from day 1 of adulthood until their last fertile day of at least 11 control and treated worms. Graph B compares the total number of eggs laid per worm in each group.

Shown in figure 70 are the effects in *C. elegans* fertility after the treatment with CGP37157. Graph A represents the number of eggs laid from day 1 of adulthood until the end of their fertile period by at least 11 worms per condition. As it is shown, only at day 2 of treatment there is a difference in the amount of eggs laid by the control and treated group being lower in the treated group. Nevertheless, when the total number of eggs laid by control and treated worms is studied (graph B), no difference can be found among them, concluding that CGP37157 does not affect *C. elegans* fertility.

## II.5.2 Effects of CGP37157 in *C. elegans* locomotion

One of the main healthspan biomarkers in *C. elegans* is locomotion maintenance while aging. It has been described that worms that exhibit fast locomotion during early adulthood (Huang et al., 2004; Pincus et al., 2011; Hahm et al., 2015), or maintain their youth speed in middle age (Hsu et al., 2009), tend to have longer lifespans compared with slow-moving worms. To explore if the treatment with CGP37157 causes an improvement in worm's locomotion, movement tracking assays were performed in control and treated populations from day 5 until day 15 of adulthood.



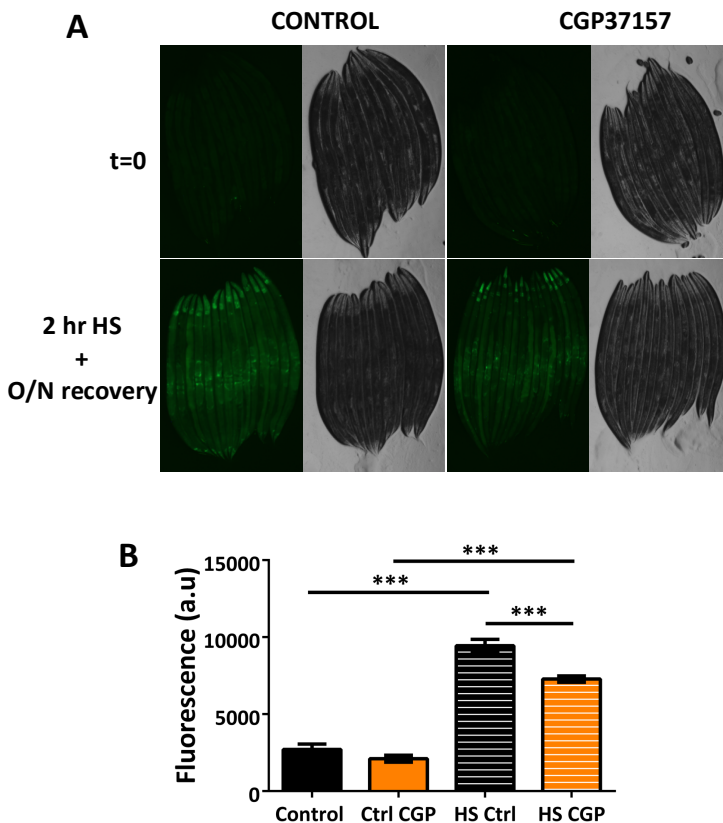
**Figure 71: Effects of CGP37157 in *C. elegans* locomotion.** Using a locomotion plugin for ImageJ, locomotion assessment in control and treated worms was made. Graph A shows the average speed of both groups expressed in mm/s; graph B represents the mean maximum speed of both populations expressed in mm/s; graph C represents the mean average distance for each day in mm; graph D shows the BLPS, body lengths per second, for each condition.

Figure 71 represents the effects of the treatment with CGP37157 in *C. elegans* locomotion. As explained above, fast locomotion during early adulthood, and maintenance of youth speed in middle age are positively correlated with lifespan. In graph A it can be observed that average speed of the worms is increased in the

treated group when compared to the control. The same or even higher effect can be observed in the maximum speed parameter (graph B). Finally, no differences were observed when the average distance and BLPS were studied, although in both cases the mean values were higher in the treated group.

### II.5.3 Effects of CGP37157 in *C. elegans hsp-12.6* expression

One of the possible effects that could have the treatment with CGP37157 is the induction of stress as a consequence of its effects in  $\text{Ca}^{2+}$  homeostasis. In this case the strain chosen to evaluate if there is cytosolic stress is TJ375 (see table 3, p76). To explore the effects of this drug in the stress response worm's pictures were taken prior and after heat shock treatment.



**Figure 72: Effects of CGP37157 in *C. elegans hsp12.6* expression in day 3 TJ375 worms.** *hsp-12.6* expression was evaluated using the strain TJ375. Graph A shows representative images of control and treated worms before and after the induction of *hsp-12.6* expression with a temporary heat-shock treatment. Graph B shows the effects of the treatment with CGP37157 before and after the HS treatment. Mean fluorescence of each group was compared to the rest using an ANOVA test.

Figure 72 shows the effects of CGP37157 in *hsp-12.6* expression. In this case, there is also evidence that the expression of this chaperone is positively correlated to lifespan. Observing the results of the experiments at day 3 of treatment, it is not possible to observe this effect in the treated worms as GFP expression compared to the control group, after HS does not reach the same levels being lower.

#### II.5.4 Effects of CGP37157 in *C. elegans* mitochondrial function

The last aging biomarker that was explored in this work is mitochondrial function by measuring ATP levels. It is important to remark that one of the few *C. elegans* mutants that were not affected by CGP37157 treatment was the mitochondrial impaired MQ1333 (*nuo-6*) strain. This fact led, together with the implication of mitochondrial  $\text{Ca}^{2+}$  levels in ATP production, to the investigation of the effects of the treatment with CGP37157 in *C. elegans* ATP levels. To that end, ATP extractions of day 5 control and treated worms were obtained, and the ATP levels of each sample studied.

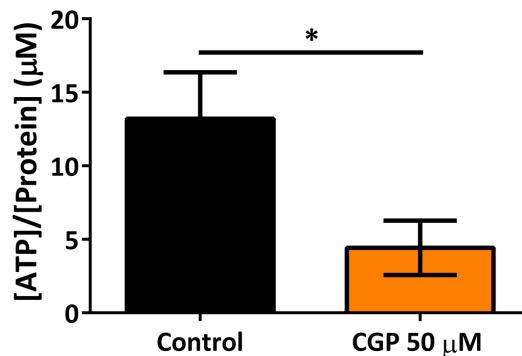


**Figure 73: Effects of CGP37157 in *C. elegans* ATP levels.** ATP levels were referenced to the total protein concentration of the samples. 6 different parallel samples for each condition were obtained and measured.

Shown in figure 73 are the effects of CGP37157 treatment in worm's ATP levels. As it can be seen, the exposure of the worms to CGP37157 causes a decrease in their ATP content indicating reduced mitochondrial activity, which could contribute to the lifespan extension in *C. elegans* as it has been demonstrated that a decrease in the ATP/AMP ratio has a prolongevity effect.

## II.6 Effects of CGP37157 in *C. elegans* sarcopenia during aging

The effects on muscle decline in *C. elegans* during aging have been widely described. Specifically, sarcomere structure of body wall muscle cells undergo a decline losing their densely packed structures and regular orientations as aging progresses (Herndon et al., 2002; Tiku et al., 2017). This fact together with the positive effects of CGP37157 in *C. elegans* locomotion led us to investigate the effects of CGP37157 in sarcopenia evolution in AQ2121 worms.

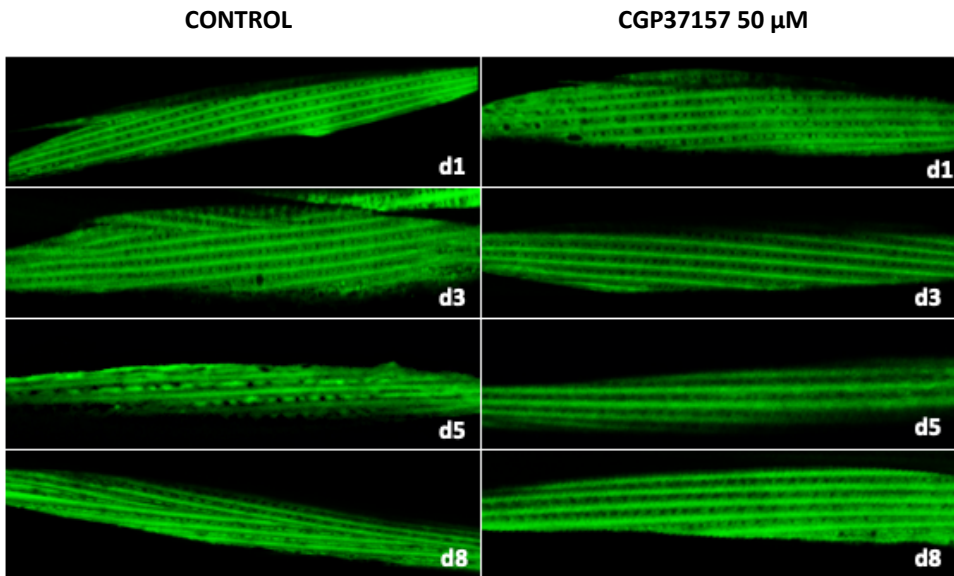


**Figure 74: Effects of CGP37157 in *C. elegans* sarcopenia development in body wall muscle cells.** AQ2121 pictures were taken every other day of control and treated worms in parallel using confocal imaging. The different pictures represent the evolution of the sarcomeric structure of body wall muscle cells as the worms age, from D1 until D8, in the absence and the presence of CGP37157.

Figure 74 represents the evolution of body wall muscle cells sarcomeric structure during aging, and the effect on this process of the treatment with CGP37157. All the pictures are representative of each day. It can be observed that at day 1 of adulthood no differences can be appreciated, indicating that all the populations used for the study began the treatment in similar conditions. At day 3 differences start to appear, as control worms start to lose some of the parallel structure while treated worms continue to present regular orientations. This effect is even more evident when representative images of day 5 and day 8 of treatment are studied. As shown in the figure, control worms start to lose either density or the sarcomeric regular distribution, while treated worms still maintain a similar structure to the one observed at day 1 of adulthood. Thus, the treatment



with CGP37157 delays the muscle decline in *C. elegans* maintaining the sarcomeric structure in body wall muscle cells.

## II.7 Effects of CGP37157 in *C. elegans* body wall muscle cells mitochondrial distribution and morphology.

It has been recently described that muscle mitochondrial structure, sarcomere structure and movement decline are highly correlated. Moreover the decline in mitochondrial network correlates strongly with the loss of movement and lifespan (Gaffney et al., 2018). Due to the effects previously described on mitochondrial function of CGP37157 and this recent discovery, the effects of the treatment with CGP37157 were studied in *C. elegans* body wall muscle cells using the strain SJ4103 and confocal imaging.

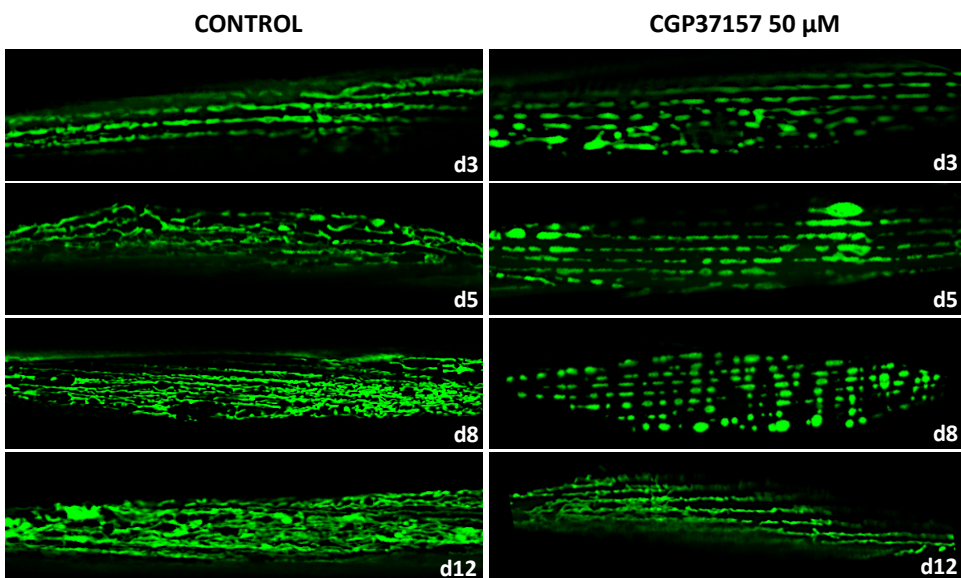


**Figure 75: Effects of CGP37157 in *C. elegans* body wall muscle cells mitochondrial distribution and morphology.** Mitochondrial structure and distribution was studied using the strain SJ4103. Pictures were taken by confocal imaging from day 3 until day 12 of adulthood in control and treated worms in parallel. All the images are representative of each day.

Represented in figure 75 is the evolution of mitochondrial structure in body wall muscle cells during aging. It also shows the effects of CGP37157 in this process. By studying the images, it is clear that mitochondrial structure suffers a decline as the organisms age. At day 1, the mitochondrial structure is quite similar to the one observed in the sarcomeric structure, representing the high

association between the ER and mitochondria in this cells. This association gets weaker during aging losing this well-organized structure. When the pictures from the control group are compared to the ones of the treated with CGP37157, it becomes clear that the treatment favors the maintenance of the mitochondrial distribution even until day 8 of adulthood. At day 12, although the structure is not as well conserved as in day 8, parallel mitochondrial distribution is still appreciated in the treated group.



**DISCUSSION**







The well-established model organism *Caenorhabditis elegans* has helped during the last decades to uncover the molecular mechanisms that modulate aging and longevity. Among the most important discoveries, the role of several metabolic pathways that play a crucial part in the aging process have been, and still are, investigated using *C. elegans*. These signaling pathways are the so called nutrient sensing pathways, and include the insulin/insulin-growth factor pathway (IIS), the AMP-activated protein kinase pathway (AMPK), the mechanistic target of rapamycin pathway (mTOR), and the sirtuins pathway (López-Otín et al., 2013; Riera et al., 2016). All these pathways have been shown to modulate longevity in *C. elegans* with different outcomes: mutations that reduce IIS and mTOR activity induce an increase in life expectancy (Lapierre and Hansen, 2012; Blackwell et al., 2019), while the reduction of the activity of AMPK and Sirtuins pathway reduce it (Mukhopadhyay et al., 2006; Lapierre and Hansen, 2012; Castillo-Quan et al., 2015). One of the main regulatory characteristics of all these pathways is the well-known fact that they do not work in an isolated manner; instead they establish multiple and complex interactions between each other making sometimes difficult to attribute the effects of certain interventions to a particular pathway.

Besides the role of nutrient sensing pathways in aging regulation, mitochondrial dysfunction is one of the main events that drives and potentiates the progressive physiological decline with aging, and the appearance of neurodegenerative diseases (Wang and Hekimi, 2015). Regarding mitochondrial function and aging, one of the oldest theories postulated to explain aging is the rate of living theory that defends the idea that aging and lifespan are regulated by the rate of energy metabolism, being lower rates positively correlated with life expectancy. Nowadays it is clear that this theory cannot fully explain the events that develop during aging progression indicating the intricated regulatory process that drives aging. Mitochondrial function and its correlation with aging has also been investigated in *C. elegans* showing that mitochondrial mutations that impair ETC activity normally increase *C. elegans* lifespan (Wang and Hekimi, 2015).

Finally, it is important to remark the role of  $\text{Ca}^{2+}$  signaling in the aging process. As organisms age,  $\text{Ca}^{2+}$  signaling gets partially impaired leading to dysfunctional cell signaling that has detrimental effects on organisms physiology. This fact led to the postulation of the “ $\text{Ca}^{2+}$  hypothesis of Alzheimer’s disease and the aging brain” linking a sustained  $\text{Ca}^{2+}$  homeostasis dysregulation to aging and the development of neurodegenerative diseases.

Due to the lack of information on how  $\text{Ca}^{2+}$  signaling modulates nutrient sensing pathways activities, and therefore lifespan, this work has focused on the study of this interrelationship using two different pharmacological interventions: the submaximal inhibition of SERCA pumps using 2,5-BHQ and thapsigargin, and



the submaximal inhibition of the mitochondrial  $\text{Na}^+/\text{Ca}^{2+}$  exchanger using CGP37157.

### SERCA inhibition and *C. elegans* lifespan

During the last years,  $\text{Ca}^{2+}$  signaling has been tightly connected to two of the key determinant hallmarks of lifespan: mitochondrial dysfunction and nutrient sensing pathways. This is why we decided to investigate the effect of submaximal inhibition of the SERCA pump in *C. elegans* lifespan.

SERCA pumps are the only mechanism in the cells responsible of restoring  $\text{Ca}^{2+}$  levels in the ER. The level of  $[\text{Ca}^{2+}]_{\text{ER}}$  is essential to determine the amount of  $\text{Ca}^{2+}$  released from the ER during cell stimulation mainly for two different reasons: ER  $\text{Ca}^{2+}$  release depends on the established  $\text{Ca}^{2+}$  gradient between the ER and the cytosol, and the activation of the channels responsible of  $\text{Ca}^{2+}$  release from the ER is driven by  $[\text{Ca}^{2+}]_{\text{ER}}$  (Yamasaki-Mann et al., 2010; Zhang et al., 2015). As a consequence, partial  $\text{Ca}^{2+}$  depletion of the ER should reduce both  $[\text{Ca}^{2+}]_{\text{cyt}}$  signaling and ER-mitochondria  $\text{Ca}^{2+}$  transfer during cell stimulation.

To test this hypothesis, two different inhibitors of SERCA pumps, 2,5-BHQ and thapsigargin have been used. 2,5-BHQ has been known to be a SERCA inhibitor for more than 30 years (Kass et al., 1989; Llopis et al., 1991). The  $K_d$  for SERCA inhibition is around 1-2  $\mu\text{M}$  (Kass et al., 1989; Llopis et al., 1991), although several off targets have been described with higher  $\text{IC}_{50}$ s including L-type  $\text{Ca}^{2+}$  channels (Nelson et al., 1994; Scamps et al., 2000; Miller et al., 2015), other  $\text{Ca}^{2+}$  channels (Scamps et al., 2000), and the PMCA (Luo et al., 2000). In addition, this compound belongs to the phenolic antioxidants family which could influence the interpretation of the results as antioxidants have been shown to modulate *C. elegans* lifespan (Pun et al., 2010). To separate the possible antioxidant effect of 2,5-BHQ from the ones caused by SERCA inhibition, the analog molecule 2,6-BHQ, that belongs to the same family as 2,5-BHQ but has no effects in SERCA activity was always used in parallel.

Our results show that 2,5-BHQ treatment was able to significantly extend *C. elegans* lifespan in a dose dependent manner, with a mean increase of 15% at the most effective dose. Moreover, the parallel experiments showed that although some lifespan extension was achieved with 2,6-BHQ treatment, the effects of the SERCA inhibitor were always higher with approximately a 3-fold change difference.



It is really challenging to know the average concentration of the drugs inside the worms, as it depends on the lipophilicity and bioavailability of the compounds used. Normally, in order to obtain effects in the worms, we have to use 10-100 fold higher drug concentrations in NGM media than the ones used in cell cultures. Considering that the most effective dose for lifespan extension was of 250  $\mu\text{M}$  when the drug was added to the NGM media, the assumption that the effects are due to SERCA inhibition becomes possible as the final concentration of the drug in the worms should be really close to the  $K_d$  for SERCA inhibition by 2,5-BHQ, although further studies are needed to confirm it.

During this work the SERCA inhibitor thapsigargin has also been used. Tg is the most potent and specific SERCA inhibitor available and it binds SERCA with a  $K_d$  in the sub-nM range (Thastrup et al., 1990). More importantly, it has also been demonstrated that this compound is able to inhibit SERCA in *C. elegans* and that concentrations above 200 nM are deleterious for worm fertility and growth (Zwaal et al., 2001). Our data show that Tg was able to induce a 10% increase in *C. elegans* lifespan in a dose dependent manner at the most effective concentration of 10 nM. This results strongly suggest that the effect of Tg is due to SERCA inhibition in *C. elegans*, as the off targets described for Tg required much higher concentrations.

Lastly, a possible effect of the metabolization of the compounds by *E. coli* OP50 cultures, the food source provided to the worms, was investigated using heat-inactivated OP50 cultures as *C. elegans* food source. This technique ensures the availability of all the nutrients needed by the worms but blocks a possible metabolization of the treatments by the bacteria. Our results show that no effect was lost for either of the treatments when bacteria were inactivated excluding that the lifespan extension by SERCA inhibitors was caused by secondary metabolites resultant from OP50 metabolism.

Once the effect of SERCA inhibitors was confirmed, the molecular mechanisms linking SERCA inhibition and lifespan extension still awaited for clarification. To try to elucidate the mechanism of action of these drugs, we investigated the effect of SERCA inhibitors in several *C. elegans* mutants. The first thing that needed to be tested was the possible induction of a caloric restriction response in the worms by the reduction of their pumping rate as a consequence of  $\text{Ca}^{2+}$  homeostatic changes induced by the treatments. To this end, the effect of both SERCA inhibitors was evaluated in the DA1113 (*eat-2*) strain, an established model of caloric restriction in *C. elegans*, that is characterized by a reduced pumping rate and increased longevity. The obtained data showed that both inhibitors induced a further increase in life expectancy in *C. elegans*, even when the drug was just orally administrated, being the most effective concentration the



same as in wild type worms. All this data suggests that the mechanism that drives lifespan extension after SERCA inhibition is not caused by a decreased food intake inducing caloric restriction.

The next step was to investigate the effects of SERCA inhibitors in *C. elegans* mutants of the nutrient sensing pathways, to evaluate the interrelationship between  $\text{Ca}^{2+}$  signaling modulation and lifespan extension through these pathways. The results obtained showed different behaviors after SERCA inhibition from different mutants. There were mutants that showed lifespan increases close to the ones observed in wild type worms after SERCA inhibition, such as the IIS pathway mutant CB1370 (*daf-2*), and the sirtuins pathway mutant VC199 (*sir-2.1*), suggesting that lifespan extension induced by SERCA inhibition does not require these two pathways to take place. The case of CF1038 (*daf-16*) mutants was less clear since a prolongevity effect was observed but the efficiency of the lifespan extension was only about 5%. DAF-16 is one of the connecting points between all nutrient sensing pathways, and the mutation used here is a lost-of-function mutation, which suggests that this transcription factor contributes at least in part to the lifespan extension observed after SERCA inhibition. Contrarily, the effects of the drugs were blocked in the mTOR pathway mutant DR412 (*daf-15*), and in the AMPK pathway mutant AGD397 (*aak-1;aak-2*), although the effects of the treatments were maintained in the mTOR pathway mutant RB1206 (*rsks-1*) and the partial AMPK pathway mutant RB754 (*aak-2*). These results suggest that both pathways are required for the lifespan extension effect of SERCA inhibitors and that the role of the mTOR pathway is not mediated by the action of RSKS-1/S6K activity. In the case of the AMPK pathway mutants, the results suggest that both catalytic subunits are able to compensate the lack of activity of each other, although further investigation is required to clarify this point. Thus, AMPK and mTOR pathway activities can respond to changes in  $\text{Ca}^{2+}$  homeostasis driven by SERCA inhibitors inducing a prolongevity effect. This result agrees with the previous finding in our lab describing that AMPK activators induced a decreased ER-mitochondria  $\text{Ca}^{2+}$  transfer through  $\text{IP}_3$  receptors (Arias-Del-Val et al., 2019).

Finally, as mentioned before, ER-mitochondria  $\text{Ca}^{2+}$  transfer through MAMs has appeared in the last years as an important mechanism in the aging process. This is why the effects of SERCA inhibitors in the mutant strain MQ1333 (*nuo-6*) were investigated. This strain has a mutation that impairs complex I of the mitochondrial respiratory chain activity leading to a reduced mitochondrial membrane potential, and therefore a reduction in ER-mitochondria  $\text{Ca}^{2+}$  transfer. Our results show that SERCA inhibitors were unable to induce changes in life expectancy in this mutants highlighting the importance of mitochondrial ETC integrity in the lifespan extension induced by SERCA inhibition. Moreover, it has been described that ETC mutants, including *nuo-6* have an increased mtROS





production that might be able to modulate longevity through AMPK pathway regulation (Wang and Hekimi, 2015).

The last fact that needed to be tested was the possible induction of the ER unfolded protein response pathway, as Tg had already been described as an inducer of ER stress in *C. elegans* at micromolar doses (Caruso et al., 2008), and it had been proven that the activation of this stress pathway affects longevity in *C. elegans* (Henis-Korenblit et al., 2010). Our results show that neither 2,5-BHQ nor Tg induced the activation of this response in *C. elegans*, and that the treated group was able to respond to an ER stress induction in the same way as the control group, discarding the possibility that the effects of SERCA inhibitors were partially caused by the activation of the ER unfolded protein response.

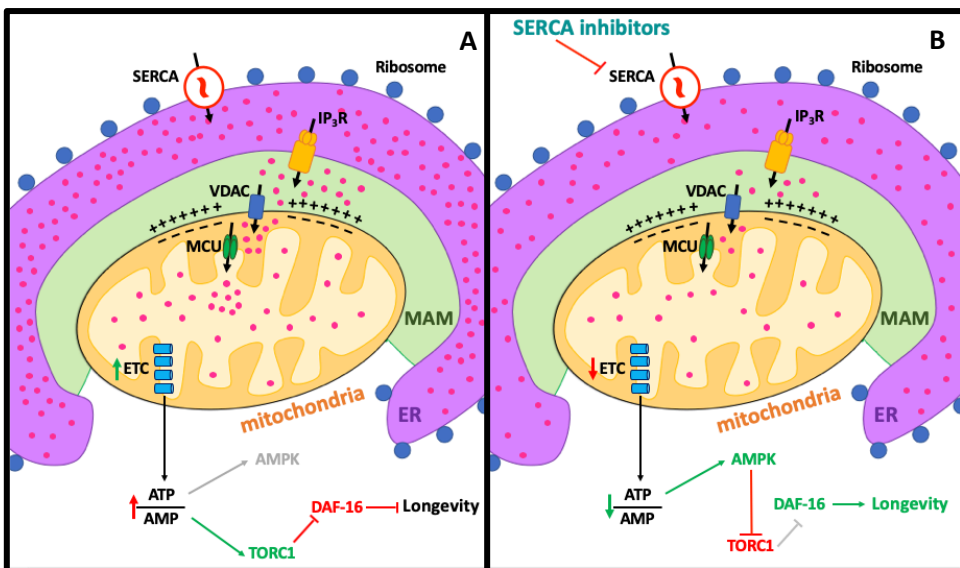


**Figure 76: Proposed mechanism for the effect of SERCA inhibitors.** Ca<sup>2+</sup> transfer from ER to mitochondria takes place in the MAMs, where IP<sub>3</sub>R in the ER membrane, VDAC porins in the outer mitochondrial membrane and MCU channels in the inner mitochondrial membrane create a Ca<sup>2+</sup> pathway between both organelles. In panel A, under control conditions, Ca<sup>2+</sup> transfer from ER to mitochondria increases mitochondrial metabolism and ATP production. The increase in the ATP/AMP ratio inhibits AMPK, activating TORC1, which has a negative impact on lifespan, in part via inhibition of DAF-16. In panel B, in the presence of the SERCA inhibitors, the decrease in the ER Ca<sup>2+</sup> content reduces ER to mitochondria Ca<sup>2+</sup> transfer. Mitochondrial metabolism is reduced and the ATP/AMP ratio decreases. This leads to activation of AMPK, inhibition of TORC1 and increase in lifespan, in part via DAF-16 activation.

In conclusion, this work has led to the discovery of new regulatory functions of Ca<sup>2+</sup> signaling in the aging process of *C. elegans*, involving the regulation of AMPK and mTOR signaling pathways through changes in mitochondrial function. We postulate that the mechanism of the effect of SERCA inhibitors in *C. elegans*



is based in the activation of the AMPK pathway, and the inhibition of the mTOR pathway via reduction of ER-mitochondria  $\text{Ca}^{2+}$  transfer and the consequent reduction of mitochondrial metabolism (figure 76).

### **CGP37157 and *C. elegans* lifespan**

The benzothiazepine CGP37157 has been used for many years as a selective inhibitor of the mitochondrial  $\text{Na}^+/\text{Ca}^{2+}$  exchanger (mNCX), the main mitochondrial  $\text{Ca}^{2+}$  efflux pathway. Besides the inhibition of the mNCX, numerous off targets have been described including the inhibition of L-type VDCC (Baron and Thayer, 1997), plasma membrane NCX (Cyz and Kiedrowski, 2003), or  $\text{Ca}^{2+}$  homeostasis modulator 1 (CALMH1)  $\text{Ca}^{2+}$  channels (Moreno-Ortega et al., 2015). Importantly, CGP37157 effects on  $\text{Ca}^{2+}$  homeostasis have proven to act as a neuroprotectant in several models of excitotoxicity (Nicolau et al., 2009; Nicolau et al., 2010; González-Lafuente et al., 2012; Martínez-Sanz et al., 2015), and usually, neuroprotective compounds have also beneficial effects in the aging process (Cooper et al., 2015; Zárate et al., 2017). Regarding the possible targets of CGP37157 in *C. elegans*, it is a difficult question because there are 10 NCX isoforms in the worm and there is no information about which one of them is responsible of mitochondrial  $\text{Ca}^{2+}$  efflux, and whether it is sensible or not to CGP37157 (Sharma et al., 2013; Sharma and O'Halloran, 2014).

As in the case of SERCA inhibitors, the effects on *C. elegans* lifespan of CGP37157 were tested using two different methods of administration: the inclusion compounds, and the direct administration through the NGM media. In both cases our results show that the treatment was able to induce a significant lifespan extension in a dose dependent manner indicating the need for submaximal inhibition of one or more of its targets to promote beneficial effects on *C. elegans* lifespan. To exclude that the effects in *C. elegans* lifespan were a consequence of the production of a secondary metabolite by OP50 metabolism of CGP37157, the effects on *C. elegans* lifespan were studied in the presence of heat-inactivated OP50 cultures, showing that the worms exhibited an even higher CGP37157-induced increase in mean life expectancy. This indicates that OP50 metabolism is unrelated with the prolongevity effects exerted by CGP37157 in *C. elegans*. Finally, the concentration of CGP37157 inside the worms was studied by HPLC-MS studies revealing that it was around 1,5  $\mu\text{M}$ , really close to the  $\text{IC}_{50}$  for the mNCX inhibition by this compound. This indicates that the effect of CGP37157 may be due to submaximal inhibition of mNCX, although other targets may also be affected at this concentration.



Once proven that the neuroprotectant CGP37157 was able to induce an increase in *C. elegans* lifespan, the mechanism of action of the drug was investigated using several *C. elegans* mutants including the caloric restriction model *eat-2*, the IIS pathway mutants *daf-2* and *daf-16*, the AMPK pathway mutants *aak-2* and *aak-1;aak-2*, the mTOR signaling pathway mutants *daf-15*, and *rsk-1*, the sirtuins pathway mutant *sir-2.1*, and the mitochondrial respiratory chain mutant *nuo-6*.

The results obtained from the survival assays in DA1113 (*eat-2*) mutants showed that CGP37157 was not inducing a caloric restriction response by decreasing the pumping rate of the worms, since the prolongevity effect of the drug was maintained in this mutants even when the drug intake was limited to oral administration.

After discarding a possible caloric restriction induction by CGP37157, the effect of this benzothiazepine was studied in *C. elegans* mutant strains of the four metabolic pathways that are known to regulate aging in *C. elegans*. The mutant strains that showed extended life expectancy after the treatment with CGP37157 were both AMPK pathway mutants, the sirtuins mutant, and the *daf-16* mutant, indicating that these pathways are not essential for the prolongevity action of CGP37157. On the contrary, the treatment with the inhibitor was unable to extend the lifespan of IIS pathway mutant *daf-2* and the mTOR mutant *daf-15*, highlighting the importance of this two pathways for the lifespan extension properties of CGP37157 in worms. In this regard, it is important to point that this two pathways are interconnected and affect lifespan in the same manner by blocking the translocation to the nucleus of DAF-16. As indicated before, CGP37157 was able to induce its prolongevity effects in *daf-16* mutants, indicating that the loss-of-function of this transcription factor is not enough to abolish the benzothiazepine effect in *C. elegans*. This suggests that even with a reduction of DAF-16 expression, the effects of CGP37157 in IIS and mTOR pathways are sufficient to induce an increase in *C. elegans* life expectancy.

Finally, the effects of CGP37157 in the mitochondrial defective ETC mutant *nuo-6*, was studied. In this case, the treatment was unable to induce any effects on lifespan. This result agrees with previous studies in cellular models where the treatment with mitochondrial oxidative phosphorylation inhibitors abolished the neuroprotectant effects of CGP37157 (Nicolau et al., 2010; González-Lafuente et al., 2012). Although the exact mechanism in charge of this effect is still unknown, the fact that the only CGP37157 mitochondrial target known until today is the mNCCX, suggests that it is highly probable that the effects in neuroprotection are mediated by the modulation of this exchanger.



## CGP37157 and Ca<sup>2+</sup> signaling

To further investigate the mechanism of action of CGP37157 in *C. elegans*, changes in Ca<sup>2+</sup> dynamics after the treatment were explored in two different muscle cell types: pharyngeal muscle cells and vulva body wall muscle cells. The rationale to study the effect in these two muscular systems is their differential regulation by the nervous system, and the refractory properties of the pharynx. The study of Ca<sup>2+</sup> signaling in pharyngeal muscle cells was performed under the stimulation of serotonin using the strains AQ2038 and AQ3055. Both strains constitutively express FRET based cameleon Ca<sup>2+</sup> probes in the pharynx with a different subcellular localization. While AQ2038 expresses the probe in the cytosol, AQ3055 strain expresses it in the mitochondria.

Cytosolic Ca<sup>2+</sup> dynamics experiments in pharyngeal muscle cells showed that CGP37157 was able to induce changes in the main parameters that define the Ca<sup>2+</sup> transients. Particularly, the distribution of the peaks included in the treated and control group showed a differential distribution according to their duration, being reduced the number of peaks that lasted more than 10 seconds in the treated group. Regarding the height and total and medium width of the Ca<sup>2+</sup> peaks, the results showed that all the parameters were reduced in the treated group even when only the peaks that lasted less than 10 seconds were used for the statistical analysis. Finally, the frequency of the peaks was increased in the treated group. All these results show that CGP37157 causes changes in the cytosolic Ca<sup>2+</sup> transients in *C. elegans*, mainly towards the reduction in [Ca<sup>2+</sup>]<sub>cyt</sub> signaling during cell stimulation.

Once cytosolic Ca<sup>2+</sup> dynamics was explored, the effects of the benzothiazepine in mitochondrial Ca<sup>2+</sup> oscillations were studied. In this case, significant changes in Ca<sup>2+</sup> dynamics were also observed, although some of them were different to the ones observed in the cytosol. Specifically, the study of Ca<sup>2+</sup> transients distribution was also different between groups, observing a decrease in long lasting peaks in the treated group, as observed in the cytosolic measurements. However, the amplitude of the mitochondrial Ca<sup>2+</sup> transients of the treated group was slightly but significantly higher, and the effects on the total and medium width of the peaks were challenging to interpret, because different results were obtained when all the peaks, or just the ones that lasted less than 10 seconds were considered in the analysis. Finally, the effects of CGP37157 in the frequency of the mitochondrial Ca<sup>2+</sup> transients were opposite to the ones observed in the cytosol. While the cytosolic oscillatory frequency was increased in the treated group, the mitochondrial frequency was significantly reduced, not observing changes in the frequency between the cytosolic and mitochondrial experiments in the control group.



All these results evidence that CGP37157 treatment causes changes in pharyngeal  $\text{Ca}^{2+}$  dynamics reducing the magnitude of  $[\text{Ca}^{2+}]_{\text{cyt}}$  transients during cell stimulation. One of the most surprising findings is the differential behavior of  $\text{Ca}^{2+}$  transients in the mitochondria when compared to the cytosol, being the most striking difference the shift in the oscillatory frequency. This result suggests that the treatment is exerting a direct effect in mitochondrial  $\text{Ca}^{2+}$  homeostatic machinery, being the most probable one the inhibition of the mNXC, since no other mitochondrial targets have been described for CGP37157.

We also wanted to investigate the possible effects of CGP37157 on pharyngeal electrophysiological properties, as action potentials in *C. elegans* are driven by  $\text{Ca}^{2+}$  instead of  $\text{Na}^+$ . The experiments showed a significant increase in the amplitude of the spikes after the treatment with CGP37157, but there were no changes in the rest of the parameters studied, including the mean frequency (Hz), the total number of pumps, the mean pump duration (ms), and the inter-pump interval (ms). The increase in the amplitude would suggest an increased  $\text{Ca}^{2+}$  entry during depolarization of pharynx cells, although the correlation of this effect with the changes in cytosolic and mitochondrial  $\text{Ca}^{2+}$  transients mentioned above is difficult to interpret.

After the study of  $\text{Ca}^{2+}$  dynamics in pharyngeal cells, the effects of CGP37157 were studied in body wall muscle cells. One of the main advantages of this tissue is that these cells do not need to be stimulated with serotonin to induce  $\text{Ca}^{2+}$  transients because they have periodic spontaneous  $\text{Ca}^{2+}$  peaks. Moreover, the magnitude of these spontaneous  $[\text{Ca}^{2+}]$  changes is much higher than that of the pharyngeal ones. In this case the effect of the treatment was studied in young and adult worms to observe the effects of CGP37157 during aging. Also, besides the study of the most effective concentration in longevity of CGP37157, 50  $\mu\text{M}$ , a 150  $\mu\text{M}$  dose was studied. Our results show that CGP37157 was also able to induce changes in vulva  $\text{Ca}^{2+}$  transients increasing the total width of the peaks, even at day 2 of treatment, while the rest of the parameters were unchanged. The same oscillatory pattern was observed at day 12 of treatment. Interestingly, the results obtained from the treatment with a higher dose of CGP37157 showed that although the same  $\text{Ca}^{2+}$  parameters were affected at day 2, the effect was smaller when compared to the 50  $\mu\text{M}$  treatment, and completely disappeared at day 12. These results show that the effect of CGP37157 in  $\text{Ca}^{2+}$  dynamics was also dose dependent being the most effective dose 50  $\mu\text{M}$  as described before for the longevity assays. The dose dependent modulation of  $\text{Ca}^{2+}$  transients by pro-longevity drugs has also been observed in the nervous system of *C. elegans* where the maintenance of neuronal  $\text{Ca}^{2+}$  transients during worms aging is only achieved at certain doses with a bell-shape response (Bazopoulou et al., 2017) . The increase in the width of the  $[\text{Ca}^{2+}]_{\text{cyt}}$  peaks may be attributed to the inhibition



of the mitochondrial  $\text{Na}^+/\text{Ca}^{2+}$  exchanger, which could delay  $\text{Ca}^{2+}$  release from mitochondria, thus extending the time required for  $[\text{Ca}^{2+}]_{\text{cyt}}$  to return to resting levels.

### CGP37157 and healthspan

During this work effects of CGP37157 on *C. elegans* lifespan and  $\text{Ca}^{2+}$  signaling have been studied, although no information about the effect on healthspan has been investigated. This is an important aspect, because not all the increases in lifespan correlate with an improvement in healthspan. As the aging research in *C. elegans* has evolved, multiple age related changes have been described including tissue, cell, and molecular changes. Among the tissue level changes, a decay in the reproductive, nervous and muscle systems have been described. Beside the changes at this level, there are also detectable changes at a cellular level, being the most important ones those related to nucleus, mitochondria, and ER morphology and activity. Finally, there are also changes at a molecular level including the modification of gene expression, the decay in RNA quality, an increase of age pigments and protein aggregation, and proteomic and metabolic changes.

All these discoveries and changes with age have led to the description of possible biomarkers of aging seeking for parameters that can reflect the physiological and functional age of the organisms (Baker and Sprott, 1988). In this sense, several potential biomarkers of aging have been proposed in *C. elegans* including physiological markers such as locomotion (Huang et al., 2004; Hsu et al., 2009; Pincus et al., 2011; Hahm et al., 2015), pharyngeal pumping rate (Huang et al., 2004), and progeny number (Pickett et al., 2013); cellular markers like the nuclear size (Tiku et al., 2017); and molecular markers including *hsp-12.6* expression (Rea et al., 2005), and mitochondrial activity (Shen et al., 2014). During the development of this work several biomarkers of aging in *C. elegans* have been studied including locomotion, progeny number, *hsp-16.2* expression, and mitochondrial activity.

The relationship and modulation of the reproductive system and aging in *C. elegans* has been deeply investigated demonstrating that changes in the activity of the reproductive system impact worms longevity (Hsin and Kenyon, 1999). Moreover, it has also been stated that there is a positive correlation between the progeny number rate and longevity (Pickett et al., 2013). Our results show that there was no difference in the total number of eggs laid by the control and the CGP37157 treated group. When the eggs laid are compared day by day, the only difference appears at day 2 of treatment being lower the rate of the treated



worms. This event was later compensated as the total number of eggs was the same for both groups. This difference is probably caused by the adaptation of the worms to the treatment, more than a direct effect of CGP37157 in the reproductive system. Thus, no effect of CGP37157 was found regarding the fertility of *C. elegans*.

The other physiological biomarker studied in this work was locomotion. It has been widely described that an improvement in locomotion, either in worms that display fast locomotion during early adulthood (Huang et al., 2004; Pincus et al., 2011; Hahm et al., 2015), or in worms that maintain their youth speed during middle age (Hsu et al., 2009), correlate positively with lifespan. When the effects of CGP37157 on *C. elegans* locomotion were studied, both their average speed (mm/s) and in their maximum speed (mm/s) were increased in middle age worms, demonstrating that the neuroprotectant CGP37157 does not only extend *C. elegans* lifespan, but it also improves their locomotion capacity, and therefore their muscular function.

Among the molecular markers that have been described, the expression of *hsp-16.2* has been evaluated after the treatment with CGP37157. This chaperone is a marker of cytosolic stress and it has been proven to correlate in a positive manner with aging (Rea et al., 2005). To assess the possible changes in *hsp-16.2* expression with the treatment, the strain TJ375 was used as GFP expression in this strain is driven by the *hsp-16.2* promoter. The results show that the treatment with CGP37157, at day 3 of adulthood, did not produce changes in GFP expression in this worms, thus no cytosolic stress was induced by the treatment. When the worms were subjected to a temporary heat shock, that drives the activation of *hsp-16.2* expression, both the control and the treated group showed a highly significant increase in GFP expression, although this expression was lower in the treated group. This could mean that CGP37157 treatment has a protective effect against cytosolic stress. To be able to establish if *hsp-16.2* could be used as a biomarker of healthspan after the treatment with CGP37157 further experiments exploring the evolution of its expression with aging would be required.

Finally, mitochondrial activity was studied by exploring ATP levels of control and treated worms. ATP levels were measured at day 5 of treatment, observing that the levels were reduced in the treated group when compared to the control group. This result indicates that mitochondrial metabolism gets reduced by CGP37157 treatment, a finding which has been previously reported to correlate positively with lifespan (Shen et al., 2014). Moreover, this result supports the previously described results of a reduced mitochondrial  $\text{Ca}^{2+}$  dynamics and the lack of effect of the neuroprotectant in the mitochondrially impaired mutant *nuo-6*, which again indicates that probably at least part of the molecular mechanism



that drives CGP37157 protective effects is due to the inhibition of the mitochondrial  $\text{Na}^+/\text{Ca}^{2+}$  exchanger.

### **CGP37157 and sarcopenia**

Sarcopenia is defined as a progressive loss of muscle mass with advancing age characterized by a decline in muscle quantity and quality (Evans, 1995; Roubenoff and Hughes, 2000). The molecular mechanisms behind the development of sarcopenia remain poorly defined. However, gene expression studies investigating human muscle with age have suggested that alterations in various metabolic pathways including the electron transport chain, the insulin signaling pathway and the mTOR pathway take part in the development of this process (Zahn et al., 2006; Phillips et al., 2013; Tang et al., 2019). Specifically, the inhibition of mTORC1 in aging mouse induces gene expression changes that reduce oxidative stress and muscle fiber damage and loss (Tang et al., 2019). Moreover, it has been recently postulated that mitochondrial deterioration in muscles and motor neurons is the primary initiator of sarcopenia and that interventions that target the improvement of mitochondrial function and proteostatic maintenance could mitigate or treat this muscle loss process (Alway et al., 2017; Coen et al., 2018).

The sarcopenia process has been demonstrated to be conserved in *C. elegans*, and recently a greater loss of mitochondrial function with aging has been associated with an earlier onset of sarcopenia in *C. elegans* (Gaffney et al., 2018). Also, the involvement of the IIS signaling pathway has been studied in this model organism by describing that *daf-2* mutants are resistant to the development of sarcopenia and associated declines in motility during aging (Duhon and Johnson, 1995; Herndon et al., 2002; Glenn et al., 2004). Due to the lack of effect of CGP37157 treatment in *daf-2*, and *daf-15* mutants, and the improved locomotion of the treated worms, we decided to investigate the possible effects of CGP37157 in sarcopenia and mitochondrial organization in *C. elegans* body wall muscle cells.

Our results show that the treatment with CGP37157 is able to delay the sarcopenia process in *C. elegans* maintaining the parallel sarcomeric structure of body wall muscle cells of treated worms when compared to the control group. Moreover, mitochondrial distribution and morphology was also improved in the worms under the benzothiazepine treatment. Since loss-of-function mutations in *daf-2* and *daf-15* blocked the effect of CGP37157, these beneficial effects in muscle integrity and maintenance may be due to the negative modulation by CGP37157 of both the IIS and the mTOR pathways.





## Concluding remarks

In conclusion, this work has described two novel pharmacological interventions that improve *C. elegans* life expectancy through the modulation of  $\text{Ca}^{2+}$  signaling. On one hand, we postulate that SERCA inhibitors induce an increase in *C. elegans* lifespan by reducing ER-mitochondria  $\text{Ca}^{2+}$  transfer. The reduction of mitochondrial  $\text{Ca}^{2+}$  uptake would induce a decrease in mitochondrial metabolism reducing the ATP/AMP ratio, activating the AMPK pathway and DAF-16 translocation to the nucleus, and inhibiting the mTOR pathway. All these metabolic changes lead to the promotion of longevity in *C. elegans*. On the other hand, the treatment with the neuroprotectant CGP37157 was also able to induce a pro-longevity effect in *C. elegans*. During this work it has been demonstrated that this compound is able to modulate cytosolic and mitochondrial  $\text{Ca}^{2+}$  dynamics. Moreover, it extends worm's lifespan by a mechanism involving IIS and mTOR pathway activities, as well as functional mitochondria, since no effect of the treatment was observed in *daf-2*, *daf-15* and *nuo-6* mutants, although the exact mechanism requires further investigation. This effect causes an improvement of locomotion in middle age worms, and a reduced mitochondrial activity. Moreover, confocal imaging experiments uncovered that CGP37157 treatment delays muscle decline associated with aging and improves mitochondrial organization and maintenance during aging in body wall muscle cells. Thus, this work has revealed a new beneficial effect of CGP37157 indicating its possible therapeutic effect on the sarcopenia process.





## CONCLUSIONS





1. Submaximal inhibition of the SERCA pump by the chronic pharmacological treatments with 2,5-BHQ and thapsigargin cause a significant increase of *C. elegans* life expectancy.
2. The effect of SERCA inhibitors does not depend on the method of administration of the drugs, either in the form of  $\gamma$ -CD inclusion compounds or directly dissolved in the NGM media, nor on the metabolization of the drugs by OP50 cultures.
3. The effects of SERCA inhibitors are not due to the induction of a caloric restriction response, as the effects were maintained in *eat-2* mutants, nor to the modulation of the activity of IIS and sirtuins signaling pathways since *daf-2* and *sir-2.1* mutants were able to respond to the treatments.
4. SERCA inhibitors did not induce any effects on the longevity of the AMPK pathway mutant *aak-1;aak-2*, nor on that of the mTOR pathway mutant *daf-15*, suggesting the implication of both pathways in the prolongevity effect exerted by SERCA inhibitors.
5. Mitochondrial respiratory chain *nuo-6* mutants did not exhibit an increased lifespan after the treatment with SERCA inhibitors indicating the necessity of a functional ETC for SERCA inhibitors to be effective.
6. SERCA inhibitors do not activate the ER stress response in *C. elegans* at the concentrations effective to increase lifespan. Moreover, the ER stress response was conserved after the treatment with SERCA inhibitors, indicating that this pathway does not take part in the prolongevity effects of SERCA inhibitors.
7. The proposed mechanism of action of SERCA inhibitors is based in a reduction of ER-mitochondria  $\text{Ca}^{2+}$  transfer, in the cellular microdomains called MAMs, reducing mitochondrial metabolism and ATP production, thus causing the activation of the AMPK pathway and the inhibition of the mTOR pathway, and then promoting the translocation of DAF-16 to the nucleus and the increase of *C. elegans* lifespan.
8. The treatment with the benzothiazepine CGP37157, already described as a neuroprotectant, produces a significant increase in the lifespan of *C. elegans* wildtype worms.
9. CGP37157 reaches a concentration inside the worms around 1,5  $\mu\text{M}$ , really close to the IC50 for the inhibition of the mNMX, and the effectiveness of the



treatment does not depend on the method of administration of the drugs, either in the form of  $\gamma$ -CD inclusion compounds or directly dissolved in the NGM media, nor on the metabolization of the drug by OP50 cultures.

10. The effects of CGP37157 are not mediated by an induction of a caloric restriction response, as the effects were maintained in *eat-2* mutants, nor by the modulation of the activity of AMPK and sirtuins signaling pathways since both *aak-2* and *aak-1;aak-2* mutants and *sir-2.1* mutants were able to respond to the treatment.
11. CGP37157 treatment did not induce any effects on the longevity of the IIS pathway mutant *daf-2*, nor on that of the mTOR pathway mutant *daf-15* suggesting the implication of both pathways in the prolongevity effect exerted by the drug.
12. Mitochondrial respiratory chain *nuo-6* mutants did not exhibit an increased lifespan after the treatment with CGP37157 indicating the necessity of a functional ETC for the treatment to be effective.
13. CGP37157 treatment induces changes in  $\text{Ca}^{2+}$  signaling in the cytosol and the mitochondria of pharyngeal muscle cells characterized by a reduced width of both cytosolic and mitochondrial  $[\text{Ca}^{2+}]$  peaks and opposite changes in both compartments in peak height and frequency.
14. Electrophysiological properties of pharyngeal pumping were also affected by CGP37157 treatment, which produced an increase in the amplitude of the depolarization, with no changes in the rest of the parameters that define the pumps.
15. CGP37157 treatment induced changes in cytosolic  $\text{Ca}^{2+}$  dynamics in vulva body wall muscle cells characterized by an increased width in the cytosolic transients. These effects were maintained until day 12 of adulthood in the treated worms at the most effective dose. Higher doses produced some effects at day 2 of treatment, but they were not maintained at day 12.
16. Several biomarkers of aging that positively correlate with an increased lifespan in *C. elegans* are modulated in worms treated with CGP37157, including an improvement in locomotion, and a reduction of mitochondrial activity. Others were not affected, such as the egg laying rate, or were reduced like *hsp-16.2* expression.

17. Development of sarcopenia gets delayed in *C. elegans* after the treatment with CGP37157 and this delay is accompanied by a maintenance of mitochondrial distribution and organization in body wall muscle cells.
18. The proposed mechanism of action of CGP37157 is based in a modulation of cytosolic and mitochondrial  $\text{Ca}^{2+}$  dynamics that are able to induce the inhibition of IIS and mTOR pathway, although the exact mechanism needs further investigation. The modulation of this pathways leads to the delay of the sarcopenia process, probably by favoring the maintenance of mitochondrial organization and distribution.
19. This thesis has for the first time revealed the possible therapeutic effects of SERCA inhibitors as modulators of AMPK and mTOR signaling pathways in the aging process, and the novel effects of CGP37157 in longevity and sarcopenia in *C. elegans*, outlining the importance of  $\text{Ca}^{2+}$  signaling in the regulation of the aging process and the appearance of aging related changes including sarcopenia and mitochondrial organization in body wall muscle cells.





**FUTURE  
PERSPECTIVES**







This thesis has revealed that calcium signaling plays a key role in the regulation of aging and that the treatment with different  $\text{Ca}^{2+}$  signaling modulators can induce an increase in the life expectancy of the model organism *C. elegans*. However, this work raises new questions and hypotheses that should be explored in order to fully understand the mechanism of action of the drugs used.

Regarding the mechanism of action of SERCA inhibitors it has been proposed that AMPK and mTOR signaling pathways activities can be modulated through changes in the activity of SERCA pumps. Moreover, it is believed that the effect is mainly mediated in the cellular microdomains called MAMs although several experiments would be needed to confirm the hypothesis. Among the proposed experiments that could help increase the understanding of SERCA inhibitors effects we propose:

- the evaluation of the changes in cytosolic and mitochondrial  $\text{Ca}^{2+}$  transients in different tissues, as it could be used as an indicator of the modulation of ER-mitochondria  $\text{Ca}^{2+}$  transfer.
- the study of the effects of SERCA inhibitors in different *C. elegans* biomarkers of aging to confirm that the treatment with the drugs does not just induce an increase in worm's life expectancy but it also improves its healthspan.
- the performance of a transcriptomic analysis that can reflect the level of expression of different members of the two signaling pathways that have been proposed to mediate the prolongevity effects. Moreover, the study of transcriptomic changes related to processes that interact with the AMPK and mTOR signaling pathways, as for example autophagy, could lead to the discovery of novel effects of the treatment.
- explore if the effects of SERCA inhibitors can improve life expectancy in different *C. elegans* strains described as neurodegenerative diseases models including Alzheimer's and Parkinson's diseases.

The work that has been done during the development of this thesis to explore the effects of CGP37157 in *C. elegans* has been more thorough being able to conclude that the compound does not only extends worm's lifespan but it also improves their locomotion and retards the sarcopenia process. However, the exact mechanism by which CGP37157 induces all these processes is not clear yet. To deeply investigate the mechanism of action of CGP37157 we propose the following experiments:



- The performance of a full transcriptomic analysis of the worms, that is already ongoing, that could be used as an indicator of the molecular and signaling pathways that modulate their activity after the treatment.
- The study of the specific isoforms of NCX in *C. elegans* that are affected by CGP37157. The expression pattern of all the isoforms is already described meaning that knowing the isoforms that variate their activity after the treatment could evidence if the phenotypic changes induced by CGP37157 are tissue specific.
- the evaluation of the effects of CGP37157 in *C. elegans* models of muscle dysfunction and sarcopenia which could indicate if the drug is able to improve muscle function or it just avoids its deterioration before deterioration appears.
- CGP37157 has also been described as neuroprotectant so the study of the effects of this treatment in neurodegenerative *C. elegans* models could be really useful to understand the possible translational applications of the treatment.



# BIBLIOGRAPHY







- Accili, D. & Arden, K. C. 2004. FoxOs at the crossroads of cellular metabolism, differentiation, and transformation. *Cell*, 117(4), pp 421-6.
- Ahumada-Castro, U., Silva-Pavez, E., Lovy, A., Pardo, E., Molgó, J. & Cárdenas, C. 2019. MTOR-independent autophagy induced by interrupted endoplasmic reticulum-mitochondrial Ca. *Autophagy*, 15(2), pp 358-361.
- Alavez, S. 2017. Homeostasis and Ageing in *C. elegans* In: Olsen, A. & Gill, M. (eds.) *Lessons from C. elegans, Healthy Ageing and Longevity 5*. Switzerland: Springer International Publishing.
- Albert, P. S. & Riddle, D. L. 1988. Mutants of *Caenorhabditis elegans* that form dauer-like larvae. *Dev Biol*, 126(2), pp 270-93.
- Altun, Z. & Hall, D. 2009a. Alimentary system, overview. In *WormAtlas* . doi:10.3908/wormatlas.1.2.
- Altun, Z. & Hall, D. 2009b. Alimentary System, Pharynx. In *WormAtlas* . doi:10.3908/wormatlas.1.3.
- Altun, Z. & Hall, D. 2009c. Epithelial system, hypodermis. In *WormAtlas* . doi:10.3908/wormatlas.1.13.
- Altun, Z. & Hall, D. 2009d. Excretory system. In *WormAtlas* . doi:10.3908/wormatlas.1.17.
- Altun, Z. & Hall, D. 2009e. Introduction. In *WormAtlas* . doi:10.3908/wormatlas.1.1.
- Altun, Z. & Hall, D. 2009f. Muscle system, nonstriated muscle. In *WormAtlas* .
- Altun, Z. & Hall, D. 2009g. Muscle system, somatic muscle. In *WormAtlas* . doi:10.3908/wormatlas.1.7
- Alvarez-Illera, P., García-Casas, P., Arias-Del-Val, J., Fonteriz, R. I., Alvarez, J. & Montero, M. 2017. Pharynx mitochondrial [Ca. *Oncotarget*, 8(34), pp 55889-55900.
- Alvarez-Illera, P., Sanchez-Blanco, A., Lopez-Burillo, S., Fonteriz, R. I., Alvarez, J. & Montero, M. 2016. Long-term monitoring of Ca<sup>2+</sup> dynamics in *C. elegans* pharynx: an in vivo energy balance sensor. *Oncotarget*, 7(42), pp 67732-67747.
- Alway, S. E., Mohamed, J. S. & Myers, M. J. 2017. Mitochondria Initiate and Regulate Sarcopenia. *Exerc Sport Sci Rev*, 45(2), pp 58-69.
- Antikainen, H., Driscoll, M., Haspel, G. & Dobrowolski, R. 2017. TOR-mediated regulation of metabolism in aging. *Aging Cell*, 16(6), pp 1219-1233.
- Apfeld, J. & Alper, S. 2018. What Can We Learn About Human Disease from the Nematode *C. elegans*? *Methods Mol Biol*, 1706, pp 53-75.
- Apfeld, J., O'Connor, G., McDonagh, T., DiStefano, P. S. & Curtis, R. 2004. The AMP-activated protein kinase AAK-2 links energy levels and insulin-like signals to lifespan in *C. elegans*. *Genes Dev*, 18(24), pp 3004-9.



- Arias-Del-Val, J., Santo-Domingo, J., García-Casas, P., Alvarez-Illera, P., Núñez Galindo, A., Wiederkehr, A., Fonteriz, R. I., Montero, M. & Alvarez, J. 2019. Regulation of inositol 1,4,5-trisphosphate-induced Ca. *Cell Calcium*, 77, pp 68-76.
- Avery, L. 1993. Motor neuron M3 controls pharyngeal muscle relaxation timing in *Caenorhabditis elegans*. *J Exp Biol*, 175 pp 283-97.
- Avery, L. & Horvitz, H. R. 1989. Pharyngeal pumping continues after laser killing of the pharyngeal nervous system of *C. elegans*. *Neuron*, 3(4), pp 473-85.
- Avery, L. & You, Y. J. 2012. *C. elegans* feeding. *WormBook*, 1-23.
- Ayyadevara, S., Alla, R., Thaden, J. J. & Shmookler Reis, R. J. 2008. Remarkable longevity and stress resistance of nematode PI3K-null mutants. *Aging Cell*, 7(1), pp 13-22.
- Baker, G. T. & Sprott, R. L. 1988. Biomarkers of aging. *Exp Gerontol*, 23(4-5), pp 223-39.
- Baron, K. T. & Thayer, S. A. 1997. CGP37157 modulates mitochondrial Ca<sup>2+</sup> homeostasis in cultured rat dorsal root ganglion neurons. *Eur J Pharmacol*, 340(2-3), pp 295-300.
- Barr, M. M. & Garcia, L. R. 2006. Male mating behavior. *WormBook*, 1-11.
- Bazopoulou, D., Chaudhury, A. R., Pantazis, A. & Chronis, N. 2017. An automated compound screening for anti-aging effects on the function of *C. elegans* sensory neurons. *Sci Rep*, 7(1), 9403.
- Beale, E. G. 2008. 5'-AMP-activated protein kinase signaling in *Caenorhabditis elegans*. *Exp Biol Med (Maywood)*, 233(1), pp 12-20.
- Ben-Zvi, A., Miller, E. A. & Morimoto, R. I. 2009. Collapse of proteostasis represents an early molecular event in *Caenorhabditis elegans* aging. *Proc Natl Acad Sci U S A*, 106(35), pp 14914-9.
- Benedetti, C., Haynes, C. M., Yang, Y., Harding, H. P. & Ron, D. 2006. Ubiquitin-like protein 5 positively regulates chaperone gene expression in the mitochondrial unfolded protein response. *Genetics*, 174(1), pp 229-39.
- Bennett, C. F. & Kaeblerlein, M. 2014. The mitochondrial unfolded protein response and increased longevity: cause, consequence, or correlation? *Exp Gerontol*, 56 pp 142-6.
- Berdichevsky, A., Viswanathan, M., Horvitz, H. R. & Guarente, L. 2006. *C. elegans* SIR-2.1 interacts with 14-3-3 proteins to activate DAF-16 and extend life span. *Cell*, 125(6), pp 1165-77.
- Berman, J. R. & Kenyon, C. 2006. Germ-cell loss extends *C. elegans* life span through regulation of DAF-16 by *kri-1* and lipophilic-hormone signaling. *Cell*, 124(5), pp 1055-68.
- Berridge, M. 2012. Cell Signalling Pathways. *Cell Signalling Biology*. [www.cellsignallingbiology.org](http://www.cellsignallingbiology.org): Portland Press Limited.
- Berridge, M., Lipp, P. & Bootman, M. 1999. Calcium signalling. *Curr Biol*, 9(5), pp R157-9.





- Berridge, M. J. 2010. Calcium hypothesis of Alzheimer's disease. *Pflugers Arch*, 459(3), pp 441-9.
- Berridge, M. J., Bootman, M. D. & Roderick, H. L. 2003. Calcium signalling: dynamics, homeostasis and remodelling. *Nat Rev Mol Cell Biol*, 4(7), pp 517-29.
- Betzer, C. & Jensen, P. H. 2018. Reduced Cytosolic Calcium as an Early Decisive Cellular State in Parkinson's Disease and Synucleinopathies. *Front Neurosci*, 12, 819.
- Betzer, C., Lassen, L. B., Olsen, A., Kofoed, R. H., Reimer, L., Gregersen, E., Zheng, J., Calì, T., Gai, W. P., Chen, T., Moeller, A., Brini, M., Fu, Y., Halliday, G., Brudek, T., Aznar, S., Pakkenberg, B., Andersen, J. P. & Jensen, P. H. 2018. Alpha-synuclein aggregates activate calcium pump SERCA leading to calcium dysregulation. *EMBO Rep*, 19(5), pii e44617.
- Bezprozvanny, I. & Mattson, M. P. 2008. Neuronal calcium mishandling and the pathogenesis of Alzheimer's disease. *Trends Neurosci*, 31(9), pp 454-63.
- Blackwell, T. K., Sewell, A. K., Wu, Z. & Han, M. 2019. TOR Signaling in. *Genetics*, 213(2), pp 329-360.
- Brenner, S. 1974. The genetics of *Caenorhabditis elegans*. *Genetics*, 77(1), pp 71-94.
- Brini, M. & Carafoli, E. 2011. The plasma membrane  $\text{Ca}^{2+}$  ATPase and the plasma membrane sodium calcium exchanger cooperate in the regulation of cell calcium. *Cold Spring Harb Perspect Biol*, 3(2), pii a004168.
- Burkewitz, K., Weir, H. J. & Mair, W. B. 2016. AMPK as a Pro-longevity Target. *Exp Suppl*, 107 pp 227-256.
- Burr, A. H. & Gans, C. 1998. Mechanical significance of obliquely striated architecture in nematode muscle. *Biol Bull*, 194(1), pp 1-6.
- Bustamante, H. A., González, A. E., Cerda-Troncoso, C., Shaughnessy, R., Otth, C., Soza, A. & Burgos, P. V. 2018. Interplay Between the Autophagy-Lysosomal Pathway and the Ubiquitin-Proteasome System: A Target for Therapeutic Development in Alzheimer's Disease. *Front Cell Neurosci*, 12, 126.
- Calì, T., Ottolini, D. & Brini, M. 2012. Mitochondrial  $\text{Ca}^{2+}$  and neurodegeneration. *Cell Calcium*, 52(1), pp 73-85.
- Carafoli, E. 2003. Historical review: mitochondria and calcium: ups and downs of an unusual relationship. *Trends Biochem Sci*, 28(4), pp 175-81.
- Carling, D. 2017. AMPK signalling in health and disease. *Curr Opin Cell Biol*, 45, pp 31-37.
- Carroll, B., Korolchuk, V. I. & Sarkar, S. 2015. Amino acids and autophagy: cross-talk and co-operation to control cellular homeostasis. *Amino Acids*, 47(10), pp 2065-88.
- Caruso, M. E., Jenna, S., Bouche-careilh, M., Baillie, D. L., Boismenu, D., Halawani, D., Latterich, M. & Chevet, E. 2008. GTPase-mediated regulation of the unfolded protein response in *Caenorhabditis elegans* is dependent on the AAA+ ATPase CDC-48. *Mol Cell Biol*, 28(13), pp 4261-74.



- Caspersen, C., Wang, N., Yao, J., Sosunov, A., Chen, X., Lustbader, J. W., Xu, H. W., Stern, D., McKhann, G. & Yan, S. D. 2005. Mitochondrial Abeta: a potential focal point for neuronal metabolic dysfunction in Alzheimer's disease. *FASEB J*, 19(14), pp 2040-1.
- Castillo-Quan, J. I., Kinghorn, K. J. & Bjedov, I. 2015. Genetics and pharmacology of longevity: the road to therapeutics for healthy aging. *Adv Genet*, 90, pp 1-101.
- Chalfie, M., Tu, Y., Euskirchen, G., Ward, W. W. & Prasher, D. C. 1994. Green fluorescent protein as a marker for gene expression. *Science*, 263(5148), pp 802-5.
- Chang, H. C. & Guarente, L. 2014. SIRT1 and other sirtuins in metabolism. *Trends Endocrinol Metab*, 25(3), pp 138-45.
- Chang, J. T., Kumsta, C., Hellman, A. B., Adams, L. M. & Hansen, M. 2017. Spatiotemporal regulation of autophagy during. *Elife*, 6, pii e18459.
- Check, E. 2002. Worm cast in starring role for Nobel prize. *Nature*, 419(6907), pp 548-9.
- Cheung, B. H., Arellano-Carbajal, F., Rybicki, I. & de Bono, M. 2004. Soluble guanylate cyclases act in neurons exposed to the body fluid to promote *C. elegans* aggregation behavior. *Curr Biol*, 14(12), pp 1105-11.
- Chisholm, A. D. & Hsiao, T. I. 2012. The *Caenorhabditis elegans* epidermis as a model skin. I: development, patterning, and growth. *Wiley Interdiscip Rev Dev Biol*, 1(6), pp 861-78.
- Chisholm, A. D. & Xu, S. 2012. The *Caenorhabditis elegans* epidermis as a model skin. II: differentiation and physiological roles. *Wiley Interdiscip Rev Dev Biol*, 1(6), pp 879-902.
- Clapham, D. E. 1995. Calcium signaling. *Cell*, 80(2), pp 259-68.
- Clapham, D. E. 2007. Calcium signaling. *Cell*, 131(6), pp 1047-58.
- Coen, P. M., Musci, R. V., Hinkley, J. M. & Miller, B. F. 2018. Mitochondria as a Target for Mitigating Sarcopenia. *Front Physiol*, 9, 1883.
- Colacurcio, D. J. & Nixon, R. A. 2016. Disorders of lysosomal acidification-The emerging role of v-ATPase in aging and neurodegenerative disease. *Ageing Res Rev*, 32, pp 75-88.
- Consortium, C. e. D. M. 2012. large-scale screening for targeted knockouts in the *Caenorhabditis elegans* genome. *G3 (Bethesda)*, 2(11), pp 1415-25.
- Consortium, C. e. S. 1998. Genome sequence of the nematode *C. elegans*: a platform for investigating biology. *Science*, 282(5396), pp 2012-8.
- Cooper, J. F., Dues, D. J., Spielbauer, K. K., Machiela, E., Senchuk, M. M. & Van Raamsdonk, J. M. 2015. Delaying aging is neuroprotective in Parkinson's disease: a genetic analysis in. *NPJ Parkinsons Dis*, 1, 15022.
- Copes, N., Edwards, C., Chaput, D., Saifee, M., Barjuca, I., Nelson, D., Paraggio, A., Saad, P., Lipps, D., Stevens, S. M. & Bradshaw, P. C. 2015. Metabolome and proteome changes with aging in *Caenorhabditis elegans*. *Exp Gerontol*, 72, pp 67-84.



- Corsi, A. K., Wightman, B. & Chalfie, M. 2015. A Transparent window into biology: A primer on *Caenorhabditis elegans*. *WormBook*, pp 1-31.
- Coughlan, K. A., Valentine, R. J., Ruderman, N. B. & Saha, A. K. 2013. Nutrient Excess in AMPK Downregulation and Insulin Resistance. *J Endocrinol Diabetes Obes*, 1(1), pp 1008.
- Cox, G. N., Kusch, M. & Edgar, R. S. 1981a. Cuticle of *Caenorhabditis elegans*: its isolation and partial characterization. *J Cell Biol*, 90(1), pp 7-17.
- Cox, G. N., Staprans, S. & Edgar, R. S. 1981b. The cuticle of *Caenorhabditis elegans*. II. Stage-specific changes in ultrastructure and protein composition during postembryonic development. *Dev Biol*, 86(2), pp 456-70.
- Cunningham, K. A., Hua, Z., Srinivasan, S., Liu, J., Lee, B. H., Edwards, R. H. & Ashrafi, K. 2012. AMP-activated kinase links serotonergic signaling to glutamate release for regulation of feeding behavior in *C. elegans*. *Cell Metab*, 16(1), pp 113-21.
- Curtis, R., O'Connor, G. & DiStefano, P. S. 2006. Aging networks in *Caenorhabditis elegans*: AMP-activated protein kinase (*aak-2*) links multiple aging and metabolism pathways. *Aging Cell*, 5(2), pp 119-26.
- Czyz, A. & Kiedrowski, L. 2003. Inhibition of plasmalemmal Na(+)/Ca(2+) exchange by mitochondrial Na(+)/Ca(2+) exchange inhibitor 7-chloro-5-(2-chlorophenyl)-1,5-dihydro-4,1-benzothiazepin-2(3H)-one (CGP-37157) in cerebellar granule cells. *Biochem Pharmacol*, 66(12), pp 2409-11.
- Dallière, N., Holden-Dye, L., Dillon, J., O'Connor, V. & Walker, R. 2019. *Caenorhabditis elegans* feeding behaviours. [https://eprints.soton.ac.uk/406590/1/DALLIERE\\_Caenorhabditis\\_elegans\\_feeding\\_AAM.pdf](https://eprints.soton.ac.uk/406590/1/DALLIERE_Caenorhabditis_elegans_feeding_AAM.pdf).
- Davidson, G. A. & Varhol, R. J. 1995. Kinetics of thapsigargin-Ca(2+)-ATPase (sarcoplasmic reticulum) interaction reveals a two-step binding mechanism and picomolar inhibition. *J Biol Chem*, 270(20), pp 11731-4.
- de la Fuente, S., Fonteriz, R. I., Montero, M. & Alvarez, J. 2013. Ca<sup>2+</sup> homeostasis in the endoplasmic reticulum measured with a new low-Ca<sup>2+</sup>-affinity targeted aequorin. *Cell Calcium*, 54(1), pp 37-45.
- Dillon, J., Andrianakis, I., Bull, K., Glautier, S., O'Connor, V., Holden-Dye, L. & James, C. 2009. AutoEPG: software for the analysis of electrical activity in the microcircuit underpinning feeding behaviour of *Caenorhabditis elegans*. *PLoS One*, 4(12), pp e8482.
- Dilova, I., Easlson, E. & Lin, S. J. 2007. Calorie restriction and the nutrient sensing signaling pathways. *Cell Mol Life Sci*, 64(6), pp 752-67.
- Doan, N. T., Paulsen, E. S., Sehgal, P., Møller, J. V., Nissen, P., Denmeade, S. R., Isaacs, J. T., Dionne, C. A. & Christensen, S. B. 2015. Targeting thapsigargin towards tumors. *Steroids*, 97, pp 2-7.



- Driscoll, M. 1995. Methods for the study of cell death in the nematode *Caenorhabditis elegans*. *Methods Cell Biol*, 46, pp 323-53.
- Duhon, S. A. & Johnson, T. E. 1995. Movement as an index of vitality: comparing wild type and the age-1 mutant of *Caenorhabditis elegans*. *J Gerontol A Biol Sci Med Sci*, 50(5), pp B254-61.
- Dwivedi, M., Song, H. O. & Ahnn, J. 2009. Autophagy genes mediate the effect of calcineurin on life span in *C. elegans*. *Autophagy*, 5(5), pp 604-7.
- Efeyan, A., Comb, W. C. & Sabatini, D. M. 2015. Nutrient-sensing mechanisms and pathways. *Nature*, 517(7534), pp 302-10.
- Ellis, H. M. & Horvitz, H. R. 1986. Genetic control of programmed cell death in the nematode *C. elegans*. *Cell*, 44(6), pp 817-29.
- Estébanez, B., de Paz, J. A., Cuevas, M. J. & González-Gallego, J. 2018. Endoplasmic Reticulum Unfolded Protein Response, Aging and Exercise: An Update. *Front Physiol*, 9, 1744.
- Evans, W. J. 1995. What is sarcopenia? *J Gerontol A Biol Sci Med Sci*, pp 5-8.
- Ferreiro, E., Oliveira, C. R. & Pereira, C. M. 2008. The release of calcium from the endoplasmic reticulum induced by amyloid-beta and prion peptides activates the mitochondrial apoptotic pathway. *Neurobiol Dis*, 30(3), pp 331-42.
- Fire, A., Xu, S., Montgomery, M. K., Kostas, S. A., Driver, S. E. & Mello, C. C. 1998. Potent and specific genetic interference by double-stranded RNA in *Caenorhabditis elegans*. *Nature*, 391(6669), pp 806-11.
- Flavell, S. W., Pokala, N., Macosko, E. Z., Albrecht, D. R., Larsch, J. & Bargmann, C. I. 2013. Serotonin and the neuropeptide PDF initiate and extend opposing behavioral states in *C. elegans*. *Cell*, 154(5), pp 1023-1035.
- Foster, T. C., Sharrow, K. M., Masse, J. R., Norris, C. M. & Kumar, A. 2001. Calcineurin links Ca<sup>2+</sup> dysregulation with brain aging. *J Neurosci*, 21(11), pp 4066-73.
- Franks, C. J., Pemberton, D., Vinogradova, I., Cook, A., Walker, R. J. & Holden-Dye, L. 2002. Ionic basis of the resting membrane potential and action potential in the pharyngeal muscle of *Caenorhabditis elegans*. *J Neurophysiol*, 87(2), pp 954-61.
- Gaffney, C. J., Pollard, A., Barratt, T. F., Constantin-Teodosiu, D., Greenhaff, P. L. & Szewczyk, N. J. 2018. Greater loss of mitochondrial function with ageing is associated with earlier onset of sarcopenia in. *Aging (Albany NY)*, 10(11), pp 3382-3396.
- Gao, S. & Zhen, M. 2011. Action potentials drive body wall muscle contractions in *Caenorhabditis elegans*. *Proc Natl Acad Sci U S A*, 108(6), pp 2557-62.
- Garcia, D. & Shaw, R. J. 2017. AMPK: Mechanisms of Cellular Energy Sensing and Restoration of Metabolic Balance. *Mol Cell*, 66(6), pp 789-800.



- García-Casas, P., Arias-Del-Val, J., Alvarez-Illera, P., Fonteriz, R. I., Montero, M. & Alvarez, J. 2018. Inhibition of Sarco-Endoplasmic Reticulum Ca<sup>2+</sup> ATPase Extends the Lifespan in *C. elegans* Worms. *Front Pharmacol*, 9, 669.
- Giles, A. C., Rose, J. K. & Rankin, C. H. 2006. Investigations of learning and memory in *Caenorhabditis elegans*. *Int Rev Neurobiol*, 69, pp 37-71.
- Glenn, C. F., Chow, D. K., David, L., Cooke, C. A., Gami, M. S., Iser, W. B., Hanselman, K. B., Goldberg, I. G. & Wolkow, C. A. 2004. Behavioral deficits during early stages of aging in *Caenorhabditis elegans* result from locomotory deficits possibly linked to muscle frailty. *J Gerontol A Biol Sci Med Sci*, 59(12), pp 1251-60.
- Golden, J. W. & Riddle, D. L. 1982. A pheromone influences larval development in the nematode *Caenorhabditis elegans*. *Science*, 218(4572), pp 578-80.
- Gomez-Suaga, P., Paillusson, S. & Miller, C. C. J. 2017. ER-mitochondria signaling regulates autophagy. *Autophagy*, 13(7), pp 1250-1251.
- González-Lafuente, L., Egea, J., León, R., Martínez-Sanz, F. J., Monjas, L., Perez, C., Merino, C., García-De Diego, A. M., Rodríguez-Franco, M. I., García, A. G., Villarroya, M., López, M. G. & de Los Ríos, C. 2012. Benzothiazepine CGP37157 and its isosteric 2'-methyl analogue provide neuroprotection and block cell calcium entry. *ACS Chem Neurosci*, 3(7), pp 519-29.
- Goodman, M. B., Hall, D. H., Avery, L. & Lockery, S. R. 1998. Active currents regulate sensitivity and dynamic range in *C. elegans* neurons. *Neuron*, 20(4), pp 763-72.
- Granatiero, V., De Stefani, D. & Rizzuto, R. 2017. Mitochondrial Calcium Handling in Physiology and Disease. *Adv Exp Med Biol*, 982, pp 25-47.
- Grandi, P. & Bantscheff, M. 2019. Advanced proteomics approaches to unravel protein homeostasis. *Drug Discov Today Technol*, 31, pp 99-108.
- Gray, J. M., Karow, D. S., Lu, H., Chang, A. J., Chang, J. S., Ellis, R. E., Marletta, M. A. & Bargmann, C. I. 2004. Oxygen sensation and social feeding mediated by a *C. elegans* guanylate cyclase homologue. *Nature*, 430(6997), pp 317-22.
- Griffin, E. F., Scopel, S. E., Stephen, C. A., Holzhauer, A. C., Vaji, M. A., Tuckey, R. A., Berkowitz, L. A., Caldwell, K. A. & Caldwell, G. A. 2019. ApoE-associated modulation of neuroprotection from A $\beta$ -mediated neurodegeneration in transgenic. *Dis Model Mech*, 12(2), ppi dmm037218.
- Gruber, J., Tang, S. Y. & Halliwell, B. 2007. Evidence for a trade-off between survival and fitness caused by resveratrol treatment of *Caenorhabditis elegans*. *Ann N Y Acad Sci*, 1100, pp 530-42.
- Hahm, J. H., Kim, S., DiLoreto, R., Shi, C., Lee, S. J., Murphy, C. T. & Nam, H. G. 2015. *C. elegans* maximum velocity correlates with healthspan and is maintained in worms with an insulin receptor mutation. *Nat Commun*, 6, 8919.
- Hansen, M., Chandra, A., Mitic, L. L., Onken, B., Driscoll, M. & Kenyon, C. 2008. A role for autophagy in the extension of lifespan by dietary restriction in *C. elegans*. *PLoS Genet*, 4(2), pp e24.



- Hansen, M., Rubinsztein, D. C. & Walker, D. W. 2018. Autophagy as a promoter of longevity: insights from model organisms. *Nat Rev Mol Cell Biol*, 19(9), pp 579-593.
- Hansen, M., Taubert, S., Crawford, D., Libina, N., Lee, S. J. & Kenyon, C. 2007. Lifespan extension by conditions that inhibit translation in *Caenorhabditis elegans*. *Aging Cell*, 6(1), pp 95-110.
- Hardie, D. G., Ross, F. A. & Hawley, S. A. 2012. AMPK: a nutrient and energy sensor that maintains energy homeostasis. *Nat Rev Mol Cell Biol*, 13(4), pp 251-62.
- Hardie, D. G., Schaffer, B. E. & Brunet, A. 2016. AMPK: An Energy-Sensing Pathway with Multiple Inputs and Outputs. *Trends Cell Biol*, 26(3), pp 190-201.
- Harman, D. 1956. Aging: a theory based on free radical and radiation chemistry. *J Gerontol*, 11(3), pp 298-300.
- Harrison, D. E., Strong, R., Sharp, Z. D., Nelson, J. F., Astle, C. M., Flurkey, K., Nadon, N. L., Wilkinson, J. E., Frenkel, K., Carter, C. S., Pahor, M., Javors, M. A., Fernandez, E. & Miller, R. A. 2009. Rapamycin fed late in life extends lifespan in genetically heterogeneous mice. *Nature*, 460(7253), pp 392-5.
- Hayashi, T. & Su, T. P. 2007. Sigma-1 receptor chaperones at the ER-mitochondrion interface regulate Ca(2+) signaling and cell survival. *Cell*, 131(3), pp 596-610.
- Henderson, S. T., Bonafè, M. & Johnson, T. E. 2006. daf-16 protects the nematode *Caenorhabditis elegans* during food deprivation. *J Gerontol A Biol Sci Med Sci*, 61(5), pp 444-60.
- Henis-Korenblit, S., Zhang, P., Hansen, M., McCormick, M., Lee, S. J., Cary, M. & Kenyon, C. 2010. Insulin/IGF-1 signaling mutants reprogram ER stress response regulators to promote longevity. *Proc Natl Acad Sci U S A*, 107(21), pp 9730-5.
- Herndon, L. A., Schmeissner, P. J., Dudaronek, J. M., Brown, P. A., Listner, K. M., Sakano, Y., Paupard, M. C., Hall, D. H. & Driscoll, M. 2002. Stochastic and genetic factors influence tissue-specific decline in ageing *C. elegans*. *Nature*, 419(6909), pp 808-14.
- Hertweck, M., Göbel, C. & Baumeister, R. 2004. *C. elegans* SGK-1 is the critical component in the Akt/PKB kinase complex to control stress response and life span. *Dev Cell*, 6(4), pp 577-88.
- Hobert, O. 2013. The neuronal genome of *Caenorhabditis elegans*. *WormBook*, 1-106.
- Hobson, R., Yook, K. & Jorgensen, E. 2017. Genetics of Neurotransmitter Release in *Caenorhabditis elegans*. El Sevier, Inc.
- Howell AM, Gilmour G, Mancebo A & AM, R. 1987. Genetic-Analysis of a large autosomal region in *Caenorhabditis elegans* by the use of a free duplication. *Genet. Res.*, 49, pp 207-213.
- Hsin, H. & Kenyon, C. 1999. Signals from the reproductive system regulate the lifespan of *C. elegans*. *Nature*, 399(6734), pp 362-6.
- Hsu, A. L., Feng, Z., Hsieh, M. Y. & Xu, X. Z. 2009. Identification by machine vision of the rate of motor activity decline as a lifespan predictor in *C. elegans*. *Neurobiol Aging*, 30(9), pp 1498-503.



- Hu, D., Cao, P., Thiels, E., Chu, C. T., Wu, G. Y., Oury, T. D. & Klann, E. 2007. Hippocampal long-term potentiation, memory, and longevity in mice that overexpress mitochondrial superoxide dismutase. *Neurobiol Learn Mem*, 87(3), pp 372-84.
- Huang, C., Xiong, C. & Kornfeld, K. 2004. Measurements of age-related changes of physiological processes that predict lifespan of *Caenorhabditis elegans*. *Proc Natl Acad Sci U S A*, 101(21), pp 8084-9.
- Ito, N., Ruegg, U. T., Kudo, A., Miyagoe-Suzuki, Y. & Takeda, S. 2013. Activation of calcium signaling through Trpv1 by nNOS and peroxynitrite as a key trigger of skeletal muscle hypertrophy. *Nat Med*, 19(1), pp 101-6.
- Jeon, S. M. 2016. Regulation and function of AMPK in physiology and diseases. *Exp Mol Med*, 48(7), pp e245.
- Jia, K., Chen, D. & Riddle, D. L. 2004. The TOR pathway interacts with the insulin signaling pathway to regulate *C. elegans* larval development, metabolism and life span. *Development*, 131(16), pp 3897-906.
- Jin, K. 2010. Modern Biological Theories of Aging. *Aging Dis*, 1(2), pp 72-74.
- Johnson, S. C., Rabinovitch, P. S. & Kaeberlein, M. 2013. mTOR is a key modulator of ageing and age-related disease. *Nature*, 493(7432), pp 338-45.
- Kaeberlein, M. 2017. Translational geroscience: A new paradigm for 21st century medicine. *Translational Medicine of Aging*, 1, pp 1-4.
- Kaeberlein, M., McVey, M. & Guarente, L. 1999. The SIR2/3/4 complex and SIR2 alone promote longevity in *Saccharomyces cerevisiae* by two different mechanisms. *Genes Dev*, 13(19), pp 2570-80.
- Kapahi, P., Kaeberlein, M. & Hansen, M. 2017. Dietary restriction and lifespan: Lessons from invertebrate models. *Ageing Res Rev*, 39, pp 3-14.
- Kapahi, P. & Zid, B. 2004. TOR pathway: linking nutrient sensing to life span. *Sci Aging Knowledge Environ*, 2004(36), pp PE34.
- Kapulkin, W. J., Kapulkin, V., Hiester, B. G. & Link, C. D. 2005. Compensatory regulation among ER chaperones in *C. elegans*. *FEBS Lett*, 579(14), pp 3063-8.
- Kashima, N., Fujikura, Y., Komura, T., Fujiwara, S., Sakamoto, M., Terao, K. & Nishikawa, Y. 2012. Development of a method for oral administration of hydrophobic substances to *Caenorhabditis elegans*: pro-longevity effects of oral supplementation with lipid-soluble antioxidants. *Biogerontology*, 13(3), pp 337-44.
- Kass, G. E., Duddy, S. K., Moore, G. A. & Orrenius, S. 1989. 2,5-Di-(tert-butyl)-1,4-benzohydroquinone rapidly elevates cytosolic Ca<sup>2+</sup> concentration by mobilizing the inositol 1,4,5-trisphosphate-sensitive Ca<sup>2+</sup> pool. *J Biol Chem*, 264(26), pp 15192-8.



- Kennedy, B. K., Berger, S. L., Brunet, A., Campisi, J., Cuervo, A. M., Epel, E. S., Franceschi, C., Lithgow, G. J., Morimoto, R. I., Pessin, J. E., Rando, T. A., Richardson, A., Schadt, E. E., Wyss-Coray, T. & Sierra, F. 2014. Geroscience: linking aging to chronic disease. *Cell*, 159(4), pp 709-13.
- Kenyon, C. 2011. The first long-lived mutants: discovery of the insulin/IGF-1 pathway for ageing. *Philos Trans R Soc Lond B Biol Sci*, 366(1561), pp 9-16.
- Kenyon, C. J. 2010. The genetics of ageing. *Nature*, 464(7288), pp 504-12.
- Khachaturian, Z. 1984. Towards theories of brain aging. Kay, DS, Barrows, GW eds. ed. Handbok of studies on psychiatry and old age. Science publishers, B.V.
- Khandia, R., Dadar, M., Munjal, A., Dhama, K., Karthik, K., Tiwari, R., Yattoo, M. I., Iqbal, H. M. N., Singh, K. P., Joshi, S. K. & Chaicumpa, W. 2019. A Comprehensive Review of Autophagy and Its Various Roles in Infectious, Non-Infectious, and Lifestyle Diseases: Current Knowledge and Prospects for Disease Prevention, Novel Drug Design, and Therapy. *Cells*, 8(7), pii E674.
- Kim, J. & Kim, E. 2016. Rag GTPase in amino acid signaling. *Amino Acids*, 48(4), pp 915-28.
- Kim, J., Kundu, M., Viollet, B. & Guan, K. L. 2011. AMPK and mTOR regulate autophagy through direct phosphorylation of Ulk1. *Nat Cell Biol*, 13(2), pp 132-41.
- Kim, J., Yang, G., Kim, Y. & Ha, J. 2016. AMPK activators: mechanisms of action and physiological activities. *Exp Mol Med*, 48, pii e224.
- Kim, W., Underwood, R. S., Greenwald, I. & Shaye, D. D. 2018. OrthoList 2: A New Comparative Genomic Analysis of Human and. *Genetics*, 210(2), pp 445-461.
- Klass, M. R. 1983. A method for the isolation of longevity mutants in the nematode *Caenorhabditis elegans* and initial results. *Mech Ageing Dev*, 22(3-4), pp 279-86.
- Kutscher, L. M. & Shaham, S. 2014. Forward and reverse mutagenesis in *C. elegans*. *WormBook*, 1-26.
- Lakowski, B. & Hekimi, S. 1998. The genetics of caloric restriction in *Caenorhabditis elegans*. *Proc Natl Acad Sci U S A*, 95(22), pp 13091-6.
- Lamming, D. W., Ye, L., Katajisto, P., Goncalves, M. D., Saitoh, M., Stevens, D. M., Davis, J. G., Salmon, A. B., Richardson, A., Ahima, R. S., Guertin, D. A., Sabatini, D. M. & Baur, J. A. 2012. Rapamycin-induced insulin resistance is mediated by mTORC2 loss and uncoupled from longevity. *Science*, 335(6076), pp 1638-43.
- Lapierre, L. R., De Magalhaes Filho, C. D., McQuary, P. R., Chu, C. C., Visvikis, O., Chang, J. T., Gelino, S., Ong, B., Davis, A. E., Irazoqui, J. E., Dillin, A. & Hansen, M. 2013. The TFEB orthologue HLH-30 regulates autophagy and modulates longevity in *Caenorhabditis elegans*. *Nat Commun*, 4, 2267.
- Lapierre, L. R. & Hansen, M. 2012. Lessons from *C. elegans*: signaling pathways for longevity. *Trends Endocrinol Metab*, 23(12), pp 637-44.





- Lee, H., Cho, J. S., Lambacher, N., Lee, J., Lee, S. J., Lee, T. H., Gartner, A. & Koo, H. S. 2008. The *Caenorhabditis elegans* AMP-activated protein kinase AAK-2 is phosphorylated by LKB1 and is required for resistance to oxidative stress and for normal motility and foraging behavior. *J Biol Chem*, 283(22), pp 14988-93.
- Lee, R. C., Feinbaum, R. L. & Ambros, V. 1993. The *C. elegans* heterochronic gene *lin-4* encodes small RNAs with antisense complementarity to *lin-14*. *Cell*, 75(5), pp 843-54.
- Lin, M. T. & Beal, M. F. 2006. Mitochondrial dysfunction and oxidative stress in neurodegenerative diseases. *Nature*, 443(7113), pp 787-95.
- Link, C. D., Cypser, J. R., Johnson, C. J. & Johnson, T. E. 1999. Direct observation of stress response in *Caenorhabditis elegans* using a reporter transgene. *Cell Stress Chaperones*, 4(4), pp 235-42.
- Lints, R. & Hall, D. 2009a. Reproductive system, overview. In *WormAtlas*. doi:10.3908/wormatlas.1.21.
- Lints, R. & Hall, D. 2009b. The cuticle. In *WormAtlas*. doi:10.3908/wormatlas.1.12.
- Llopis, J., Chow, S. B., Kass, G. E., Gahm, A. & Orrenius, S. 1991. Comparison between the effects of the microsomal Ca(2+)-translocase inhibitors thapsigargin and 2,5-di-(t-butyl)-1,4-benzohydroquinone on cellular calcium fluxes. *Biochem J*, 277 ( Pt 2), pp 553-6.
- Lockery, S. R., Hulme, S. E., Roberts, W. M., Robinson, K. J., Laromaine, A., Lindsay, T. H., Whitesides, G. M. & Weeks, J. C. 2012. A microfluidic device for whole-animal drug screening using electrophysiological measures in the nematode *C. elegans*. *Lab Chip*, 12(12), pp 2211-20.
- Long, X., Spycher, C., Han, Z. S., Rose, A. M., Müller, F. & Avruch, J. 2002. TOR deficiency in *C. elegans* causes developmental arrest and intestinal atrophy by inhibition of mRNA translation. *Curr Biol*, 12(17), pp 1448-61.
- Ludtmann, M. H. R. & Abramov, A. Y. 2018. Mitochondrial calcium imbalance in Parkinson's disease. *Neurosci Lett*, 663, pp 86-90.
- Luo, D., Nakazawa, M., Yoshida, Y., Cai, J. & Imai, S. 2000. Effects of three different Ca(2+) pump ATPase inhibitors on evoked contractions in rabbit aorta and activities of Ca(2+) pump ATPases in porcine aorta. *Gen Pharmacol*, 34(3), pp 211-20.
- López-Otín, C., Blasco, M. A., Partridge, L., Serrano, M. & Kroemer, G. 2013. The hallmarks of aging. *Cell*, 153(6), pp 1194-217.
- López-Otín, C., Galluzzi, L., Freije, J. M. P., Madeo, F. & Kroemer, G. 2016. Metabolic Control of Longevity. *Cell*, 166(4), pp 802-821.
- MacMillan, D., Currie, S., Bradley, K. N., Muir, T. C. & McCarron, J. G. 2005. In smooth muscle, FK506-binding protein modulates IP3 receptor-evoked Ca2+ release by mTOR and calcineurin. *J Cell Sci*, 118(Pt 23), pp 5443-51.



- Mair, W., Morante, I., Rodrigues, A. P., Manning, G., Montminy, M., Shaw, R. J. & Dillin, A. 2011. Lifespan extension induced by AMPK and calcineurin is mediated by CRTC-1 and CREB. *Nature*, 470(7334), pp 404-8.
- Mango, S. E. 2007. The *C. elegans* pharynx: a model for organogenesis. *WormBook*, 1-26.
- Marchi, S., Bittremieux, M., Missiroli, S., Morganti, C., Patergnani, S., Sbrano, L., Rimessi, A., Kerkhofs, M., Parys, J. B., Bultynck, G., Giorgi, C. & Pinton, P. 2017. Endoplasmic Reticulum-Mitochondria Communication Through Ca. *Adv Exp Med Biol*, 997, pp 49-67.
- Martínez, G., Duran-Aniotz, C., Cabral-Miranda, F., Vivar, J. P. & Hetz, C. 2017. Endoplasmic reticulum proteostasis impairment in aging. *Aging Cell*, 16(4), pp 615-623.
- Martínez-Sanz, F. J., Lajarín-Cuesta, R., Moreno-Ortega, A. J., González-Lafuente, L., Fernández-Morales, J. C., López-Arribas, R., Cano-Abad, M. F. & de los Ríos, C. 2015. Benzothiazepine CGP37157 Analogues Exert Cytoprotection in Various in Vitro Models of Neurodegeneration. *ACS Chem Neurosci*, 6(9), pp 1626-36.
- Marx, J. 2002. Nobel Prize in Physiology or Medicine. Tiny worm takes a star turn. *Science*, 298(5593), pp 526.
- Mattson, M. P. 2004. Pathways towards and away from Alzheimer's disease. *Nature*, 430(7000), pp 631-9.
- McGhee, J. D. 2007. The *C. elegans* intestine. *WormBook*, 1-36.
- McKay, J. P., Raizen, D. M., Gottschalk, A., Schafer, W. R. & Avery, L. 2004. eat-2 and eat-18 are required for nicotinic neurotransmission in the *Caenorhabditis elegans* pharynx. *Genetics*, 166(1), pp 161-9.
- Meléndez, A. & Levine, B. 2009. Autophagy in *C. elegans*. *WormBook*, 1-26.
- Mendes, C. C., Gomes, D. A., Thompson, M., Souto, N. C., Goes, T. S., Goes, A. M., Rodrigues, M. A., Gomez, M. V., Nathanson, M. H. & Leite, M. F. 2005. The type III inositol 1,4,5-trisphosphate receptor preferentially transmits apoptotic Ca<sup>2+</sup> signals into mitochondria. *J Biol Chem*, 280(49), pp 40892-900.
- Michaux, G., Legouis, R. & Labouesse, M. 2001. Epithelial biology: lessons from *Caenorhabditis elegans*. *Gene*, 277(1-2), pp 83-100.
- Miller, L., Greensmith, D. J., Sankaranarayanan, R., O'Neill, S. C. & Eisner, D. A. 2015. The effect of 2,5-di-(tert-butyl)-1,4-benzohydroquinone (TBQ) on intracellular Ca<sup>2+</sup> handling in rat ventricular myocytes. *Cell Calcium*, 58(2), pp 208-14.
- Missiroli, S., Bonora, M., Patergnani, S., Poletti, F., Perrone, M., Gafà, R., Magri, E., Raimondi, A., Lanza, G., Tacchetti, C., Kroemer, G., Pandolfi, P. P., Pinton, P. & Giorgi, C. 2016. PML at Mitochondria-Associated Membranes Is Critical for the Repression of Autophagy and Cancer Development. *Cell Rep*, 16(9), pp 2415-27.
- Mitchell, D. H., Stiles, J. W., Santelli, J. & Sanadi, D. R. 1979. Synchronous growth and aging of *Caenorhabditis elegans* in the presence of fluorodeoxyuridine. *J Gerontol*, 34(1), pp 28-36.



- Miyawaki, A., Llopis, J., Heim, R., McCaffery, J. M., Adams, J. A., Ikura, M. & Tsien, R. Y. 1997. Fluorescent indicators for Ca<sup>2+</sup> based on green fluorescent proteins and calmodulin. *Nature*, 388(6645), pp 882-7.
- Mizunuma, M., Neumann-Haefelin, E., Moroz, N., Li, Y. & Blackwell, T. K. 2014. mTORC2-SGK-1 acts in two environmentally responsive pathways with opposing effects on longevity. *Aging Cell*, 13(5), pp 869-78.
- Mizushima, N., Levine, B., Cuervo, A. M. & Klionsky, D. J. 2008. Autophagy fights disease through cellular self-digestion. *Nature*, 451(7182), pp 1069-75.
- Moerman, D. G. & Williams, B. D. 2006. Sarcomere assembly in *C. elegans* muscle. *WormBook*, 1-16.
- Montero, M., Alvarez, J., Scheenen, W. J., Rizzuto, R., Meldolesi, J. & Pozzan, T. 1997. Ca<sup>2+</sup> homeostasis in the endoplasmic reticulum: coexistence of high and low [Ca<sup>2+</sup>] subcompartments in intact HeLa cells. *J Cell Biol*, 139(3), pp 601-11.
- Morciano, G., Marchi, S., Morganti, C., Sbrano, L., Bittremieux, M., Kerkhofs, M., Corricelli, M., Danese, A., Karkucinska-Wieckowska, A., Wieckowski, M. R., Bultynck, G., Giorgi, C. & Pinton, P. 2018. Role of Mitochondria-Associated ER Membranes in Calcium Regulation in Cancer-Specific Settings. *Neoplasia*, 20(5), pp 510-523.
- Moreno-Ortega, A. J., Martínez-Sanz, F. J., Lajarín-Cuesta, R., de Los Rios, C. & Cano-Abad, M. F. 2015. Benzothiazepine CGP37157 and its 2'-isopropyl analogue modulate Ca<sup>2+</sup> entry through CALHM1. *Neuropharmacology*, 95, pp 503-10.
- Mrak, R. E. & Griffin, W. S. 2007. Common inflammatory mechanisms in Lewy body disease and Alzheimer disease. *J Neuropathol Exp Neurol*, 66(8), pp 683-6.
- Mukhopadhyay, A., Oh, S. W. & Tissenbaum, H. A. 2006. Worming pathways to and from DAF-16/FOXO. *Exp Gerontol*, 41(10), pp 928-34.
- Murphy, C. T. & Hu, P. J. 2013. Insulin/insulin-like growth factor signaling in *C. elegans*. *WormBook*, 1-43.
- Murshid, A., Eguchi, T. & Calderwood, S. K. 2013. Stress proteins in aging and life span. *Int J Hyperthermia*, 29(5), pp 442-7.
- Nagai, T., Yamada, S., Tominaga, T., Ichikawa, M. & Miyawaki, A. 2004. Expanded dynamic range of fluorescent indicators for Ca(2+) by circularly permuted yellow fluorescent proteins. *Proc Natl Acad Sci U S A*, 101(29), pp 10554-9.
- Nagarajan, A., Ning, Y., Reisner, K., Buraei, Z., Larsen, J. P., Hobert, O. & Doitsidou, M. 2014. Progressive degeneration of dopaminergic neurons through TRP channel-induced cell death. *J Neurosci*, 34(17), pp 5738-46.
- Napolitano, G. & Ballabio, A. 2016. TFEB at a glance. *J Cell Sci*, 129(13), pp 2475-81.



- Nelson, E. J., Li, C. C., Bangalore, R., Benson, T., Kass, R. S. & Hinkle, P. M. 1994. Inhibition of L-type calcium-channel activity by thapsigargin and 2,5-t-butylhydroquinone, but not by cyclopiazonic acid. *Biochem J*, 302 ( Pt 1), pp 147-54.
- Nelson, F. K., Albert, P. S. & Riddle, D. L. 1983. Fine structure of the *Caenorhabditis elegans* secretory-excretory system. *J Ultrastruct Res*, 82(2), pp 156-71.
- NemaMatrix. 2019. <https://nemamatrix.com/product-category/phenotyping-products/screenchip-system/>.
- Nicolau, S. M., de Diego, A. M., Cortés, L., Egea, J., González, J. C., Mosquera, M., López, M. G., Hernández-Guijo, J. M. & García, A. G. 2009. Mitochondrial Na<sup>+</sup>/Ca<sup>2+</sup>-exchanger blocker CGP37157 protects against chromaffin cell death elicited by veratridine. *J Pharmacol Exp Ther*, 330(3), pp 844-54.
- Nicolau, S. M., Egea, J., López, M. G. & García, A. G. 2010. Mitochondrial Na<sup>+</sup>/Ca<sup>2+</sup> exchanger, a new target for neuroprotection in rat hippocampal slices. *Biochem Biophys Res Commun*, 400(1), pp 140-4.
- Nussbaum-Krammer, C. I., Neto, M. F., Brielmann, R. M., Pedersen, J. S. & Morimoto, R. I. 2015. Investigating the spreading and toxicity of prion-like proteins using the metazoan model organism *C. elegans*. *J Vis Exp*, 95), pp 52321.
- Ogawa, A., Firth, A. L., Smith, K. A., Maliakal, M. V. & Yuan, J. X. 2012. PDGF enhances store-operated Ca<sup>2+</sup> entry by upregulating STIM1/Orai1 via activation of Akt/mTOR in human pulmonary arterial smooth muscle cells. *Am J Physiol Cell Physiol*, 302(2), pp C405-11.
- Organization, W. H. 2018. *Ageing and health*. <https://www.who.int/news-room/fact-sheets/detail/ageing-and-health> .
- Palmer, A. E. & Tsien, R. Y. 2006. Measuring calcium signaling using genetically targetable fluorescent indicators. *Nat Protoc*, 1(3), pp 1057-65.
- Pan, H. & Finkel, T. 2017. Key proteins and pathways that regulate lifespan. *J Biol Chem*, 292(16), pp 6452-6460.
- Paolisso, G., Gambardella, A., Ammendola, S., D'Amore, A., Balbi, V., Varricchio, M. & D'Onofrio, F. 1996. Glucose tolerance and insulin action in healthy centenarians. *Am J Physiol*, 270(5 - Pt 1), pp E890-4.
- Patergnani, S., Suski, J. M., Agnoletto, C., Bononi, A., Bonora, M., De Marchi, E., Giorgi, C., Marchi, S., Missiroli, S., Poletti, F., Rimessi, A., Duszynski, J., Wieckowski, M. R. & Pinton, P. 2011. Calcium signaling around Mitochondria Associated Membranes (MAMs). *Cell Commun Signal*, 9, 19.
- Peng, H., Liu, J., Sun, Q., Chen, R., Wang, Y., Duan, J., Li, C., Li, B., Jing, Y., Chen, X., Mao, Q., Xu, K. F., Walker, C. L., Li, J., Wang, J. & Zhang, H. 2013. mTORC1 enhancement of STIM1-mediated store-operated Ca<sup>2+</sup> entry constrains tuberous sclerosis complex-related tumor development. *Oncogene*, 32(39), pp 4702-11.



- Phillips, B. E., Williams, J. P., Gustafsson, T., Bouchard, C., Rankinen, T., Knudsen, S., Smith, K., Timmons, J. A. & Atherton, P. J. 2013. Molecular networks of human muscle adaptation to exercise and age. *PLoS Genet*, 9(3), pii e1003389.
- Pickett, C. L., Dietrich, N., Chen, J., Xiong, C. & Kornfeld, K. 2013. Mated progeny production is a biomarker of aging in *Caenorhabditis elegans*. *G3 (Bethesda)*, 3(12), pp 2219-32.
- Pierce, S. B., Costa, M., Wisotzkey, R., Devadhar, S., Homburger, S. A., Buchman, A. R., Ferguson, K. C., Heller, J., Platt, D. M., Pasquinelli, A. A., Liu, L. X., Doberstein, S. K. & Ruvkun, G. 2001. Regulation of DAF-2 receptor signaling by human insulin and ins-1, a member of the unusually large and diverse *C. elegans* insulin gene family. *Genes Dev*, 15(6), pp 672-86.
- Pincus, Z., Smith-Vikos, T. & Slack, F. J. 2011. MicroRNA predictors of longevity in *Caenorhabditis elegans*. *PLoS Genet*, 7(9), pii e1002306.
- Porta, E. A. 2002. Pigments in aging: an overview. *Ann N Y Acad Sci*, 959, pp 57-65.
- Post, M. R., Lieberman, O. J. & Mosharov, E. V. 2018. Can Interactions Between  $\alpha$ -Synuclein, Dopamine and Calcium Explain Selective Neurodegeneration in Parkinson's Disease? *Front Neurosci*, 12, 161.
- Pun, P. B., Gruber, J., Tang, S. Y., Schaffer, S., Ong, R. L., Fong, S., Ng, L. F., Cheah, I. & Halliwell, B. 2010. Ageing in nematodes: do antioxidants extend lifespan in *Caenorhabditis elegans*? *Biogerontology*, 11(1), pp 17-30.
- Qureshi, M. A., Haynes, C. M. & Pellegrino, M. W. 2017. The mitochondrial unfolded protein response: Signaling from the powerhouse. *J Biol Chem*, 292(33), pp 13500-13506.
- Raffaello, A. & Rizzuto, R. 2011. Mitochondrial longevity pathways. *Biochim Biophys Acta*, 1813(1), pp 260-8.
- Rainey, A. & Davidson, M. 2019. *ZEISS tutorials. Spectral imaging FRET with biosensors* [Online]. Available:<http://zeisscampus.fsu.edu/mobile/tutorials/spectralimaging/spectralfret/indexmobile.html>.
- Rea, S. L., Wu, D., Cypser, J. R., Vaupel, J. W. & Johnson, T. E. 2005. A stress-sensitive reporter predicts longevity in isogenic populations of *Caenorhabditis elegans*. *Nat Genet*, 37(8), pp 894-8.
- Rhoades, J. L., Nelson, J. C., Nwabudike, I., Yu, S. K., McLachlan, I. G., Madan, G. K., Abebe, E., Powers, J. R., Colón-Ramos, D. A. & Flavell, S. W. 2019. ASICs Mediate Food Responses in an Enteric Serotonergic Neuron that Controls Foraging Behaviors. *Cell*, 176(1-2), pp 85-97.e14.
- Riddle, D., Blumenthal, T. & Meyer, B. 1997a. *C. elegans II. 2nd edition. Section IV, Anatomy*: Cold Spring Harbor (NY): Cold Spring Harbor Laboratory Press.
- Riddle, D., Blumenthal, T., Meyer, B. & editors. 1997b. *C. elegans II. 2nd edition. Section II, Neurotransmitter Metabolism and Function*. Cold Spring Harbor (NY): Cold Spring Harbor Laboratory Press;.



- Riera, C. E., Merkwirth, C., De Magalhaes Filho, C. D. & Dillin, A. 2016. Signaling Networks Determining Life Span. *Annu Rev Biochem*, 85, pp 35-64.
- Rimessi, A., Giorgi, C., Pinton, P. & Rizzuto, R. 2008. The versatility of mitochondrial calcium signals: from stimulation of cell metabolism to induction of cell death. *Biochim Biophys Acta*, 1777(7-8), pp 808-16.
- Rios, E. & Brum, G. 1987. Involvement of dihydropyridine receptors in excitation-contraction coupling in skeletal muscle. *Nature*, 325(6106), pp 717-20.
- Rizzuto, R. & Pozzan, T. 2006. Microdomains of intracellular Ca<sup>2+</sup>: molecular determinants and functional consequences. *Physiol Rev*, 86(1), pp 369-408.
- Robida-Stubbs, S., Glover-Cutter, K., Lamming, D. W., Mizunuma, M., Narasimhan, S. D., Neumann-Haefelin, E., Sabatini, D. M. & Blackwell, T. K. 2012. TOR signaling and rapamycin influence longevity by regulating SKN-1/Nrf and DAF-16/FoxO. *Cell Metab*, 15(5), pp 713-24.
- Rossi, A., Pizzo, P. & Filadi, R. 2019. Calcium, mitochondria and cell metabolism: A functional triangle in bioenergetics. *Biochim Biophys Acta Mol Cell Res*, 1866(7), pp 1068-1078.
- Roubenoff, R. & Hughes, V. A. 2000. Sarcopenia: current concepts. *J Gerontol A Biol Sci Med Sci*, 55(12), pp M716-24.
- Roy, D., Kahler, D. J., Yun, C. & Hubbard, E. J. A. 2018. Functional Interactions Between. *G3 (Bethesda)*, 8(10), pp 3293-3309.
- Rubinsztein, D. C., Codogno, P. & Levine, B. 2012. Autophagy modulation as a potential therapeutic target for diverse diseases. *Nat Rev Drug Discov*, 11(9), pp 709-30.
- Ruf, V., Holzem, C., Peyman, T., Walz, G., Blackwell, T. K. & Neumann-Haefelin, E. 2013. TORC2 signaling antagonizes SKN-1 to induce *C. elegans* mesendodermal embryonic development. *Dev Biol*, 384(2), pp 214-27.
- Régimbald-Dumas, Y., Frégeau, M. O. & Guillemette, G. 2011. Mammalian target of rapamycin (mTOR) phosphorylates inositol 1,4,5-trisphosphate receptor type 2 and increases its Ca(2+) release activity. *Cell Signal*, 23(1), pp 71-9.
- Sakai, N., Ohno, H., Tomioka, M. & Iino, Y. 2017. The intestinal TORC2 signaling pathway contributes to associative learning in *Caenorhabditis elegans*. *PLoS One*, 12(5), pii e0177900.
- Sala-Vila, A., Navarro-Lérida, I., Sánchez-Alvarez, M., Bosch, M., Calvo, C., López, J. A., Calvo, E., Ferguson, C., Giacomello, M., Serafini, A., Scorrano, L., Enriquez, J. A., Balsinde, J., Parton, R. G., Vázquez, J., Pol, A. & Del Pozo, M. A. 2016. Interplay between hepatic mitochondria-associated membranes, lipid metabolism and caveolin-1 in mice. *Sci Rep*, 6, 27351.
- Salminen, A. & Kaarniranta, K. 2012. AMP-activated protein kinase (AMPK) controls the aging process via an integrated signaling network. *Ageing Res Rev*, 11(2), pp 230-41.
- Samuel, B. S., Rowedder, H., Braendle, C., Félix, M. A. & Ruvkun, G. 2016. *Caenorhabditis elegans* responses to bacteria from its natural habitats. *Proc Natl Acad Sci U S A*, 113(27), pp E3941-9.



- Sanz-Blasco, S., Valero, R. A., Rodríguez-Crespo, I., Villalobos, C. & Núñez, L. 2008. Mitochondrial Ca<sup>2+</sup> overload underlies Abeta oligomers neurotoxicity providing an unexpected mechanism of neuroprotection by NSAIDs. *PLoS One*, 3(7), pii e2718.
- Sarkis, G. J., Ashcom, J. D., Hawdon, J. M. & Jacobson, L. A. 1988. Decline in protease activities with age in the nematode *Caenorhabditis elegans*. *Mech Ageing Dev*, 45(3), pp 191-201.
- Scamps, F., Vignes, S., Restituto, S., Campo, B., Roig, A., Charnet, P. & Valmier, J. 2000. Sarco-endoplasmic ATPase blocker 2,5-Di(tert-butyl)-1, 4-benzohydroquinone inhibits N-, P-, and Q- but not T-, L-, or R-type calcium currents in central and peripheral neurons. *Mol Pharmacol*, 58(1), pp 18-26.
- Screaton, R. A., Conkright, M. D., Katoh, Y., Best, J. L., Canettieri, G., Jeffries, S., Guzman, E., Niessen, S., Yates, J. R., Takemori, H., Okamoto, M. & Montminy, M. 2004. The CREB coactivator TORC2 functions as a calcium- and cAMP-sensitive coincidence detector. *Cell*, 119(1), pp 61-74.
- Sergiev, P. V., Dontsova, O. A. & Berezkin, G. V. 2015. Theories of aging: an ever-evolving field. *Acta Naturae*, 7(1), pp 9-18.
- Sharma, V., He, C., Sacca-Schaeffer, J., Brzozowski, E., Martin-Herranz, D. E., Mendelowitz, Z., Fitzpatrick, D. A. & O'Halloran, D. M. 2013. Insight into the family of Na<sup>+</sup>/Ca<sup>2+</sup> exchangers of *Caenorhabditis elegans*. *Genetics*, 195(2), pp 611-9.
- Sharma, V. & O'Halloran, D. M. 2014. Recent structural and functional insights into the family of sodium calcium exchangers. *Genesis*, 52(2), pp 93-109.
- Shaye, D. D. & Greenwald, I. 2011. OrthoList: a compendium of *C. elegans* genes with human orthologs. *PLoS One*, 6(5), pii e20085.
- Shen, E. Z., Song, C. Q., Lin, Y., Zhang, W. H., Su, P. F., Liu, W. Y., Zhang, P., Xu, J., Lin, N., Zhan, C., Wang, X., Shyr, Y., Cheng, H. & Dong, M. Q. 2014. Mitoflash frequency in early adulthood predicts lifespan in *Caenorhabditis elegans*. *Nature*, 508(7494), pp 128-32.
- Shtonda, B. & Avery, L. 2005. CCA-1, EGL-19 and EXP-2 currents shape action potentials in the *Caenorhabditis elegans* pharynx. *J Exp Biol*, 208(Pt 11), pp 2177-90.
- Slack, C. & Tullet, J. 2018. Signal Transduction Pathways in Ageing. *Subcell Biochem*, 90, pp 323-350.
- Son, H. G., Altintas, O., Kim, E. J. E., Kwon, S. & Lee, S. V. 2019. Age-dependent changes and biomarkers of aging in *Caenorhabditis elegans*. *Aging Cell*, 18(2), pii e12853.
- Song, B. M. & Avery, L. 2013. The pharynx of the nematode *C. elegans*: A model system for the study of motor control. *Worm*, 2(1), pii e21833.
- Song, R., Sarnoski, E. A. & Acar, M. 2018. The Systems Biology of Single-Cell Aging. *iScience*, 7, pp 154-169.
- Soto, C. 2003. Unfolding the role of protein misfolding in neurodegenerative diseases. *Nat Rev Neurosci*, 4(1), pp 49-60.



- Starkov, A. A. & Beal, F. M. 2008. Portal to Alzheimer's disease. *Nat Med*, 14(10), pp 1020-1.
- Steger, K. A., Shtonda, B. B., Thacker, C., Snutch, T. P. & Avery, L. 2005. The *C. elegans* T-type calcium channel CCA-1 boosts neuromuscular transmission. *J Exp Biol*, 208(Pt 11), pp 2191-203.
- Stiernagle, T. 2006. Maintenance of *C. elegans*. *WormBook*, 1-11.
- Strange, K. 2006. An overview of *C. elegans* biology. *Methods Mol Biol*, 351, pp 1-11.
- Strange, K. 2016. Drug Discovery in Fish, Flies, and Worms. *ILAR J*, 57(2), pp 133-143.
- Sugiura, M., Fuke, S., Suo, S., Sasagawa, N., Van Tol, H. H. & Ishiura, S. 2005. Characterization of a novel D2-like dopamine receptor with a truncated splice variant and a D1-like dopamine receptor unique to invertebrates from *Caenorhabditis elegans*. *J Neurochem*, 94(4), pp 1146-57.
- Sulston, J. E. & Horvitz, H. R. 1977. Post-embryonic cell lineages of the nematode, *Caenorhabditis elegans*. *Dev Biol*, 56(1), pp 110-56.
- Sulston, J. E., Schierenberg, E., White, J. G. & Thomson, J. N. 1983. The embryonic cell lineage of the nematode *Caenorhabditis elegans*. *Dev Biol*, 100(1), pp 64-119.
- Sun, J., Folk, D., Bradley, T. J. & Tower, J. 2002. Induced overexpression of mitochondrial Mn-superoxide dismutase extends the life span of adult *Drosophila melanogaster*. *Genetics*, 161(2), pp 661-72.
- Sundaram, M. V. & Buechner, M. 2016. The *Caenorhabditis elegans* Excretory System: A Model for Tubulogenesis, Cell Fate Specification, and Plasticity. *Genetics*, 203(1), pp 35-63.
- Tang, H., Inoki, K., Brooks, S. V., Okazawa, H., Lee, M., Wang, J., Kim, M., Kennedy, C. L., Macpherson, P. C. D., Ji, X., Van Roekel, S., Fraga, D. A., Wang, K., Zhu, J., Wang, Y., Sharp, Z. D., Miller, R. A., Rando, T. A., Goldman, D., Guan, K. L. & Shragar, J. B. 2019. mTORC1 underlies age-related muscle fiber damage and loss by inducing oxidative stress and catabolism. *Aging Cell*, 18(3), pii e12943.
- Templeman, N. M. & Murphy, C. T. 2018. Regulation of reproduction and longevity by nutrient-sensing pathways. *J Cell Biol*, 217(1), pp 93-106.
- Thastrup, O., Cullen, P. J., Drøbak, B. K., Hanley, M. R. & Dawson, A. P. 1990. Thapsigargin, a tumor promoter, discharges intracellular  $\text{Ca}^{2+}$  stores by specific inhibition of the endoplasmic reticulum  $\text{Ca}^{2+}$ -ATPase. *Proc Natl Acad Sci U S A*, 87(7), pp 2466-70.
- Tiku, V., Jain, C., Raz, Y., Nakamura, S., Heestand, B., Liu, W., Späth, M., Suchiman, H. E. D., Müller, R. U., Slagboom, P. E., Partridge, L. & Antebi, A. 2017. Small nucleoli are a cellular hallmark of longevity. *Nat Commun*, 8, 16083.
- Treiman, M., Caspersen, C. & Christensen, S. B. 1998. A tool coming of age: thapsigargin as an inhibitor of sarco-endoplasmic reticulum  $\text{Ca}^{2+}$ -ATPases. *Trends Pharmacol Sci*, 19(4), pp 131-5.





- Trojanowski, N. F., Raizen, D. M. & Fang-Yen, C. 2016. Pharyngeal pumping in *Caenorhabditis elegans* depends on tonic and phasic signaling from the nervous system. *Sci Rep*, 6, 22940.
- Tullet, J. M. 2015. DAF-16 target identification in *C. elegans*: past, present and future. *Biogerontology*, 16(2), pp 221-34.
- Vadysirisack, D. D. & Ellisen, L. W. 2012. mTOR activity under hypoxia. *Methods Mol Biol*, 821, pp 45-58.
- Vallese, F., Barazzuol, L., Maso, L., Brini, M. & Cali, T. 2020. ER-Mitochondria Calcium Transfer, Organelle Contacts and Neurodegenerative Diseases. *Adv Exp Med Biol*, 1131, pp 719-746.
- van Heemst, D., Beekman, M., Mooijaart, S. P., Heijmans, B. T., Brandt, B. W., Zwaan, B. J., Slagboom, P. E. & Westendorp, R. G. 2005. Reduced insulin/IGF-1 signalling and human longevity. *Aging Cell*, 4(2), pp 79-85.
- Varshney, L. R., Chen, B. L., Paniagua, E., Hall, D. H. & Chklovskii, D. B. 2011. Structural properties of the *Caenorhabditis elegans* neuronal network. *PLoS Comput Biol*, 7(2), pii e1001066.
- Vellai, T., Takacs-Vellai, K., Zhang, Y., Kovacs, A. L., Orosz, L. & Müller, F. 2003. Genetics: influence of TOR kinase on lifespan in *C. elegans*. *Nature*, 426(6967), pp 620.
- Wang, J., Robida-Stubbs, S., Tullet, J. M., Rual, J. F., Vidal, M. & Blackwell, T. K. 2010. RNAi screening implicates a SKN-1-dependent transcriptional response in stress resistance and longevity deriving from translation inhibition. *PLoS Genet*, 6(8), pii e1001048.
- Wang, X. & Zheng, W. 2019. Ca<sup>2+</sup> homeostasis dysregulation in Alzheimer's disease: a focus on plasma membrane and cell organelles. *FASEB J*, 33(6), pp 6697-6712.
- Wang, Y. & Hekimi, S. 2015. Mitochondrial dysfunction and longevity in animals: Untangling the knot. *Science*, 350(6265), pp 1204-7.
- White, J. G., Southgate, E., Thomson, J. N. & Brenner, S. 1986. The structure of the nervous system of the nematode *Caenorhabditis elegans*. *Philos Trans R Soc Lond B Biol Sci*, 314(1165), pp 1-340.
- Wilhelm, T., Byrne, J., Medina, R., Kolundžić, E., Geisinger, J., Hajduskova, M., Tursun, B. & Richly, H. 2017. Neuronal inhibition of the autophagy nucleation complex extends life span in post-reproductive. *Genes Dev*, 31(15), pp 1561-1572.
- Wojda, U., Salinska, E. & Kuznicki, J. 2008. Calcium ions in neuronal degeneration. *IUBMB Life*, 60(9), pp 575-90.
- Wolff, S. & Dillin, A. 2006. The trifecta of aging in *Caenorhabditis elegans*. *Exp Gerontol*, 41(10), pp 894-903.
- Wolkow, C. & Hall, D. 2015. Introduction to the Dauer Larva, Overview. In *WormAtlas* .
- Woods, A., Dickerson, K., Heath, R., Hong, S. P., Momcilovic, M., Johnstone, S. R., Carlson, M. & Carling, D. 2005. Ca<sup>2+</sup>/calmodulin-dependent protein kinase kinase-beta acts upstream of AMP-activated protein kinase in mammalian cells. *Cell Metab*, 2(1), pp 21-33.



- Workgroup, A. s. A. C. H. 2017. Calcium Hypothesis of Alzheimer's disease and brain aging: A framework for integrating new evidence into a comprehensive theory of pathogenesis. *Alzheimers Dement*, 13(2), pp 178-182.e17.
- Wyss-Coray, T. & Rogers, J. 2012. Inflammation in Alzheimer disease-a brief review of the basic science and clinical literature. *Cold Spring Harb Perspect Med*, 2(1), pii a006346.
- Xu, S., Hsiao, T. I. & Chisholm, A. D. 2012. The wounded worm: Using *C. elegans* to understand the molecular basis of skin wound healing. *Worm*, 1(2), pp 134-8.
- Xu, Y. & Park, Y. 2018. Application of. *Prev Nutr Food Sci*, 23(4), pp 275-281.
- Yamasaki-Mann, M., Demuro, A. & Parker, I. 2010. Modulation of endoplasmic reticulum Ca<sup>2+</sup> store filling by cyclic ADP-ribose promotes inositol trisphosphate (IP<sub>3</sub>)-evoked Ca<sup>2+</sup> signals. *J Biol Chem*, 285(32), pp 25053-61.
- Yang, W. & Hekimi, S. 2010. Two modes of mitochondrial dysfunction lead independently to lifespan extension in *Caenorhabditis elegans*. *Aging Cell*, 9(3), pp 433-47.
- Yao, Y., Tsuchiyama, S., Yang, C., Bulteau, A. L., He, C., Robison, B., Tsuchiya, M., Miller, D., Briones, V., Tar, K., Potrero, A., Friguet, B., Kennedy, B. K. & Schmidt, M. 2015. Proteasomes, Sir2, and Hxk2 form an interconnected aging network that impinges on the AMPK/Snf1-regulated transcriptional repressor Mig1. *PLoS Genet*, 11(1), pii e1004968.
- Yavari, A., Bellahcene, M., Bucchi, A., Sirenko, S., Pinter, K., Herring, N., Jung, J. J., Tarasov, K. V., Sharpe, E. J., Wolfien, M., Czibik, G., Steeples, V., Ghaffari, S., Nguyen, C., Stockenhuber, A., Clair, J. R. S., Rimbach, C., Okamoto, Y., Yang, D., Wang, M., Ziman, B. D., Moen, J. M., Riordon, D. R., Ramirez, C., Paina, M., Lee, J., Zhang, J., Ahmet, I., Matt, M. G., Tarasova, Y. S., Baban, D., Sahgal, N., Lockstone, H., Puliyadi, R., de Bono, J., Siggs, O. M., Gomes, J., Muskett, H., Maguire, M. L., Beglov, Y., Kelly, M., Dos Santos, P. P. N., Bright, N. J., Woods, A., Gehmlich, K., Isackson, H., Douglas, G., Ferguson, D. J. P., Schneider, J. E., Tinker, A., Wolkenhauer, O., Channon, K. M., Cornall, R. J., Sternick, E. B., Paterson, D. J., Redwood, C. S., Carling, D., Proenza, C., David, R., Baruscotti, M., DiFrancesco, D., Lakatta, E. G., Watkins, H. & Ashrafian, H. 2017. Mammalian  $\gamma$ 2 AMPK regulates intrinsic heart rate. *Nat Commun*, 8(1), 1258.
- Zahn, J. M., Sonu, R., Vogel, H., Crane, E., Mazan-Mamczarz, K., Rabkin, R., Davis, R. W., Becker, K. G., Owen, A. B. & Kim, S. K. 2006. Transcriptional profiling of aging in human muscle reveals a common aging signature. *PLoS Genet*, 2(7), pp e115.
- Zhang, J. Z., Waddell, H. M. & Jones, P. P. 2015. Regulation of RYR2 by sarcoplasmic reticulum Ca(2+). *Clin Exp Pharmacol Physiol*, 42(6), pp 720-6.
- Zhao, H., Li, T., Wang, K., Zhao, F., Chen, J., Xu, G., Zhao, J., Chen, L., Li, L., Xia, Q., Zhou, T., Li, H. Y., Li, A. L., Finkel, T., Zhang, X. M. & Pan, X. 2019. AMPK-mediated activation of MCU stimulates mitochondrial Ca. *Nat Cell Biol*, 21(4), pp 476-486.
- Zhao, J., Brault, J. J., Schild, A., Cao, P., Sandri, M., Schiaffino, S., Lecker, S. H. & Goldberg, A. L. 2007. FoxO3 coordinately activates protein degradation by the autophagic/lysosomal and proteasomal pathways in atrophying muscle cells. *Cell Metab*, 6(6), pp 472-83.



- Zhou, B., Kreuzer, J., Kumsta, C., Wu, L., Kamber, K. J., Cedillo, L., Zhang, Y., Li, S., Kacergis, M. C., Webster, C. M., Fejes-Toth, G., Naray-Fejes-Toth, A., Das, S., Hansen, M., Haas, W. & Soukas, A. A. 2019. Mitochondrial Permeability Uncouples Elevated Autophagy and Lifespan Extension. *Cell*, 177(2), pp 299-314.e16.
- Zinzalla, V., Stracka, D., Oppliger, W. & Hall, M. N. 2011. Activation of mTORC2 by association with the ribosome. *Cell*, 144(5), pp 757-68.
- Zwaal, R. R., Van Baelen, K., Groenen, J. T., van Geel, A., Rottiers, V., Kaletta, T., Dode, L., Raeymaekers, L., Wuytack, F. & Bogaert, T. 2001. The sarco-endoplasmic reticulum Ca<sup>2+</sup> ATPase is required for development and muscle function in *Caenorhabditis elegans*. *J Biol Chem*, 276(47), pp 43557-63.
- Zárate, S., Stevnsner, T. & Gredilla, R. 2017. Role of Estrogen and Other Sex Hormones in Brain Aging. Neuroprotection and DNA Repair. *Front Aging Neurosci*, 9, 430.